



**A University of Sussex DPhil thesis**

Available online via Sussex Research Online:

<http://sro.sussex.ac.uk/>

This thesis is protected by copyright which belongs to the author.

This thesis cannot be reproduced or quoted extensively from without first obtaining permission in writing from the Author

The content must not be changed in any way or sold commercially in any format or medium without the formal permission of the Author

When referring to this work, full bibliographic details including the author, title, awarding institution and date of the thesis must be given

Please visit Sussex Research Online for more information and further details

# **Investigation of Operational Conditions of Steam Traps through Acoustic Emission**

**Eur Ing Christopher M. R. A. Poczka**  
**MEng CEng MIMechE**

Submitted for the degree of Doctor of Philosophy  
University of Sussex  
December 2011

UNIVERSITY OF SUSSEX

CHRISTOPHER M. R. A. POCZKA , DOCTOR OF PHILOSOPHY

INVESTIGATION OF OPERATIONAL CONDITIONS OF STEAM TRAPS THROUGH  
ACOUSTIC EMISSIONABSTRACT

*Steam is widely used in the process industry; in sectors ranging from food preparation to clothing production to sterilisation in hospitals. The process industry is one of the main energy users. With energy efficiency and the reduction of carbon emissions high on current political agendas, the Steam Industry, which led the early industrial revolution, is looking for innovative energy saving solutions to reduce emissions.*

*A key component of the steam and condensate loop is the Steam Trap, which separates the condensate from the steam and maintains an efficient and safe steam system. Steam Traps are basic mechanical devices and their faults are difficult to diagnose due to the two-phase flow of steam and condensate. Current testing methods are manual in nature, time consuming and costly. This thesis investigates the use of acoustic condition monitoring techniques to understand the relationship between acoustic emission and steam leakage.*

*In this investigation, a number of Steam Traps have been tested at several typical pressure and condensate load operation conditions and the respective acoustic emissions have been recorded. The characteristics of the heterodyne circuit, used to record acoustic data, have been investigated. The resulting acoustic signals of major types of Steam Traps have been systematically analysed against these operating conditions and steam leakage rates. Time, Frequency and Time-Frequency methods have been applied to acoustic signals and the results evaluated through statistical methods. Finally, Steam Traps are categorised by their acoustic response and a number of analysis techniques and approaches are presented.*

# Declaration

I hereby declare that this thesis, either in the same or different form, has not been previously submitted to this or any other University for a degree.

Signature:

Christopher M. R. A. Poczka



# Acknowledgements

**Whether you think that you can,  
or that you can't,  
you are usually right.**  
*Henry Ford*

First and foremost, I would like to thank the Royal Commission for the Exhibition of 1851 for the award of the Industrial Fellowship. I am deeply indebted to the Royal Commission for the many opportunities this Fellowship has provided to me including studying for this PhD. The financial and peerage support during the three year fellowship is warmly acknowledged.

I would like to thank my academic supervisor, Dr William W. J. Wang from the University of Sussex for his support and advice throughout the course of this research. I also want to acknowledge Spirax Sarco Limited, my employer, for supporting me in my studies for my PhD and especially Richard Carmichael and Jeremy Miller.

My parents have been a great source of motivation and support throughout my life, especially during my studies. Thank you for everything.

I am grateful to the members of the Research Department and all of the test shop staff at Spirax Sarco past and present for their help in carrying out this research. I am also grateful to many opportunities that were presented to me during my studies and especially to have met so many interesting people. Long may friendships and memories last.

Last, but certainly not least, I would like to thank my wife Michele for her endless support and encouragement.

**Love, Live, Learn**

# Copyright Permissions

The author would like to acknowledge the following copyright holders and thank them for their permission to reproduce their material. Further reproduction prohibited without permission. The following list appears in the order in which the Figures appear in the text:

Copyright is claimed on Figures 1.1, 2.1, 2.3, 2.4, 2.6, 2.7, 2.8, 2.9, 2.10 and 2.11. Copyright holders are Spirax Sarco. Spirax Sarco permits the reproduction of the Figures, further reproduction prohibited without permission.

Copyright is claimed on Figure 2.12 and Figure 2.13. Copyright holders are British Standard Institute. BSI permits the reproduction of Figure 1 and 2 from "PSE/007 Committee from Methods for Determination of Steam Loss of Automatic Steam Traps - BS EN 27841:1991. Technical report, PSE/007 Industrial Valve, 1991."

Copyright is claimed on Figure 2.14. Copyright holders are Elsevier. Elsevier permits the reproduction of Figure 2 from "I. Macleod, R. Rowley, M. Beesley, and P. Olleya. Acoustic monitoring techniques for structural integrity. Nuclear Engineering and Design, Vol. 129, Iss. 2, pp 191-200, 1991."

Copyright is claimed on Figure 2.15 and Figure 2.17. Copyright holders are the Society of Petroleum Engineers. The Society of Petroleum Engineers permits the reproduction of Figure 1 and Figure 2 from "Chien, S.F. 1990. Predicting Wet-Steam Flow Regime in Horizontal Pipes. J Pet Technol 42 (3):356-362. SPE-17574-PA. doi:10-2118/14574-PA."

Copyright is claimed on Figure 2.16. Copyright holders are Spirax Sarco. Spirax Sarco permits the reproduction of the Figure, further reproduction prohibited without permission.

Copyright is claimed on Figure 2.18 and Figure 2.19. Copyright holders are Oxford University Publishing. Oxford University Publishing permits the reproduction of Figure 3.15 (Page 84) and Figure 3.20 (Page 89) from "Christopher E. Brennen. Cavitation and Bubble Dynamics (Oxford Engineering Science Series) Oxford University Press, USA, 1995."

Copyright is claimed on Figure 3.6. Copyright holders are Spirax Sarco. Spirax Sarco permits the reproduction of the Figure, further reproduction prohibited without permission.

# Contents

<b>Abstract</b>	<b>ii</b>
<b>Declaration</b>	<b>iii</b>
<b>Acknowledgements</b>	<b>iv</b>
<b>Copyright Permissions</b>	<b>v</b>
<b>List of Tables</b>	<b>x</b>
<b>List of Figures</b>	<b>xi</b>
<b>Nomenclature</b>	<b>xvi</b>
<b>1 Overview of the Investigation</b>	<b>1</b>
1.1 Steam Process Industry and Steam Traps . . . . .	1
1.2 Current Steam Trap Condition Monitoring Approach . . . . .	2
1.3 Problem Definition and Objectives of this Investigation . . . . .	3
1.4 Significance of the Investigation to Knowledge . . . . .	4
1.5 Motivation and Extension of the Knowledge through the Investigation . . . . .	4
1.6 Structure of Thesis . . . . .	5
<b>2 Introduction to Steam Traps, Applications and Quality Assessment Techniques</b>	<b>6</b>
2.1 Steam Trap Types and Their Function . . . . .	6
2.1.1 Velocity Traps . . . . .	9
2.1.2 Thermostatic Traps . . . . .	10
2.1.3 Mechanical Traps . . . . .	11
2.1.4 Steam Trap Operation Conditions . . . . .	13
2.1.5 General Steam Trap Failure Modes . . . . .	14
2.1.6 Specific Steam Trap Failure Modes . . . . .	14
2.2 Condition Monitoring of Steam Traps . . . . .	16
2.2.1 Condition Monitoring Techniques Applied to Steam Traps . . . . .	16
2.2.2 SWOT Analysis of Steam Trap Measurement Techniques . . . . .	19
2.2.3 Existing Steam Trap Diagnostic Equipment . . . . .	20
2.3 Steam Wastage Measurement . . . . .	22
2.3.1 Steam Wastage Measurement Standard . . . . .	22
2.4 Published Steam Trap Information and Wastage Data . . . . .	25
2.5 Acoustic Emission of Steam Traps . . . . .	26
2.5.1 Sources and Reasons of Acoustic Emission . . . . .	27

2.5.2	Acoustics Emission in Steam and Condensate . . . . .	28
2.5.3	Measurement of Acoustic Emission of Steam Traps . . . . .	29
2.5.4	Acoustic Condition Monitoring Techniques applied to Steam Traps . . . . .	31
2.6	Two-Phase Flow and Cavitation in Pipelines . . . . .	32
2.6.1	Occurrence of Two-Phase Flow . . . . .	32
2.6.2	Two-Phase Flow Regimes in Horizontal and Vertical Pipes . . . . .	33
2.6.3	Bubble Dynamics and Cavitation . . . . .	38
2.6.4	Water Hammer . . . . .	41
2.6.5	Flow Induced Vibration . . . . .	41
2.7	Overview of Digital Signal Processing for Condition Monitoring . . . . .	41
2.7.1	Time Domain, Frequency and Time-Frequency . . . . .	42
2.7.2	Signal Processing Techniques for Flows . . . . .	46
2.7.3	Analysis of Signals . . . . .	46
2.8	Condition Monitoring in Related Industrial Applications . . . . .	47
2.8.1	Pipe Leak Detection . . . . .	47
2.8.2	Valve Leak Detection . . . . .	48
2.8.3	Flow Measurement . . . . .	49
2.9	Relevant Signal Processing Methods . . . . .	50
2.10	PESTLE Analysis on Condition Monitoring for Steam Traps . . . . .	51
2.10.1	Political Factors . . . . .	52
2.10.2	Economic Factors . . . . .	52
2.10.3	Sociocultural Factors . . . . .	53
2.10.4	Technological Factors . . . . .	53
2.10.5	Legal Factors . . . . .	53
2.10.6	Environmental Factors . . . . .	54
2.11	Summary . . . . .	55
<b>3</b>	<b>Experimental Design for Steam Trap Wastage and Acoustic Measurement</b>	<b>56</b>
3.1	Testing Setup and Methodology . . . . .	56
3.2	Setup of Steam Wastage Rig for Testing of Steam Traps . . . . .	57
3.2.1	Steam Wastage Standard . . . . .	57
3.2.2	St Georges Steam Wastage Rig (SGR) Specification and Design . . . . .	57
3.2.3	Runnings Road Steam Wastage Rig (RRR) Specification and Design . . . . .	58
3.2.4	Comparison of Operation of the two rigs and consideration of BSEN 27841 . . . . .	59
3.3	Steam Wastage Measurement Data Acquisition and Processing . . . . .	60
3.3.1	Data Acquisition Hardware . . . . .	61
3.3.2	Steam Wastage Rig Sensors . . . . .	62
3.3.3	Steam Wastage Calculation Algorithm . . . . .	64
3.4	Acoustic Data Acquisition . . . . .	65
3.4.1	Acoustic Sensor . . . . .	65
3.4.2	Experimental Setup for Acoustic Signal Acquisition . . . . .	66
3.4.3	Acoustic Data and Signal Recording Software . . . . .	66
3.5	Steam Trap Test Experimental Procedure . . . . .	68
3.5.1	Overview . . . . .	68
3.5.2	Procedure . . . . .	68
3.6	Summary . . . . .	69

<b>4</b>	<b>Experiments on the Heterodyne Stethoscope Response</b>	<b>70</b>
4.1	Background to the Heterodyne Investigation . . . . .	70
4.1.1	Heterodyne Process . . . . .	70
4.1.2	Frequency Modulation . . . . .	70
4.1.3	Implementation . . . . .	71
4.2	The Heterodyne Circuit used in the Experiments . . . . .	72
4.2.1	Probe Heterodyne Circuit Specification . . . . .	73
4.2.2	Assumptions on the Heterodyne Effects . . . . .	73
4.3	Probe Experimental Setups Data Acquisition and Analysis . . . . .	73
4.3.1	Heterodyne Circuit Investigation . . . . .	73
4.3.2	Stethoscope Module Investigation . . . . .	78
4.3.3	Investigation of Combined Heterodyne and Stethoscope . . . . .	85
4.4	Time-Frequency Analysis Investigation of the Frequency Folding Effect of the Heterodyne Circuit . . . . .	90
4.5	Corrected Assumptions on the Heterodyne Effects . . . . .	90
4.6	Summary . . . . .	91
<b>5</b>	<b>Operational Conditions and Process Parameters</b>	<b>93</b>
5.1	Acoustically Detected Steam Trap Failure Modes . . . . .	93
5.2	Data Analysis Approach . . . . .	95
5.2.1	Data Analysis Methodology . . . . .	95
5.2.2	Re-sampling of Acoustic Data . . . . .	96
5.2.3	Application of Analysis Techniques to Acoustic Steam Trap Data Analysis . . . . .	96
5.3	Overview of the Key Parameter Analysis . . . . .	99
5.3.1	Multivariate Analysis of Test Parameters . . . . .	101
5.3.2	Analysis of Trap Type and Pressure / Condensate Load Relationship . . . . .	103
5.4	Acoustic Analysis Techniques applied to the Steam Wastage Data . . . . .	109
5.5	Summary . . . . .	110
<b>6</b>	<b>Fixed Orifice Steam Trap Analysis</b>	<b>111</b>
6.1	Acoustic Signals for Fixed Orifice Trap . . . . .	111
6.1.1	Characteristics of the Acoustic Signals . . . . .	112
6.1.2	Feature Extraction of Acoustic Trap Signals . . . . .	116
6.2	Application of Signal Processing . . . . .	118
6.2.1	Time Domain Analysis . . . . .	118
6.2.2	Frequency Domain Analysis . . . . .	122
6.2.3	Time-Frequency Analysis . . . . .	132
6.3	Summary . . . . .	141
<b>7</b>	<b>Non-Impulsive Steam Trap Analysis</b>	<b>143</b>
7.1	Acoustic Signals for Non-Impulsive Trap . . . . .	143
7.1.1	Characteristics of the Acoustic Signals . . . . .	144
7.2	Application of Signal Processing . . . . .	148
7.2.1	Time Domain Analysis . . . . .	148
7.2.2	Frequency Domain Analysis . . . . .	154
7.2.3	Time-Frequency Analysis . . . . .	164
7.3	Summary . . . . .	173

<b>8</b>	<b>Impulsive Steam Trap Analysis</b>	<b>175</b>
8.1	Acoustic Signals for Impulsive Trap . . . . .	175
8.2	Application of Signal Processing . . . . .	176
8.2.1	Characteristics of the Acoustic Signals . . . . .	176
8.2.2	Time Domain Analysis . . . . .	179
8.2.3	Frequency Domain Analysis . . . . .	185
8.2.4	Time-Frequency Analysis . . . . .	196
8.3	Summary . . . . .	207
<b>9</b>	<b>Key Results Summary</b>	<b>208</b>
9.1	Steam Trap Test Rig . . . . .	208
9.2	Heterodyne Circuit . . . . .	208
9.3	Common Features in the Signal Analysis . . . . .	209
9.3.1	Orifice Traps Common Features . . . . .	209
9.3.2	Non-Impulsive Traps Common Features . . . . .	209
9.3.3	Impulsive Traps Common Features . . . . .	209
9.4	Sources of Error . . . . .	209
<b>10</b>	<b>Conclusions and Recommendations</b>	<b>211</b>
10.1	Contribution to Knowledge . . . . .	211
10.2	Recommendations and Further Work . . . . .	213
10.3	Final Summary Overview . . . . .	213
	<b>References</b>	<b>215</b>
<b>A</b>	<b>Additional Steam Trap Information</b>	<b>224</b>
A.1	List of Steam Trap Manufacturers . . . . .	224
A.2	Carbon Trust Calculation . . . . .	225
<b>B</b>	<b>Heterodyne Circuit Information</b>	<b>226</b>
<b>C</b>	<b>Steam Wastage Rig</b>	<b>228</b>
C.1	Pictures Steam Wastage Rig . . . . .	228
C.1.1	St Georges Road Test Shop . . . . .	228
C.1.2	Runnings Road Test Shop . . . . .	232
C.2	Steam Wastage Rig Schematics . . . . .	234
C.2.1	St Georges Road Test Shop . . . . .	234
C.2.2	Runnings Road Test Shop . . . . .	236
C.3	LabView Data Acquisition Software . . . . .	237
C.3.1	Software Overview Diagram . . . . .	237
C.3.2	LabView Flow Diagrams . . . . .	240
C.3.3	List of SubVIs in Program . . . . .	244
C.3.4	List of Associated INI and DLM Files . . . . .	244
C.3.5	Matlab Steam Wastage Calculation for LabView . . . . .	247
<b>D</b>	<b>List of Data Files</b>	<b>249</b>
D.1	Fixed Orifice . . . . .	249
D.2	Non-Impulsive . . . . .	250
D.3	Impulsive . . . . .	251

# List of Tables

1.1	Steam Trap Condition Monitoring Techniques . . . . .	3
2.1	Steam Trap Specification Information . . . . .	14
2.2	Steam Trap Failure Modes . . . . .	14
2.3	SWOT Steam Trap Condition Monitoring Techniques . . . . .	19
2.4	SWOT Diagnostic Devices . . . . .	21
2.5	Steam Trap Condition Monitoring Products . . . . .	22
2.6	Spirax Sarco Steam Wastage Data . . . . .	26
2.7	Steam Trap Failure Percentage . . . . .	26
4.1	Convergence Results of Multiple Input Signals . . . . .	85
5.1	Signal Processing Techniques applied to Steam Traps . . . . .	97
5.2	Operational Parameter Analysis Data Summary . . . . .	97
5.3	Table of Test Parameters . . . . .	100
5.4	Operational Condition Condensate and Pressure Indicator . . . . .	103
6.1	Fixed Orifice Trap Acoustic Data Summary . . . . .	112
6.2	Fixed Orifice Trap Condensate and Pressure Indicator . . . . .	118
7.1	Float Trap Acoustic Data Summary . . . . .	144
7.2	Float Trap Condensate and Pressure Indicator . . . . .	148
8.1	Thermodynamic Trap Acoustic Data Summary . . . . .	176
8.2	Thermodynamic Trap Condensate and Pressure Indicator . . . . .	180
D.1	Fixed Orifice Trap Acoustic Complete Data List . . . . .	249
D.2	Float Trap Acoustic Complete Data List . . . . .	250
D.3	Thermodynamic Trap Acoustic Complete Data List . . . . .	251

# List of Figures

1.1	Products Made with Steam . . . . .	1
2.1	Examples of Steam Traps . . . . .	7
2.2	Steam Trap Type Overview . . . . .	7
2.3	Steam System Overview (from [89]) . . . . .	8
2.4	Thermodynamic Steam Trap (from [91]) . . . . .	9
2.5	Fixed Orifice Trap . . . . .	10
2.6	Balance Pressure Trap (from [91]) . . . . .	11
2.7	Balance Pressure Trap Cross-section (from [91]) . . . . .	11
2.8	Bimetal Trap (from [91]) . . . . .	12
2.9	Bimetal Strip (from [91]) . . . . .	12
2.10	Float Trap Cross-section (from [91]) . . . . .	12
2.11	Inverted Bucket Trap (from [91]) . . . . .	13
2.12	ISO RIG Method A (from [71]) . . . . .	23
2.13	ISO RIG Method B (from [71]) . . . . .	24
2.14	Frequency Response from a Small Orifice in a Steam Pipeline (from [54]) . . . . .	31
2.15	Horizontal Flow Regimes (from [25]) . . . . .	34
2.16	Horizontal Flow Regimes observed in Experiments (from [84]) . . . . .	35
2.17	Wet Steam Flow Regimes (from [96]) . . . . .	36
2.18	Cavitation Frequency Response (from [11]) . . . . .	39
2.19	Cavitation Frequency Response (from [11]) . . . . .	40
3.1	SGR Rig Steam Trap Test Station Diagram . . . . .	58
3.2	SGR Test Area - Tank and Weight Scales . . . . .	59
3.3	SGR Test Area - Steam Trap Test Setup . . . . .	59
3.4	SGR Rig Steam Trap Test Station Diagram . . . . .	59
3.5	Runnings Road Steam Wastage Rig . . . . .	60
3.6	Heterodyne Probe Nomenclature . . . . .	66
3.7	UP100 Experimental Hardware Setup . . . . .	67
3.8	UP100 Clamp on Steam Pipe . . . . .	67
3.9	Acoustic Recording Software Setup . . . . .	67
4.1	Heterodyne Module connected to the Oscilloscope . . . . .	74
4.2	Heterodyne Module connected to the PCMCIA Card . . . . .	75
4.3	Heterodyne Module Oscilloscope Time Domain Plot . . . . .	76
4.4	Heterodyne Module PCMCIA Card Time Domain Plot . . . . .	76
4.5	Heterodyne Module PCMCIA Card Frequency Domain Plot . . . . .	77
4.6	Stethoscope Module Investigation Experimental Setup . . . . .	78



4.7	Stethoscope Module Test Setup . . . . .	79
4.8	Hammer for Impulse . . . . .	79
4.9	Stethoscope Module Time Domain Plot . . . . .	80
4.10	16 Stethoscope Signal Average (Magnitude before averaging FFTs) . . . . .	80
4.11	16 Stethoscope Signal Average (Magnitude after averaging FFTs) . . . . .	81
4.12	Stethoscope Module Signal Average for 2 samples . . . . .	82
4.13	Stethoscope Module Signal Average for 4 samples . . . . .	83
4.14	Stethoscope Module Signal Average for 8 samples . . . . .	83
4.15	Stethoscope Module Signal Average for 24 samples . . . . .	83
4.16	Stethoscope Module Signal Average for 32 samples . . . . .	83
4.17	Stethoscope Module Convergence Results . . . . .	84
4.18	Percentage Difference on Convergence for Modulus FFT and Complex FFT . . . . .	84
4.19	Combined Module Responses in the Frequency Domain . . . . .	86
4.20	Dynamic Combined Module Response Experimental Setup . . . . .	87
4.21	Dynamic Combined Frequency Signal Response . . . . .	88
4.22	Dynamic Combined Module Response Time Frequency . . . . .	89
4.23	Dynamic Combined Module Response Time Frequency (Zoomed) . . . . .	89
4.24	Time-Frequency Representation of Heterodyne Module using a Frequency Sweep . . . . .	90
5.1	Data Analysis Approach . . . . .	96
5.2	Fixed Orifice Trap Data Review . . . . .	98
5.3	Float Trap Data Review . . . . .	98
5.4	Thermodynamic Trap Data Review . . . . .	99
5.5	Interdependence of Key Parameters in Steam Wastage Determination . . . . .	100
5.6	Steam Saturation Curve . . . . .	101
5.7	Multi-Variate Analysis of Steam Trap Test Conditions . . . . .	102
5.8	Operational Parameter Analysis Colour Legend . . . . .	103
5.9	Fixed Orifice Pressure vs. RMS and Kurtosis Load Review . . . . .	105
5.10	Fixed Orifice Condensate Load vs. RMS and Kurtosis Review . . . . .	106
5.11	Float Trap Pressure vs. RMS and Kurtosis Review . . . . .	106
5.12	Float Trap Kurtosis Condensate Load vs. RMS and Kurtosis Review . . . . .	107
5.13	Thermodynamic Trap Pressure vs. RMS and Kurtosis Review . . . . .	108
5.14	Thermodynamic Trap Condensate Load vs. RMS and Kurtosis Review . . . . .	108
6.1	Orifice Trap 5 barg Low Steam Wastage Time Plot . . . . .	113
6.2	Orifice Trap 5 barg Low Steam Wastage Time Plot Zoomed . . . . .	113
6.3	Orifice Trap 5 barg Medium Steam Wastage Time Plot . . . . .	114
6.4	Orifice Trap 5 barg Medium Steam Wastage Time Plot Zoomed . . . . .	114
6.5	Orifice Trap 5 barg High Steam Wastage Time Plot domain . . . . .	115
6.6	Orifice Trap 5 barg High Steam Wastage Time Plot Zoomed . . . . .	115
6.7	Orifice Colour Legend . . . . .	118
6.8	Orifice Trap Time Domain RMS and Kurtosis . . . . .	119
6.9	Orifice Trap Time Domain Standard Deviation and Maximum . . . . .	120
6.10	Orifice Trap Time Domain Variance and Mean . . . . .	120
6.11	Orifice Trap Time Domain Sum and Median . . . . .	121
6.12	Orifice Trap FFT 5 barg CL=9.5 kg/hr SWV=4.62 kg/hr . . . . .	123
6.13	Orifice Trap FFT 5 barg CL=43.7 kg/hr SWV=1.65 kg/hr . . . . .	124

6.14 Orifice Trap FFT 5 barg CL=87.5 kg/hr SWV=0.57 kg/hr . . . . .	124
6.15 Orifice Trap FFT 10 barg CL=14.1 kg/hr SWV=7.79 kg/hr . . . . .	125
6.16 Orifice Trap FFT 10 barg CL=53.1 kg/hr SWV=2.51 kg/hr . . . . .	125
6.17 Orifice Trap FFT 10 barg CL=107 kg/hr SWV=0.27 kg/hr . . . . .	126
6.18 Orifice Trap FFT 15 barg CL=13.8 kg/hr SWV=11.63 kg/hr . . . . .	126
6.19 Orifice Trap FFT 15 barg CL=61.4 kg/hr SWV=3.6 kg/hr . . . . .	127
6.20 Orifice Trap FFT 15 barg CL=87.5 kg/hr SWV=-0.26 kg/hr . . . . .	127
6.21 Orifice Trap Frequency Domain RMS and Kurtosis . . . . .	128
6.22 Orifice Trap Frequency Domain Standard Deviation and Maximum . . . . .	129
6.23 Orifice Trap Frequency Domain Variance and Mean . . . . .	129
6.24 Orifice Trap Frequency Domain Sum and Median . . . . .	130
6.25 Orifice Trap Frequency Domain Frequency Bins Part 1 . . . . .	131
6.26 Orifice Trap Frequency Domain Frequency Bins Part 2 . . . . .	131
6.27 Orifice Trap STFT 5 barg CL=9.5 kg/hr SWV=4.62 kg/hr . . . . .	133
6.28 Orifice Trap STFT 5 barg CL=43.7 kg/hr SWV=1.65 kg/hr . . . . .	133
6.29 Orifice Trap STFT 5 barg CL=87.5 kg/hr SWV=0.57 kg/hr . . . . .	134
6.30 Orifice Trap STFT 10 barg CL=14.1 kg/hr SWV=7.79 kg/hr . . . . .	134
6.31 Orifice Trap STFT 10 barg CL=53.1 kg/hr SWV=2.51 kg/hr . . . . .	135
6.32 Orifice Trap STFT 10 barg CL=107 kg/hr SWV=0.27 kg/hr . . . . .	135
6.33 Orifice Trap STFT 15 barg CL=13.8 kg/hr SWV=11.63 kg/hr . . . . .	136
6.34 Orifice Trap STFT 15 barg CL=61.4 kg/hr SWV=3.6 kg/hr . . . . .	136
6.35 Orifice Trap STFT 15 barg CL=87.5 kg/hr SWV=-0.26 kg/hr . . . . .	137
6.36 Orifice Trap STFT RMS and Kurtosis . . . . .	138
6.37 Orifice Trap STFT Standard Deviation and Maximum . . . . .	139
6.38 Orifice Trap STFT Variance and Mean . . . . .	139
6.39 Orifice Trap STFT Sum and Median . . . . .	140
6.40 Orifice Trap STFT Frequency Bins Part 1 . . . . .	140
6.41 Orifice Trap STFT Frequency Bins Part 2 . . . . .	141
7.1 Float Trap 5 barg Low Steam Wastage Time Plot . . . . .	145
7.2 Float Trap 5 barg Low Steam Wastage Time Plot Zoomed . . . . .	145
7.3 Float Trap 5 barg Medium Steam Wastage Time Plot . . . . .	146
7.4 Float Trap 10 barg Low Steam Wastage Time Plot Zoomed . . . . .	146
7.5 Float Trap 5 barg High Steam Wastage Time Plot . . . . .	147
7.6 Float Trap 5 barg High Steam Wastage Time Plot Zoomed . . . . .	147
7.7 Float Trap Colour Legend . . . . .	148
7.8 Float Trap Time Domain RMS and Kurtosis . . . . .	149
7.9 Float Trap Time Domain Kurtosis Only . . . . .	150
7.10 Float Trap Time Domain Standard Deviation and Maximum . . . . .	151
7.11 Float Trap Time Domain Variance and Mean . . . . .	151
7.12 Float Trap Time Domain Sum and Median . . . . .	152
7.13 Float Trap Time Domain Median Only . . . . .	152
7.14 Float Trap FFT 5 barg CL=10 kg/hr SWV=1.88 kg/hr . . . . .	155
7.15 Float Trap FFT 5 barg CL=10 kg/hr SWV=2.71 kg/hr . . . . .	156
7.16 Float Trap FFT 5 barg CL=30 kg/hr SWV=4.08 kg/hr . . . . .	156
7.17 Float Trap FFT 10 barg CL=10 kg/hr SWV=0.68 kg/hr . . . . .	157
7.18 Float Trap FFT 10 barg CL=10 kg/hr SWV=1.68 kg/hr . . . . .	157

7.19	Float Trap FFT 10 barg CL=10 kg/hr SWV=4.1 kg/hr . . . . .	158
7.20	Float Trap FFT 10 barg CL=10 kg/hr SWV=7.48 kg/hr . . . . .	158
7.21	Float Trap FFT 10 barg CL=60 kg/hr SWV=-0.39 kg/hr . . . . .	159
7.22	Float Trap FFT 15 barg CL=10 kg/hr SWV=9.29 kg/hr . . . . .	159
7.23	Float Trap Frequency Domain RMS and Kurtosis . . . . .	160
7.24	Float Trap Frequency Domain Standard Deviation and Maximum . . . . .	160
7.25	Float Trap Frequency Domain Variance and Mean . . . . .	161
7.26	Float Trap Frequency Domain Sum and Median . . . . .	162
7.27	Float Trap Frequency Domain Frequency Bins Part 1 . . . . .	162
7.28	Float Trap Frequency Domain Frequency Bins Part 2 . . . . .	163
7.29	Float Trap STFT 5 barg CL=10 kg/hr SWV=0.65 kg/hr . . . . .	165
7.30	Float Trap STFT 5 barg CL=10 kg/hr SWV=2.71 kg/hr . . . . .	166
7.31	Float Trap STFT 5 barg CL=30 kg/hr SWV=4.08 kg/hr . . . . .	166
7.32	Float Trap STFT 10 barg CL=10 kg/hr SWV=0.68 kg/hr . . . . .	167
7.33	Float Trap STFT 10 barg CL=10 kg/hr SWV=1.68 kg/hr . . . . .	167
7.34	Float Trap STFT 10 barg CL=10 kg/hr SWV=4.1 kg/hr . . . . .	168
7.35	Float Trap STFT 10 barg CL=10 kg/hr SWV=7.48 kg/hr . . . . .	168
7.36	Float Trap STFT 10 barg CL=60 kg/hr SWV=-0.39 kg/hr . . . . .	169
7.37	Float Trap STFT 15 barg CL=10 kg/hr SWV=9.29 kg/hr . . . . .	169
7.38	Float Trap STFT RMS and Kurtosis . . . . .	170
7.39	Float Trap STFT Standard Deviation and Maximum . . . . .	170
7.40	Float Trap STFT Variance and Mean . . . . .	171
7.41	Float Trap STFT Sum and Median . . . . .	171
7.42	Float Trap STFT Frequency Bins Part 1 . . . . .	172
7.43	Float Trap STFT Frequency Bins Part 2 . . . . .	172
8.1	Thermodynamic Trap 15 barg High Steam Wastage Time Plot . . . . .	177
8.2	Thermodynamic Trap 15 barg High Steam Wastage Time Plot Zoomed . . . . .	177
8.3	Thermodynamic Trap 15bar Medium Steam Wastage Time Plot . . . . .	178
8.4	Thermodynamic Trap 15bar Medium Steam Wastage Time Plot Zoomed . . . . .	179
8.5	Thermodynamic Trap 15 barg Low Steam Wastage Time Plot . . . . .	179
8.6	Thermodynamic Trap 15 barg Low Steam Wastage Time Plot Zoomed . . . . .	180
8.7	Thermodynamic Trap Colour Legend . . . . .	181
8.8	Thermodynamic Trap Time Domain RMS and Kurtosis . . . . .	181
8.9	Thermodynamic Trap Time Domain Standard Deviation and Maximum . . . . .	182
8.10	Thermodynamic Trap Time Domain Variance and Mean . . . . .	183
8.11	Thermodynamic Trap Time Domain Sum and Median . . . . .	183
8.12	Thermodynamic Trap FFT 5 barg CL=10 kg/hr SWV=0.19 kg/hr . . . . .	187
8.13	Thermodynamic Trap FFT 15 barg CL=10 kg/hr SWV=1.62 kg/hr . . . . .	188
8.14	Thermodynamic Trap FFT 15 barg CL=35 kg/hr SWV=1.12 kg/hr . . . . .	188
8.15	Thermodynamic Trap FFT 15 barg CL=45 kg/hr SWV=0.38 kg/hr . . . . .	189
8.16	Thermodynamic Trap FFT 15 barg CL=60 kg/hr SWV=-0.37 kg/hr . . . . .	189
8.17	Thermodynamic Trap FFT 20 barg CL=10 kg/hr SWV=10.96 kg/hr . . . . .	190
8.18	Thermodynamic Trap FFT 20 barg CL=10 kg/hr SWV=9.65 kg/hr . . . . .	190
8.19	Thermodynamic Trap FFT 20 barg CL=50 kg/hr SWV=7.38 kg/hr . . . . .	191
8.20	Thermodynamic Trap FFT 20 barg CL=55 kg/hr SWV=1.39 kg/hr . . . . .	191
8.21	Thermodynamic Trap Frequency Domain RMS and Kurtosis . . . . .	192

8.22	Thermodynamic Trap Frequency Domain Standard Deviation and Maximum . . .	192
8.23	Thermodynamic Trap Frequency Domain Variance and Mean . . . . .	193
8.24	Thermodynamic Trap Frequency Domain Sum and Median . . . . .	194
8.25	Thermodynamic Trap Frequency Domain Frequency Bins Part 1 . . . . .	194
8.26	Thermodynamic Trap Frequency Domain Frequency Bins Part 2 . . . . .	195
8.27	Thermodynamic Trap STFT 5 barg CL=10 kg/hr SWV=0.19 kg/hr . . . . .	199
8.28	Thermodynamic Trap STFT 15 barg CL=10 kg/hr SWV=1.62 kg/hr . . . . .	199
8.29	Thermodynamic Trap STFT 15 barg CL=35 kg/hr SWV=1.12 kg/hr . . . . .	200
8.30	Thermodynamic Trap STFT 15 barg CL=45 kg/hr SWV=7.38 kg/hr . . . . .	200
8.31	Thermodynamic Trap STFT 15 barg CL=60 kg/hr SWV=-0.37 kg/hr . . . . .	201
8.32	Thermodynamic Trap STFT 20 barg CL=10 kg/hr SWV=10.96 kg/hr . . . . .	201
8.33	Thermodynamic Trap STFT 20 barg CL=10 kg/hr SWV=9.65 kg/hr . . . . .	202
8.34	Thermodynamic Trap STFT 20 barg CL=50 kg/hr SWV=7.28 kg/hr . . . . .	202
8.35	Thermodynamic Trap STFT 20 barg CL=55 kg/hr SWV=1.39 kg/hr . . . . .	203
8.36	Thermodynamic Trap STFT RMS and Kurtosis . . . . .	203
8.37	Thermodynamic Trap STFT Standard Deviation and Maximum . . . . .	204
8.38	Thermodynamic Trap STFT Variance and Mean . . . . .	204
8.39	Thermodynamic Trap STFT Sum and Median . . . . .	205
8.40	Thermodynamic Trap STFT Frequency Bins Part1 . . . . .	206
8.41	Thermodynamic Trap STFT Frequency Bins Part 2 . . . . .	206
B.1	UP100 Heterodyne Probe Specification . . . . .	227
C.1	SGR Rig Vessel and Flow Line . . . . .	228
C.2	SGR Rig Test Area Setup . . . . .	229
C.3	SGR Rig Condensate Heat Exchanger and Injection Setup . . . . .	229
C.4	SGR Rig Vessel Control Panel . . . . .	230
C.5	SGR Rig National Instruments Hardware . . . . .	230
C.6	SGR Rig National Instruments Hardware . . . . .	231
C.7	SGR Rig Data Acquisition . . . . .	231
C.8	Runnings Road Steam Trap Rig . . . . .	232
C.9	Runnings Road Rig Steam Trap Test Station . . . . .	232
C.10	Runnings Road Rig Panel . . . . .	233
C.11	Runnings Road Rig Data Acquisition . . . . .	233
C.12	SGR Rig Schematic 1 - Steam Inlet to Vessel . . . . .	234
C.13	SGR Rig Schematic 2 - Steam Inlet to Vessel . . . . .	235
C.14	RR Rig Schematic . . . . .	236
C.15	LabView Start-up User Interface . . . . .	237
C.16	LabView Data Test Setup User Interface . . . . .	237
C.17	LabView Data Acquisition User Interface . . . . .	238
C.18	LabView Sensor Calibration Coefficient User Interface . . . . .	238
C.19	LabView Data Presentation User Interface Screen 1 . . . . .	239
C.20	LabView Data Presentation User Interface Screen 2 . . . . .	239
C.21	LabView Front GUI Flow Chart . . . . .	240
C.22	LabView Data Acquisition Flow Chart Part 1 . . . . .	241
C.23	LabView Data Acquisition Flow Chart Part 2 . . . . .	242
C.24	LabView Data Acquisition Flow Chart Part 3 . . . . .	243

# Nomenclature

$\delta p$	change in pressure $Pa$
$\Delta t$	time interval, $s$
$\delta z$	change in height, $m$
$\dot{m}_G$	mass flow of gas, $kg/s$
$\dot{m}_L$	mass flow of liquid, $kg/s$
$\mu$	mean value
$\mu_G$	dynamic viscosity of gas fraction, $kg/(s \cdot m)$
$\mu_L$	dynamic viscosity of liquid fraction, $kg/(s \cdot m)$
$\rho$	density of the medium, $kg/m^3$
$\rho_G$	density of the gas fraction, $kg/m^3$
$\rho_L$	density of the liquid fraction, $kg/m^3$
$\sigma$	Cavitation number
$\sigma_i$	Incipient cavitation number
$\sigma_{SD}$	standard deviation
$\theta_1$	initial water temperature in the calorimeter tank, $^{\circ}C$
$\theta_2$	final water temperature in the calorimeter tank, $^{\circ}C$
$c$	longitudinal wave speed or sound speed, $m/s$
$c_p$	specific heat constant of the calorimeter material, $kJ/(kg \cdot ^{\circ}K)$
$d_i$	internal pipe diameter, $m$
$dB$	Decibel, $dB$
$E(t)$	the expected value of the quantity $t$
$Fr_G$	Froude number, dimensionless
$g$	acceleration due to gravity, $9.81 m/s^2$
$h_{f1}$	initial specific enthalpy of water in the calorimeter, $kJ/kg$
$h_{f2}$	final specific enthalpy of the condensate and water in the calorimeter, $kJ/kg$

$h_{fgs}$	specific enthalpy of the evaporation at steam inlet conditions, $kJ/kg$
$h_{fi}$	specific enthalpy of the liquid at the trap inlet temperature, $kJ/kg$
$h_{fo}$	specific enthalpy of the liquid at the trap outlet temperature, $kJ/kg$
$h_{fs}$	specific enthalpy of the liquid at steam inlet conditions, $kJ/kg$
$h_{gi}$	specific enthalpy of the saturated steam at the trap inlet temperature, $kJ/kg$
$h_{go}$	specific enthalpy of the saturated steam at the trap outlet temperature, $kJ/kg$
$I_E$	impulse / energy produced by each cavitation event
$K$	Parameter $K$ , dimensionless
$m_1$	mass of calorimeter plus water, at the start, $kg$
$m_2$	mass of calorimeter plus water, at the finish, $kg$
$m_f$	final mass of water and condensate in the calorimeter, $kg$
$m_i$	initial mass of water in the calorimeter, $kg$
$m_t$	mass of calorimeter tank, $kg$
$m_c$	mass of condensate collected in the separating tank, $kg$
$m_{st}$	mass of steam collected in the condensing tank, $kg$
$mA$	milli Ampere, $mA$
$N_E$	number of cavitation events per unit time
$p_S$	sound pressure level
$q_{ms}$	steam loss / flow rate, $kg/hr$
$Re_G$	Reynolds number for the gas fraction, dimensionless
$Re_L$	Reynolds number for the liquid fraction, dimensionless
$T$	Parameter $T$ , dimensionless
$t_s$	sample interval
$V$	Volts, $V$
$X$	Martenelli number, dimensionless
$x$	a number of values
$Z_0$	characteristic acoustic impedance, $Ns/m^3$
.wav	Waveform Audio File Format
AE	Acoustic Emission
barg	pressure measurement in bar gauge, 1 bar = 100 kilo pascals
BP	Balance Pressure Steam Trap

CBM	Condition Based Maintenance
CF	Crest Factor
CL	Condensate Load, $kg/hr$
DDE	Dynamic Data Exchange
DFT	Discrete Fourier Transform
DSP	Digital Signal Processing
EN 27841	Steam Wastage Measurement Standard
ERT	Electrical Resistance Tomography
FFT	Fast Fourier Transform
FO	Fixed Orifice Steam Trap
FT	Float Steam Trap
GUI	Graphical User Interface
IB	Inverted Bucket Steam Trap
NDT	Non-Destructive Testing
PCMCIA	Personal Computer Memory Card International Association - Data Acquisition Card Interface
PSD	Power Spectral Density
PZT	Lead Zirconate Titanate
RMS	Root Mean Square
RRR	Runnings Road Steam Wastage Rig
SGR	St Georges Road Steam Wastage Rig
SM	Bi-Metal Steam Trap (Special Metal)
STFT	Short-Time Fourier Transform
SubVI	Subordinate Visual Instrument
SWV	Steam Wastage Value, $kg/hr$
TD	Thermodynamic Steam Trap
VB	Visual Basic
VI	Visual Instrument

Figure 1.1: Products Made with Steam



heated to above its saturation temperature. Steam is a transparent gas when it is under pressure. The grey colour usually associated with steam occurs when the ambient pressure drops below the vapour pressure thus allowing steam to condense and form small liquid droplets which change the translucency of the gas. This is often observed at power plant cooling towers or in the home when a kettle or pan of water is boiling. At standard temperature and pressure, an equal mass of steam occupies approximately 1,600 times the volume of water.

Steam is an excellent energy transport and transfer medium due to its high latent heat capacity. For this reason, it is used widely in the process industry. Other advantages of steam are that it is odourless, non-hazardous and can be easily controlled and managed. For all of these reasons, steam is a widely used process fluid in many industries as cited by Spirax Sarco, the Valve User Magazine and Oliver Lyle [91, 48, 53].

The “Steam and Condensate Loop” is the route the water takes through the process. This process starts in the boiler room with pretreated water, where the water is heated in a boiler, creating steam. Steam is then distributed through a network of pipes to the relevant process locations (as shown in Figure 2.3 on page 8). As steam transfers its energy, it condenses back to water. This condensate is then removed by Steam Traps, collected and piped back to the hotwell completing the cycle. The hotwell receives the returned condensate and supplies this to the boiler as make-up water.

Steam has a higher specific enthalpy than water at a given pressure and temperature, which means that steam can carry more energy per unit mass than water. In steam systems, the steam is transported through use of pressure differences and thus does not need any pumps. Similarly, the condensate returns to the hotwell that feeds the boiler with little need for pumping. This is another reason why steam can be economically advantageous as most of the time, it does not require pumps for motion. Other industrial applications include district heating, such as the installation of ConEdison in New York and CPCU in Paris. In those applications, a number of co-generation power plants supply steam which is piped through the city to supply buildings with heat. The capacity for steam to effectively transfer energy is also used in non-industrial applications such as cooking, cleaning, mixing and heating.

## **1.2 Current Steam Trap Condition Monitoring Approach**

Steam Traps can be tested in two ways: continuous and instantaneous. In continuous monitoring, a sensor which relays the status of the trap to a centralised reporting station is permanently attached to the steam trap. In instantaneous monitoring, a survey is carried out manually using a portable Steam Trap diagnostic device. A survey engineer will visit the plant and diagnose

each trap manually using the device on an annual/bi-annual basis. This approach provides an instantaneous snapshot of the condition of the plant but does not provide continuous feedback on the condition of Steam Traps, allowing faults potentially to be undetected for some period of time. Steam Traps leaking for a long period of time can result in high energy loss, affecting the profitability of a steam plant.

Steam Traps can be diagnosed using several measurement technologies, which are often used in conjunction with each other. These techniques are detailed in Table 1.1. As most surveys are instantaneous in nature, the most widely used methodology is ultrasonic-based acoustic emission. Usually, this is applied by either an ultrasonic stethoscope or an automatic tester.

Technology	Measurement	Advantages	Disadvantages
Optical	Infra-red, Visual, Laser	Externally applied measurement	Little differentiation between phases
Acoustic	Ultrasonic Sound	Externally applied measurement	Ambient signals can influence measurement
Thermal	Temperature	Externally applied measurement	No differentiation between steam and condensate
Conductivity	Conductivity	Accurate measure of good /bad threshold	Internally applied measurement
Heat Transfer	Heat Flux	Differentiation between steam and condensate	Internally applied measurement

Table 1.1: Steam Trap Condition Monitoring Techniques

### 1.3 Problem Definition and Objectives of this Investigation

The need for a reliable and more consistent automatic diagnosis of Steam Traps is evident. A review of the currently available systems for diagnosing Steam Wastage shows that these can be improved. Currently, the main method to interpret data in instantaneous diagnosis uses the human brain. This process could be optimised by the use of electronics, making diagnosis more consistent and repeatable. However, to develop such a process, a good understanding of the Steam Trap's acoustic emission profiles is required. This work focuses on the digital signal processing aspects related to the acoustic emission only. The objectives of this research are summarised as follows:

- Develop a suitable test rig and experimental setup.
- Obtain an in-depth understanding of failure conditions in Steam Traps.
- Build an understanding of the relationship between Steam Trap acoustics and operational conditions.

- Apply digital signal processing techniques and statistical measurements to diagnosis of Steam Trap data.

## 1.4 Significance of the Investigation to Knowledge

The work carried out as part of this research is novel. There are several areas of new knowledge and applications that have not been presented previously. The following is a summary of this work's contribution to scientific knowledge:

- 1) The acoustic emission properties of Steam Traps have been systematically evaluated.
- 2) Characteristics of heterodyne signal have been analysed.
- 3) The relationship between the acoustic emission and Steam Wastage, Pressure and Condensate Load have been assessed for a number of conditions.
- 4) Inherent random operational behaviour has been discovered for three types of Steam Trap.
- 5) The complexity of multiple parameter analysis in relation to operational traps has been discussed.

## 1.5 Motivation and Extension of the Knowledge through the Investigation

Throughout this investigation, the author obtained new knowledge in several areas using key literature:

- The background to Digital Signal Processing was learned using many books, but specifically from these sources: [83] [44].
- The Steam Wastage Rig was designed in partial accordance with British Standard EN 27841:1991 [71].
- Instrumentation for the Steam Wastage Rig was developed using using National Instruments Hardware and LabView software. The following materials were used by the author to learn the graphical programming software: [61, 62].
- The data was processed using Matlab and information from the following references: [55], [56], [57], [45] and [23].
- Standards relating to Steam Traps were studied [70] and [69].

- This thesis was prepared using L<sup>A</sup>T<sub>E</sub>X based typesetting software and written using the reference material contained in [58].

Patent applications which the Author has been involved with:

- Patents relating to the design of Steam Traps: [18], [21] and [17].
- Patent relating to Steam Trap Condition Monitoring [19].
- Patent relating to condensate return analysis with respect to Steam Wastage Measurement [22].

Additionally a number of confidential reports were issued as part of the Author's work at Spirax Sarco, the details of which cannot be disclosed.

## 1.6 Structure of Thesis

The following provides an overview of the structure of the Thesis.

<b>Chapter 1</b>	Introduction to the investigation, the structure of the Thesis and other key background information.
<b>Chapter 2</b>	Introduction to Steam Traps and methods for Steam Trap analysis. Key scientific topics: background to the investigation, including topics such as two-phase flow, acoustics and digital signal processing.
<b>Chapter 3</b>	The experimental setup in terms of Steam Trap testing and acoustic data capture.
<b>Chapter 4</b>	Investigating the properties of the heterodyne circuit and the effects this has on the acoustic data collected.
<b>Chapter 5</b>	An overview of the key parameters, a first pass analysis and an overview of the data used.
<b>Chapters 6,7 and 8</b>	Applying digital signal processing techniques to analyse the acoustic data of three Steam Trap profiles.
<b>Chapter 9</b>	Highlighting the common features in the analyses of the three different acoustic categories.
<b>Chapter 10</b>	Discussing the results and concluding the outcome of the research, defining the contribution to knowledge and suggesting further work.

*This chapter provided a brief overview of this investigation, highlighting the contribution to knowledge as well as outlining the subsequent chapters. The next chapter provides an introduction to Steam Traps, Steam Trap Condition Monitoring and Steam Wastage Measurement methods. A PESTLE analysis is also presented providing context to the importance of this work.*

## Chapter 2

# Introduction to Steam Traps, Applications and Quality Assessment Techniques

*This chapter reviews the background information involved in this research work, providing relevant details of Steam Traps, Steam Wastage Measurement and Steam Trap condition monitoring. Thereafter, this chapter presents relevant technical background information on acoustics and two-phase flow. The connection between acoustic emission and steam flow is made. Following on, an overview of digital signal processing is presented. The chapter concludes with a summary of the key points from these background topics. This chapter provides a brief introduction to the above mentioned subjects, readers versed in such content may wish to proceed to Chapter 3.*

### 2.1 Steam Trap Types and Their Function

The literal meaning of a Steam Trap is, of course something that traps steam. A Steam Trap is primarily used in applications in which it is necessary to discharge condensate from a steam-filled space without the loss of steam. The ASME PTC 39-2005 standard [5] defines a Steam Trap as:

“A device which permits the removal of condensate and air and other non-condensable gases, for steam systems at or below saturated steam temperature, and prevents or limits the discharge of live steam.”

Figure 2.3 on page 8 shows a pictorial section of a steam system with Steam Traps circled in red for clarity, taken from Spirax Sarco’s Product Overview literature [89], where examples of heat

exchange and steam distribution are displayed.

Information on Steam Traps has largely been obtained from the “Steam and Condensate Loop Book” by Spirax Sarco [91] and “The efficient use of steam” by Oliver Lyle [53]. Information was also obtained from the technical training course provided by Spirax Sarco [85]; Information relating to the Steam Wastage Measurement was taken from BS EN 27841:1991, the standard for Steam Wastage Measurement [69].

There are various types of Steam Traps (see Figure 2.1). The six most common types can be divided into 3 major categories (see Figure 2.2) based on their operational mode:

- 1) Velocity Traps - change in fluid dynamic
- 2) Thermostatic Traps - change of fluid temperature
- 3) Mechanical Traps - change in fluid density



Figure 2.1: Examples of Steam Traps

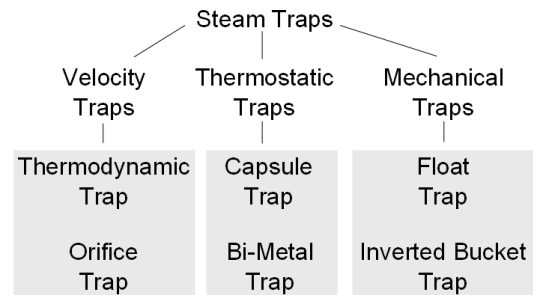


Figure 2.2: Steam Trap Type Overview

For the purposes of this study, Spirax Sarco Steam Traps will be the focus as this work is supported by Spirax Sarco Limited. An extensive list of manufacturers is supplied in the Appendix, Section A.1.

The following Sections will expand on the three major categories of Steam Traps, explaining their operational features, starting with Velocity Traps on page 9.

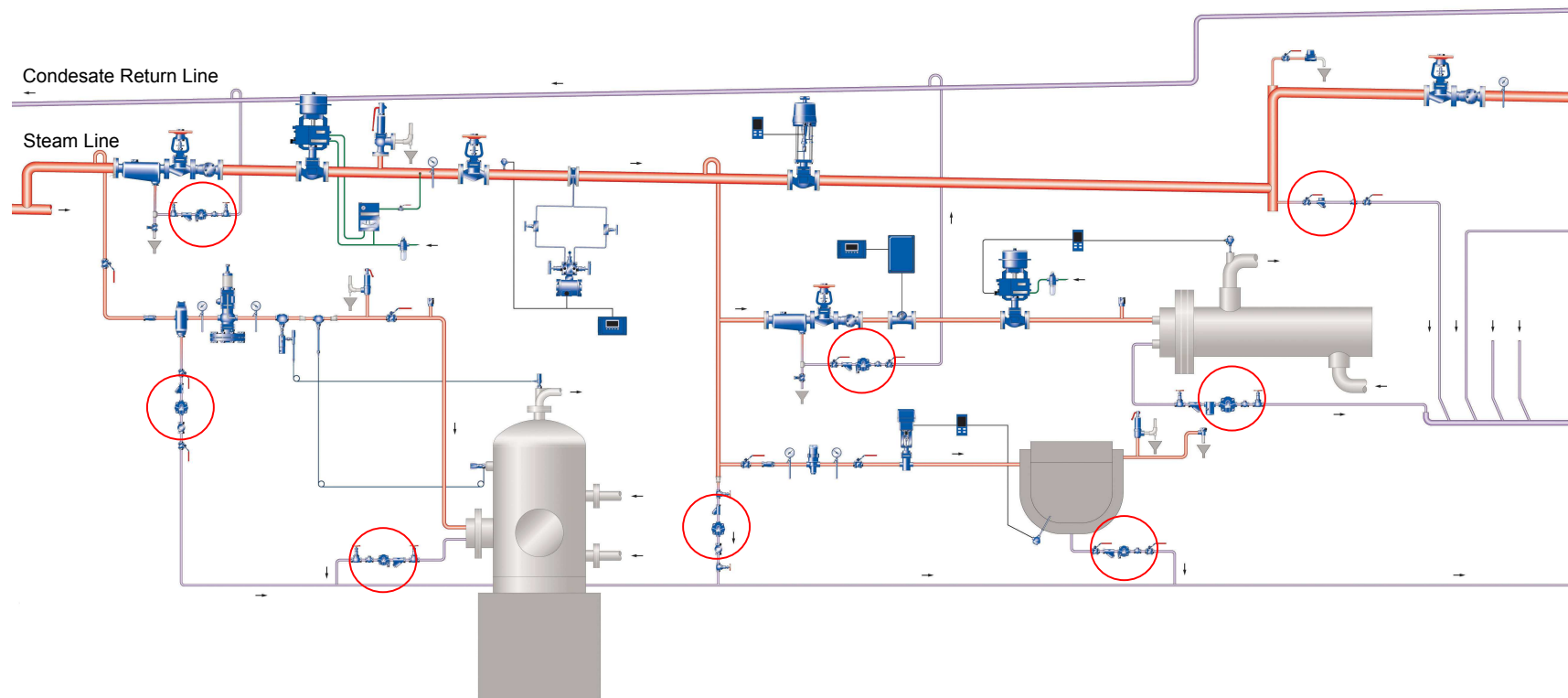


Figure 2.3: Steam System Overview (from [89])

### 2.1.1 Velocity Traps

#### Thermodynamic Trap

The Thermodynamic Trap is a very simple device using only a disc which opens and closes (similar to a check valve) as seen in Figure 2.4.

Although several theories on the working principle of this trap exist, the most widely accepted states that this trap uses the density and differences in specific volumes between steam and condensate to open and close the trap. When condensate passes through the trap, the disc is in the open position and condensate passes through the 'head' space past the disc and to an outlet. On the other hand, when steam flows past the disc, a lower pressure below the disc is created, causing the disc to close. Steam in the head must condense before the disc can open again.

The Thermodynamic Trap is generally used where there is a small and fairly constant level of condensate generated; applications include the mains drainage of steam distribution lines and small constant applications. As the Thermodynamic Trap backs up condensate quite readily, it is not well suited for steam processes with changing condensate loads. This is also a reason why this trap is only available for smaller pipe sizes, generally, up to 1 inch diameter.

#### Orifice Traps

The Orifice Trap is the simplest of all traps as is just a small hole with no mechanism. This trap utilises a simple orifice and the choking effect of orifices together with the density/volume fraction differences between steam and condensate. Differential pressure between the system and

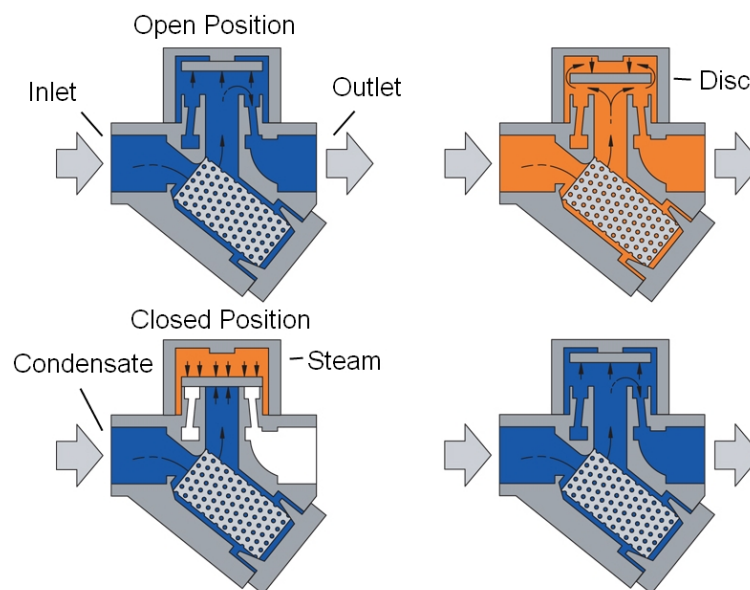


Figure 2.4: Thermodynamic Steam Trap (from [91])



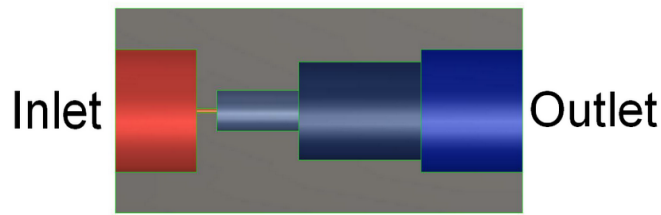


Figure 2.5: Fixed Orifice Trap

the outlet of the trap from high pressure to low /near atmospheric pressure causes condensate to flash off. For large amounts of condensate, the pass area of the orifice cannot adapt to the higher load, causing condensate to back up. In the event that there is little or no condensate up-stream of the trap, the flashing effect does not take place and the trap will leak steam. As steam has a far higher specific volume (and thus a longer residence-time), this slows the flow of steam and causes choking in the orifice. The Figure 2.5 shows the cross-section of such a trap.

This behaviour highlights that Orifice Traps have to be carefully sized for the application, as they have no mechanism to adjust to changing conditions. For this reason, this trap type is suitable for fixed conditions where there is little or no modulation and is suitable for continuous use. Applications include long runs of steam distribution pipe, which is required to be at pressure 24 hours a day continuously.

### 2.1.2 Thermostatic Traps

The Thermostatic Trap group includes the Bi-metal and Capsule Traps. These traps are generally slow to react and will back up more condensate compared to the other trap types. These are mainly used for mains distribution drainage and for non-critical applications. These traps do have a very good start up performance as when they get cold, the pass area is equal to the fully open orifice. Only once the trap reaches working temperature does the mechanism start to operate. For this reason, these traps are used specifically as air vents for steam systems and on clean steam systems, where air and condensate removal are of high importance within the process. The Capsule Trap is the most widely used trap of this category.

#### Capsule Traps

The Capsule Trap is also known as the Balance Pressure Trap seen in Figure 2.6. This type of trap utilises differences in fluid temperature for operation. The capsule element (as seen in Figure 2.7) is filled with a mixture of water and alcohol which expands and contracts with temperature change. The vapour temperature of the mixture within the bellows can be set by altering the ratio of water and alcohol. When steam surrounds the capsule, it causes the bellows to expand, forcing

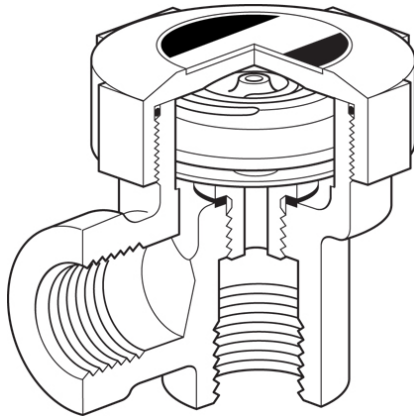


Figure 2.6: Balance Pressure Trap (from [91])

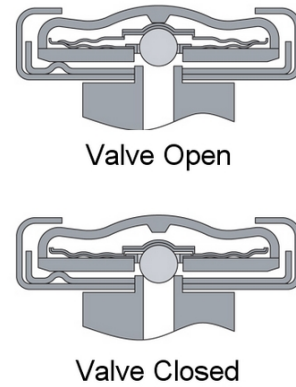


Figure 2.7: Balance Pressure Trap Cross-section (from [91])

a ball bearing into the seat of the trap and sealing the valve. Conversely, when condensate below saturation temperature surrounds the bellows, the bellows contracts, allowing the condensate to pass through the trap. For this reason, this trap inherently backs up condensate to make the mechanism work. As thermostatic exchange is slow, this trap also has a longer time constant between actuations. It is also commonly used to vent air in steam systems.

### Bi-metal Traps

Bi-metal Traps utilise bi-metallic strips (two metal strips with different thermal coefficients of expansion fused together), as a mechanism to open and close the valve. Figure 2.8 shows a cross-section of the Bi-metal Trap with the bi-metal disc stack at its centre and Figure 2.9, the temperature effect on the metal is shown. As with the Capsule Trap, heat (steam) alters the shape of the strip so that it will close the valve; condensate will cool the metal strip, returning it to its original shape, opening the valve. These Steam Traps are used in systems in which a small amount of condensate is of advantage and, once again, react very slowly. They are very good for high pressure applications and, for that reason, are frequently used in power station systems.

## 2.1.3 Mechanical Traps

### Float Traps

The Float Trap uses the effect of density and buoyancy of condensate in conjunction with a float to open and close the valve and is shown in Figure 2.10. As the condensate level rises in the containment chamber, the float rises and lifts a lever-connected ball from the valve seat, allowing the condensate to drain through the valve orifice. As the condensate level in the chamber decreases, the lever-connected ball reseats over the valve, sealing the trap. This type of trap reacts imme-

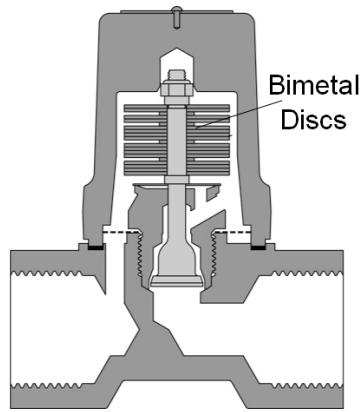


Figure 2.8: Bimetal Trap (from [91])

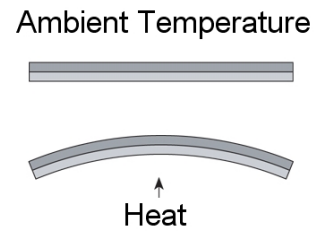


Figure 2.9: Bimetal Strip (from [91])

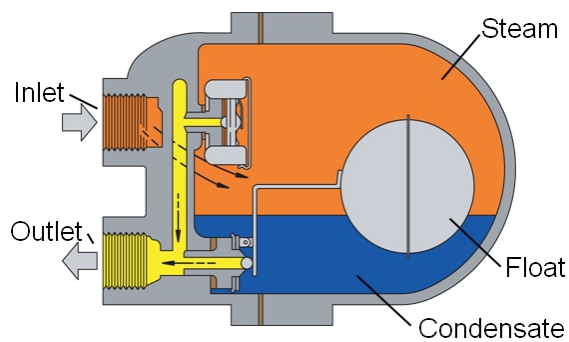


Figure 2.10: Float Trap Cross-section (from [91])

diately to the condensate load presented, but is not very effective at high pressure as the float buoyancy needs to balance the valve seating forces. For this reason, some Float Trap models have operational pressure range limits matching the orifice size of valve seat with the float buoyancy; otherwise, the trap may not open and the float could collapse

Float Traps are also very susceptible to “water hammer” damage, which is the impacting of slugs of condensate travelling at high speeds creating a very high instantaneous pressure peak capable of bursting the float. This, of course, would render the trap motionless, resulting in a build-up of condensate. In the specific model depicted in Figure 2.10, the Float Trap is combined with a balance pressure capsule to provide air venting capability.

### Inverted Bucket Traps

The Inverted Bucket Trap is similar to the Float Trap, but can be used in higher pressure applications and is less susceptible to water hammer. Figure 2.11 shows the Inverted Bucket Trap at the different stages of its cycle. It has a floating bucket as a mechanism and requires a water seal to work (see Figure 2.11).

The working cycle comprises steam entering the inverted bucket providing buoyancy and

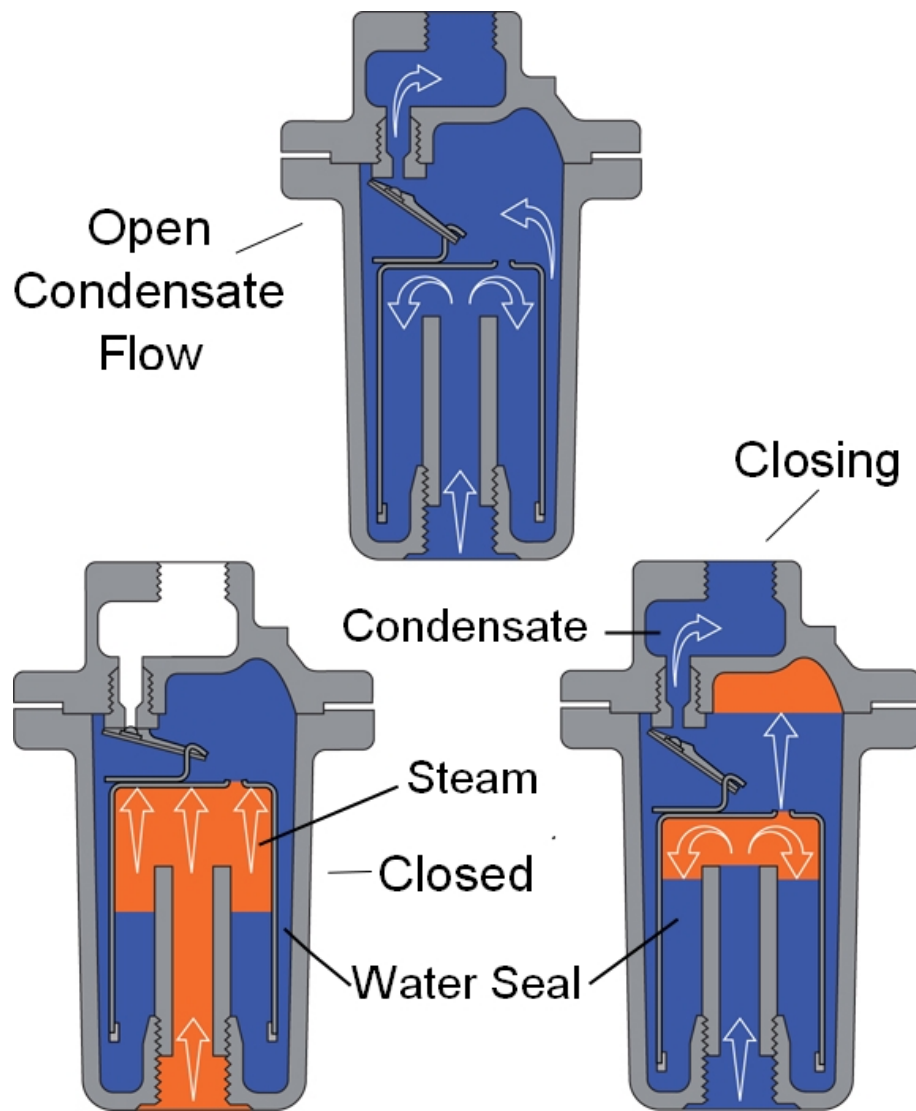


Figure 2.11: Inverted Bucket Trap (from [91])

causing the valve to close. Once the steam in the inverted bucket condenses, the bucket sinks, due to its own weight, thus causing the valve to open for condensate to drain away. This type of trap is not very good at start up, due to its retention of air. The water seal is crucial in the operation of this type of trap as displacement of the seal can result in high loss of steam from the system.

#### 2.1.4 Steam Trap Operation Conditions

Lyle cites Float Traps as continuous/intermittent, and Balance Pressure Traps as semi-continuous [53]. Survey Engineers consider Thermostatic Steam Traps as the same category as Balance Pressure Traps; Inverted Bucket Traps are continuous/intermittent as well as impulsive in nature; Thermodynamic Traps are intermittent and impulsive in nature; Orifice Traps are continuous as they have no mechanisms.

	Type of Discharge	Opening Force	Closing force	Temperature of Condensate	Condensate Drained
<b>Thermo-dynamic</b>	Impulse	Differential pressure	Differential pressure	Saturation	As Formed
<b>Orifice</b>	Continuous	N/A	N/A	Saturation	As Formed, based on size
<b>Capsule</b>	Semi-Continuous	Steam pressure	Differential Pressure	Below Saturation	After cooling
<b>Bi-metal</b>	Semi-Continuous	Steam pressure	Differential Pressure	Pre-set temperature	At pre-set temperature
<b>Float</b>	Continuous	Buoyancy	Weight of bucket	Saturation	Instantly
<b>Inverted Bucket</b>	Intermittent	Weight of bucket	Buoyancy	Saturation	As Formed

Table 2.1: Steam Trap Specification Information

### 2.1.5 General Steam Trap Failure Modes

There are three basic categories of Steam Trap Failure Modes:

Failure mode	Symptom	Manifestation
<b>Failed Open</b>	Rapid cycling, high steam usage	Loud discharge, visible steam leak
<b>Failed Closed</b>	Quiet and cold	Blocked, damaged mechanism
<b>External Failure</b>	Normal Operation, high steam usage	External leak, gasket failure

Table 2.2: Steam Trap Failure Modes

As Table 2.2 indicates, the “Failed Open” failure mode causes high steam usage, loss of steam and a consequent higher cost of operation. “Failed Closed” causes inefficiency, loss of function and is, potentially dangerous in that a build-up of condensate can develop into “water hammer” which can damage the system as explained in the Department of Energy publication [31]. “External Failure” can be caused by any number of reasons, but is usually the result of old or damaged pipes, corrosion/erosion, gasket failure, etc.. An example of this is the failure of the district heating steam line in New York as explained in the incident investigation [13]. The investigation into the cause of failure pointed at water hammer being the main cause, which was a result of the Steam Traps not removing the condensate.

### 2.1.6 Specific Steam Trap Failure Modes

Steam losses can be either 1) Direct, i.e., steam losses due to flow of steam or 2) Indirect, i.e., steam losses due to insulation and the design/operating principle of the Trap. Indirect steam losses are

much more difficult to define as they result from environmental, radiation, trap size and material from which the trap is made and condensate load conditions.

### **Velocity Traps**

As described in the previous section, the operation of the Thermodynamic Trap results from changes in the fluid dynamics of the steam and condensate phases. Both the Thermodynamic Trap and the Orifice Trap use the flashing principle to throttle the flow of condensate. As the Thermodynamic Trap relies on the radiation heat loss from the head to operate the disc, environmental conditions can affect operation and cycling. When the ambient temperature is high, the trap will cycle very rarely; when the ambient temperature is cold, the trap will cycle more, resulting in faster wear and tear of the trap. For this reason, some traps are fitted with insulated covers to reduce heat transfer. Generally, Thermodynamic Traps cycling faster than 10 times a minute are deemed to have failed. Due to the clear response of the trap when cycling, it is fairly easy to diagnose this type of Steam Trap, as it is either open or closed. Although chapter 11 in the Steam and Condensate Loop Book [91] states that Thermodynamic Traps cannot have a varying degree of failure, research in Spirax Sarco has shown that it is possible to determine, to a limited degree, the severity of failure of a Thermodynamic Trap by considering the opening and closing action in quantity and type of event.

Under low condensate load, the Steam Wastage from a Thermodynamic Trap can be as low as 0.5kg/hr, but this will depend on the ambient conditions.

### **Thermostatic Traps**

As described previously, the Thermostatic Trap uses temperature to distinguish between steam and condensate. This type of trap should not leak steam under normal conditions, as the trap backs up condensate until the active element has sufficiently cooled, causing a significant amount of condensate to be collected in the drop-leg pipe this trap requires. The design of the condensate collection for this trap dictates that the drop-leg pipe not be insulated or lagged which leads to indirect steam loss. The Thermostatic Trap also has a slow response time which will allow steam to leak when the trap closes.

“No Load” laboratory tests indicate that a typical steam loss of approximately 0.5kg/hr can be expected.

### **Mechanical Traps**

The Float Trap uses a float to remove condensate as soon as it forms. As the orifice for removal of condensate is below the water line, a water seal is created and steam loss minimised. Although

this is the case for steady flows, if the flow is dynamic and varying, steam bubbles can pass through the water, much like air travels through the eye of a vortex. Many Float Traps are fitted with a Thermostatic Capsule (the mechanism from a Balance Pressure Trap) to assist in venting air. Although this “hybrid” trap is better at venting air, it also means that there are two paths for steam leakage.

Float Traps have the highest indirect steam loss due to size and design of the trap. To reduce these losses, Float Traps are carefully lagged to reduce heat loss during operation and freezing if not in use and located outside.

Inverted Bucket Traps require steam bubbling through the water seal to make the bucket buoyant. Heat loss is required to lower the bucket and open the trap. One of the main failures occurring in this type of trap is the failure of the water seal, allowing steam to collect at the top of the trap. If the bucket does not rise, steam collecting in the top of the trap can escape.

Steam loss for “no load” conditions is approximately 0.5kg/hr, but this can vary due to insulation and environmental conditions in which this trap is operating.

## **2.2 Condition Monitoring of Steam Traps**

The advantages and responsibilities for Condition Monitoring and Management of Plant according to File [32] are:

- 1) Maintain plant and equipment in full working conditions;
- 2) Minimise downtime and restore failed process equipment as quickly as possible;
- 3) Maximise the economic life of plant and equipment;
- 4) Optimise the cost and effort with respect to the points above; and
- 5) Provide information which can be used to establish policies for replacement of equipment and future capital investments.

Furthermore, reports and industrial advice by ConEddisison and Spirax Sarco highlight the importance of a Steam Trap Maintenance and Survey Program to accomplish the above tasks in an ongoing and timely manner [91, 26].

### **2.2.1 Condition Monitoring Techniques Applied to Steam Traps**

The following Condition Monitoring Techniques describe current measurement techniques and methods used for testing Steam Traps, some of which are covered by a Carbon Trust publication [15] and steam trap manufacturer’s information, such as from Armstrong and Spirax Sarco.

### **Visual Measurement**

Steam Traps can be monitored visually by use of a sight glass situated upstream from the trap. However, a sight glass is not always useful, as steam is translucent when under pressure and is difficult to distinguish from condensate. Also, a sight glass can develop scaling, obscuring visual observation depending on the pipe work and the age of installation.

If the trap outlet is piped to atmospheric conditions, the output of the trap can be considered visually, but it is worth remembering that condensate will partially flash off into steam due to the pressure drop and it would require an experienced survey engineer to distinguish the flash off from live steam.

In short, although visual measurement is possible, it is the least reliable of all the methods.

### **Audio Measurement**

Low frequency acoustics was an early method of diagnosing Steam Trap behaviour. Early methodology was crude, employing a screw driver to act as a wave guide by holding the tip of the screw driver against the trap and the handle of the screw driver to one's ear. A similar design based on a stethoscope from a doctor is presented by TLV in [101]. This methodology has been refined, over the years, to employ a stethoscope instead of a screw driver, but even this method can be contaminated by ambient environmental noise and it is difficult to distinguish steam from condensate.

Again, although audio measurement is possible, it is not a reliable method for diagnosing Steam Trap behaviour.

### **Ultrasonic Measurements**

Ultrasonic measurement (acoustic sensors that respond to frequencies above 20kHz) uses amplified high frequency signals which attenuate rapidly to identify the source of sound. Low frequency noise is also detectable, allowing an assessment of a broader frequency spectrum than just the high frequency audio measurement. For this reason, ultrasonic measurement is also used in condition monitoring for rotating machinery and other industrial processes.

The hand-held ultrasonic sensor sold and used by Spirax Sarco's Steam Trap survey engineers is the UP 100. This device includes a sensor and electronics which modulate a frequency response of between 38-42kHz (high frequency) to 300Hz-5kHz (low frequency) using a heterodyne circuit [88]. According to the audio tapes on steam trap diagnosis [4] and webinars on air and steam system surveys [103, 104], an ultrasonic stethoscope 36-44kHz is sufficient to amplify the sound of flowing steam.



### **Thermal Measurements**

Thermocouples, infra-red and thermal imaging cameras are the devices normally employed in the measurement of temperature. Thermocouples are normally placed in the flow upstream of the Steam Trap, as shown in [28] where Cypress Envirosystem describe a temperature measurement taken up stream and downstream of the Steam Trap. ARI describes the use of two temperature probes and a heating element in their patent [35], which is further described in Section 2.2.3. Rozlosnik in [79] discusses the use of infra-red and thermal imaging cameras taking external temperature measurements to diagnose Steam Traps. In addition, Spirax Sarco survey engineers often use hand-held infra-red measurement devices to supplement other kinds of measurement (e.g. acoustic) in diagnosing Steam Trap behaviour.

### **Conductivity Measurement**

Steam has low electrical conductivity, whereas condensate (unless very pure) has high electrical conductivity. Spirax Sarco has developed an internal conductivity-based measurement device ("Spiratec") for use with Steam Traps [90]. This device utilises a weir and orifice to create a differential pressure which displaces the mass of condensate within the device. If steam flow is present, a normally submerged sensor is uncovered through increased differential pressure. This in turn exposes the sensor to steam, thus reducing the measured conductivity and, ultimately, raises an alarm through connected electronics.

As with other internally fitted measurement techniques, the Spiratec does have some disadvantages. It is costly to purchase and install as it must be fitted into the pipework upstream of the Steam Trap and industrially hard wired, as described in [86]. Furthermore, the sensor seal provides an additional avenue for steam leakage and the sensor can experience scaling similar to the sight glass in visual measurement.

### **Heat Transfer Coefficient**

Thermal measurement covers the use of temperature for Steam Trap monitoring, on the other hand heat transfer coefficient is a measure of heat flow. Condensate and steam can be determined by the measurement their respective heat transfer rates. This can also be used as an internal measurement technique for Steam Trap diagnostics. When this measurement is applied effectively, it can accurately distinguish between steam, condensate and air, as the heat transfer coefficients differ by magnitudes of ten, respectively. A sensor of this kind has not been commercially produced, although some prior art exists in terms of patents [80].

Method	Strengths	Weaknesses	Opportunities	Threats
<b>Visual</b>	Simple implementation	Internal	Observe fluid flow regimes	Difficult to install and monitor continuously
<b>Audio</b>	External measurement	Unclear	External application	Prone to environmental noise interference
<b>Ultra-sonic</b>	External measurement	Expensive due to sensor and electronics	Easy implementation	None
<b>Thermal</b>	Simple implementation	Unclear diagnosis results	Poor measure of good / bad threshold	Environmental effect can change diagnosis
<b>Conductivity</b>	Simple implementation	Internal measurement	Existing installed based	Prone to leakage and failure of sensor
<b>Heat Transfer</b>	Temperature	Internal measurement	Not widely used	Not accurate enough, only binary output

Table 2.3: SWOT Steam Trap Condition Monitoring Techniques

### 2.2.2 SWOT Analysis of Steam Trap Measurement Techniques

SWOT Analysis (Strengths, Weaknesses, Opportunities and Threats) is a tool used to summarise and compare different options (in this case, measurement technique options). Strengths and Weaknesses are internal factors; Opportunities and Threats are external factors. The outline in Table 2.3 was taken from Gillespie, Foundations of Economics [37].

Overall, the most commonly applied measurement techniques are ultrasonic and thermal as cited in Frank [34], Bloch [8] and Rockwell [78]. In some cases, these are combined to give a more complete diagnostic result, but the need for an experienced person undertaking the survey cannot be overemphasised. The use of ultrasonic acoustic emission measurement devices is widely known in the industry, as reported by respected sources Orlove [65], Rozlosnik [79], and Goodmann [38].

Thermal and acoustic measurements have also been evaluated and, as stated earlier, thermal measurement was found to be unsuitable, on its own, to differentiate between steam and condensate due to the radiant heat of the Steam Trap body as described in Rozlosnik [79] and Goodmann [38]. In terms of a retro-fitable, external diagnostic method of measurement, it is clear that the acoustic emission approach is the most appropriate one to choose. However, this measurement technique can also be enhanced by using a thermal-based device (e.g., a temperature probe or Infra-red hand-held device).

### 2.2.3 Existing Steam Trap Diagnostic Equipment

Existing Steam Trap Diagnostic Equipment can be categorised as either 1) Hand-held or 2) Static.

#### Handheld Diagnostic Devices

Devices in this category use predominantly, ultrasonic sensors detecting acoustic emission from Steam Traps. The sensor detects the ultrasonic vibration and uses frequency shifting principles to shift the ultrasonic signal from the high ultrasonic frequency range to a low frequency range detectable by the human ear. Examples of such devices include the UE Systems UP100 and the CTRL UL101.

There are automated devices which are similar to the devices described above, but which interpret signals by use of algorithms and electronics rather than the human ear. Examples of such devices include the TLV Trapman, the Miyawaki Dr. Trap and the Gestra VKP40.

The measurement method for these devices is instantaneous, so depending on when the data is acquired and the process stage of the Steam Trap, a false interpretation or diagnosis may be made. In comparative tests, these devices are often unable to accurately distinguish between high condensate load and high steam loss.

#### Static Diagnostic Devices

Static Diagnostic Devices for Steam Traps are fixed to the Steam Trap or pipe adjacent to the trap and monitor the trap continuously. These devices diagnose Steam Traps and report a pass/fail measurement based on Acoustic and/or Thermal measurement methods.

Such systems include the thermal-based device from Cyrus Environment Systems which uses up and down steam temperature measurement of the trap to diagnose whether the trap is leaking. An acoustic device example is the Armstrong Steam Eye.

One further example, which should be mentioned is a product of ARI, a Steam Trap supplier. This is a proprietary Steam Trap system (CONA) which uses two internal temperature measurements; one sensor driven by a fixed heater and the other sensor measuring the resulting temperature as described in the relating patent [35]. Depending on the condition of the steam and condensate, the heat transfer rates will be different and steam and condensate volumes can be estimated. This method is not widely used, as it is contained internally within the Steam Trap and is limited to ARI Steam Traps.

The hand-held devices have limited Steam Wastage Measurement capability, as they feedback only high/low thresholds of leakage rather than a scalar value. Even the continuous measurement provided by the Static Devices provide “Failed” or “OK” feedback based on threshold values and do not include allowances for process variation.

Device	Strengths	Weaknesses	Opportunities	Threats
<b>TLV Trapman</b>	Automatic steam trap diagnosis	Instantaneous measurement	Measurement accuracy	Established product
<b>Gestra VKP40</b>	Vibration and temperature	Instantaneous measurement	Only Gestra traps can accurately be tested	Established product
<b>Miyawaki Dr Trap</b>	Vibration and temperature	Instantaneous measurement	Only Miyawaki traps can accurately be tested	Established product
<b>Armstrong SteamEye</b>	Continuous measurement	Limited diagnostic results	Poor measure of good / bad threshold	Established product
<b>Ari Cona</b>	Continuous measurement	Temperature only measurement	Can only be used with ARI traps	Existing product
<b>Cyrus Environmental</b>	Continuous measurement	Temperature only measurement	Temperature measurement alone has limited accuracy	Existing product

Table 2.4: SWOT Diagnostic Devices

### SWOT Analysis of Existing Products

Table 2.4 compares existing products in accordance with the SWOT Analysis.

It is clear that Ultrasonic Measurement is the best technology available for external diagnosis of Steam Traps, as seen in Table 2.5. Further, the combination of Thermal and Acoustic technologies will enhance diagnosis.

It is clear from a review of existing products that the equipment available does not offer any clear information how measurement is achieved. The Author's work aims to investigate the relationship between ultrasonic heterodyne data and Steam Wastage to understand how steam traps can be diagnosed.

Supplier	Measurement Method	Advantages	Disadvantages
TLV Trapman	Vibration and temperature	Portable, Significant Library of traps	Level of accuracy
Gestra VKP40	Vibration and temperature	Portable	Only Gestra traps can accurately be tested
Miyawaki Dr Trap	Vibration and temperature	Portable	Only Miyawaki traps can accurately be tested
Armstrong SteamEye	Vibration and temperature	On-line continuous monitoring	Poor measure of good / bad threshold
Ari System Cona	Temperature only	On-line continuous monitoring	Wired communications, binary output
Cyrus Enviro Systems	Temperature only	On-line continuous monitoring, wireless	Temperature measurement has limited accuracy

Table 2.5: Steam Trap Condition Monitoring Products

## 2.3 Steam Wastage Measurement

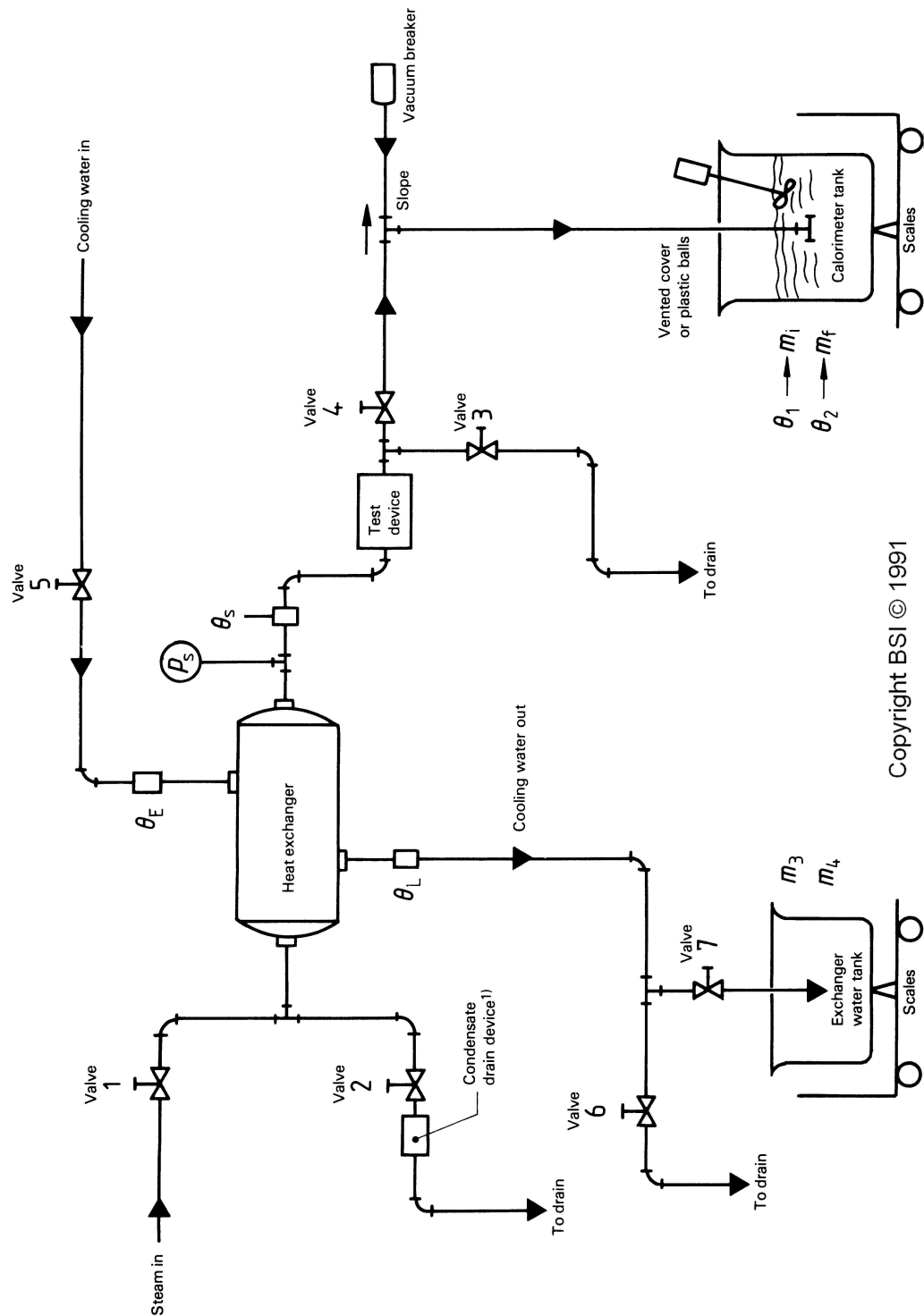
### 2.3.1 Steam Wastage Measurement Standard

There are two test methods described by the Standard BS EN 27841:1991 also known as the ISO 7841:1988 [71]. The standard was developed by the British Standards PSE/7 committee, which is responsible for industrial valves and automatic steam traps in the United Kingdom. The committee is also responsible for the UK contribution to European and international standardisation work. The two test methods described in the standard use the similar test process, but different measurements and calculations to determine the steam leakage rate. A key feature of this work led to the development of an expanded Steam Wastage Rig to methodically analyse Steam Traps as seen in Figure 2.12 and 2.13.

The first method, “A”, as shown in Figure 2.12, requires the fluid flow from the Steam Trap to be directed into a tank partially filled with cold water, known as the sparge tank. This water is necessary to condense any steam contained in the fluid from the trap. Over time, the change in mass and temperature of the tank is then measured along with pressure and temperature conditions at the Steam Trap. These measurements are then used to calculate the mass fraction of steam and condensate as in the formula below.

$$q_{ms} = \left[ \frac{m_f h_{f2} - m_i h_{f1} - h_{fs}(m_f - m_i) + c_p \cdot m_t(\theta_2 - \theta_1)}{h_{fgs}} \right] \cdot \frac{3600}{\Delta t} \quad (2.1)$$

These measurements must be extremely accurate, otherwise Steam Wastage will be misdiag-

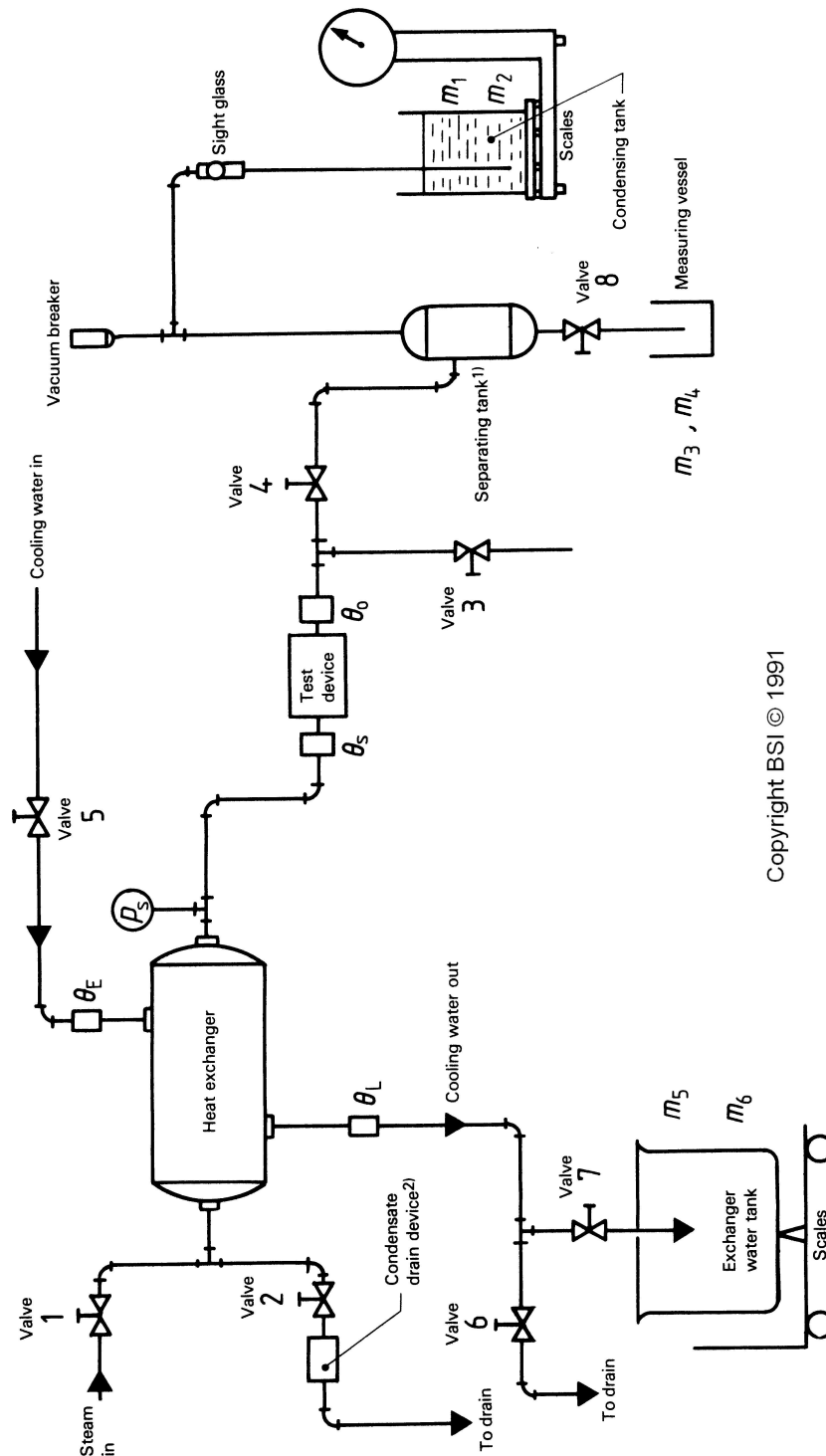


Copyright BSI © 1991

Figure 2.12: ISO RIG Method A (from [71]). ©British Standards Institution (BSI www.bsigroup.com). Extract reproduced with permission. Source: BS EN 27841:1991 Methods for determination of steam loss of automatic steam traps. Further reproduction prohibited without permission. From details see Permissions section.

nosed.

The second method, "B", as shown in Figure 2.13, requires the separation of steam and condensate. The steam is captured in the sparge tank and measured once condensed; the condensate



Copyright BSI © 1991

Figure 2.13: ISO RIG Method B (from [71]). ©British Standards Institution (BSI www.bsigroup.com). Extract reproduced with permission. Source: BS EN 27841:1991 Methods for determination of steam loss of automatic steam traps. Further reproduction prohibited without permission. From details see Permissions section.

is collected from the separator in a separate tank and measured. Steam Wastage can then be calculated with these two measurements, however, this method relies heavily on the efficiency of the separator. Steam Wastage using method "B" can be determined using the formula below.

$$q_{ms} = \left[ \frac{m_{st}(hg_o - hf_i) - m_c(hf_i - hf_o)}{hg_s - hf_s} \right] \cdot \frac{3600}{\Delta t} \quad (2.2)$$

## 2.4 Published Steam Trap Information and Wastage Data

The essence of steam and associated products is based on established science and technology and form part of a long established industry. Today, although steam is a widely used process fluid, it is not widely taught within the education system nor is there much non-industrial research available. As a result, publications tend to be, primarily, limited to non-peer reviewed papers with subjective conclusions.

For example, a paper published by Nishal Ramadas discusses the application of acoustic data for Steam Trap diagnosis [76]. Ramadas was employed by Spirax Sarco to consider the feasibility of Acoustic Steam Trap Condition Monitoring. His approach considered a number of Steam Traps in small populations; application of a power spectrum estimation; and Principal Component Analysis to arrive at the conclusion that it was possible to diagnose the condition of the Steam Trap. The use of the heterodyne circuit was not investigated and assumptions were made regarding the source of the acoustic emission. This conference paper was submitted and is in the public domain.

Rozlosnik [79] and Goodmann [38] evaluated acoustic and thermal measurement approaches to Condition Monitoring of Steam Traps. Although good results were found using only Acoustic Measurements, it was found that the diagnosis could be enhanced by applying Thermal Measurements in combination with Acoustic Measurements. Thermal Measurements alone were found to be insufficient for reliable diagnosis.

No other public condition monitoring literature has been found for Steam Traps. It is clear, though, that other industrial partners are working on the development of new techniques, but published work in this field is rare.

Table 2.6 summarises steam leakage values for four trap types. These values are for new traps on low load conditions and as no trap can achieve zero leakage, it does highlight the importance of having a suitable steam system maintenance program to minimise steam losses. It is worth noting that there is always a radiation loss associated with the steam trap, which can be significantly less if it has been lagged with insulation. For worn traps, the figures of leakage through the trap would be increased.

All Steam Traps in a steam system will leak some steam. The amount of leakage depends, largely, on type of trap, the age of the system and whether a continuous maintenance program is



	Through trap	No-load From trap	Total	Through trap	Reasonable load From trap	Total
Thermo-static	0.5	0.5	1.0	Nil	0.5	0.5
Float	Nil	1.4	1.4	Nil	1.4	1.4
Inverted Bucket	0.5	1.2	1.7	Nil	1.2	1.2
Thermo-dynamic	0.5	0.25	0.75	Nil	0.25	0.25
Measured with the International Standard ISO 7841 (1988) and the European Standard CEN 27841 (1991)						

Table 2.6: Spirax Sarco Steam Wastage Data

Programme Frequency	None	Annual	Bi-annual
Spirax Sarco	20%	10%	5%
UE Systems	50%	25%	12%
US Department of Energy	20%	-	-
Energy Management News	40%	6%	-

Table 2.7: Steam Trap Failure Percentage

being implemented. The US Department of Energy suggests in [31] that the use of fixed diagnostic equipment on Steam Traps can reduce the leakage rate to 1% .

In a case study published by the Carbon Trust [14], the survey of a large petrochemical site having over 13000 Steam Traps, highlighted that 314 traps had failed open and were leaking steam. The resulting replacement and improvement programme reduced the steam requirement of the site by over 4t/hr, saving over 23GWh of energy annually.

An article in Energy Management News [77] covered issues related to the management of a population of Steam Traps and provided a number of typical field examples where steam plant had been investigated for Steam Trap failures. The article reported that a reduction of steam trap failure from 40% to 6% was achieved following the implementation of steam trap management programme.

Figures of the percentage of traps typically leaking depending on an implemented maintenance programme have been found from several sources, some of which have been outlined above, which are summarised in Table 2.7.

## 2.5 Acoustic Emission of Steam Traps

The following list provides key definitions which have been taken from Oxford Dictionary of Physics [46] and “Fundamentals of Noise and Vibration” by Norton and Karczub [64] and are central to this work:

- Vibration is “A repetitive periodic change in displacement with respect to a reference point”.

- Sound is “the periodical mechanical vibrations and waves in gasses liquids and solids elastic media”.
- Acoustics is “the study of sound and waves”.
- Audible Vibrations are “Vibrations in the order of 20Hz to 20kHz”.
- Ultrasound is “Vibrations above 20kHz”.
- Acoustic emission is “the generation of elastic waves through external factors, such as mechanical loading”.

### 2.5.1 Sources and Reasons of Acoustic Emission

Acoustic emission (AE) signals are widely used in the field of Non-Destructive Testing (NDT). Fast energy releases, caused by operational conditions and or faults with the equipment, generate a spectrum of waves starting at the low Hz level and ranging up to several MHz. AE is commonly understood to be a resultant of a localised energy release, causing waves to propagate through the material and the associated structure. The frequency range of the acoustic emissions varies by application. Examples of typical frequency bands, as described by Williams in [106], are:

#### 1) Structural Mechanics

- (a) Structural dynamic applications in the range of 0.1-100Hz;
- (b) Rotor dynamics from about 50Hz to 1kHz; and
- (c) Mechanical Failures such as bearing wear and leaks in pipelines in the range of 1kHz to 100kHz.

#### 2) Material Science

- (a) Growing cracks found in the range of 50kHz to 1 MHz; and
- (b) Ultrasonic Non-Destructive Testing of metals between 1-10MHz.

AE can also be related to irreversible releases of energy and sources include friction, cavitation and impact. The latter examples are related to the acoustic sources in a Steam Trap. The AE approach is advantageous as the frequency band of AE lies above the background noise, allowing the feature selection for classification to be performed outside the background noise frequency range and thus providing an improved signal to noise ratio.

In terms of the application of AE to condition monitoring, acoustic signals are acquired from an object and monitored to locate and/or define the standard operating conditions. Threshold techniques and other methods are used to define out of bounds data and signal an alarm.

In preventative maintenance, a correlation between the specific events and their associated intensity or duration of time are used. This approach can be used to determine the onset of a failure or to document the progression of the fault condition. Using such procedures allows maintenance to be scheduled before critical failure and with a minimum amount of disruption to the processes. As AE is a passive approach, processes can remain in service during the inspection, reducing the down time. For this reason, it is very suited to continuous condition monitoring.

In addition to NDT, acoustic emission monitoring has also been applied to process monitoring. Applications include the detection of upsets in fluidized beds and the detection of end points in batch granulation and mixture optimisation for chemical processing.

### **Acoustic Emission in Pipes**

Acoustic emission in pipes has several sources caused by the fluid-structure-interaction. Specifically, acoustic emission arises from the release of energy from fluid phase exchange. These acoustic emission signals are transferred through the pipe wall to the surface where they can be picked up by an external sensor as described by Kocis and Figura in [51]. Low frequency vibrations are caused by geometrical changes and fluid flow excitation of the natural frequencies of the pipe. Over and above the fluid structure interaction in steam and condensate systems, the nature of the fluid is multi-phase further adding to the sources of acoustic emission.

In terms of the higher frequencies, turbulence of the flow higher regimes adds significant energy to the energy signature of the flows and through that to the acoustic emission. Nakamura [60] states that two-phase flow regimes are notoriously difficult to map and recreate as they are inherently very unstable. It is clear that the inherent instability of two-phase flow regimes will make the exact determination of conditions difficult.

Nakamura lists the sources of acoustic noise in pipe systems as:

- 1) Unstable fluid flow when the flow velocity surpasses a critical value; and
- 2) Vibration due to oscillating flow.

### **2.5.2 Acoustics Emission in Steam and Condensate**

The use of acoustic emission signals for Non-Destructive Testing (NDT) and condition monitoring is widely accepted. There have been extensive applications in the use of ultrasonics for the detection of air leakage, as described by webinar on air system surveys [103], many of which are threshold or manual based.

The different flow regimes within the flow as described in Section 2.6 result in acoustic signal generation. The steam and condensate both have highly different densities, which are pressure

dependant and differ by orders of magnitude. The characteristic impedance of a medium, such as air, rock or water is a material property. The attenuation of the high frequency noise is high as the density of the steam is low and the transition to the steel and thus the sensor is low. The acoustic impedance (similar to electrical impedance) is governed by:

$$Z_0 = \rho \cdot c \quad (2.3)$$

Blazquez [7] suggests that acoustic emission of gasses and liquids through small holes produces ultrasound emissions in the band of 40kHz, whereas condensate discharge at low speed does not produce ultrasound. However, a blowing trap contains ultrasound.

Ao et al. [3] discuss the application of ultrasonics for a clamp on flow measurement for gas, steam and compressed air. In this application, the ultrasound is used through a set of transducers as both active and passive and the time of flight is used to calculate a flow rate.

### 2.5.3 Measurement of Acoustic Emission of Steam Traps

Acoustic sensors detect elastic waves propagating through a medium, such as a pipe. These can both be active and passive and operate in a frequency range of low kHz to 1MHz. Active transducers are used in flow metering or medical ultrasound equipment for example, where signals are created using the transducer. The source signal rebounds from the subject being investigated and is subsequently analysed. AE tools on the other hand are just passive, they do not actively produce signals. Rather, they passively detect acoustic emission of the subject being investigated. Applications include crack propagation in material and vibration analysis of rotating machinery.

#### Application of Acoustic Emission to Two-Phase Flow Measurement

Although numerous products exist for this application, little peer reviewed information is available on steam and condensate metering as a lot of the information is industrial based research and confidential in nature. Many investigations have been conducted into the classification and metering of two-phase flow of gasses and oil for application in the petrochemical industry, as well as mixtures of air and water. Wang and Tong [105] showed that two-phase flow measurement is possible by measuring the noise in pressure readings from a pressure transmitter in an orifice plate flow measurement device. The noise resulting from the pressure fluctuations and turbulence allows the two-phase flow to be inferred.

### Acoustics Emission in Steam Traps

Steam Trap acoustic emission has a number of sources, but is always related to change in energy, such as:

- 1) Changes in flow path and velocity: either changes in the dimensions of the pipe or directional changes in the flow. As steam has a specific volume approximately 1600 times that of condensate at atmospheric conditions, the flow velocities are far higher than condensate when constrained in a pipe. When flow accelerates and changes from laminar to turbulent, the transition releases energy, which can be measured.
- 2) Pressure drop: When the fluids observe a pressure drop some of the condensate changes phase and flashes into steam. When steam passes through a pressure drop it dries and can even turn to superheated steam.
- 3) Phase change / Cavitation: Cavitation and flashing of the condensate as it is released by the Steam Trap. The frequency peak depends on the viscosity of the liquid. For low viscosity, the frequency range of 20-30kHz should be used. For high viscosity, and the frequency range of 40-60kHz as described by Rozlosnik [79]
- 4) Two-phase flow (as mentioned above in the previous point). When condensate transfers from a pressurised liquid to an atmospheric vapour, it releases energy related to the transfer between the different phases. Wang and Tong [105] described two-phase flow as a Stochastic Process and that a noise signature generated by an orifice can be approximated as white noise. Bubble flow is also associated with acoustic emission. When bubbles collapse, they emit acoustic emission depending on the pressure and the void fraction. Although the flow of condensate usually follows a river type flow, the flow can take on flow regimes such as annular, wave, intermittent, dispersed and stratified. Acoustic emission resulting from changes in the gas volume fraction in intermittent slug flow was described by Addali et al. in [1]. A correlation between the acoustic emission energy and slug velocities was found for a range of liquid and gas velocities.
- 5) The mechanism used in Steam Traps makes noise when operating. Thermodynamic Traps observe a clear impulse-like response when the mechanisms open, Balance Pressure Traps can breathe and Float Traps observe a periodic, wave-like opening and closing motion.

The most reported frequency range of high frequency detection equipment for gaseous system is between 40kHz to 45kHz. There is no reason for this specific frequency range, although references have been made that this range can be linked with gas escaping small orifices. Macleod et

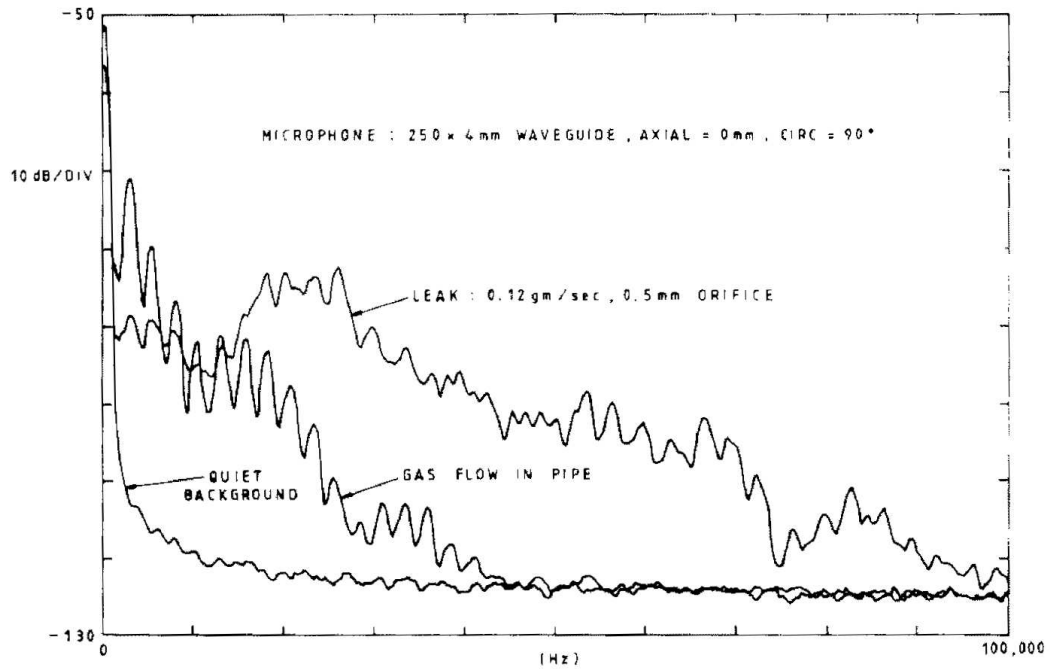


Fig. 2. Acoustic gas leak detection using air-borne noise.

Figure 2.14: Frequency Response from a Small Orifice in a Steam Pipeline (from [54]). ©1991 Elsevier. Reproduced with permission of the copyright owner. Further reproduction prohibited without permission. From details see Permissions section.

al. [54] investigated leaks on nuclear power plant and found that a gaseous leak yielded high energy levels of acoustic emission in frequency range of 35kHz to 50kHz (see Figure 2.14), whereas gas flow and background noise high energy levels were limited to below 30kHz.

UESystems, a supplier of acoustic condition monitoring equipment and provider of steam system monitoring training, claims in a web lecture on air survey work that the measurement of gasses can be adequately undertaken using ultrasonic detection. For Steam Trap surveys, it specifically suggested that a stethoscope be tuned to about 25kHz, which will be high enough to reduce the low frequency mechanism emission, but low enough to identify “rushing steam” through the mechanism which was described in a technical report [102]. UESystems also claims in a lecture on air leak surveys [103], that the measurement of gasses can be adequately measured using a frequency band of 25kHz to 40kHz which agrees with Macleod et al..

#### 2.5.4 Acoustic Condition Monitoring Techniques applied to Steam Traps

Three other investigations have been undertaken by other parties.

Ramadas [76] showed the application of acoustic emission techniques to Steam Traps for a heating application. This work was carried out at Spirax Sarco in parallel to this investigation. The work used the same Steam Wastage that was designed for this research. Ramadas used similar heterodyne data as well as the same data acquisition equipment. Although there is some overlap

of the work, the investigation by Ramadas was not as detailed as aspects such as the heterodyne frequency shifting circuit response were not investigated or considered by the author. There was also no clear understanding of the reasons for the acoustic emission generation mechanisms.

Spasova investigated the raw acoustic emission to Steam Traps. Relationships between the two-phase flow regimes and the acoustic emission were established for a number of operational conditions of Steam Traps. The work highlighted a number of frequency bands with resonant peaks which were related to the two-phase flow. Using these frequency bands, a number of algorithms could be created for the mapping of Steam Wastage. It is worth noting that Spasova's work did not use heterodyne-based data and that a significant amount of test work was conducted using the research rig established as part of this work. Although the author has had sight of this work, further details of Spasova's work and reports [84] cannot be disclosed due to confidentiality reasons.

Allgood investigated acoustic emission related to Steam Traps, but used a low-frequency accelerometer for the work, which was reported in [2]. Short-Time Fourier Transforms and Wavelets were applied as well as Fourier transforms and time domain processing. The analysis was not very effective due to the low-frequency accelerometer used to collect the data. This highlights the reason for choosing a heterodyne circuit to condition the signal.

All these investigations were carried out by or in conjunction with Spirax Sarco. No other relevant research related to Steam Traps and acoustic emission has been discovered.

## **2.6 Two-Phase Flow and Cavitation in Pipelines**

### **2.6.1 Occurrence of Two-Phase Flow**

The term "Multiphase Flow" is defined as flow that consists of a mixture of the three phases: gas, liquid and solid. Fluid flow in pipes in steam systems is of a liquid and gas phase mixture, also referred to as condensate and steam respectively. Steam systems have, in comparison with an air and water system, a continuous heat loss and thus there are usually both liquid and gas flow at any instance of flow. Pressure drops, dynamic changes and heat exchange can also result in phase changes, where steam can condense to condensate as well as condensate flash off to become steam. Two-phase flow is complicated and dynamic. Internal and confidential research at Spirax Sarco has shown that two-phase flow is affected by a number of parameters including pipe size and geometrical changes, fluid pressure and temperature and other fluid properties, such as density and enthalpy. The measurement of two-phase flow can be difficult due to the differing flow regimes, densities, etc.. Due to this uncertainty of phase composition it is very difficult to meter two-phase flow, especially in steam and condensate systems.

## 2.6.2 Two-Phase Flow Regimes in Horizontal and Vertical Pipes

Two-phase flow regimes are of great importance to industry and its processes. For this reason, there is a lot of research undertaken in the modelling and understanding of two-phase flow. One of the challenges of a steam system is that the inside of a pipe cannot be seen. Using sight glasses in experiments with Steam Traps, it has been shown that the steam under pressure forces the condensate around the wall of the pipe. Depending on the void fraction of the mixture, the flow regime changes. Sources such as Hewitt [42], Nakamura [60] and Barton [6] describe the fluid flow of the two phases in horizontal and vertical pipes for steam and condensate flows. A number of agreed pipe flow regimes are described, which can be observed by changing the conditions within the pipe. The flow regimes are dictated by the void fractions of the liquid and gas phase, which in turn result in different vibration and acoustic emission profiles. According to Nakamura [60], two-phase flow can be characterised by a number of flow regimes. The list starts with a high liquid phase and transits to a high gas phase void fraction:

- 1) Bubbly Flow - Mainly liquid flow with gas bubbles dispersed within. The gas flow rate and the resulting flow induced forces are low.
- 2) Stratified Flow - Stratified flow with the gas flowing on the top and the liquid on the bottom in horizontal piping with a smooth interface layer between the phases.
- 3) Stratified Wavy flow - This flow regime is the same as the stratified flow regime, but the interface layer between the phases is wavy rather than smooth.
- 4) Plug Flow - Low turbulence and the gas bubbles are large and intermittent.
- 5) Slug Flow - Similar to plug flow although the liquid phase is even more separated and a bullet-like phase. This flow regime manifest as water hammer when a slug impacts on an elbow or section of pipe where there is a directional change.
- 6) Annular Mist Flow - Even lower liquid phase, with the gas phase in the centre of the pipe and the liquid phase around the perimeter, forming an annular ring of liquid.
- 7) Mist Flow - Mainly gas phase, this flow regime is opposite to the first regime, bubbly flow. The flow is mainly high speed gas phase with small liquid droplets suspended in the flow.

Brennen [12] covers in detail two-phase flow regimes and the associated flow maps. Taitel and Dukler [96] investigated two-phase flow and established flow maps detailing the different flow regimes. Street et al. [93] investigated the two-phase gas-liquid flow in vertical pipes and concluded that the light phase moves in relation to the dense phase and also that resulting pressure



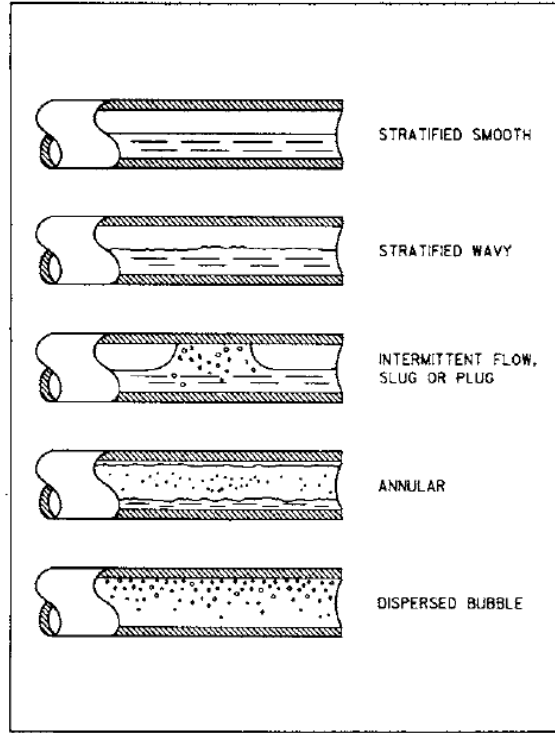


Figure 2.15: Horizontal Flow Regimes (from [25]). ©1990 SPE. Reproduced with permission of the copyright owner. Further reproduction prohibited without permission. From details see Permissions section.

fluctuations are periodic in nature of the fluid density at any pipe location. Figure 2.15 shows the horizontal flow regimes and the typical visualisations.

Some of these flow regimes presented have been re-created and validated in several experiments by Spasova [84] using the Steam Wastage Rigs at Spirax Sarco. Example images of the flow regimes are shown in Figure 2.16. The clear differentiation between the different flow regimes can be seen and the similarities with Figure 2.15 are clear.

Figure 2.17 shows an example of a flow regime map for two-phase flow by Taitel and Dukler from 1976 referred to by Street and Tek in [93]. As the flow regime map is composed of three graphs a number of parameters need to be evaluated, as detailed by Thome in [99]. These parameters are: the Martenelli parameter  $X$ , the Froude number  $Fr_G$  and parameters  $T$  and  $K$ . The Martenelli parameter  $X$ , is given by Equation 2.4.

$$X = \left[ \frac{(\delta p / \delta z)_L}{(\delta p / \delta z)_G} \right]^{1/2} \quad (2.4)$$

The Froude number  $Fr_G$  is given by Equation 2.5:

$$Fr_G = \frac{\dot{m}_G}{[\rho_G(\rho_L - \rho_G)d_i g]^{1/2}} \quad (2.5)$$

Parameter  $T$  is given by Equation 2.6:

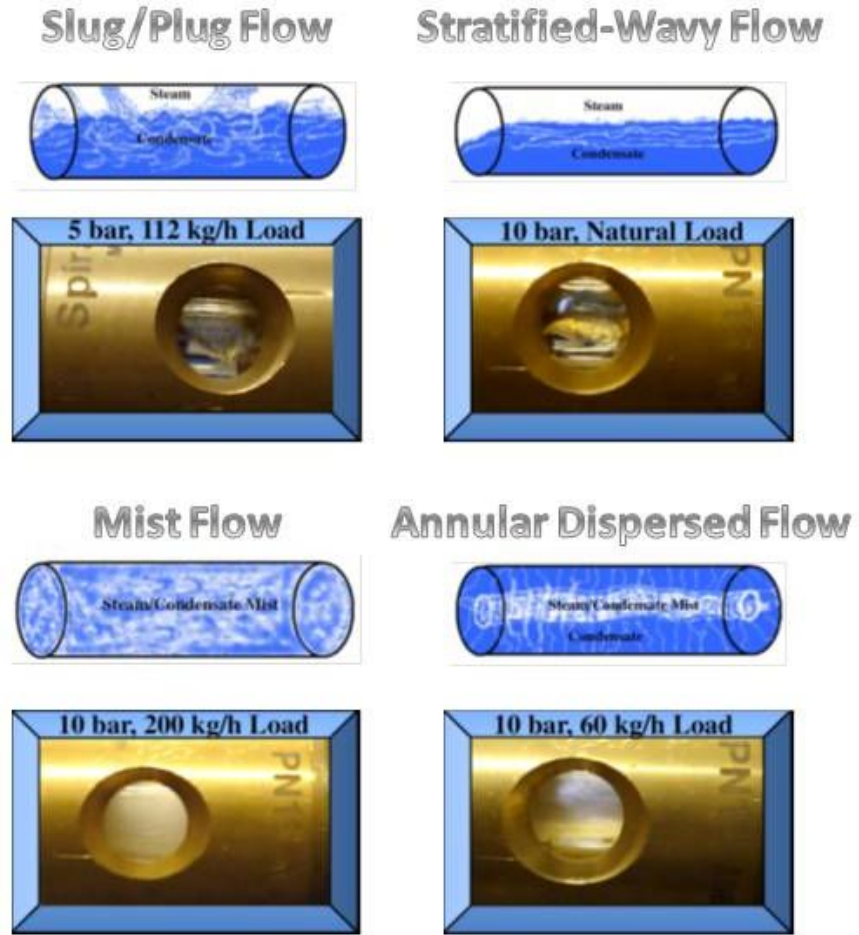


Figure 2.16: Horizontal Flow Regimes observed in Experiments (from [84]) ©2009 Spirax Sarco. Reproduced with permission of the copyright owner. Further reproduction prohibited without permission. From details see Permissions section.

$$T = \left[ \frac{|\delta p / \delta z|_L}{g(\rho_L - \rho_G)} \right]^{1/2} \quad (2.6)$$

Parameter  $K$  is given by Equation 2.7:

$$K = Fr_G Re_L^{1/2} \quad (2.7)$$

Furthermore, the Reynolds number for the gas and liquid phase is given by Equations 2.9 and 2.8 respectively:

$$Re_L = \frac{\dot{m}_L d_i}{\mu_L} \quad (2.8)$$

$$Re_G = \frac{\dot{m}_G d_i}{\mu_G} \quad (2.9)$$

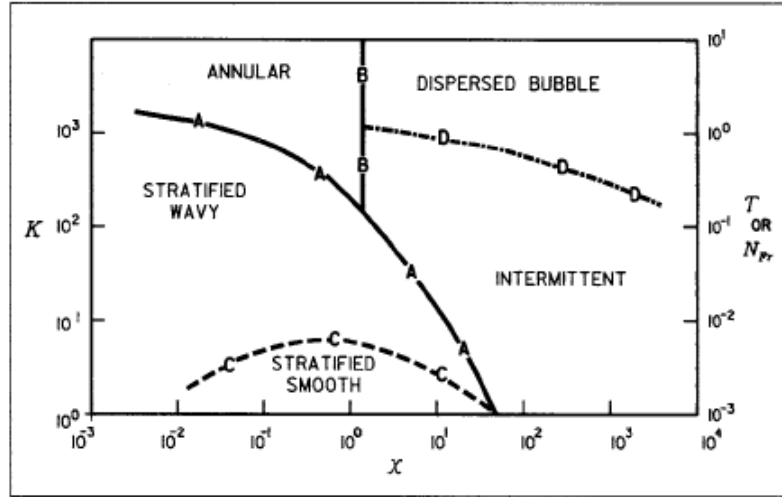


Figure 2.17: Wet Steam Flow Regimes (from [96]). ©1990 SPE. Reproduced with permission of the copyright owner. Further reproduction prohibited without permission. From details see Permissions section.

Additionally, the pressure gradient  $(\delta p / \delta z)_k$ , where  $k$  is defined as  $L$  or  $G$  depending on whether a liquid or gas phase is being considered, is given by Equation 2.10:

$$(\delta p / \delta z)_k = \frac{2f_k \dot{m}_k^2}{\rho_k d_i} \quad (2.10)$$

where  $f_k$  is defined as follows for laminar flow (where  $Re_k < 2000$ ):

$$f_k = \frac{16}{Re_k} \quad (2.11)$$

For flows with a  $Re_k$  higher than 2,000 (including the transition regime of between 2,000 to 10,000), the turbulent flow friction factor Equation is used (Equation 2.12)

$$f_k = \frac{0.079}{Re_k^{1/4}} \quad (2.12)$$

To use the flow map firstly, the Martinelli parameter and Froude number are evaluated to establish whether the flow pattern is in the annular region or below that. If the result falls in the lower left zone of Figure 2.17 then  $K$  is evaluated. In the centre of the graph,  $X$  and  $K$  are used to establish whether a flow is fully stratified or stratified wavy. For the right zone, if the number falls in the top half then parameter  $T$  is calculated. Then if  $T$  and  $X$  fall in the bottom half then the flow regime is determined to be wavy. The work detailed above is based on empirical data. From these equations it is clear that the determination of flow regimes is ambiguous and cannot be simply determined. The purpose of outlining the equations above is not cover in depth the subject of two-phase flow, but provide an introduction of the complexity of this subject matter.

Zhou et al. [109] investigated the two-phase flow regime identification through high speed photography. Seven flow regimes were created using air (gas phase) and water (liquid phase) and classified. Although the approach of imaging is not the approach taken by this investigation, this paper highlights the complexity of diagnosing two-phase flow regimes. The accuracy was 100% in the application of this approach, although several classifiers have to be employed to reduce the variables and the support vector machines approach was applied for final classification.

Tan et al. [98] investigated the application of Electrical Resistance Tomography (ERT) to the determination of flow regimes. Statistical features are derived through time series statistical analysis together with 1D and 2D wavelet analysis. These features are then considered using a data fusion approach, all of which acts as an input to the vector support machine algorithm for the recognition of the flow regime. The fluids used for this investigation were air and water. It was shown that provided the features could be adequately be defined this approach would be suitable for the identification to two-phase flow regimes.

Hua et al. [43] discuss the determination of flow regimes using measurements from a pipeline transducer. The fluids used were air and water and a support vector machine algorithm was applied to the data for classification. Although the approach taken by the authors was successful in providing a diagnosis of the flow regime, it was found that in deviation cases this approach could result in an erroneous determination of the flow regime. Nevertheless, this non-invasive flow metering approach is closely linked with this investigation, highlighting possible sources for errors. Another point worth noting is that the power spectra considered were up to 2kHz, which is below the ultrasonic range.

Tambouratzis and Pázsit [97] describe the application of neural networks to neutron radiography images from a nuclear reactor. This paper is very relevant as it considers the fluids steam and water in a steam application (nuclear reactor). Although the coolant cycle is not the same application as condensate return from Steam Traps, parallels can be drawn. This application utilises statistical features for the determination of two-phase flow regimes. Self-organising aspects are facilitated through the application of Neural Networks as well as through mean-based ratios, allowing the system to be self-aligning. The need for careful management of the data was highlighted as two-phase flow is not deterministic. Lastly, the non-invasive approach is very relevant to acoustic emission.

Sun et al. [94] describe the two-phase flow regime identification using a differential pressure sensor from a venturi meter. The fluids used were air and water and Hilbert-Huang transform was applied to the signals for feature generation. As the energy levels for single-phase data and the bubbly flow were both low, they can be difficult to distinguish. Nevertheless, the rules-based approach worked for all other energy levels. Furthermore, the pipe size and flow rate had little

influence on the clarity of the data. It is also worth noting that the sample frequency was very low (200Hz).

### 2.6.3 Bubble Dynamics and Cavitation

Hahn et al. [40] describe the acoustic emission from a fresh water jet and air jet as it penetrates the surface of a pool of fresh water. The investigation utilises frequency spectra to analyse the resulting acoustic emission. Spectra peaks found in the region below 1kHz region are caused by the oscillations of the resonance cavity created in the freshwater pool. As water and air is used this does not directly relate to Steam Trap operation, but the cavitation observed in the experiment may be observed in Float Traps, supporting the argument for the use of ultrasonics to isolate the steam leakage for other physical acoustic emission sources.

Boyd and Varley [9] investigated the acoustic emission from bubble columns. In the experiment air was sparged from the bottom of a column vessel, allowing bubbles to form and rise through the water. The acoustic emission from the bubble creation was shown to be within the 1kHz range and the emission spectrum peaks were related to the modal resonant frequencies excited by the bubble formation within the column. This was investigated for gas hold-up of up to 20% and a correlation between the changes in the gas hold-up and the frequency were found. The author concludes that this method could be usefully applied to situations where the bubble dispersion is not visible. For Steam Traps, this could be a useful indicator although the frequency responses are in the 0-1000Hz range.

Two-phase flows and their dynamics result in pressure fluctuations which can result in cavitation. Cavitation occurs when the ambient pressure reduces to below vapour pressure of the liquid, causing some of the liquid phase to change to the vapour phase and is usually detected as noise, rather than by visual inspection. Bubble and Cavitation flow is described by Brennen in [11].

Cavitation bubbles collapsing result in a high energy release and noise, which results from the momentary high pressure generated as the contents of the bubble are highly compressed. This phenomenon was discovered by Reynolds and vaporisation discovered by Parsons. Cavitation has been the interest of a significant amount of research.

All flows have a cavitation number,  $\sigma$ , even when they are not cavitating. For a flow situation cavitation must be considered when either pressure decreases or flow velocity increases, as these conditions could result in the overall pressure reaching the vapour pressure and cavitation to occur. To allow this relationship to be explored, the cavitation number is used as defined by Equation 2.13.

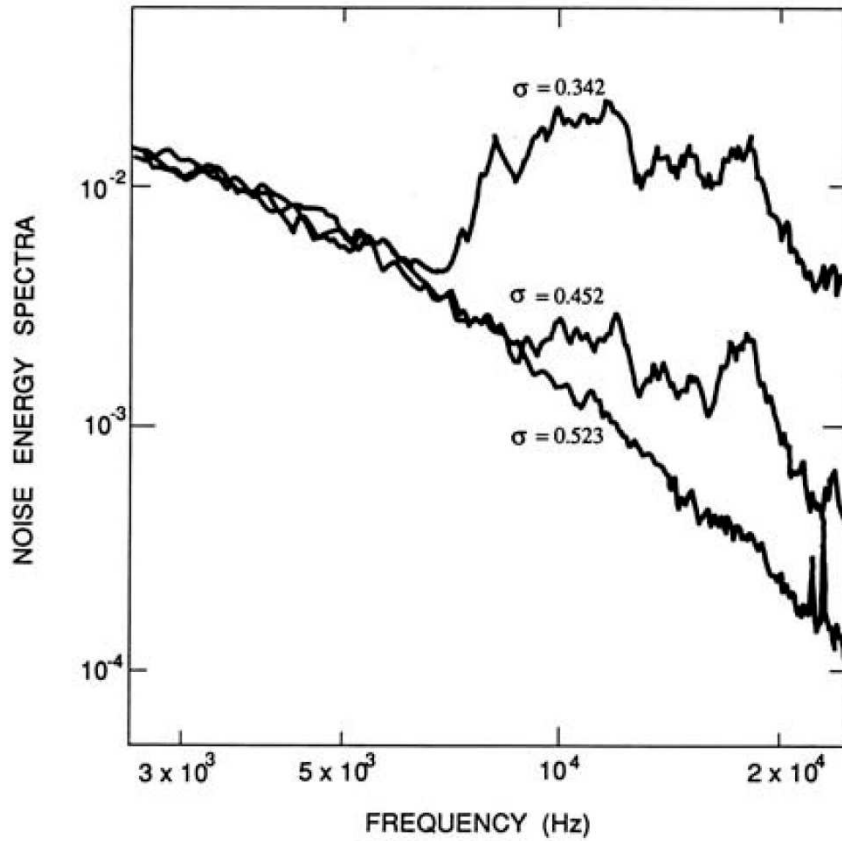


Figure 2.18: Cavitation Frequency Response (from [11]). ©1995 UOP. Reproduced with permission of the copyright owner. Further reproduction prohibited without permission. From details see Permissions section.

$$\sigma = \frac{p_{\infty} - p_V(T_{\infty})}{\frac{1}{2}\rho_L U_{\infty}^2} \quad (2.13)$$

In Equation 2.13,  $p_V$  is the vapour pressure, at a reference temperature of  $(T_{\infty})$ . If  $p_{\infty}$  is large compared to  $p_V(T_{\infty})$  or  $U_{\infty}$  is sufficiently small, the cavitation number  $\sigma$  will be large and single phase flow will occur. As the cavitation number reduces, nucleation will occur at some point. This value of  $\sigma$  is known as the incipient cavitation number  $\sigma_i$ .

Typical acoustic emission noise spectra due to cavitating and non-cavitating flow through an orifice of a hydraulic control valve are shown in Figure 2.18. The lowest curve ( $\sigma = 0.523$ ) represents the turbulent noise from the non-cavitating flow. As can be seen from the figure, the noise level dramatically increases above about 5 kHz for flows with a lower incipient cavitation number ( $\sigma = 0.452$  and  $\sigma = 0.342$ ). Furthermore, the spectral peaks between 5 kHz and 10 kHz correspond to the expected natural frequencies of bubble nuclei in flow.

The analytical analysis for cavitation noise is built up from knowledge of the collapse of a single bubble. It is difficult to apply many of the proposed models as they rely on idealised scenarios, not considering thermal effects and non-condensable gasses, which will exist in a steam

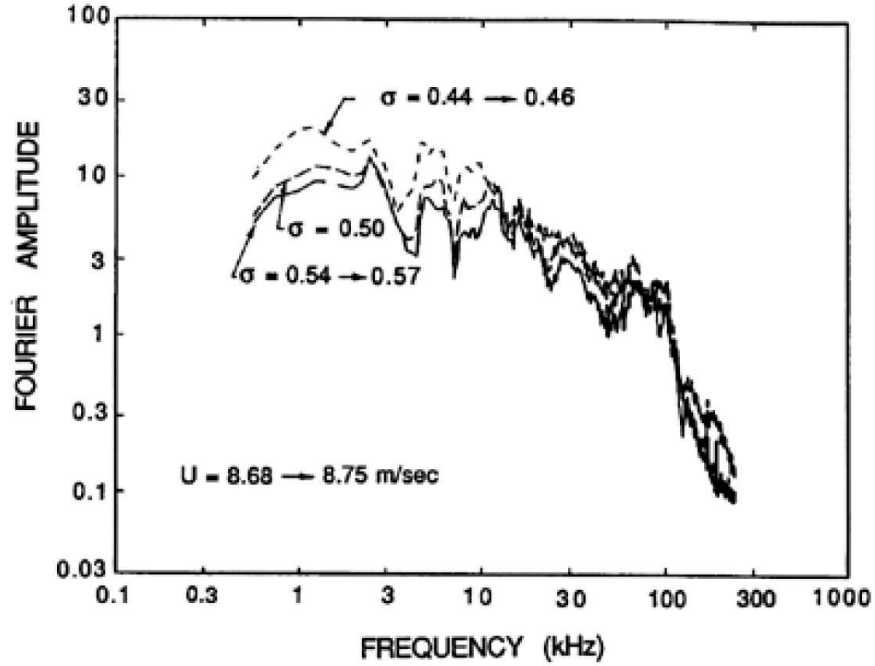


Figure 2.19: Cavitation Frequency Response (from [11]). ©1995 UOP. Reproduced with permission of the copyright owner. Further reproduction prohibited without permission. From details see Permissions section.

system application. The typical frequency spectra contained in single bubble noise are shown in Figure 2.19. Depending on the conditions, the acoustic decay of the noise has been found to be practically between  $f^{-2/5}$  and  $f^{-2}$ .

A typical frequency response spectrum for a single bubble in flow is shown in Figure 2.19. This response would also correspond to the overall cavitation noise spectrum, provided the bubble collapse events are randomly distributed in time. In the frequency range of up to 50kHz, the spectra exhibits an  $f^{-1}$  decay. It should be noted that the rapid decay beyond 80kHz is due to the limitation of the recording equipment.

Considering the synthesis of cavitation noise from the noise produced by individual cavitation bubbles or events, Brennen suggests that provided the events can be considered to occur randomly in time then the sound pressure level,  $p_S$ , will be given Equation 2.14.

$$p_S = I_E \cdot N_E \quad (2.14)$$

In Equation 2.14, the impulse produced by each event is denoted by  $I_E$  and the number of events per unit time is denoted by  $N_E$ .

#### **2.6.4 Water Hammer**

Water hammer is a condition where high-pressure impulses are observed within the pipe system. Steam moves at a higher velocity than condensate within the pipe system. Pipe distribution systems are usually designed for a steam pipe velocity of between 25m/s to 40m/s, but condensate moves at lower speed (typically under 5m/s). When condensate pools sufficiently, a slug can be created, acting like a bullet in the barrel of a rifle, accelerating along the length of the pipe until it impacts a bend or change in direction of the pipe. The high-velocity impact causes a pressure wave to propagate, which in turn can damage Steam Traps and even break pipes if sufficiently severe and repeated in action.

The causes for water hammer can be poor start-up, or shut-down, the lack of insulation resulting in more condensate being created as well as failed steam traps. Owen published papers on the propulsion of an isolated slug through a pipe [66] and on the impact of water slugs on wet steam meters (Owen et al. [67]). These investigations do not deal with the detection of water hammer, but investigate the effect of water hammer on the operation of Steam Traps. Providing Steam Traps work as expected and good steam system operational procedures are implemented, water hammer should not be expected to occur.

#### **2.6.5 Flow Induced Vibration**

The characteristics of the excitation force depend on the two-phase flow patterns being observed. Several flow regime maps estimate the resulting flow regimes based on flow conditions, rates and other existing physical properties. Experiments with air and water have shown that vibration generally increases with flow velocity. Nakamura [60] described slug flow and the experiment showed that the amplitude was less dependent on the two-phase flow velocity. In plug flow, on the other hand, vibration amplitudes were strongly related to two-phase flow velocity even though amplitudes were small. These discoveries also indicate that an increase in pressure in a steam system would result in an increase in velocity and thus a higher level of pipe vibrations.

### **2.7 Overview of Digital Signal Processing for Condition Monitoring**

Digital Signal Processing is frequently applied to the field of condition monitoring problems. Applications range from steam turbines in power stations to engines in cars, examples of which are listed in Braun [10] and Norton and Karczub [64]. In this section, Digital Signal Processing is introduced and its relevance to condition monitoring in industry is highlighted. Signal analysis



techniques can be categorised into four types:

- 1) Signal magnitude analysis - e.g. probability densities, mean values, variance, skewness and extreme values.
- 2) Time domain analysis of individual signals - e.g. correlations, covariances and impulse responses.
- 3) Frequency domain analysis of individual signals - e.g. spectral densities, frequency responses, coherences and cepstrum analysis.
- 4) Dual analysis of signals in time or frequency domain - cross correlation between two signals, either frequency or time domain.

### 2.7.1 Time Domain, Frequency and Time-Frequency

Analogue signals are continuous in nature. Digital signals are a collection of discrete data points with respect to time. A signal (recorded as a series of discrete data points in the time domain) can be transformed into the frequency domain by the use of signal processing techniques using the Fourier Transform. The algorithm when applied in the digital context is referred to as the Discrete Fourier Transform (DFT) and the Fast Fourier Transform (FFT). An analysis combining both time and frequency domain will also be covered through the Short-Time Fourier Transform (STFT), as well as associated techniques.

#### Time Domain

Time domain signal processing is the analysis of the signals with respect to time. Discrete signals in the time domain are made up of amplitude and corresponding time values. Depending on the sampling frequency, the number of data points will vary, higher sampling rates will provide more detail, but also require an increased computational effort. Commonly evaluated measures in the time domain include Minimum and Maximum values, Sum of Total Signal, as well as statistical indicators such as Mean, Kurtosis, Root Mean Square, Standard Deviation and Variance.

One time domain measure frequently used in bearing condition monitoring is the Crest Factor, which is a measure of the severity of the amplitude peaks versus the Root Mean Square of the signal. The Crest Factor is defined mathematically in Equation 2.15.

$$CR = \frac{Peak\ Level}{RMS} \quad (2.15)$$

This measure is used in applications such as roller bearings, cavitation and gear tooth wear, any applications where there may be impacts as part of the failure mechanism as cited by Braun in

[10]. A frequency representation of the signal may not show the impacts if the noise is random or non-periodic. A further advantage of this approach is that it is simple to calculate using the time domain signal only. Even though the value as such may not be deterministic, a trend of the Crest Factor may be sufficient to show degradation occurring. This measure, applied to Thermodynamic Traps, could yield some diagnostic merit due to the impact nature of the Thermodynamic Trap mechanism.

### Frequency Domain

The frequency domain provides a representation of a time domain signal in terms of frequency, in other words, how much energy is contained at a certain frequency. The Fourier Transform is the most common technique used to calculate this transform. It was discovered by Joseph Fourier (1768-1830) during study of conduction of heat in two dimensional objects. This problem was mathematically expressed as differential equations and Fourier solved this using an infinite series of trigonometric sine and cosine terms, as shown in the identity 2.16 to solve the problem.

$$e^{j\omega t} = \cos(\omega t) + j \sin(\omega t) \quad (2.16)$$

Years after this solution had been presented, Fourier developed the Fourier integral to analyse non-periodic functions. These expressions are defined by the following equations, the Fourier Transform and the Inverse Fourier transform, in Equations 2.17 and 2.18 respectively, where  $F(\omega)$  is the Fourier transform of the signal  $f(t)$ . Equation (2.17) is also known as the “Continuous Fourier Transform”.

$$F(\omega) = \int_{-\infty}^{+\infty} f(t) \cdot e^{-j\omega t} dt \quad (2.17)$$

$$f(t) = 1/2\pi \cdot \int_{-\infty}^{+\infty} F(\omega) \cdot e^{j\omega t} d\omega \quad (2.18)$$

The inverse Fourier Transform from Equation 2.18 can be rewritten in term of sine and cosine rather than complex exponentials.

Digital signals have to be sampled as a discrete sample. The signal  $f(t)$  is converted into a discrete signal  $f(n)$  by taking  $n = 1, 2, 3, \dots, N$  samples at time  $t = nt_s$ , where  $t_s$  is the sample interval. This transformation from continuous to discrete is referred to as “Discrete Fourier transform (DFT)”. The mathematical definition is defined as:

$$F(m) = \sum_{n=1}^N f(n) \cdot e^{-\frac{j2\pi nm}{N}} \quad (2.19)$$

Therefore, Equation (2.19) can be rewritten again as:

$$F(m) = \sum_{n=1}^N f(n) \left[ \cos\left(\frac{2\pi nm}{N}\right) + j \sin\left(\frac{2\pi nm}{N}\right) \right] \quad (2.20)$$

The computational implementation of the Fourier transform is referred to as the Fast Fourier Transform (FFT), which is an optimised implementation of the Fourier Transform utilising powers of 2 to dramatically increase the speed of computation. The most common Fast Fourier Transform algorithm was published by Cooley and Tukey in 1965 [27]. The first value of the Fast Fourier Transform yields the RMS offset, but the instantaneous time domain information is lost.

Real world applications with complicated signals which include transients or pulses (“non-stationary signals”), which cannot be easily investigated using either time domain or frequency domain processing. For this processing requirement time-frequency methods have been developed to present a signal in terms of both time and frequency. One of these methods is an expansion of the Fourier Transform resulting in the “Short-Time Fourier Transform”.

### Time-Frequency Domain

Time-frequency signal processing can be very useful as it can highlight changes in frequency with respect to time, providing a two-dimensional analysis of the signal. The process to achieve this is by computing a number of Fourier Transforms by dividing the signal into short time-period segments, multiplying these by a window function  $s(t) \cdot g(t - \tau)$  and evaluating the Fourier Transform for the frequency content of that section. For this reason, the method is referred to as the Short-Time Fourier Transform (STFT). Mathematically this can be defined as:

$$STFT(\tau, \omega) = \int_{-\infty}^{+\infty} s(t) \cdot g(t - \tau) e^{-j\omega t} dt \quad (2.21)$$

where:

$s(t)$  = signal in time domain

$g(t)$  = window function

The time and frequency resolution when calculating the Short-Time Fourier Transform is dependent on the shape and length of the window function. This compromise between time resolution and frequency resolution is an important aspect in this type of frequency analysis. Provided the shape and size of the window function remain constant throughout, an analysis of the results will be comparable. Further detail on windows is provided in the next section.

**Window functions and Spectrum Leakage** The equation for the STFT shows a time-based signal which is multiplied by a window function. The Fourier Transform of the resulting signal provides only the frequency components within the limited time period or otherwise the length of the window. The size and shape of the window is application dependent. Examples of windows are the Hanning window and Hamming window. The use of these “distribution-based” windows can reduce the spectral leakage compared with a rectangular window, as tail-off is not as “abrupt”.

The window can be moved along the time domain. The width of window function is dependent on the events being processed and is significant so that most of the frequency details within the limited time period can be identified. Due to the window function and the Heisenberg uncertainty principle, there is a clear resolution issue with this signal processing approach, either there is a good frequency resolution with less time or there is good temporal resolution with poor frequency clarity.

As mentioned, due to the limited frequency resolution in a digitally sampled system, a frequency may fall between two frequency bins, causing components to be reflected and leak into adjacent bins. This effect is known as spectrum leakage.

### **Fault Diagnostic Techniques**

Sharif and Grosvenor [81] listed a number of fault diagnostic techniques for the application in Process Plant Condition Monitoring:

- 1) Logical Method - Detailed knowledge is used to establish a hypothesis and test the hypothesis to solve the fault.
- 2) Algorithmic Method - Using Flowcharts, guiding an operator through the determination of the fault condition.
- 3) Functional Systems Documentation - Based on “divide and Test” this approach divides plant into blocks with defined inputs and outputs, each of which can be tested layers, drilling down until the system with a fault is identified.
- 4) Expert System - This approach reviews individual cases rules are created for specific classifications. This approach requires calibration and future updates as additional failure modes are identified. This is named an expert system as it requires an expert in the field to define the criteria by which the system diagnoses the condition.
- 5) Statistical System - This approach uses statistical parameters to determine the fault condition, allowing abnormal states to be identified. Multivariate Statistical Process Control is an extension to this approach allowing several variables to be considered in parallel.

- 6) Model Based - Based on mathematical modelling, a model representation of the plant can be designed, allowing faults to be investigated. This may be enhanced by Statistical approaches and Kalman Filtering. Fuzzy Logic is another approach from this category.
- 7) Artificial Neural Networks - Artificial Neural Networks rely on training data and examination data to classify the relationship between input and output parameters. This approach is modelled on the function of the human brain and is limited by the training data. If a certain fault is not trained, the system will not recognise it. This approach is an extension to Fuzzy Logic.
- 8) State Transition Diagrams - This method is often used in Programmable Logic Controllers, the system will show the current state as well as the next state allowing an operator identify the problem.

From the list of possible fault detection approaches, a number could be usefully applied to Steam Trap condition monitoring including: Expert Systems, Statistical System and Model Based.

### **2.7.2 Signal Processing Techniques for Flows**

This section will consider certain Signal Processing Techniques and considerations that have to be taken when applying these techniques. The research from these papers provide analogous approaches which could be applied to Steam Trap condition monitoring.

The application of signal analysis to multiphase flow measurement was applied by Pusayatanont in [73]. The techniques applied were in the time and frequency domains as well as well as joint approaches such as the Short-Time Fourier Transform.

### **2.7.3 Analysis of Signals**

Norton and Karczub [64] provides a good background to the Noise and Vibration Analysis for Engineers. Signals can be classified as deterministic or random. Deterministic Signals can be described by mathematical relationship, whereas random signals are defined by probabilities and statistical measures. Signals can also be classified as continuous or transient with respect to time. Transient signals change significantly with respect to time. For this reason, it is more appropriate to analyse the total amount of energy in a transient signal. On the other hand, the average power is a more appropriate measure for continuous signals. For these reasons, transient signals use units of energy and continuous deterministic signals use units relating to power (energy per time unit).

Random signals cannot be described with mathematical relationships, as they have a time history that is neither transient nor periodic. Relevant measures are RMS values, variance, probability distributions, correlation functions and power spectral densities.

Most random signals can be defined as stationary in nature, meaning they are time-invariant, examples of which are atmospheric gust velocities and vibrations associated with a spacecraft during various stages of the launch process. Even if a random signal is non-stationary (in other words, features such as the Power Spectral Density vary with time), these signals can be broken up into smaller quasi-stationary signals. Generally, industrial noise signals are either stationary deterministic (e.g. sinusoidal), stationary random or transient. Whether a signal is defined as stationary or non-stationary depends on the probability distribution. Depending on the time scale at which a signal is being considered, most signals can be described as being stationary, in other words, if the signal features impulses, if the signal sample is long enough and includes a representative number of impulses, the signal could be determined to be stationary.

In steam systems, there are many parts that could produce a random response, examples of which include changes in piping, turbulent flow, orifices and thermodynamic or flow regime changes.

Four types of statistical functions are used to describe random signals:

- 1) Means-square value and variance - Provide information about the amplitude of the signal
- 2) Probability distributions - Provide statistical information on the amplitude domain of the signal
- 3) Correlation functions - Provide statistical information on the time domain of the signal
- 4) Spectral density functions - Provide statistical information

The next section will review applications in related fields of Condition Monitoring

## **2.8 Condition Monitoring in Related Industrial Applications**

As mentioned previously, little published work has been found on Condition Monitoring of Steam Traps. Therefore, a number of related subject matters have been reviewed and a number of key papers are presented below, divided into relevant areas of interest.

### **2.8.1 Pipe Leak Detection**

Taghvaei et al. [95] applied cepstrum analysis to the detection of leaks in pipes carrying water. A sharp impulse signal was created using a solenoid valve and a quick opening and closing action, sending a pressure pulse down the pipe. The system response was mapped for the undamaged system. Subsequently, holes were drilled in the pipe to simulate leaking conditions. These signals were analysed using cepstrum wavelet and cross-correlation analysis. A correlation was found

between the leak size and the amplitude ratios of the resonant peaks of the pressure waves and reflections. This work would not be suitable for a steam system, as pressure waves would not be acceptable to processes and the two-phase flow nature (as well as possible inclusion of non-condensable gasses) could cause the system to be highly unreliable .

Srinivasan et al. [92] investigated the acoustic emission from the injection of different substances (water, argon and hydrogen) and steam/water into sodium in an evaporator. The acoustic emission signals were analysed by calculating the power spectral density (PSD) as well as other parameters. The PSD showed peak frequencies in the region between 35kHz to 45kHz approximately, which the authors relate to the injection of substances.

### **2.8.2 Valve Leak Detection**

There are several papers describing the estimation of leakage. Thompson and Zolkiewski [100] investigated through valve leakage using nitrogen, argon, carbon dioxide and helium. A spectrum analyser from Bruel&Kaer was used to analyse the signals under the various test conditions. The authors highlight that when discharging to atmosphere, acoustic emission peaks have been found in the range of 32-44 kHz in a bandwidth of about 5-6kHz. However, analysis of this paper focusses on frequencies below 20kHz. The work highlighted that the acoustic emission is independent of leak rate, pressure drop and set-up of the piping, but is affected by the diameter of the pipe. Interestingly, an orifice was found to provide the same response as the valve when replaced. Although the results were found to be repeatable, this method does not provide a universal application and complements other techniques. The conclusion of this investigation highlights that the analysis of signals below 20kHz is only possible when a high signal to noise ratio is possible. For larger leaks or high background noise application, higher frequency approaches must be used. This approach is very applicable to valves, where there is low dynamic noise from the dynamic motion of the mechanism, which is not the case in most of the Steam Traps.

Sharif and Grosvenor [82] investigates the internal leakage of air through a valve as a continuation of the work by Thompson and Zolkiewski [100]. As Thompson's work was related to below 20kHz acoustic emission, which is affected by low frequency industrial noise, this paper reviewed the effect of industrial noise on this approach. The paper demonstrated that low levels of leakage at low pressures can be detected by acoustic emission (AE). The application of a 20-100kHz resonant sensor picked up noise in the low kHz region resulting from background noise from machinery as well as features resulting from the leak in the valve. It is worth noting that, although the 20-100kHz sensor was more sensitive, the 0.1-1MHz sensor required less filtering. The improvement in the results over Thompson were achievable due to the technical advances in data acquisition and filtering equipment.

Püttmer and Rajaraman. [75] investigate the measurement of leakage through a valve in accordance with ANSI/FCI 70-2 and IEC 60534-4. This approach requires valves to be closed and water to be used as a test medium, which is impossible in the case of a Steam Trap, as the mechanism is automatic and flow is two-phase, sometimes including non-condensable gasses. The paper suggests that due to poor correlation, the determination of leakage rate from acoustic emission level measurement as applied to control valves is not possible.

Kaewwaewnoi et al. [49] investigated the relationship between internal leakage through a valve and the resulting acoustic emission using power spectra. The experimental setup was created as well as theoretical calculations made. It was discovered that the theoretically derived sound was very much in agreement with the acoustic emission signal power. The experiments were carried out with water and air. A good correlation between the acoustic emission response and the leakage rate was proven. However, the correlation factors were different between air and water, further highlighting the limits of this approach in relation to steam, as the two-phase flow of steam and condensate changes between the liquid and gas phase are continuously based on flow conditions.

Chen et al. [24] investigated the integrity of hydraulic seals as applied to a water hydraulic cylinder both through experimentation as well as simulation. It was demonstrated that internal leakages below 1.0 l/min can be predicted. It was also concluded that energy-based approaches are more suitable than the acoustic emission count rate or peak PSD data in interpreting the acoustic emission signal generated by internal leakage in an hydraulic cylinder. Finally, AE RMS values and internal valve leakage are both very much in a linear relationship and could therefore be applied to a quantitative acoustic emission model for the assessment of leakage.

### 2.8.3 Flow Measurement

Pusayatanont et al. [72] investigated the use of conventional flow meters for the metering of multiphase flow, more specifically steam and its dryness fraction. The methodologies applied were the power spectrum, and the Fast Fourier Transform. In terms of the correlation between the measured and estimated steam dryness, the error was defined as at 1.6%, based on a power spectrum density equation in the range of 30-250Hz.

Kim [50] investigated the measurement of the two-phase flow in single-phase turbine and vortex flow meters using air and water mixtures. Wavelet and time-frequency methods were applied to the signals, which clearly extracted the vortex shedding frequency. The noise from the two-phase flow however was not clearly identifiable using these methods.

Evans et al. [30] discusses the use of the time domain signal for non-intrusive flow measurement of water and air by considering the acoustic emission from pipe work. A strong determin-



istic relationship between the standard deviation of the frequency averaged acoustic emission signal and the flow rate is shown. The experimental results show a near quadratic relationship between the signal noise and flow rate in the pipe and the dependency on materials and diameter is presented.

Lay-Ekuakille et al. present the application of the FFT and STFT to signals from a pressure transmitter to determine the leakage from water pipes and reduce water leaks. A simulated system of water pipes was used to create data. Both linear and quadratic regression were applied to ensure the frequency data was comparable. The paper demonstrates the application of the STFT to leak detection determination [52].

Jardine et al. [47] outline Condition Based Maintenance (CBM) summarising and reviewing the recent development in time, frequency and time-frequency domain analysis approaches. The increase in multi-sensor approaches are also covered as well as algorithms provided for different applications.

## 2.9 Relevant Signal Processing Methods

Yella et al. [108] describe pattern recognition and processing methods for application to acoustic emission. The paper overviews the application of signal processing and feature extraction techniques, specifically support vector machines and Multi-Layer Perceptron neural network to woodworking applications. The assessment of wooden structure using NDT methods was proven possible.

Hauptmann et al. [41] discuss the state of the art of ultrasonic sensors as applied to monitoring of flow; current large-scale applications involve level and flow measurement. The limitations of this approach are also highlighted and commercial examples presented. The challenges and lack of maturity of ultrasonic approaches are discussed, highlighting that the trend for use of ultrasonics in monitoring is increasing, suggesting that in-line concentration and particle size measurement is expected to see the most significant impact in industry.

Püttmer [74] discusses new ultrasonic sensor applications in industry, highlighting that the need for continuous condition monitoring requires a condition monitoring system for all key plant components. The links with industrial application are also highlighted.

Yang et al. [107] investigated the monitoring of cavitation noise by applying vector support machines to butterfly valves. Statistical methods were used to identify stationary features. Using this signal, the support vector machines were trained and classified. The classification has also been compared with that of a self-organising neural network. The success rate of classification was 100% for both training and test sets. The use of these advance techniques in condition-based

maintenance is highlighted as well as the consequences on realtime system are discussed.

The application of RMS as a measure of leakage in a high-pressure coolant system in nuclear reactors is described in Morozov [59]. The approach described in the paper utilises an acoustic sensor, communication cables and interpretation hardware. Acoustic signals are analysed for two features. Firstly, the Power Spectrum Density is used in the setup to evaluate the frequency spectrum being recorded from the process. Secondly, the signal proportional to the logarithm of the RMS of the acoustic signal is used to evaluate changes in the process allowing leakage to be evaluated.

Wang and Tong [105] used the measurement of differential pressure noise from orifices for a range of steam dryness rates and pressure values to measure two-phase flow. A theoretical model was developed and fitted to a practical model. The results of the study create a measure of two-phase flow in real time using only one orifice. Statistical measures for the measurement of two-phase flow have been applied based on the stochastic nature of the samples used.

**Discussion** Following the review of the published literature, the following key points can be summarised:

- 1) It is clear that the acoustic signals for the Steam Traps will not be deterministic in nature and possibly require a multi-variable approach and statistical analysis of the signals due to the chaotic randomness of the flow regimes.
- 2) The application of time and frequency approaches has been reviewed and there is merit in covering both domains as well as the joint time-frequency domain in the analysis of the acoustic emission due to the changing nature of the acoustic signal of traps during their operation.
- 3) From a classification point of view, basic statistical approaches will be applied and reviewed.

This chapter has presented the theoretical background to this investigation. However, little specific literature has been found on the condition monitoring of Steam Traps. It is uncertain whether no work has been carried out in this field of study or whether any results are not available due to confidentiality reasons.

## 2.10 PESTLE Analysis on Condition Monitoring for Steam Traps

The PESTLE analysis tool is a method used to analyse issues using the six key areas. PESTLE is an acronym for Political, Economic, Social, Legal, Technological and Environmental as described by Gillespie in [37]. The section summarises the reasons for this research, providing an application-based context for the work and highlighting the value of this research contribution.

### 2.10.1 Political Factors

The reduction of energy consumption, energy wastage and harmful emissions has been, and continues to be, widely reported in the media and has become an important agenda item for many institutions and countries around the world today, as evidenced by current environmental directives listed below:

- UK Carbon Reduction Commitment
- UK Climate Change Levy
- EU Renewables Directive
- EU Emissions Trading Scheme
- Intergovernmental Panel on Climate Change
- Kyoto Protocol successor agreement
- United Nations Framework for Climate Change

Although it appears that using energy more efficiently and wasting less energy are obvious Economic Factors, sometimes Political Factors can influence industrial behaviour, leading to the adoption of less damaging environmental operating protocols. Directives, such as listed above, are not necessarily more or less economically advantaged, but rather form a cooperative body of political will to improve the use of finite energy resources and decrease pollution. The Department for the Environment, Food and Rural Affairs published the guidance on how to measure and report greenhouse gas emissions for UK businesses and organisations.

### 2.10.2 Economic Factors

Industry in the UK is estimated to consume approximately 250,000GWh of fossil fuel per annum of which 35% is used in steam boilers as reported by the Carbon Trust [16]. The estimated cost of a tonne of steam has increased from approximately £12-15 in 2005 to approximately £22-25 per tonne in 2011.

Approximately 15% to 21% of Steam Traps in industrial plants in the USA without a regular maintenance program are reported as “Failed”, indicating higher carbon emissions than there should be as indicated in a report by the US Department of Energy [31]. Spirax Sarco estimates “Failed” rates could be as low as 5% for Steam Traps with a regular maintenance program.

The Carbon Trust was established to increase innovation as well as trading activities related to energy saving activities. In addition, climate change is a key part of the overall Seventh Framework Programme which in total provides up to €50.5 billion of funding for innovation support.

A Steam Trap working 8,400 hours a year and leaking an average of 10.8kg/hr (which has been found to be a reasonable estimate) will result in carbon emissions of 13.97t/yr (see Appendix A.2). This calculation was based on part of a Carbon Trust grant application as part of this research [20].

Also, Directives created by Political Factors will have a direct impact on Economic Factors of the industrial world by introducing financial penalties or incentives for the environmental impact in the way a product is brought to market or managed.

### **2.10.3 Sociocultural Factors**

Social and Cultural influences on business vary from country to country and it is important that such factors are considered. The design of an efficient Steam Trap condition monitor could have wide-reaching energy saving implications such as: reducing energy required to raise steam, reduced carbon emissions by reducing the energy and reducing the fresh water processed by the plant to make up for lost steam.

With increased legislation, there will be more pressure on companies. ISO 14001 is an environmental accreditation that companies hold to show their approach to the environment and this could be affected by the use of the energy monitor.

### **2.10.4 Technological Factors**

The UK market for Condition Monitoring Equipment has increased by 18% from £130 million to £160 million in 2008-09 according to Plemsoll Portfolio Analysis which was mentioned in an article in Process Engineering [68]. This is a clear indication that Condition Monitoring is essential to efficiency performance improvements driven by political and economic factors, not to mention the current recession. Also, dramatic increases in adoption of wireless systems in industrial settings and the reduction in cost of producing small electronic devices are making development of a Condition Monitoring device a much more realistic proposition than ever before.

### **2.10.5 Legal Factors**

The Climate Change Act in the UK in November 2008 provides for a legally binding target to cut carbon emissions to 80% by 2050, to be achieved through action in the UK and abroad. An interim reduction in emissions of at least 34% by 2020 was also established. Both of these targets are measured against the pre-industrialisation carbon emissions baseline in 1990 in the Climate Change Act 2008 [29].

Key outputs are:

- 1) Carbon budgeting system which caps emissions over five-year periods, for which the Government must report to Parliament, its policies and proposals to meet the budgets;
- 2) Further measures to reduce emissions, which include options to introduce domestic emissions trading schemes, supported through, among others, a Carbon Reduction Commitment Energy Efficiency Scheme, measures on biofuels, powers to introduce pilot financial incentive schemes in England for household waste; and
- 3) A requirement for the Government to issue guidance on how companies should report their greenhouse gas emissions, and to review the contribution reporting could make to emissions reductions by 1 December 2010.

Carbon trading became law in 2010 in the UK with a charge of £1000 per ton of  $CO_2$  emissions for high and medium industrial users of energy. The main aim of this act of law is to encourage transition towards a low carbon economy within the UK and demonstrate leadership and responsibility towards the goals set out in the Copenhagen 2009 Global Agreement to the reduction of carbon emissions after the year 2012.

In terms of the European Union, more ambitious targets have been established beyond the agreements in the Kyoto Protocol by the European Climate Change Programme. This programme seeks to prevent temperature increases beyond 2 degrees C above pre-industrial levels. Improvements as part of this programme include: the improvement in energy efficiency by 20%, the increase of energy from renewables sources to 20% of all energy and to cut greenhouse gas emissions, at a minimum, by 20% from the levels in 1990.

To achieve these ambitious targets, the EU Emissions Trading Scheme has been established as well as a number of standards and regulations.

#### **2.10.6 Environmental Factors**

This research work contributes to the reduction of Steam Wastage and associated additional carbon emissions. The environment is defined by the Environment Agency as the land, air and water, all of which are effected by increased emissions. The reduction of industrial emissions will form a part of the measure that can be taken to reduce risk of further climate change.

Additionally, fresh water is becoming a scarce resource as highlighted by the Economist Magazine in a recent article [39]. The reduction of atmospheric steam losses will reduce the need for make-up water to replace the “lost” steam in a process as well as reduce the boiler chemicals required.

## 2.11 Summary

The chapter has introduced Steam Traps and their applications. The current state of surveying and the methods used have been discussed. Possible opportunities for signal processing and pattern recognition techniques have been proposed. The chapter has introduced the source of the acoustic emission, two-phase flow and digital signal processing. Literature that is of interest has also been highlighted.

The key findings are listed below:

- The likely sources of the acoustic emission have been presented, including cavitation and two-phase flow. The complexity of two-phase flow has been highlighted, especially in reference to expected flow regimes.
- Relevant signal processing approaches have been covered including frequency, and time Frequency opportunities for signal processing and pattern recognition techniques have been proposed.
- No specific knowledge or research into the acoustic emission from Steam Traps has been found. The author is aware of other confidential work carried out at Spirax Sarco related to Steam Traps which cannot be discussed due to confidentiality reasons.
- A Pestle Analysis has been used to set the greater context of this research. Environmental and economic impacts have been highlighted.

*The next chapter will be covering the experimental setup of the rig and the data acquisition software/hardware used to gather the data for this investigation.*

## Chapter 3

# Experimental Design for Steam Trap Wastage and Acoustic Measurement

*This chapter presents an overview of the experimental setup, both for testing of Steam Traps and acoustic data capture. The steam plant layout, the Steam Wastage Rig and the necessary sensors for the data acquisition are described at a basic level. The design of the data acquisition hardware and software used to evaluate the Steam Wastage Rig as well as the hardware and software aspects of the acoustic data acquisition are described in more detail. Lastly, a review of the captured data is presented as an introduction to the subsequent data analysis chapters.*

### 3.1 Testing Setup and Methodology

The research work carried out in this thesis requires two data sets to be analysed simultaneously:

- 1) Steam Wastage data needs to be obtained for different Steam Traps in a number of typical operating conditions.
- 2) Acoustic data needs to be obtained for different Steam Traps in a number of typical operating conditions.

Both these datasets must be recorded in parallel, so that the two data sets can be subsequently analysed and correlated for comparisons to be made.

Two Steam Wastage Rigs were designed to facilitate the testing of the Steam Traps. The steam is provided from a boiler to the rig. The condensate is water raised in pressure and temperature and injected into the rig. Electronic software and hardware record sensor readings and evaluate the Steam Wastage Value by calculation of an energy balance.

The next section describes the Steam Wastage Rigs.

## 3.2 Setup of Steam Wastage Rig for Testing of Steam Traps

### 3.2.1 Steam Wastage Standard

Two Steam Wastage Rigs were built to evaluate the steam loss from Steam Traps using the Steam Wastage standard BS EN 27841:1991. The Steam Wastage standard has been introduced in Section 2.3.1. In this section, the detail for the two rigs utilised in this research are covered. The first rig, St Georges Road Steam Wastage Rig (SGR), is based on the method A of the standard and the other, Runnings Road Steam Wastage Rig (RRR), is based on method B.

### 3.2.2 St Georges Steam Wastage Rig (SGR) Specification and Design

The Steam Wastage Rig according to method A of the BS EN 27841:1991 standard was designed and built in Spirax Sarco's St Georges Road test shop by Research Department staff and the author. This rig allows steam plant conditions to be simulated. The standard is limited to very low condensate loads due to the assumptions made. For this reason, the rig had to be extended in terms of the limits of the standard to simulate a representative set of operational conditions. A process identification diagram for the flowline and water injection is provided in Figure 3.1.

In the case of the St Georges Steam Wastage Rig a condensate load of up to 200 kg/hr and an operating pressure of up to 20 barg can be generated, limited by the steam flowline fittings. The steam is provided from a central steam generator, which can operate at up to 69 barg. At the starting point of the flowline is a 750 litre pressure vessel. The steam to the vessel is provided at a maximum of 39 barg to the central vessel. Air at 40barg as well as water at up to 5 barg can also be supplied, neither of which are used in the Steam Wastage Rig setup.

From the vessel, a 2 inch diameter flow-line extends out to which the Steam Trap test setup is connected. A condensate injection point is fitted to the flow line, approximately 4 metres downstream from the vessel. A further 4 metres from the injection point, a separator is installed to simulate a dirt pocket. The outlet of the separator is piped to a drop-leg, similar to a standard Steam Trap installation and includes Steam Trap isolations valves as well as a strainer. A process identification diagram is provided in Figure 3.4 and photographs of the actual setup are shown in Figures 3.2 and 3.3. In the case of method A, only one capture tank is used, as the mass balance and temperature difference of the sparge tank are evaluated to calculate the Steam Wastage Value and condensate load. Schematics and pictures relating to the rigs are also provided in Appendix C.3.2.



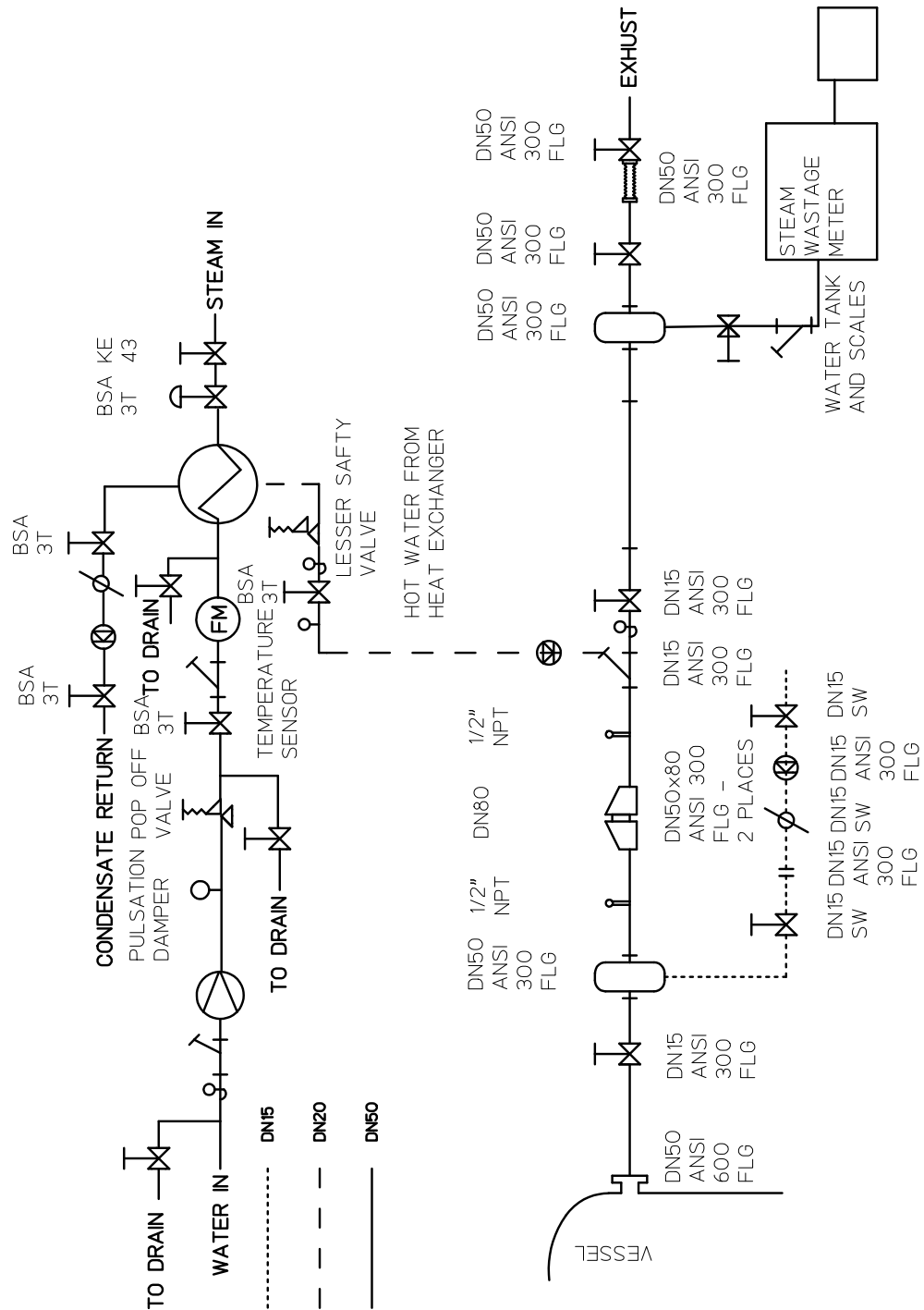


Figure 3.1: SGR Rig Steam Trap Test Station Diagram

### 3.2.3 Runnings Road Steam Wastage Rig (RRR) Specification and Design

The Steam Wastage Rig at the Runnings Road site pre-existed this research project and was constructed by colleagues at Spirax Sarco. This rig has been designed within the limitations of the BS EN 27841 standard for very accurate calculation of the Steam Wastage. For this reason, this rig can only operate at up to 16 barg of pressure and a condensate load of 15 kg/hr. To attain high

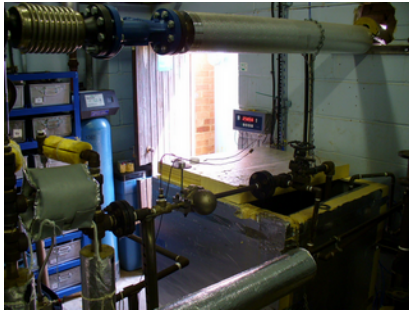


Figure 3.2: SGR Test Area - Tank and Weight Scales



Figure 3.3: SGR Test Area - Steam Trap Test Setup

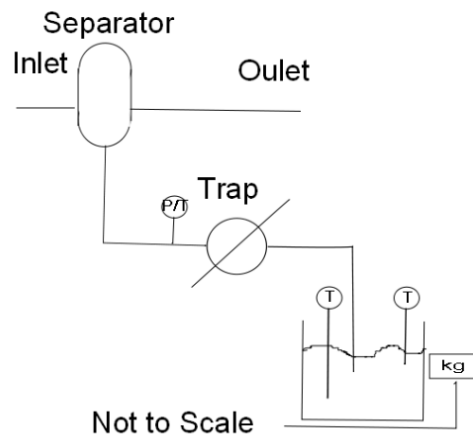


Figure 3.4: SGR Rig Steam Trap Test Station Diagram

accuracy in calculation, the scales of the rig have a small range (maximum weight measurement of 15 kg load) but also a high measurement resolution at 0.05 kg. The rig is supported by a custom designed LabView based Data Acquisition and Steam Wastage Evaluation software.

### 3.2.4 Comparison of Operation of the two rigs and consideration of BSEN 27841

As mentioned at the start of the chapter, the importance of the data acquisition is to record the acoustic signals and accurately calculate steam wastage over a given period. Both methods for Steam Trap characterisation suggested EN 27841 suffer from the dynamic and non-stationary behaviour of Steam Traps. As Steam Traps generally do not leak continuously, or sometimes exhibit temporary damage, i.e., through dirt on the seat, an average Steam Wastage Value measured over a relatively long time period, such as 5, 10 or 15 minutes is not representative of the instantaneous leakage at any given moment. Providing these instantaneous events are periodic and repeat several tens of times during a 5 minute test for example, the averaging will not affect the results. However, if these events are temporary, i.e. a change occurs during the acquisition time (some



Figure 3.5: Runnings Road Steam Wastage Rig

dirt is removed for example), then the acoustic signal and averaged Steam Wastage Value will not match the recorded acoustic signal. For these reasons, a Steam Wastage Meter was designed based on the Spiratec Steam Trap diagnostic device [90]. However, data from this device is not included in this investigation.

Additionally, Steam Wastage Measurement using the EN 27841 standard is only applicable to small leakages and low condensate loads. These conditions only represent the worst case scenario of a Steam Trap operation and not the normal operational conditions. For this reason, one of the rigs built to method B, is designed to the standard, whilst the other rig exceeds the standard requirements.

It is worth noting that a Spirax Sarco internal report conducted by National Engineering Laboratories [63] described the use of the Steam Wastage Standard for diagnosis of Steam Wastage in Steam Traps on a previously designed test rig that was no longer available. The report found a remarkable repeatability of results that has not been possible to be reproduced in the new rig. The reason for this may be that the current work is focussed on establishing Steam Wastage Values for the full operational range of a trap, rather than for limited number of “ideal scenario” tests, which are described in the standard.

### 3.3 Steam Wastage Measurement Data Acquisition and Processing

The design of the data acquisition and Steam Wastage calculation software for the SGSWR was conducted as part of this research. The following sections discuss the hardware used to establish the Steam Wastage measurement, as well as an overview of the sensors used. An overview of the LabView software, written to calculate the Steam Wastage, is also covered.

### 3.3.1 Data Acquisition Hardware

The data acquisition hardware used to acquire parameters from the SGR Steam Wastage Rig are discussed in this section. Initially, two PICOlog devices were used and weight measurement manually collected. However, the author decided to make a number of improvements to the rig and designed a LabView based acquisition system which also acquired the weight data, details of which are provided in the subsequent sections.

#### Picotech Hardware

The data acquisition system initially utilised on the SGR rig was based on a PICOlog analogue to digital voltage converter (ADC11) and thermocouple converter (TC08) for 4-20mA and T-type thermocouples respectively. The driver PICOlog software was configured to handle the thermocouple channels and the 4-20mA channels for the pressure readings, porting them from the hardware via USB to the operating system on the laptop computer. The mass reading from the scales were manually recorded from the display of the weighing scales at a 1 minute rate and entered into the spreadsheet by the operator.

As indicated, this setup had several shortcomings, primarily from the manual recording of the mass values from the scales as well as the slow acquisition rate of 1 sample/minute for the other measurements. This procedure resulted in a lot of human error and poor timing of the measured points.

#### National Instruments Hardware

A LabView data acquisition system was designed using a LabView 8.5 Development package software. The design for the LabView system introduced automatic weight acquisition, a sampling rate of 1 sample per 2 seconds and an automated recording system including weight measurement and storage of test results.

The hardware consisted of a USB cDAQ9011 chassis with a thermocouple NI9211 and 4-20mA NI9203 sensor input modules. The weighing scale indicator is also directly connected to the computer using a serial connection to transmit the current mass from the weighing scale display to the software. To facilitate the transfer, an RS232 serial link was designed using an EasySync "Serial-to-USB" converter and the standard RS232 library within LabView.

This LabView system is designed to record all required data channels (four temperature, one pressure and one serial communications measurement) at 2 second intervals. A suitable visual instrument was designed to stream current data values to the display screen during the setup phase of a test. Once a test is started, the data is displayed on the screen and simultaneously recorded to an array. Once the acquisition period has been completed, the data is manipulated

using an embedded Matlab script to evaluate the Steam Wastage Value and Condensate Load. Finally, the data is written to a comma-separated value file for the test. Key information is also logged into a test log which contains all the test activities conducted, akin with the index in a book.

The advantages of this improved system are that the process is automated, the acquisition rate is faster and more precise and the data is collated in a more organised manner. The LabView system has improved the Steam Wastage Rig performance and the completion rate of tests. It has also allowed the time duration of the tests to be reduced from 15 minutes to 10 minutes and following some further validation to 5 minutes per test run.

### **3.3.2 Steam Wastage Rig Sensors**

The Steam Wastage calculation relies on the acquisition of analogue signals of pressure, temperature and weight for the calculation of Steam Wastage of a Steam Trap. These individual sensors are described below:

#### **Pressure**

The pressure sensor is a standard pressure transducer providing a 4-20 mA output for a given range of input pressure. The sensor contains a bellows with a strain gauge sputtered onto a thin plate. When the thin plate is pressurised, it bows and the strain gauge measures the strain which can be related to the internal pressure of the bellows. The in-built electronics convert this measurement into a 4-20 mA signal for re-transition. These sensors are off-the-shelf and are available in several pressure ranges. The range used on the SGSWR is a 0-40 barg sensor and is sold by Spirax Sarco.

In terms of data acquisition, the pressure transducer was connected to the National Instruments cDAQ through a 4-20 mA module. This module features channel separation and individual 24-bit resolution capture signal with a range of 0-20mA. The 4mA is a standard DC offset of the loop which provides the power for the instrumentation to work. The “raw” signal has a span of 16mA, which is correlated with the pressure output. Due to this relationship between mA and pressure, the sensors are calibrated before installation to ensure the signals are accurate. This signal was sampled with 10Hz frequency, averaged and then compared by test to ensure that no noise fluctuations caused the signal to be biased.

#### **Thermocouple**

Thermocouples utilise the Seebeck effect [46]. In thermocouples, two dissimilar metals are joined. When this joint experiences a temperature gradient, a voltage difference, which can be measured

and related to temperature, is created. Two types have been utilised in the rigs; type-K and type-T.

Type-K thermocouples are chromel-alumel and are most commonly used in industry as the measurable temperature range is very broad; from  $-200$  to  $+1350$  °C. The measurement sensitivity is approximately  $41$  V/°C. Type-T thermocouples consist of copper-constantan metals and the measurable temperature range is lower from  $-200$  to  $350$  °C. In this application, the type-T is more advantageous as the temperature range is more closely matched to the observation range. Consequently the type-T results in a better measurement resolution, as the measurement sensitivity is comparable with the type-K at  $43$  V/°C.

### Scales

The weighing scales used in the rig utilise a four-way strain gauge bridge mounted under a plate upon which the weigh tank is placed. This strain gauge bridge is connected directly to a display unit which converts the strain gauge signal to a mass reading using a Wheatstone Bridge. The display unit provided an RS232 serial communication retransmit output which was used to transmit the signal from the display to the Easysync Serial-to-USB converter attached to the data acquisition computer. Using these communication protocols, the measurement was transferred to the computer and used in the calculation in LabView.

### Sensor Calibration

Sensor measurements have an associated accuracy range. If higher accuracy is required, calibration can provide certainty on the accuracy of the sensor signal. In the case of thermocouple and pressure sensors, a tight accuracy is required to ensure accurate data is recorded and evaluated. As the transfer functions for both sensors are linear, a straight forward calibration procedure, which will be described in a subsequent section, can be implemented [33].

All sensors were calibrated before the rig was commissioned and are checked regularly. In the case of the individual sensors, these procedures are detailed below:

- 1) **Pressure Sensor** is tested using the calibration equipment, which is a standard dead weight tester for pressure transducers. From the calibration curve, the calibration factors are calculated and factors imported into the LabView Software.
- 2) **Temperature Sensor** is tested using a thermocouple calibration device which uses a high precision heating element to provide a precise amount of heat and is regularly externally calibrated. The thermocouples are placed in the device and the output measured. These values can be compared and a calibration correlation be produced. When tested, the thermocouples showed less than  $0.5$  °C drift at  $200$  °C.

- 3) **Scales** are tested and calibrated by an external calibration contractor on an annual basis. The advantage of the RS232 link is that any calibration effects are dealt with upstream of the data capture, i.e. in the display unit of the device. This approach negates the need to adjust the weight measurement in the LabView software.

The author additionally designed a visual instrument module in the LabView software to allow for calibration constants to be adjusted in the software. As a security measure, only authorised users could log in to this software module.

### **3.3.3 Steam Wastage Calculation Algorithm**

As mentioned previously, the data acquisition system initially utilised on the SGRSWR was based on PICOlog hardware and an excel-based Visual Basic (VB) software. Subsequently, this was upgraded to National Instruments hardware and software. The following sections cover the details of the software setup.

#### **PICOlog Data Calculation Software**

In PICOlog data was transferred to Microsoft Excel using Dynamic Data Exchange (DDE) protocol within a VB script in Excel. The mass reading from the scales had to be manually recorded from the display of the weighing scales and entered into the spreadsheet. Readings of the pressure and temperature sensors were taken every 1 minute over a period of 15 minutes per test run. The VB script also performed the Steam Wastage value calculations on the completed dataset.

#### **LabView Steam Wastage Evaluation Software**

The LabView software, which was designed by the author for the rig as part of this research project, is made up of several levels of Visual Instruments (VI) , which are individual programs based on visual programming. Several VIs have been written and are combined to create the Steam Wastage software. The complete software contains seven VIs , which are Graphical User Interfaces (GUI) visible to the user, as well as seventeen subordinate VIs (SubVI), subroutines which run in the background and are not visible. Further, one initialisation file, one integrated Steam Wastage table, a password list and calibration file were created. An alphabetical list of the main graphical VIs is provided below:

- 1) Acquire Data.vi - GUI for data acquisition.
- 2) Calibration SWR.vi - GUI for calibration of sensors.
- 3) Global.vi - Used to exchange values between VIs (not seen by user).

- 4) Login User.vi - GUI for User Login.
- 5) Setup Test.vi - GUI to setup a test and enter details of the Steam Trap and test conditions.
- 6) Toplevel SWR.vi - Master GUI linking all the GUIs (acts as a navigation pane).
- 7) View SWR results.vi - GUI to view the results of current and past test data.

Further details of the software, as well as the list of SubVIs are provided in Appendix C.3.3.

### **Data Acquisition Screen and Steam Wastage Data Presentation**

The Steam wastage was presented in a tabular form in a GUI and saved for future reference in a .CSV file. A picture of the GUI is provided in Appendix C.20.

A number of screen shots are provided in Appendix Section C.3 highlighting the complicated nature of the new system.

## **3.4 Acoustic Data Acquisition**

The acoustic data was recorded using laptop and PCMCIA data acquisition with a 16-bit A/D converter and 16 input channels. A single channel can be recorded at a sample rate of 200kHz, but as the channels are multiplexed, if more than one channel is used, the maximum rate is 100kHz divided by the number of channels used, i.e. if two channels are used, the maximum sample rate would be 50kHz per channel. The PCMCIA card was chosen for high data rate and portability. The specific PCMCIA card used was a DAS16/16 from Measurement Computing to convert analogue signal from the acoustic sensor to a digital signal. Channel 0 and channel 1 were used for the acoustic data acquisition at a rate of 50kHz. The heterodyne signal is a narrowband signal with a range from 0-5kHz and a drop-off of about 10kHz. No additional filtering was applied to the input signal, as the PCMCIA card includes hardware anti-aliasing and, furthermore, the signal has been oversampled by approximately 5 times using the 50kHz.

### **3.4.1 Acoustic Sensor**

The input sensor used to record the acoustic data capture was the UE Systems UP100. This is a hand-held probe for condition monitoring of rotating machinery and other devices. The probe has a narrowband bimorph Lead Zirconate Titanate (PZT) ultrasonic sensor centred at 40kHz. The bandwidth of the sensor is approximately  $\pm 3$ kHz. The sensor attaches to probe, which has an internal heterodyne circuit, providing an audio jack output. This circuit transfers the ultrasonic signal to a lower frequency bandwidth which can be heard by an operator. Parts of the probe are (taken from [88, 87]):





Figure 3.6: Heterodyne Probe Nomenclature

- 1) Stethoscope Module
- 2) Heterodyne Module

The UP100 Probe is the complete unit consisting of both Stethoscope and Heterodyne Modules.

### 3.4.2 Experimental Setup for Acoustic Signal Acquisition

The Stethoscope Module was clamped onto the pipe using a special clamp and stand-off to provide thermal barrier as in Figure 3.8. The Stethoscope Module was connected to the UP100 Heterodyne Module using a coaxial cable. From the Heterodyne Module, the data was transferred into a breakout box via a 2.5mm jack audio cable and then recorded using a C-based software application using drivers for the PCMCIA card as in Figure 3.7. The Heterodyne Module includes an attenuation control for use with the headphones. The attenuation control was set to 40 dB, which allowed the signals to be recorded without clipping to ensure no aliasing is introduced. The input voltage on the DAQ card was set to  $\pm 5$  volts to reduce the quantisation error of the bipolar input signal.

### 3.4.3 Acoustic Data and Signal Recording Software

The software saves the acoustic data as a .dat file with a filename made up of date and a time stamp, which is recorded and placed in a chronological order in the folder structure. A Graphical User Interface allowed the recording to be managed and controlled, as seen in Figure 3.9.



Figure 3.7: UP100 Experimental Hardware Setup

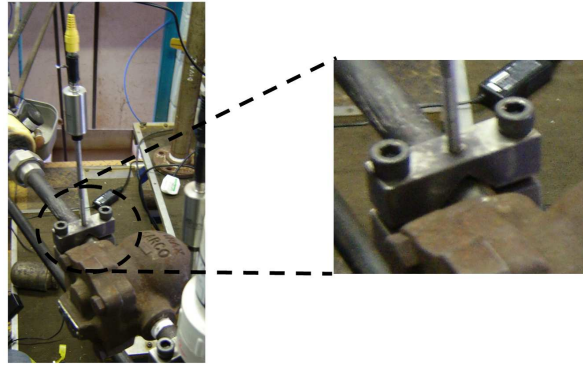


Figure 3.8: UP100 Clamp on Steam Pipe

Figure 3.9: Acoustic Recording Software Setup

The details of the test are recorded in a text file with the same name. Furthermore, the text files were collated into a comma separated (.CSV) index file within the same folder, with each successful recording appended to the bottom of the file. This software was designed by an external contractor for the purposes of this project.

The acoustic data is saved as a .dat file encoded using 16-bit unsigned integer encoding and the associated test information is collated in a text file of the same name. The filename has been chosen as the date and time of the test, as this was deemed the most straight forward and unique method to identify files and prevent over writing of any existing file.

## 3.5 Steam Trap Test Experimental Procedure

### 3.5.1 Overview

The Steam Wastage Rig has been described at length in Section 3.2. This section covers a brief procedure for the data capture.

### 3.5.2 Procedure

This procedure assumes that the rig has been prepared for use according to the standard operating procedure and that a suitable trap is installed in the flow line. In terms of operating the rig, the general process is as follows:

- 1) Set pressure and condensate load.
- 2) Once the conditions are set, warm up the flow line using the trap bypass valve.
- 3) Once the flow line is warm, open the trap stop valve to warm the trap through, ensuring the bypass valve is closed.
- 4) Once warm, the rig should be reset, i.e. the tanks emptied if necessary.
- 5) Ensure that the data acquisition software for both the Steam Wastage calculation and acoustic data acquisition is ready.
- 6) Close the bypass valve and open the valve for the rig.
- 7) Run the test for the necessary time (5,10 or 15 minute).
- 8) Ensure all data is recorded.
- 9) Close the main valve, open bypass valve.
- 10) Reset the rig, i.e. empty the tanks, if necessary.
- 11) Setup the next condition (pressure, condensate load and Steam Trap) and repeat test steps 2 to 10, or shut the rig down, gradually venting the steam pressure.

The procedure for an individual test is repeated a number of times (usually four), to allow variability of test data to be reviewed. The list above covers the outline procedure for data acquisition.

### 3.6 Summary

This chapter has presented the experimental setup used, both from a Steam Wastage and acoustic point of view. An overview has been provided of the National Instruments data acquisition hardware and software used. The acoustic setup introduced the Heterodyne Probe as the acoustic data acquisition sensor. The key findings are listed below:

- A test rig was successfully designed and built to simulate a number of steam trap operating conditions. Much of the requirements of the BSEN standard have been adhered to. However, in terms of the allowable condensate load, the allowable value in the standard has been extended to allow real operational conditions to be tested.
- A Steam Wastage calculation and data acquisition system was designed and implemented. National Instruments software (LabView) and hardware (NI DAQ) were used. These changes improved the usability of the Steam Wastage Rig as well as providing an improved method for recording experiments.
- The acoustic emission data acquisition set-up used was presented. The software and hardware worked and provided good quality data for the subsequent analysis.
- The Acoustic Sensor Probe (UP100) was introduced.

*The acoustic probe has been introduced as a lead to the next chapter which will investigate the heterodyne circuit and its properties. A number of tests and results will be presented to characterise the performance of both the Stethoscope Module and Sensor Probe. The data acquisition software/hardware used to gather data for this work is also briefly covered.*

## Chapter 4

# Experiments on the Heterodyne Stethoscope Response

*This chapter presents the analysis of the ultrasonic heterodyne probe. The sensor and probe electronics are analysed using signal generator-based data recordings, which are processed using time and time-frequency methods. The results of several simulated input signals are presented together with an explanation of the acoustic data and an overview of digital signal processing.*

### 4.1 Background to the Heterodyne Investigation

#### 4.1.1 Heterodyne Process

Heterodyning is translation of frequencies by the generation of new frequencies by multiplying two waveforms. This process can be used to move information in the frequency range. In the case of the device used in this investigation, it is implemented in the UP 100 device.

#### 4.1.2 Frequency Modulation

The acoustic probe used in this investigation uses frequency translation. In frequency translation, there are two methods:

- 1) Frequency multiplication where all frequencies are multiplied by a constant factor.
- 2) Heterodyning can also be defined as a mixing process in which all frequencies are shifted by a fixed amount.

The key difference between the two methods is that the multiplying method preserves frequency ratio while its bandwidth is multiplied. Heterodyning, on the other hand, preserves

frequency differences and maintains the bandwidth of the input signal. Both processes are non-linear. The heterodyne circuit used in this investigation is a frequency translation circuit, which translates the incoming signal by a fixed amount up or down within the frequency domain [36].

The original heterodyne technique was pioneered by Canadian inventor-engineer Reginald Fessenden in 1901 in an improvement of the communication of Morse code. A "heterodyne" receiver has a local oscillator that was adjusted to be close in frequency to the signal being received, so that when the two signals were mixed, the difference or "beat" frequency was in the audible range.

In radio communications, the heterodyne circuit is widely-used to transmit and receive radio signals, where information is transmitted within a spread (bandwidth) around the selected frequency. At the receiver, a detector mixes the incoming signal with a waveform generated by an internal oscillator, at the same selected frequency as the source signal. The two frequencies are subtracted from each other by mixing, resulting in an audible frequency signal, which is the difference between the two frequencies. Pitch, volume and duration are all reproduced through this process by the radio receiver.

Heterodynes are the resulting frequencies from the mixing process. Fundamentally, the mixing of two frequencies creates two new frequencies, according to the properties of the sine function: one at the sum of the two frequencies mixed, and the other at their difference. Typically, only one of the new frequencies is desired; the higher one after modulation and the lower one after demodulation. The other signal is filtered out.

### 4.1.3 Implementation

The heterodyne circuit can be regarded as a black box with an input and an output. Linearity in practical implementations of heterodyne circuits is restricted to limited ranges of the input signal magnitude. Moreover, the frequency ranges are limited and the bandwidth of the output signal will depend on the bandwidth of the input signal.

Heterodyne circuits can also be three-port devices where the third port is the input for the mixing frequency. In that case, the operating range is dictated by the input of the mixing frequency. The bandwidth is dictated by the input signal and the linearity of the heterodyne is defined by the frequencies that can be successfully shifted. Noise present in the mixing frequency will influence the output; in applications, the noise factor of the mixer is important.

If a non-linear two-port assembly is used with both signal and mixing frequencies applied to the input, the output may contain not only the sum and difference of the frequencies, but also harmonics. Thus, frequencies used and filters applied must be carefully selected to reduce such effects.

The mixed signal  $M(t)$  of two signals  $A \cos w_c t$  and  $B \cos w_s t$  is given by:

$$M(t) = A \cos w_c t B \cos w_s t \quad (4.1)$$

Considering the application of a heterodyne mixer in an ideal multiplier this follows:

$$M(t) = \frac{AB}{2} \cos(w_c + w_s)t + \frac{AB}{2} \cos(w_c - w_s)t \quad (4.2)$$

## 4.2 The Heterodyne Circuit used in the Experiments

The heterodyne is essentially a blackbox with unknown characteristics. The input sensor provides a pickup for the acoustic energy and the electronics perform the frequency manipulations resulting in a significantly changed, narrowband, signal output. Details of the probe and the electronics used could not be obtained from the manufacturer.

For this reason, it is important to understand how the heterodyne circuit and sensor manipulate the input signals to allow the signals to be evaluated properly and Steam Traps to be analysed. There is a clear requirement in this chapter to show that the resulting acoustic signal processed by the heterodyne is sufficiently detailed to allow Steam Traps to be analysed.

Provided the richness of information is contained in the signal, the advantages of using a heterodyne are:

- 1) The down-sampling and compacting of the signal through the heterodyne reduces the required sampling rate for acquisition and thus lower cost hardware can be used.
- 2) Less memory is required for the storage of the signal as a lower sample rate can be used.
- 3) Computationally, more intense techniques can be applied to the analysis, without requiring high power analysis equipment, as the information of the signal is contained in the lower bandwidth.

The heterodyne circuitry and the effects of frequency shifting have not been previously investigated for this instrument. There was no information available from the manufacturer on the signal response and signal manipulation by the electronics. The primary purpose of this chapter is to understand the specific frequencies being passed through the circuitry by:

- 1) Systematically analysing the components of the probe.
- 2) Simulating a number of signal inputs and analysing the respective responses.
- 3) Providing conclusive results to underpin the findings from the analysis chapters.

The following sections discuss the tests carried out to clarify the points above.

### 4.2.1 Probe Heterodyne Circuit Specification

The terminology for the Heterodyne Probe components used in this research has been defined in Section 3.4.1. As explained in Chapter 3, the heterodyne circuit contained in the Heterodyne Probe, transfers a narrow bandwidth signal from the ultrasonic frequency domain to the low frequency audio band which can be detected by the human ear. The heterodyne circuit used in the UP100 is a mixer type in which a carrier frequency is mixed with the input signal. The carrier frequency is approximately 38kHz and is mixed with the input signal from the UP100 Sensor, which has a bandwidth of approximately  $\pm 3$  kHz centred at around 40 kHz [88, 87].

### 4.2.2 Assumptions on the Heterodyne Effects

A heterodyne circuit can be used to shift a signal in the frequency domain. As mentioned previously, this is the same method utilised in the AM radio signal modulation. It is assumed that the heterodyne circuit has two functions in this application:

- 1) Filtering the signal through its narrow band response.
- 2) Frequency shifting, by shifting the high frequencies of 40kHz into audible range (approximately 500-4500 kHz).

Linearity in practical implementations of heterodyne circuits is restricted to limited ranges of the input signal magnitude. Moreover, the frequency range is limited and the bandwidth of the output signal will depend on the bandwidth of the input signal.

## 4.3 Probe Experimental Setups Data Acquisition and Analysis

Three experimental setups were created to investigate the Stethoscope and Heterodyne module systematically:

- 1) Heterodyne Circuit - both oscilloscope and PCMCIA data acquisition.
- 2) Stethoscope Module - impulse signal input recorded using PCMCIA data acquisition.
- 3) Complete Response of the UP100 Probe - using an ultrasonic tone generator and PCMCIA data acquisition.

### 4.3.1 Heterodyne Circuit Investigation

A digital oscilloscope (LeCroy Wavejet 324A) and a Agilent Technologies signal generator (33220A) were used to investigate the response by providing a fixed input signal and displaying the output



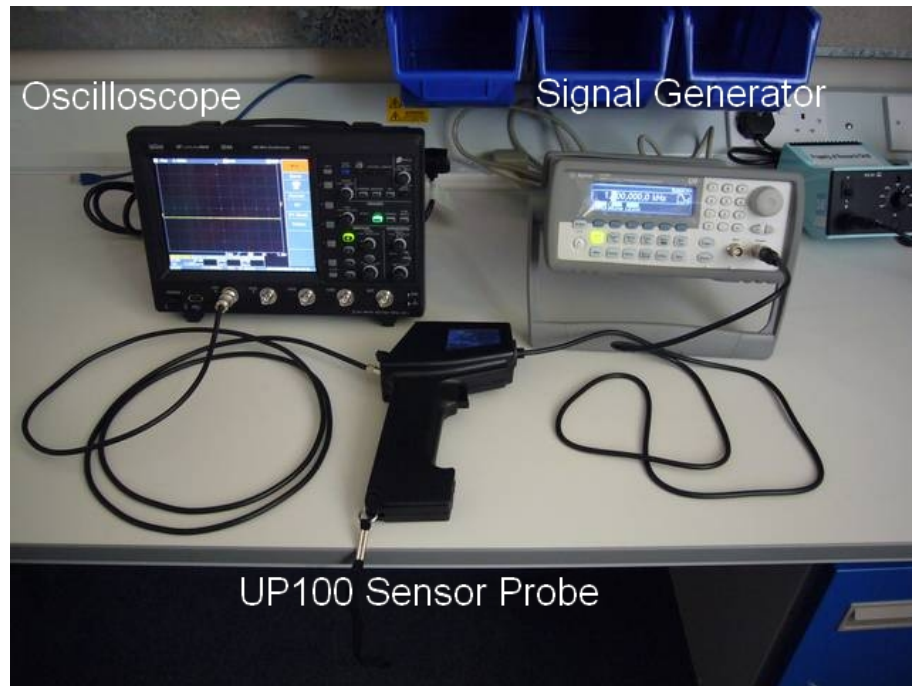


Figure 4.1: Heterodyne Module connected to the Oscilloscope

on the oscilloscope. The signal generator also allowed a linear frequency sweep to be performed, which allowed the heterodyne circuit response to be mapped in relation to the frequency input, essentially providing a frequency input versus frequency output map.

The signal generator was used as the input device to the Heterodyne Module using a BNC to RCA cable with 75 ohm impedance. The output of the Heterodyne Probe was connected to the oscilloscope as can be seen in Figure 4.1. A linear signal sweep ranging from 20 Hz to 80 kHz was conducted using the signal generator over a duration of 15 seconds.

As an extension to this work, the oscilloscope was removed and replaced with the Measurement Computing DAS16/16 PCMCIA data acquisition card to acquire the data for further analysis using Matlab. This signal was sampled using 200 kHz and recorded with the PCMCIA card connected to the PC using a Matlab script.

In this setup, the Heterodyne Module was connected to the PCMCIA breakout box using a standard 3.5 mm mono jack and cable. The breakout box was connected to the PCMCIA card through a ribbon cable as can be seen in Figure 4.2. The probe includes a variable gain setting and it is also worth noting that in application, the variable gain setting was found to be best set at 40 dB for all traps, allowing for sufficient dynamic range for impulsive as well as non-impulsive signal responses.

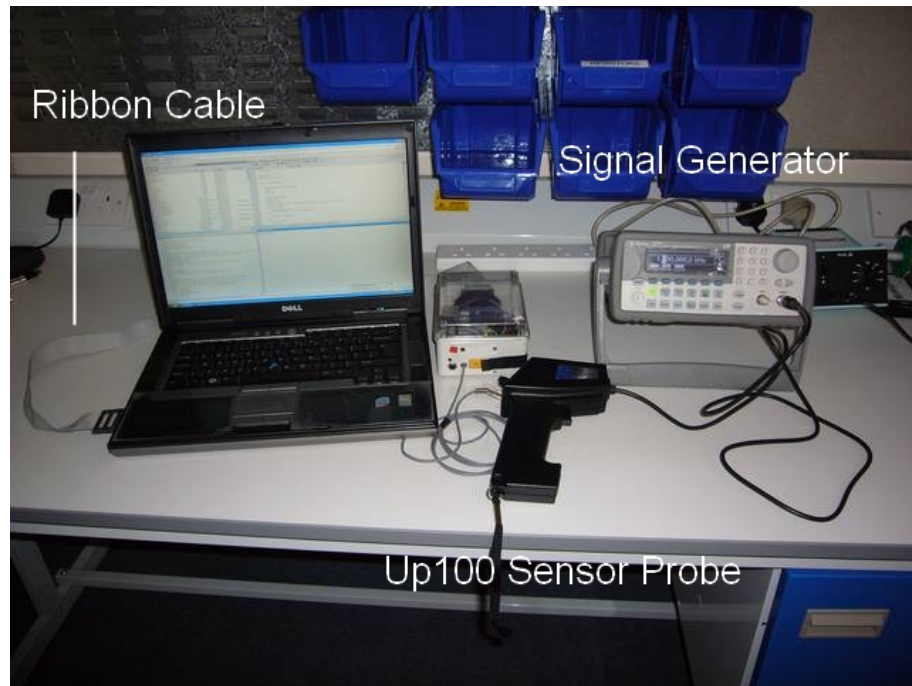


Figure 4.2: Heterodyne Module connected to the PCMCIA Card

### Time Domain Analysis

The time domain representation of the recorded heterodyne transformed signal are provided in Figures 4.3 and 4.5 for the oscilloscope and PCMCIA card respectively. It is clear, comparing the two plots that the signals recorded are similar. The lower frequencies appear higher than expected. The signal sweep in horizontal axis (in Figure 4.3) is time, but as a frequency sweep is being performed, the time is linearly proportional with frequency. The resulting figures can be defined as an input frequency versus a resulting output amplitude with respect to the input frequency.

As confirmation of the frequency sweep output of the Agilent Signal Generator, the “raw” signal excluding the Heterodyne Probe was recorded using the same data acquisition equipment. As can be seen from Figure 4.4, the signal sweep for 20 Hz to 80 kHz is flat and fairly constant in the time domain. Equally, considering the frequency domain plot, the signal is flat with no changes in features. It should be noted that a peak is observed at just over 30kHz, which may be an artefact of the circuitry and noteworthy for the further analysis. No other specific features were highlighted as part of this comparison.

### Frequency Domain Analysis

Figure 4.5 shows the time domain and frequency domain plots for a 20 Hz to 80 kHz frequency sweep including the Heterodyne Module. The time domain features clearly the amplitude modulation with frequency. The highest amplitude is achieved at around 37 kHz, which relates to

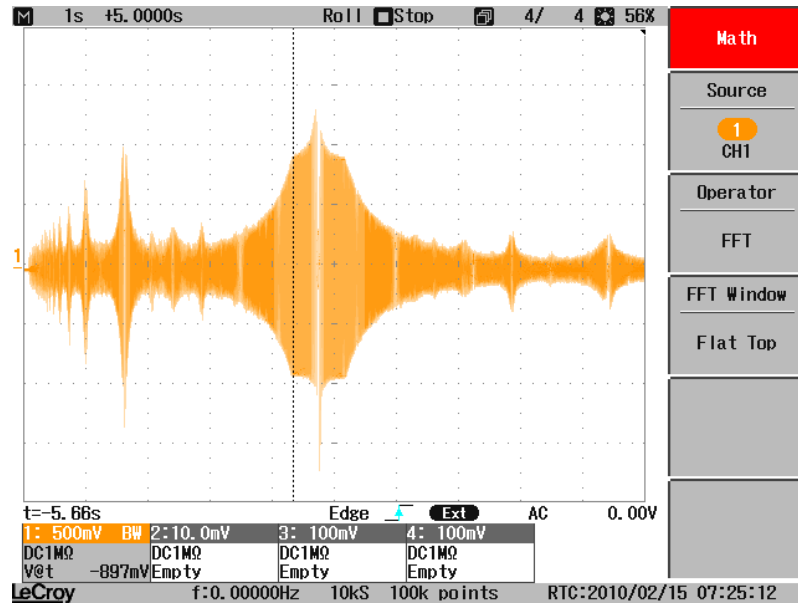


Figure 4.3: Heterodyne Module Oscilloscope Time Domain Plot

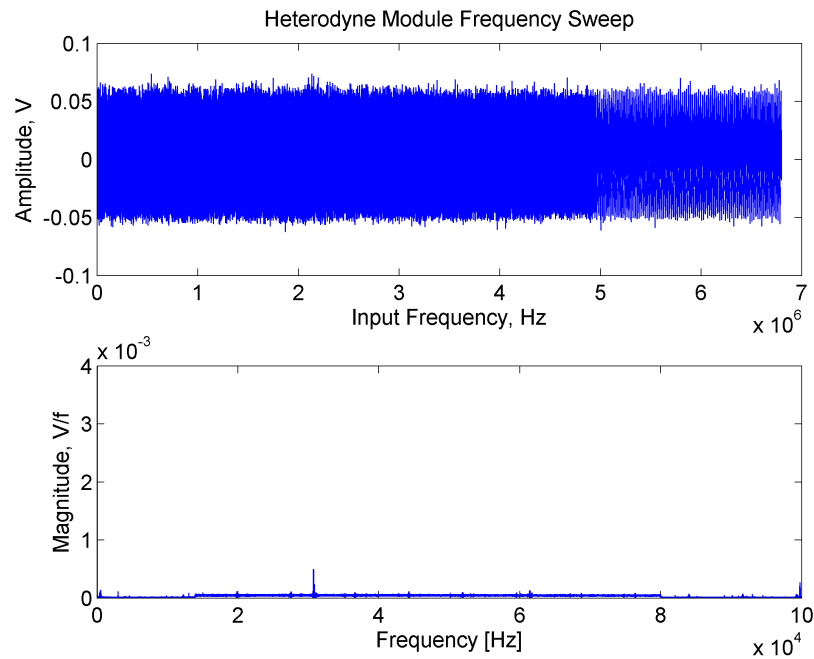


Figure 4.4: Heterodyne Module PCMCIA Card Time Domain Plot

the carrier frequency of the heterodyne circuit. The minimum with the highest maxima on either side is due to the crossing over of the input frequency with the oscillator frequency. It is worth noting that as the time domain signal was a frequency sweep, the time domain has been plotted with respect to frequency rather than time, to show the changes of input frequency to output amplitude.

The Fast Fourier Transform (FFT) analyses the frequencies transferred by the Heterodyne. Due to the sweep of the signal generator, the amplitude of the frequencies reduce as the frequencies

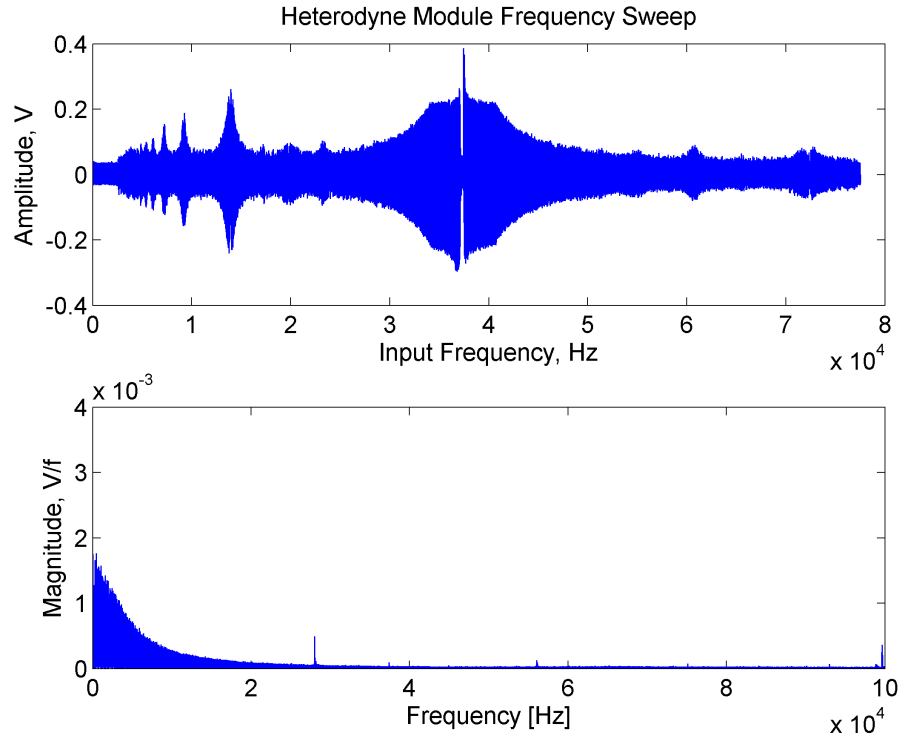


Figure 4.5: Heterodyne Module PCMCIA Card Frequency Domain Plot

increases. This could be explained by the power of the signal generator being constant and as power is related to the amplitude squared, as the frequency increases, the power decreases as a function of the square root of frequency. Another noteworthy point is that a significant peak just below the 30 kHz mark is observed, similar to the peak in the simulated signal experiment, which was observed at just over 30 kHz.

It must also be noted that the frequency sweep used in this investigation is an artificial signal and not akin with the input provided by the sensor. However, it allows the relative frequency responses to be analysed through a common input.

A time frequency analysis of the data will be presented in Section 4.4, expanding on how the frequencies are transposed by the circuitry.

## Discussion

Considering Figure 4.5, there are a number of key resonances that appear periodically throughout the lower frequency part of the signal in the time domain. These harmonics may be a fragment of the way the electronic circuitry has been implemented. Furthermore, it is clear that the input signal is not filtered around 40kHz bandwidth, but rather the whole signal is amplified by a complicated response curve (see in Figure 4.5). The sensor will contribute its own signal response, which will have to be compounded with the heterodyne circuitry effects. A clear conclusion is

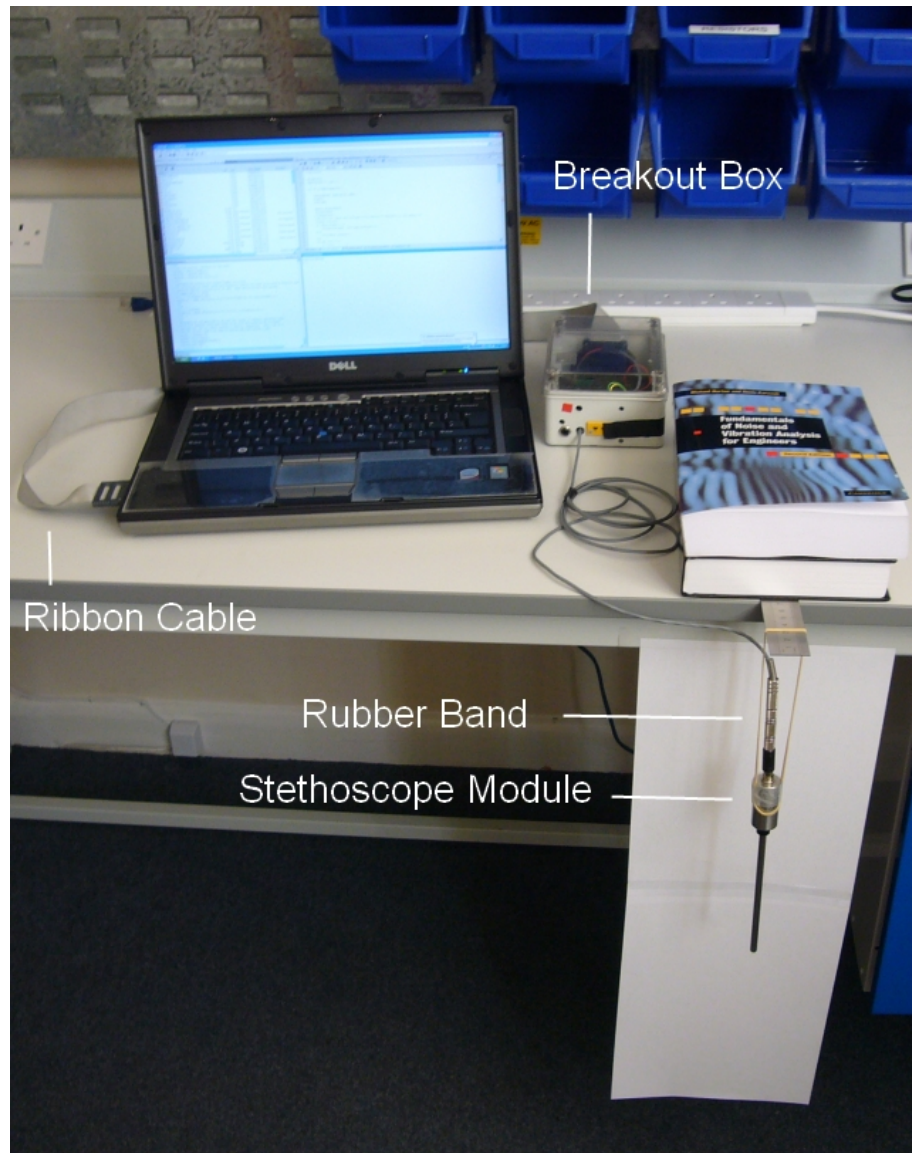


Figure 4.6: Stethoscope Module Investigation Experimental Setup

that not only 38-44 kHz signals are transferred by the probe, but rather that all frequencies are passed to a higher or lower degree.

#### 4.3.2 Stethoscope Module Investigation

The first test analysed only the heterodyne circuit, displaying the output using the oscilloscope and through the PCMCIA DAQ card. In this next experiment, the Stethoscope Module was investigated by attaching it directly to the PCMCIA data acquisition card without passing the signals through the Heterodyne Module. This allowed the Stethoscope Module to be excited and the “raw” sensor response be recorded digitally for further analysis in Matlab. Figure 4.6 shows the overall experimental setup for this test.

The Stethoscope Module was suspended from a ruler using a rubber band, as seen in Figure



Figure 4.7: Stethoscope Module Test Setup



Figure 4.8: Hammer for Impulse

4.7. The sensor was excited by a hammer strike, to create a sharp, instantaneous signal with a wide frequency response. This impulse input signal was chosen as theoretical signal response includes all frequencies from zero to infinity. Furthermore, this was a signal that could easily be created and replicated. The hammer used in the experiments is displayed in Figure 4.8. The signals were sampled using 200 kHz using the PCMCIA card and the Matlab script with 5 second length of recording to capture the hammer strike event.

### Time Domain

In total, 32 signals were recorded which were reviewed to ensure the data had been suitably recorded. Following the quality review, some signals were re-recorded. Figure 4.9 shows four example plots of the time domain signals response of suspended hammer strikes as recorded through the PCMCIA data acquisition card.

Figure 4.9 shows two examples of unsuitable and two examples of suitable hammer strike test recordings. The top two diagrams show signals that were unsuitable because the one on the left displays a low signal to noise ratio and the one on the right displays a repeated impact (the sensor touched the hammer on the rebound). The lower two plots show two suitable examples in which the expected time domain response is a sharp impulse signal with a high signal to noise ratio and little or no signal after the initial impulse.

### Frequency Domain

Sixteen impulse signals were used to calculate a representative FFT. Figure 4.10 shows the frequency domain FFT representation adding both the real and imaginary parts of the individual FFTs and then averaging them to obtain an “combined average response”. The blue traces repre-



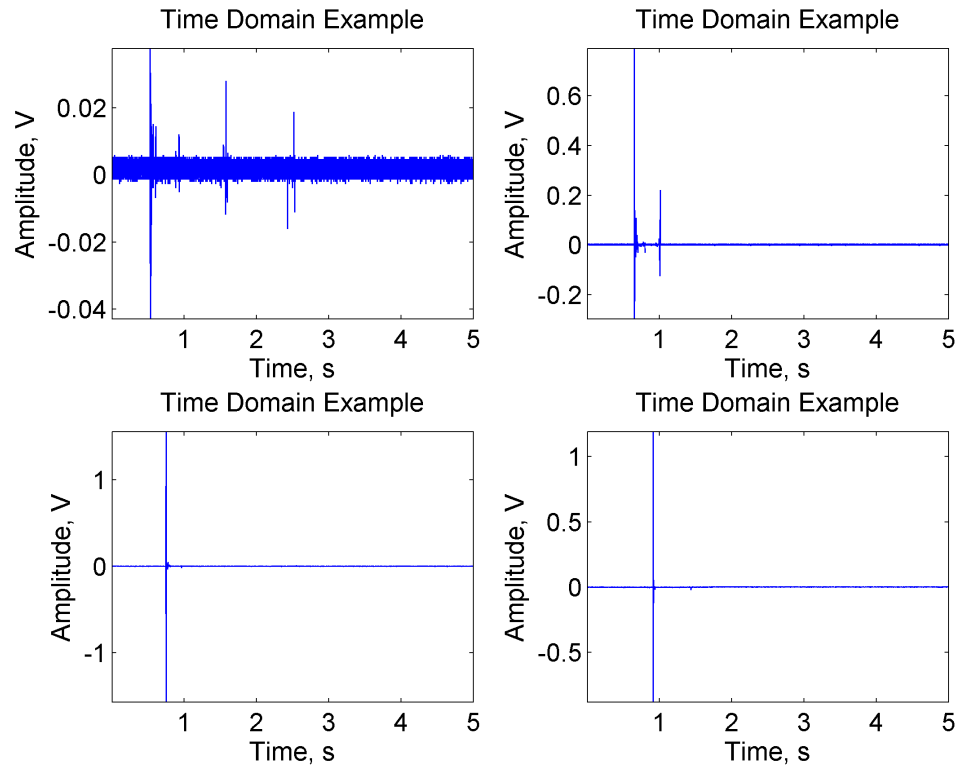


Figure 4.9: Stethoscope Module Time Domain Plot

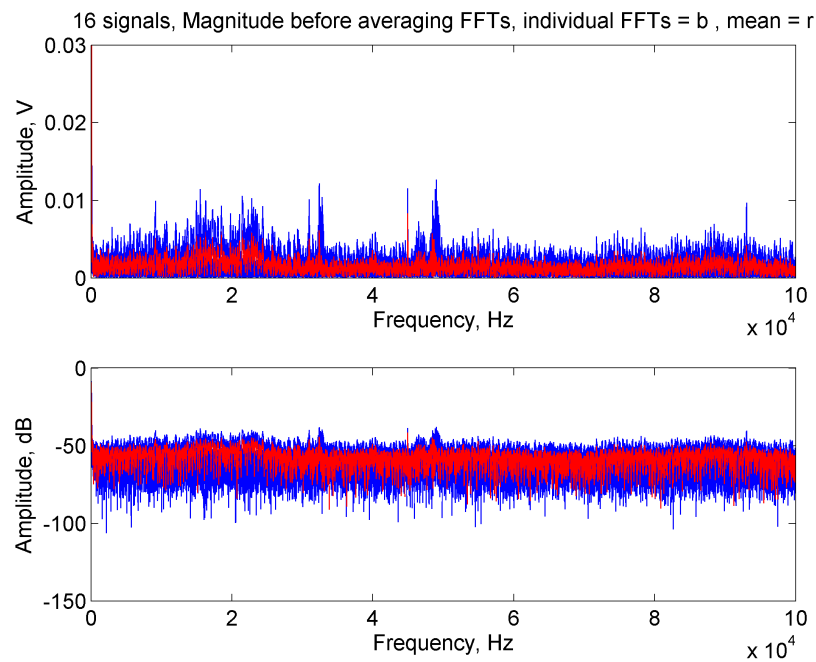


Figure 4.10: 16 Stethoscope Signal Average (Magnitude before averaging FFTs)

sents the individual FFTs; the red is the average FFT. Top y-axis is amplitude; bottom plot y-axis is dB scale.

Figure 4.11 shows the frequency domain FFT representation using only the modulus (exclud-

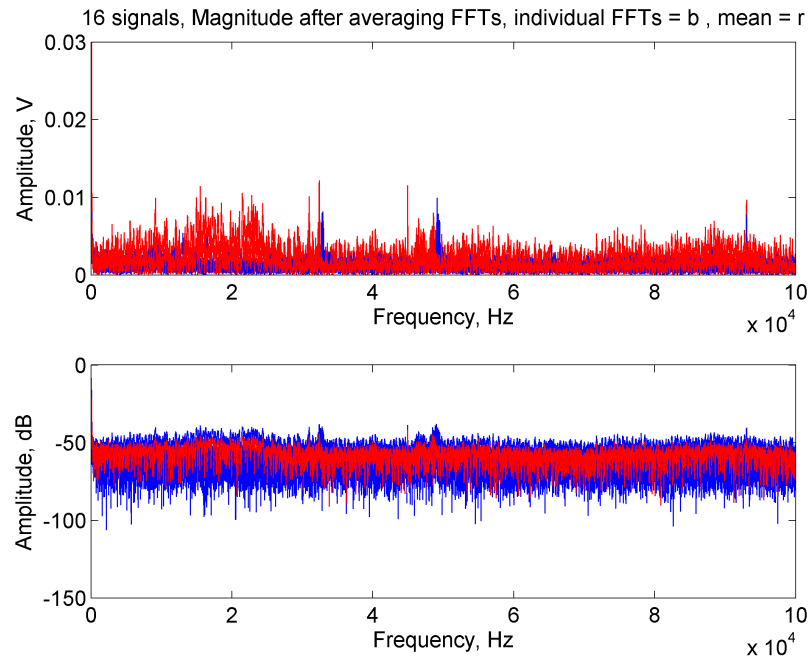


Figure 4.11: 16 Stethoscope Signal Average (Magnitude after averaging FFTs)

ing imaginary component) of the individual FFTs before averaging a number of signal to obtain an “combined average response”. The blue traces represent the individual FFTs; the red trace is the average of all the sample FFTs. Top y-axis is amplitude; bottom plot y-axis is dB scale.

**Discussion** The FFT of each of the signals was computed using the complete signal (including imaginary component) before averaging. The blue trace is the original signal; the red is the average FFT of 16 signals. Top y-axis is amplitude; bottom plot y-axis is dB scale.

The calculation of the modulus after the averaging the FFTs results in a lower average signal output (-70 db, +/-10 db bandwidth approximately) with a broader average signal bandwidth. The signal that has the modulus calculated before the averaging provides a higher signal output (-57 db, +/-5 db bandwidth approximately).

In terms of an average value, it is clear that the calculation of the modulus after the averaging gives a lower average signal output (-73 db, +/-10 db bandwidth approx) with a broader average signal bandwidth. The signal that has the modulus calculated before the averaging process provides a higher signal output (-60 db, +/-5 db bandwidth approx) with a difference of 3 db. This, of course, is understood as averaging a large number of FFTs (including both real and imaginary parts) will result in the average value approaching zero.



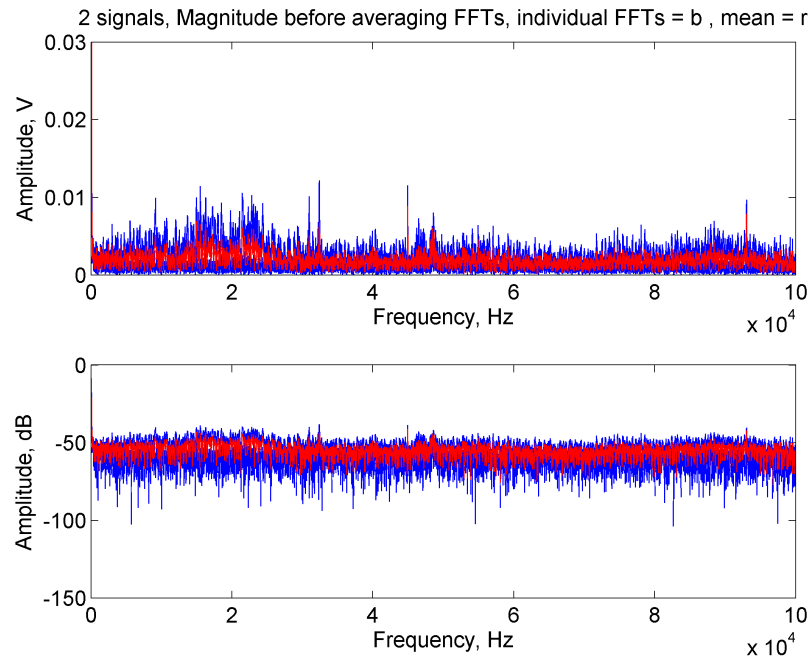


Figure 4.12: Stethoscope Module Signal Average for 2 samples

### Stethoscope Module Frequency Response Convergence

As mentioned previously, 32 signals have been recorded as the hammer strike approach is inherently variable. To establish whether the data sets provide convergence, the data sets have been processed in 2, 4, 8, 16, 24 and 32 signal batch sizes.

In terms of the information displayed, the blue trace is the FFT plotted for each signal on top of each other. The red line is the average for the number of signals being reviewed. As an example, Figure 4.12 shows the magnitude of the Fourier Transform and combined mean of the respective FFT spectra. Signals of 4, 8, 24 and 32 are shown in Figures 4.13, 4.14, 4.15 and 4.16 respectively. Figure 4.10 illustrates the 16 signal FFT response. It should be noted that this data was sampled with 200 kHz (the highest sampling hardware available) and that Ramadas [76] indicated that the piezo material is responsive to input frequencies up to about 80 kHz. In addition, the Data Acquisition hardware included anti-aliasing hardware feature. Even though the signal does not appear to fall off in Figure 4.10 after 80kHz, for these reasons, sampling at 200 kHz should be sufficient to avoid aliasing within the data.

Reviewing the sensor responses, there seems to be peaks at around 18 kHz, 30 kHz and 45 kHz although the location of the peaks vary depending on the batch size of data being considered. This is of interest as the Heterodyne Module circuitry has a low and high frequency response. Considering Figure 4.5 if these peaks coincide, the signal could be amplified and passed through the circuit to the data acquisition, resulting in the higher frequency as well as lower frequency noise being transmitted through this process.

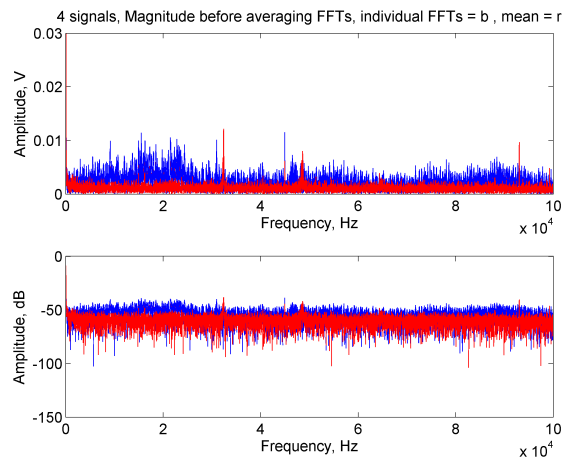


Figure 4.13: Stethoscope Module Signal Average for 4 samples

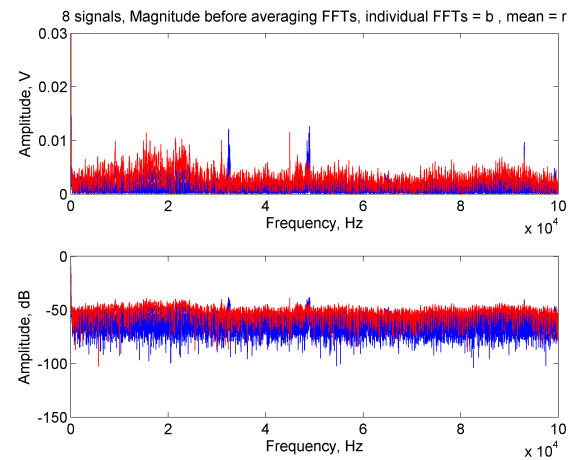


Figure 4.14: Stethoscope Module Signal Average for 8 samples

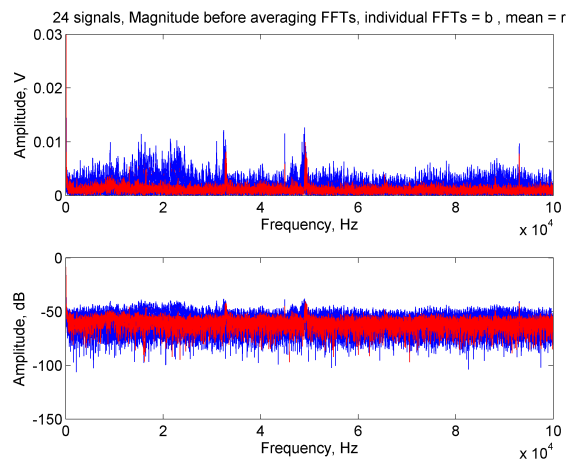


Figure 4.15: Stethoscope Module Signal Average for 24 samples

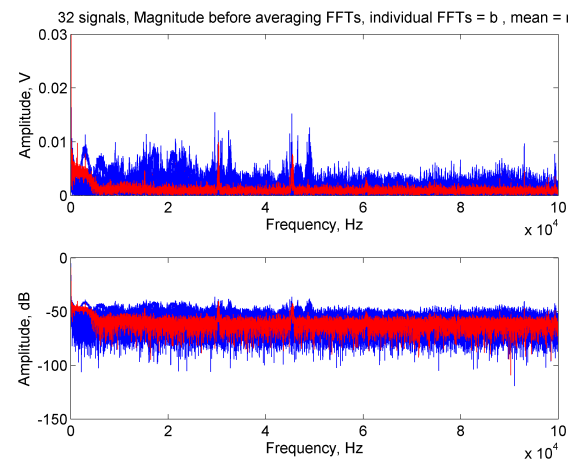


Figure 4.16: Stethoscope Module Signal Average for 32 samples

**Convergence Analysis** Figure 4.17 summarises the mean values for six sets of FFT averages to analyse convergence of the mean value. Each set contains an increasing number of data sets; specifically the sets contain 2, 4, 8, 16, 24 and 32 sets FFTs which are averaged to calculate a mean value. Additionally, Table 4.1 summarises the calculated mean values and % differences for the six individual data set collections.

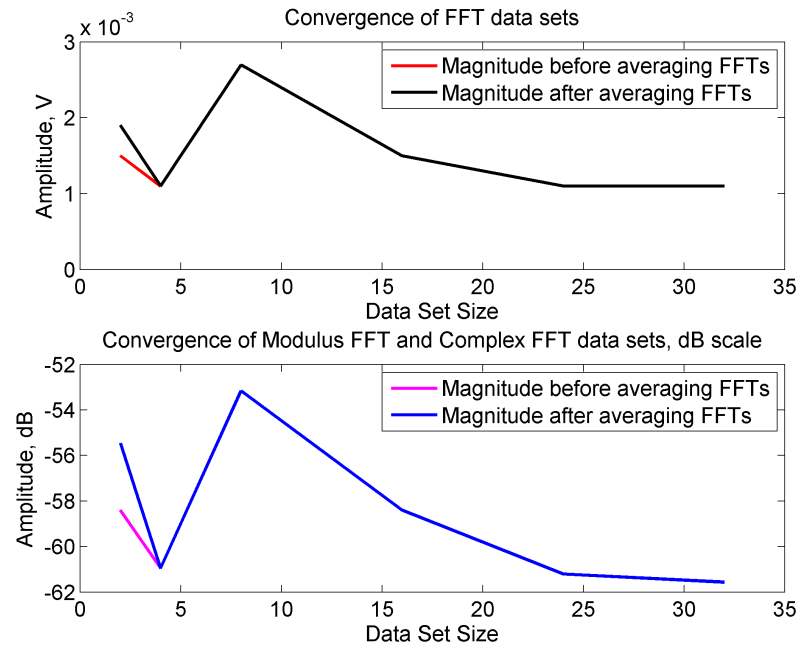


Figure 4.17: Stethoscope Module Convergence Results

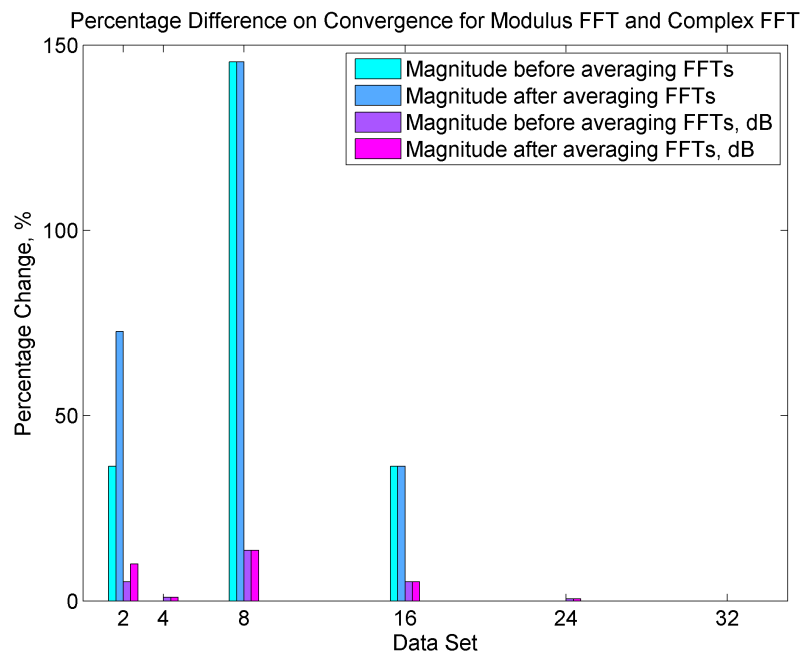


Figure 4.18: Percentage Difference on Convergence for Modulus FFT and Complex FFT

Signal	2	4	8	16	24	32
<b>Magnitude before averaging FFTs</b>	0.0015	0.0011	0.0027	0.0015	0.0011	0.0011
<b>Difference %</b>	-36.3	0.0	-145.4	-36.6	0.0	0.0
<b>Magnitude before averaging FFTs, dB</b>	-58.3	-60.9	-53.1	-58.3	-61.2	-61.5
<b>Difference %</b>	5.1	0.9	13.6	5.1	0.5	0.0
<b>Magnitude after averaging FFTs</b>	0.0019	0.0011	0.0027	0.0015	0.0011	0.0011
<b>Difference %</b>	-72.7	0.00	-145.4	-36.36	0.0	0.0
<b>Magnitude after averaging FFTs, dB</b>	-55.4	-60.9	-53.1	-58.3	-61.2	-61.5
<b>Difference %</b>	9.9	0.9	13.6	5.1	0.5	0.00

Table 4.1: Convergence Results of Multiple Input Signals

**Discussion** Table 4.1 shows that averaging 24 data sets, the highest difference in mean value is 0.57% for the dB scale measurement. In this case, the convergence level has been defined as a change of mean value of less than 1 % of the dB value. The decrease in percentage deviation as the data set size increases is graphically shown in Figure 4.18. The average of 24 and 32 samples is less than 0.57 % and is thus deemed to be suitable for further investigation in the subsequent section.

### 4.3.3 Investigation of Combined Heterodyne and Stethoscope

Two approaches used to investigate the combined response of the Heterodyne Circuit and Stethoscope module are outlined below:

- 1) By analytically combining the responses of the first test (electronics only) and second test (sensor only). This was carried out by multiplying the FFTs for the two parts (sensor and heterodyne responses), i.e. the hammer strike sensor signals with the response of the heterodyne circuit to the frequency sweep.
- 2) By using an electronic 40 kHz signal generator tester for ultrasonic probes to simulate an input signal. To create low frequency signal akin with a moving mechanism, a set of keys and a metal pin were tapped against the connected wave guide during some of the data acquisition.

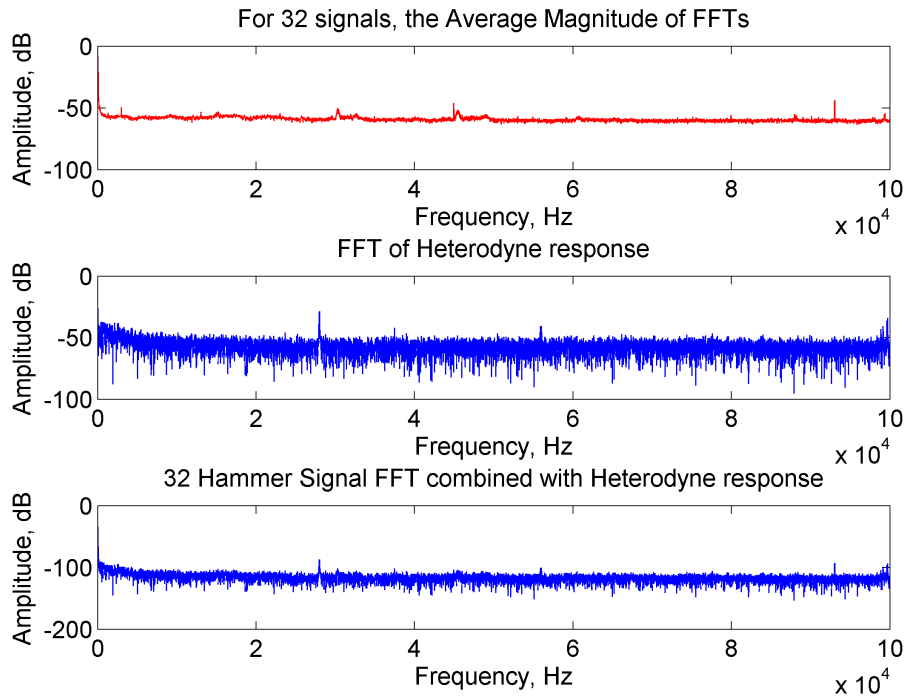


Figure 4.19: Combined Module Responses in the Frequency Domain

These approaches allowed the complete system to be analysed, taking into account the Stethoscope Module as well as the Heterodyne Module.

#### Analytical Investigation of Combined Response

The combined signal response of the Stethoscope Module and Heterodyne Module was evaluated using example signals of each of the separate test cases and multiplying them with each other. For reference, Figure 4.4 shows the time domain of signal from Heterodyne in the upper half of the figure and the FFT in the lower half of the figure. The signal was recorded using the 40 dB gain setting on the heterodyne circuit with an input signal sweep from 20 Hz to 80 kHz using a digital signal generator over duration of 10 seconds. For reference, Figure 4.9 shows the time domain impulses and Figure 4.16 shows the FFT response for the hammer strike signal.

An FFT was computed for the signal sweep, with 10,000 steps, as it was for the hammer strike signals. The length of the FFT was kept constant, so that the multiplication could be readily carried out. The resulting combined signal of both sensor and Heterodyne responses is shown in Figure 4.19. The top plot in the figure is the averaged FFT of the hammer strike for 32 samples. The middle plot in the figure is the FFT of the Heterodyne to the frequency sweep and the lowest plot is the combined FFT of both signals. As the resulting signal (the lowest plot) is a multiplication of the two above, the dB scale is the lowest (an addition of the two other scales).

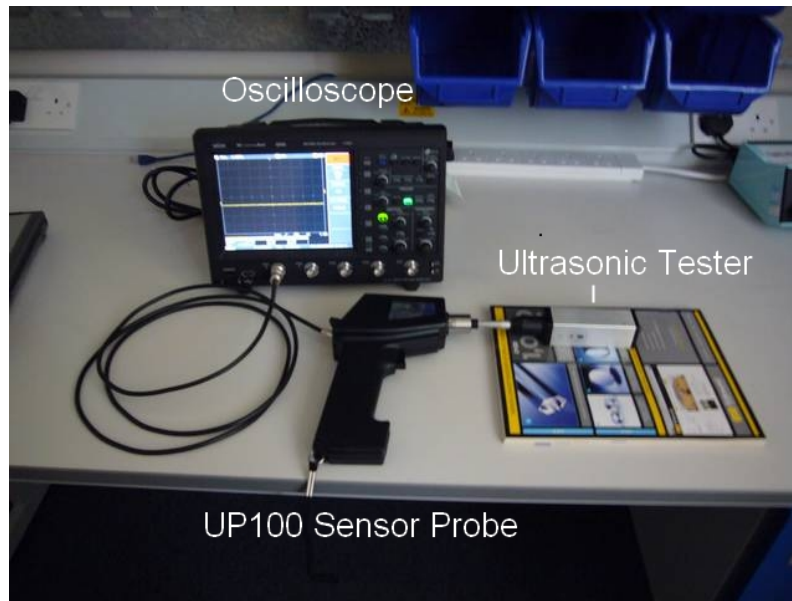


Figure 4.20: Dynamic Combined Module Response Experimental Setup

The signal response is broad and flat. There is no specific resonance highlighted, however very low peaks are observed in the three locations (18, 30, 45 kHz approximately). These are all artefacts from the Heterodyne FFT response, which are visible in the middle plot of Figure 4.19 and referred to in the FFT analysis section (Section 4.3.1) on the heterodyne circuit.

### Experimental and Dynamic Combined Module Response

The synthesis of an experimental signal analogous to a Steam Trap was difficult to achieve as the frequency range required would have to stretch from below 1 kHz to above 45 kHz. Furthermore, the signal would have to be created deterministically so that the signal transformation could be accurately analysed thereafter. As the creation of such a complicated signal was not possible given the resources available, an alternative solution was applied. An ultrasonic tester was used to create a 40 kHz base signal on a wave guide and a low frequency signal was superimposed. This low frequency signal was created by either a set of keys or a metal pin impacting the wave guide connection between the signal generator and sensor. Although this signal is artificially created, it is analogous to a Thermodynamic Trap operation. The experimental setup is shown in Figure 4.20.

The ultrasonic tester, although undefined in terms of the exact signal output (other than a wave at approximately 40 kHz), provides an insight into the overall response of the sensor unit. Reviewing the Fourier Transform on the dB scale (as seen in Figure 4.21), there is a response at 48 kHz for both the keys and the tester. The other peak worth noting is the 40 kHz signal, which is the resultant of the tester exciting the piezo material.

The purpose of this “Dynamic Combined Module Response” basic simulation was to simulate

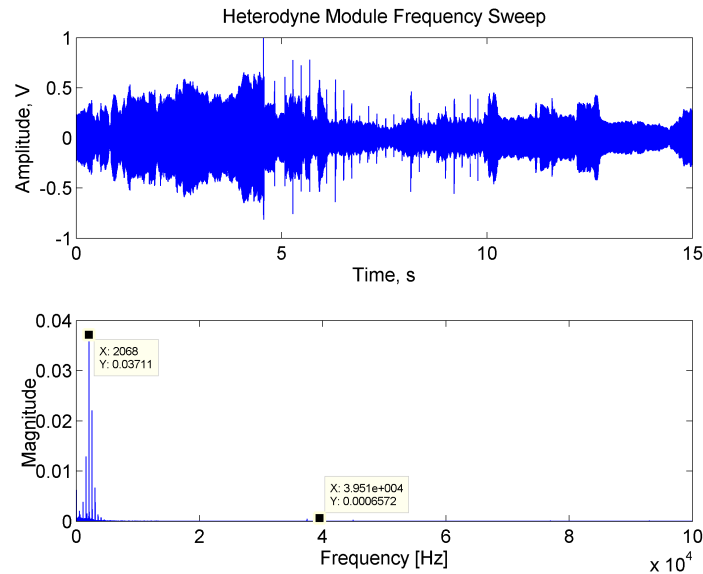


Figure 4.21: Dynamic Combined Frequency Signal Response

an impact-like Steam Trap with simulated high frequency data to evaluate the differences between the change. This insight allows the dynamic changes in the Heterodyne Module to be observed and understood, providing further understanding on how the heterodyne responds to both the low frequency and high frequency “shift” signal. A time domain representation is shown in the upper half of Figure 4.22.

As the signal response is dynamic, i.e. it changes over time, a time-frequency map was calculated using the Matlab code below:

```
[s,f,t,p]=spectrogram(data,256,1,512,50000);
figure;
contourf(t,f,10*log10(abs(p)),'edgecolor','none');
grid on; axis tight;
ylabel('Frequency');xlabel('Time');
```

The resulting map is shown in the lower half of Figure 4.22. The clear changes in the signal are apparent. There is a clear base signal that stretches across the lower frequency band between approximately 1 to 3 kHz and is visible in high intensity across the time changes. Interestingly the high frequency impacts from the pin are visible in the higher frequencies (6-8 kHz), but not in the low frequency band, as they are overshadowed by the high frequency signal resulting from the 40 kHz signal generator.

Figure 4.23 magnifies the signal between time stamps of 5 and 7 seconds, showing that there are clear impulses that provide an even distribution across the frequency spectrum (vertical axis) as expected from a true impulse response. Again, the strong horizontal band response from the ul-

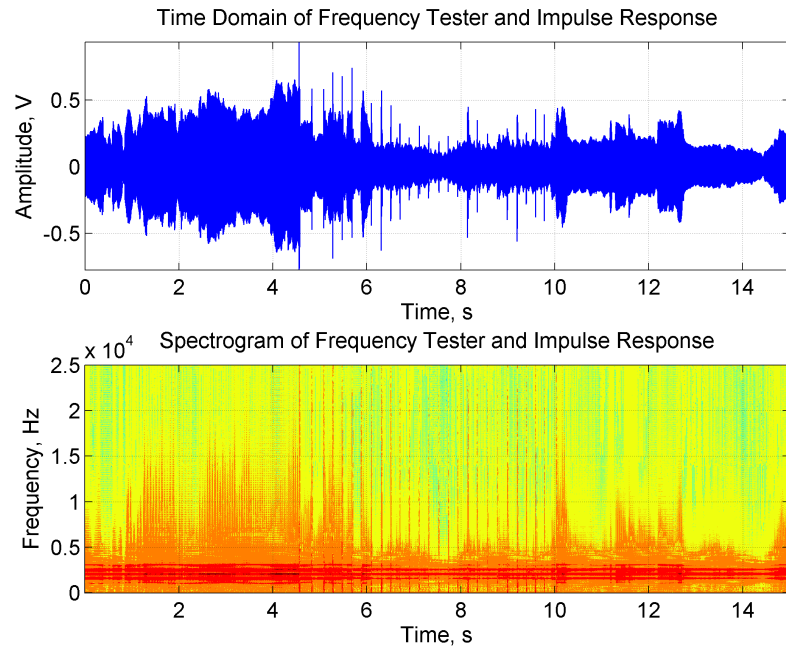


Figure 4.22: Dynamic Combined Module Response Time Frequency

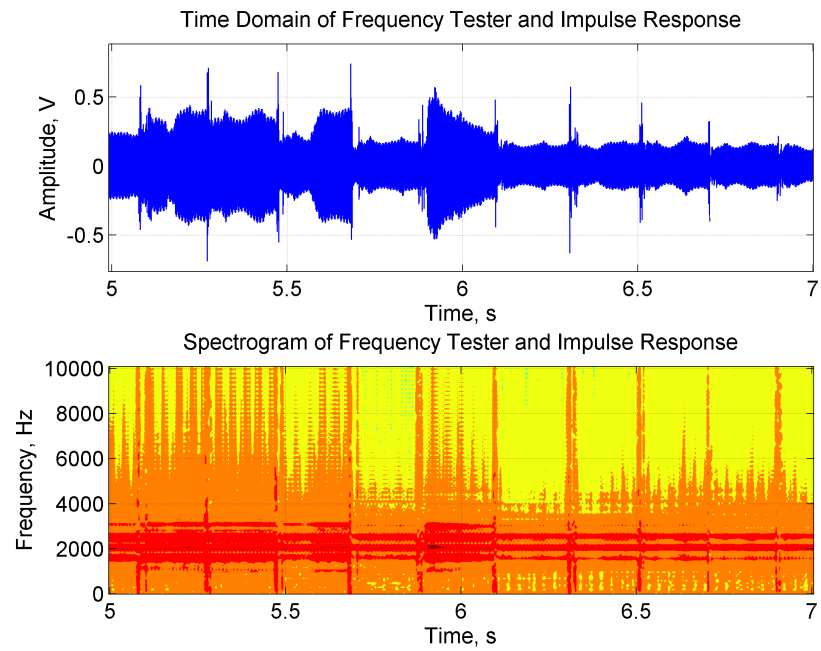


Figure 4.23: Dynamic Combined Module Response Time Frequency (Zoomed)

trasonic tester can be seen, having been heterodyned to the low frequency range. The bandwidth of the response is consistent at about 2 kHz across the time (horizontally). In this magnified plot of the STFT, the vertical stripes from the impacts and the low horizontal high frequency conversion are more clearly displayed.



## 4.4 Time-Frequency Analysis Investigation of the Frequency Folding Effect of the Heterodyne Circuit

The frequency conversion properties of the heterodyne circuit have been investigated in the previous sections. To further understand the behaviour of the heterodyne circuit with respect to frequency shifting, the frequency sweep data previously analysed was again analysed using a time-frequency analysis. The analysis shows how individual frequencies contribute to the signal response as a whole.

Using the swept input signal (initially reviewed using the Fourier Transform), a time-frequency map has been created. The resulting map is shown in Figure 4.24.

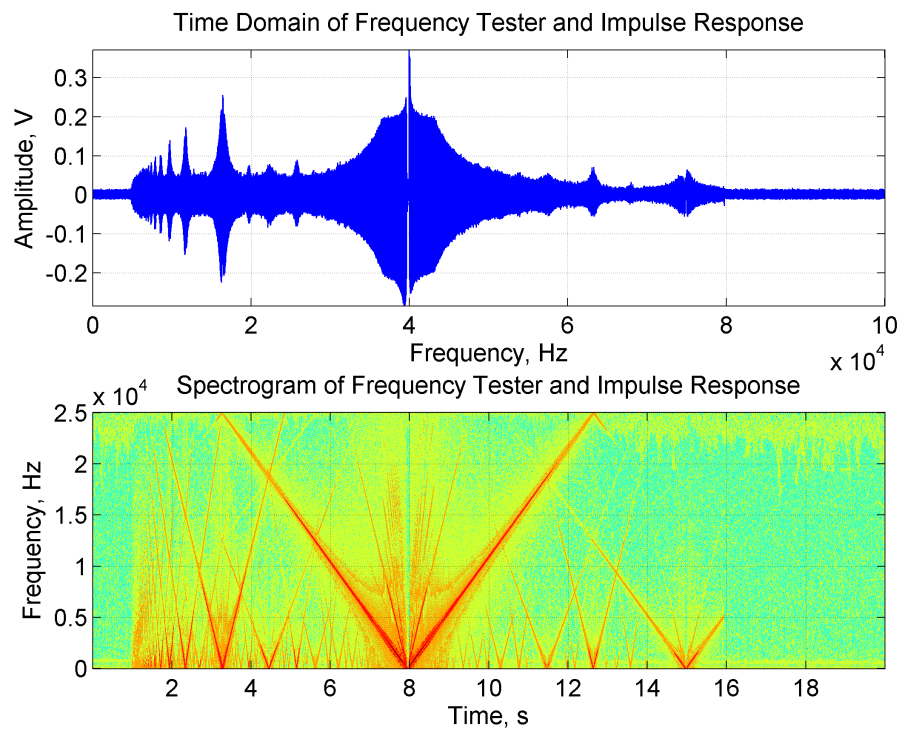


Figure 4.24: Time-Frequency Representation of Heterodyne Module using a Frequency Sweep

As highlighted in Chapter 2, the frequency range between 1 kHz to 44 kHz can be used for the detection of Steam Trap behaviour. It is clear from the time frequency analysis that all frequencies are folded into the low frequency domain, shown clearly in Figure 4.24.

## 4.5 Corrected Assumptions on the Heterodyne Effects

It was earlier assumed that the heterodyne circuit has two functions. These assumptions (Section 4.2.2) have now been investigated and validated:

1) *“Filtering the signal through its narrow band response.”*

This has been disproven through the systematic analysis on components of the probe. The resulting signal is not narrow band, nor filtered. The response of the heterodyne is broadband in nature and encompasses frequencies along the whole spectrum, not just centred around 38-43 kHz as suggested previously. All frequency components pass through the circuit and are detectable in the output of the probe. This was proven by both frequency and time frequency analysis.

2) *“Frequency shifting, of the high frequencies in a 4-5 kHz bandwidth around 40kHz into audible range (approximately 500-4500 kHz).”*

This has been proven through the frequency and time-frequency experimentation.

## 4.6 Summary

In addition to investigation of the two assumptions above, the following findings and observations have been made:

- The performance of the heterodyne has been systematically investigated. The two core components (Stethoscope Module and Heterodyne Probe) have been individually evaluated and the combined response assessed using a deterministic signal.
- The signal strength in the high frequency ultrasonic is reduced in amplitude once the signal is transposed to the low frequency band.
- In terms of Probe response from the input signal sweep a number of input frequencies have been identified that provide a higher amplitude response. These are located at 10 kHz, 13 kHz and 40 kHz.
- In terms of the Stethoscope Module response, the hammer strike experiment provided a sharp, impulse-like, response. Due to the nature of the hammer strike experiment, it is not entirely repeatable, providing minor inconsistency. However, the data has been carefully checked for inconsistencies and in some cases repeated to ensure representative signals are used in the analysis.
- The combined signal response analysis shows that the response is flat across the frequency bandwidth, with a small peak seen at around 40 kHz.
- Lastly, the analysis of the input frequency sweep was presented. A time-frequency analysis was undertaken highlighting the frequency shifting properties of the heterodyne probe. A key discovery has been that although the frequencies at the ultrasonic range are amplified,

where high energy low frequency signals exist these are still maintained by the transformation.

*The acoustic probe has been introduced as a lead to the next chapter which will investigate the heterodyne circuit and its properties. A number of tests and results will be presented to characterise the performance of both the Stethoscope Module and Sensor Probe. The data acquisition software/hardware used to gather data for this work is also briefly covered.*

## Chapter 5

# Operational Conditions and Process Parameters

*This chapter analyses the influence of key parameter of Pressure, Temperature, Condensate Load and Steam Trap Type on the acoustic emission. The composition of data for each trap set is presented. A review of acoustic representations of failure modes for different Steam Traps is provided. Lastly, an introduction to the signal processing chapters' structure is also presented.*

### 5.1 Acoustically Detected Steam Trap Failure Modes

This Section explains how the acoustic profiles of Steam Traps were divided for this research. For this section, a number of acoustic samples were converted to .wav files. As the data was in the audio frequency range due to the heterodyne circuit, this conversion could be readily processed using standard approaches included in the Matlab m-file library (wavwrite.m). These audio files were compared with statements from survey engineers and acoustic Steam Trap diagnosis training tapes and webinars, [4] and [103, 104] respectively.

The different trap types observe individual responses as detailed below:

- 1) **Thermodynamic Trap** - This trap has a clear and sharp opening/closing sequence. Failure of the trap can manifest in a high cycling rate; quiet periods between cycles indicate a working trap.
- 2) **Orifice Trap** - This trap has no mechanism and thus a continuous emission, which is very difficult to diagnose.
- 3) **Capsule Trap** - This trap can be difficult to diagnose as it has a long cycling time, which is dependent on the sub-cool threshold and the operational conditions at the trap.

- 4) **Bi-metal Trap** - Same as the Capsule Trap but with a longer delay.
- 5) **Float Trap** - This trap emits a continuous acoustic emission and can be soft sounding, due to the large casting and the dynamics of the trap.
- 6) **Inverted Bucket Trap** - There is a definitive open and closing sequence, but modulations can occur, especially under small condensate loads

From the brief introduction above, the operational acoustic emission profiles of Steam Traps can be divided into three overall categories:

- 1) Continuous Condensate Discharge - This occurs when a trap is undersized, or when the load exceeds the trap's capacity, for example, at start-up or when other traps have failed closed. The sound is softer than the sound of leaking steam.
- 2) Continuous Modulating - This condition occurs when the trap has small loads and it is continuously opening and closing. This often occurs on mains drainage and other continuous operation applications.
- 3) Blow Through - This is when steam leaks from the Steam Trap. There is a significant roar, which is high pitched and loud.

Taking the previous categories into account, Steam Traps have been classified into three primary acoustic emission profiles for the purposes of this investigation. The placing of Steam Traps with the respective categories in the list does not imply that a trap cannot exhibit characteristics of any of the other categories, but that the primary operational acoustic emission Profile of the trap is the category under which the trap is listed. These primary operational modes are:

- 1) Continuously Discharging - The Orifice Trap is the only trap operating in this way, as there is no mechanism to facilitate modulation. It is always continuously discharging in its operational behaviour.
- 2) Non-Impulsive - The Float Trap, Balance Pressure Trap and Bi-metal Trap belong to this category, as they primarily operate in this mode of operation.
- 3) Impulse Discharge - The Thermodynamic Trap and the Inverted Bucket Trap have a clear and impulse like opening and closing sequence.

These three profiles will be used to structure the analysis of the Steam Traps in the subsequent analysis chapters.

## 5.2 Data Analysis Approach

For the subsequent analysis chapters, data has been divided into three categories based on the acoustic emission profile, i.e.:

- 1) Fixed Orifice - stationary signals - using the Fixed Orifice Trap as an example.
- 2) Non-Impulsive - pseudo stationary signals with inherent time-based modulations. There may still be stationary signals, but also mechanism related modulation. The Float Trap is used as an example for this category.
- 3) Impulsive - Clear, sharp impulses overlaid onto a low level background noise. The Thermodynamic Trap is used as an example of this category.

Thereafter, the datasets used in the analysis chapters have been separated into pressure and condensate load conditions. These different operating conditions, coupled with the mechanisms of operation, resulted in different Steam Wastage Values . This section reviews the Steam Wastage data used in this research work. A full list of data sets is included in Appendix D.

In the following analysis chapters data sets are further divided by pressure and condensate load conditions, as the intensity of the acoustic signal changes. Furthermore, this approach allows for a more systematic and analytical approach to review the acoustic data.

The importance of the orifice data is that it allows the steam and condensate flows to be determined separately. As there is no mechanism to plug the orifice, due to the differential pressure across the orifice either steam, condensate or a mixture of both has to be flowing through. This allows for a “purist” analysis of the acoustic emission and, for this reason, this will be analysed first.

### 5.2.1 Data Analysis Methodology

The data analysis approach presented in subsequent chapters follows an established process as highlighted in a number of sources [76, 83, 23]:

Firstly, using the previously acquired data, data will be preprocessed for feature selection. This may include filtering, re-sampling and other conditioning work. With the prepared signals, the feature selection is undertaken by analysing the signals under a variety of conditions. This will be followed by classification and finally some pattern recognition will be applied. This is an iterative process and may require a number of loops to be undertaken on the feature selection and classification to ensure a suitable model for identification of Steam Wastage can be found. The approach is shown diagrammatically in [108] and reproduced in Figure 5.1.

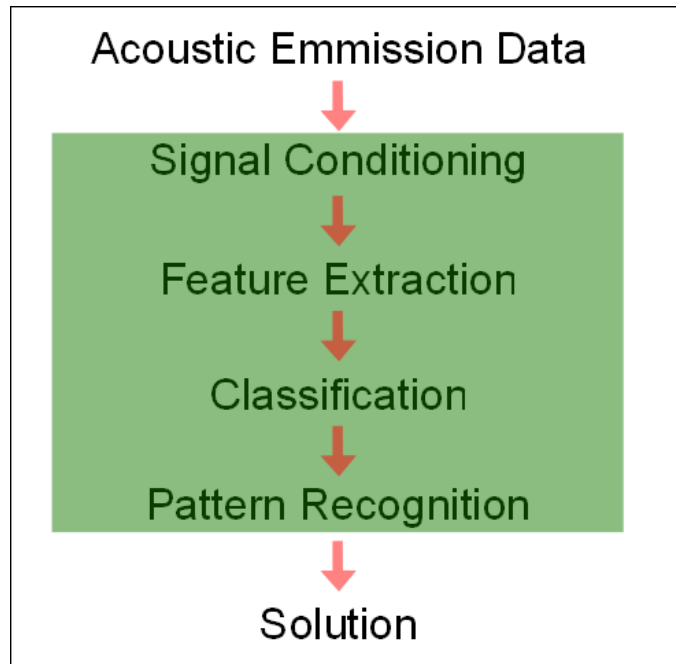


Figure 5.1: Data Analysis Approach

### 5.2.2 Re-sampling of Acoustic Data

Due to the signal being significantly oversampled, computation of the acoustic signal is re-sampled at 20kHz using decimation. This process allows for four times the bandwidth of the “active” signal, which is acceptable within the limits of the Nyquist criterion. In decimation, the full signal 50kHz is reduced by re-sampling only the  $n$ th point within the data set, thus reducing the overall sampling and signal size. This has significant computational advantages, especially when using more computationally intensive processes such as the Short-Time Fourier Transform. As in this case, the factor is a non-integer factor (equal to 2.5); Matlab was used to decimate the signal using an in-built function (resample.m).

### 5.2.3 Application of Analysis Techniques to Acoustic Steam Trap Data Analysis

Based on the results from the heterodyne investigation and the overview above, the following analysis methods will be applied to the different Steam Trap groups. These are listed in Table 5.1.

#### Acoustic Data Review by Steam Trap Type

As mentioned previously, for each of the three acoustic profiles identified, one specific trap type will be used as a representative example of this performance. The table below shows the data categories and the associated Steam Trap types with the related data availability.

Data Type	Trap Type	Applied Methods
Fixed Orifice	Fixed Orifice	Time, Frequency and Time Frequency Analysis
Non-Impulsive	FT, SM, BP	Time, Frequency and Time Frequency Analysis
Impulsive	TD, IB	Time, Frequency and Time Frequency Analysis

Table 5.1: Signal Processing Techniques applied to Steam Traps

Data Type	Trap Type	Data Type	Applied Methods
Fixed Orifice	Fixed Orifice	Heterodyne	Full data set of pressure and condensate data
Non-Impulsive	FT	Heterodyne	Partial set of pressure and condensate data
Impulsive	TD	Heterodyne	Partial set of pressure and condensate data

Table 5.2: Operational Parameter Analysis Data Summary

The data being considered varies by trap type but is within the pressure range of 5 barg to 20 barg, which reflects a substantial proportion of operating conditions seen in industrial process industry. The condensate load is largely dictated by the test rig as well as the conditions of the Steam Trap. The data that is presented as part of this analysis ranges from a low 10 kg/hr to 120 kg/hr. The upper range in terms of condensate load is only attained by the Fixed Orifice Trap. To provide a means to review the data, the spread of condensate and pressure values have been plotted to allow a ready comparison of the data displayed in the Table 5.2.

**Fixed Orifice Data** The data for the Fixed Orifice Trap shown in Figure 5.2, displays a good spread of measurements across both pressure and condensate load ranges. The geometrical and in some cases, linear relationship is caused by the simplicity of this trap. As there is no mechanism to interfere with the operation, the values recorded in the experimentation are clearly related.

**Float Trap** The Float Trap data, shown in Figure 5.3, presents a good spread of pressure conditions (one of the experimental control parameters), but the condensate loads recorded are not as widely ranged as the previously presented data for the Fixed Orifice trap. The reason for this is that the mechanism causes a throttling of the flow through the trap, reducing the amount of condensate that can be cleared.

**Thermodynamic Trap** The Thermodynamic Trap data shown in Figure 5.4 presents also a good spread of pressure conditions although the condensate loads are not as widely ranging as the



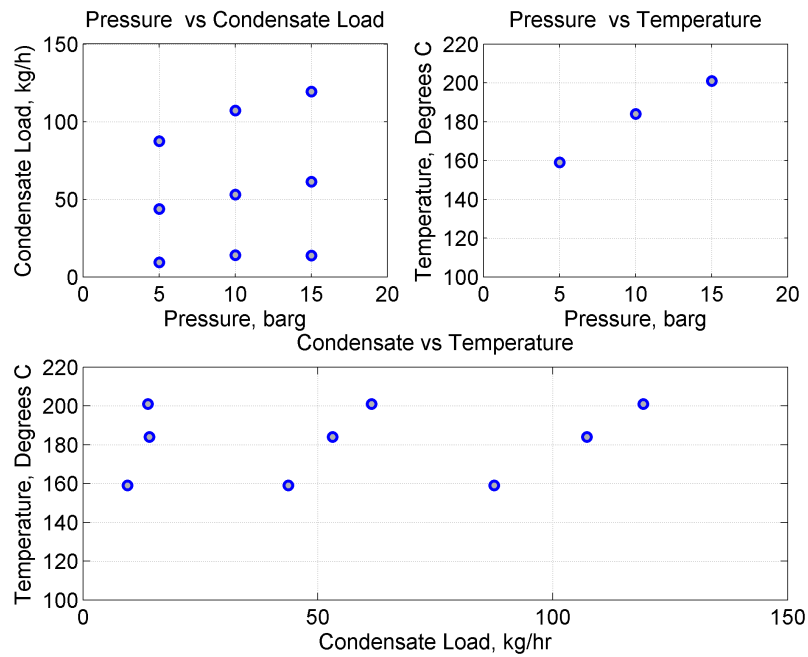


Figure 5.2: Fixed Orifice Trap Data Review

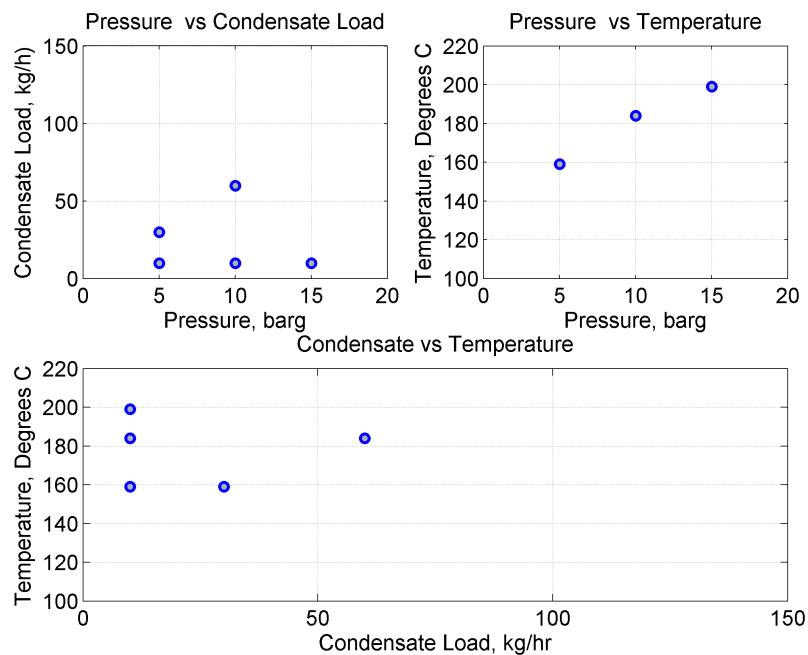


Figure 5.3: Float Trap Data Review

Fixed Orifice trap. This trap has a low flow rate due to its construction. For this reason, the main application is on steam distribution pipe condensate drainage. Furthermore, the mechanism, a disc moving inside the trap, much like a check valve causes a throttling of the flow through the trap, reducing the amount of condensate that can be cleared.

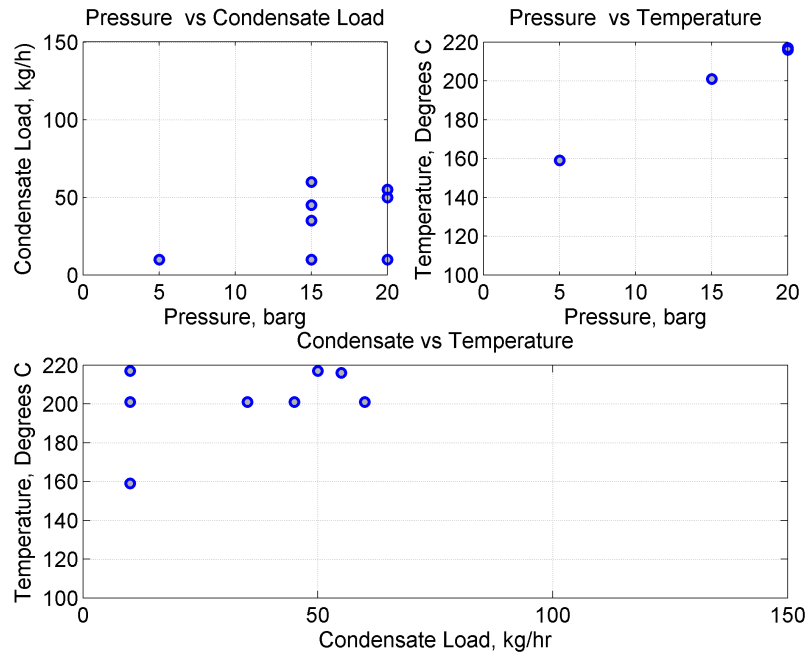


Figure 5.4: Thermodynamic Trap Data Review

**General Comments** As can be seen in Figures 5.2, 5.3 and 5.4 the pressure and temperature are related, reflected by the steam saturation curve in Figure 5.6, which is explained in the next section.

### 5.3 Overview of the Key Parameter Analysis

The key parameter analysis focuses on deterministic parameters which are part of the test setup. Deterministic parameters can be defined by a set number of parameters and are limited in choice. In other words, they can be bound to a range of specific and definable values. In the Steam Trap analysis, these deterministic parameters include the Steam Trap type as well as measurable values of condensate load, pressure and temperature.

As highlighted in Chapter 2, acoustic emission is a result of two-phase flow, fluid structure interaction and the response of the Steam Trap. To allow the acoustic emission to be analysed in relation to Steam Wastage, the impact and contribution of the primary, deterministic parameters must first be understood. A list of possible primary parameters are provided in Table 5.3.

The Steam Wastage Value is affected by all of the parameters shown in Table 5.3, making it difficult for a definitive analysis to be undertaken without considering the interdependencies of these parameters individually. Reviewing the list, it is worth noting that the Steam Trap size is fixed for this investigation to 1/2 inch size. The design of Steam Traps by different manufacturers are comparable thus only Spirax Sarco Steam Traps are being investigated (other than the Fixed

Parameter	Range of Values (Approximate)	Included
Steam Wastage	0 - 20kg/hr	Yes
Steam Trap Type	TD, FT, FO, IB, SM, BP	Yes
Pressure	0-20 barg	Yes
Temperature	100 - 200 °C	Yes
Condensate Load	0 - 200 kg/hr	Yes
Pipe Size	1/2, 3/4, 1 inch	No
Pipe Fitting	Screwed, Welded, Flanged, etc.	No
Manufacturers	See Appendix	No

Table 5.3: Table of Test Parameters

Orifice trap, which is not manufactured by Spirax Sarco). Alternative steam line designs and connections also have not been considered. All traps have been tested in a horizontal setup with screwed connections. The test line setup followed the recommended Steam Trap and condensate line design in the product support literature and “Steam and Condensate Loop” book [91]. In Figure 5.5 a graphical representation of the interdependence of the 5 key parameters is shown in the form of a Venn diagram.

In the Venn Diagram, the Steam Wastage Value is depicted as the central interface in Figure 5.5 surrounded by three clear, two-parameter intersections, which can be identified and named as:

- 1) Interface 1 - Pressure / Temperature and Steam Trap type relationship
- 2) Interface 2 - Steam Trap type and Condensate relationship
- 3) Interface 3 - Steam Trap type and Pressure relationship

In an effort to reduce the dimensionality of this research investigation, these three interfaces (where two circles are overlapping) are important to be understood prior to analysing and un-

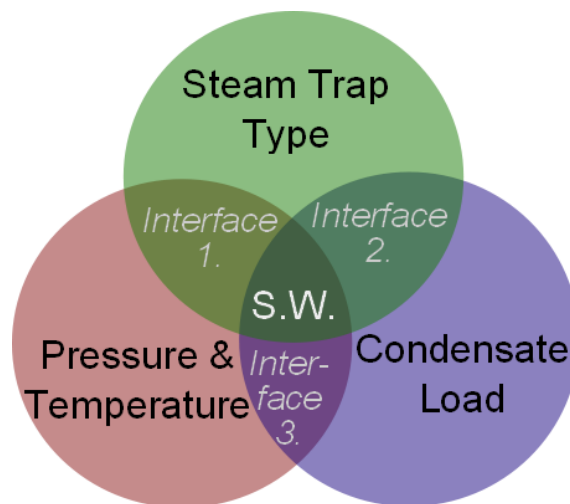


Figure 5.5: Interdependence of Key Parameters in Steam Wastage Determination

derstanding the relationship of acoustic emission and Steam Wastage Values. In this Chapter, the overlapping segments will be first to be considered, allowing the interdependence between the respective two parameters of the overlapping segments to be established. Thereafter, Steam Wastage is considered (located graphically in the centre of the Venn diagram) for each of the three Steam Trap groupings.

These parameters (other than the Steam Trap type) are all indications of the operational conditions of the Steam Trap and can be controlled or measured. As saturated steam was used to test Steam Traps, the pressure and temperature are correlated deterministically by the steam saturation curve, which can be seen in Figure 5.6. For this reason, the pressure and temperature parameters are displayed as one entity in the Venn diagram.

In the remainder of this section, the pressure-temperature dependence (which is highlighted by the steam saturation curve relationship) is further investigated. Thereafter, the relationship between the Steam Trap type and pressure or condensate load is reviewed to complete the understanding of the interface relationships.

### 5.3.1 Multivariate Analysis of Test Parameters

This section reviews the pressure-temperature dependence on the basis of operational variables. The four parameters being considered are: Pressure, Temperature, Condensate Load and Steam Wastage. A multivariate analysis is used to review these experimental parameters to highlight trends and relationships between these parameters. Figure 5.7 displays pressure, condensate load and temperature plotted against each other in a matrix format. It is worth noting that where the parameter is plotted against itself (e.g. Pressure vs. Pressure) a histogram is displayed showing the distribution of the data. This graph shows that the experimental data used in this investigation is well distributed across all conditions, although each set of trap data does not cover all of the conditions when compared to Figures 5.2, 5.3 and 5.4. The only relationship not distributed across the domain is the temperature-pressure relationship, as seen in the bottom left and top right

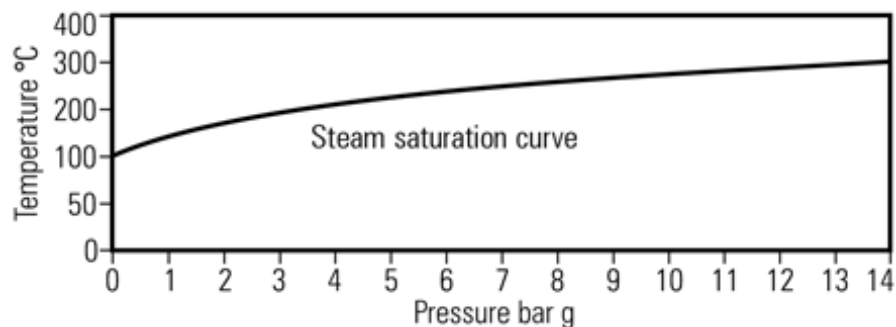


Figure 5.6: Steam Saturation Curve

quadrants of Figure 5.7, which is explained in the next section.

### Pressure-Temperature Relationship

As can be seen, Steam Wastage Measurement is related to pressure and temperature conditions at the Steam Trap. Comparing Figures 5.6 and 5.7, the relationship between the pressure and temperature and the steam saturation curve is shown.

A conclusion from this analysis is that provided the steam is saturated, the Steam Wastage calculations introduced in Chapter 2 work. One of the assumptions of the Steam Wastage Measurement standard ([71]) is that it is restricted to saturated steam conditions only, allowing the enthalpy values of the steam and condensate to be fixed by conservation of energy. As only saturated conditions will be used by this investigation, the temperature effects can be neglected and only pressure considered. For this reason, only pressure, condensate load and trap type will be covered in the next chapters when Steam Trap data is analysed.

### Pressure-Condensate Load Relationship

The interdependence between condensate and pressure is also depicted in Figure 5.7. There is no specific relationship between the pressure and the condensate load. The data is widely distributed

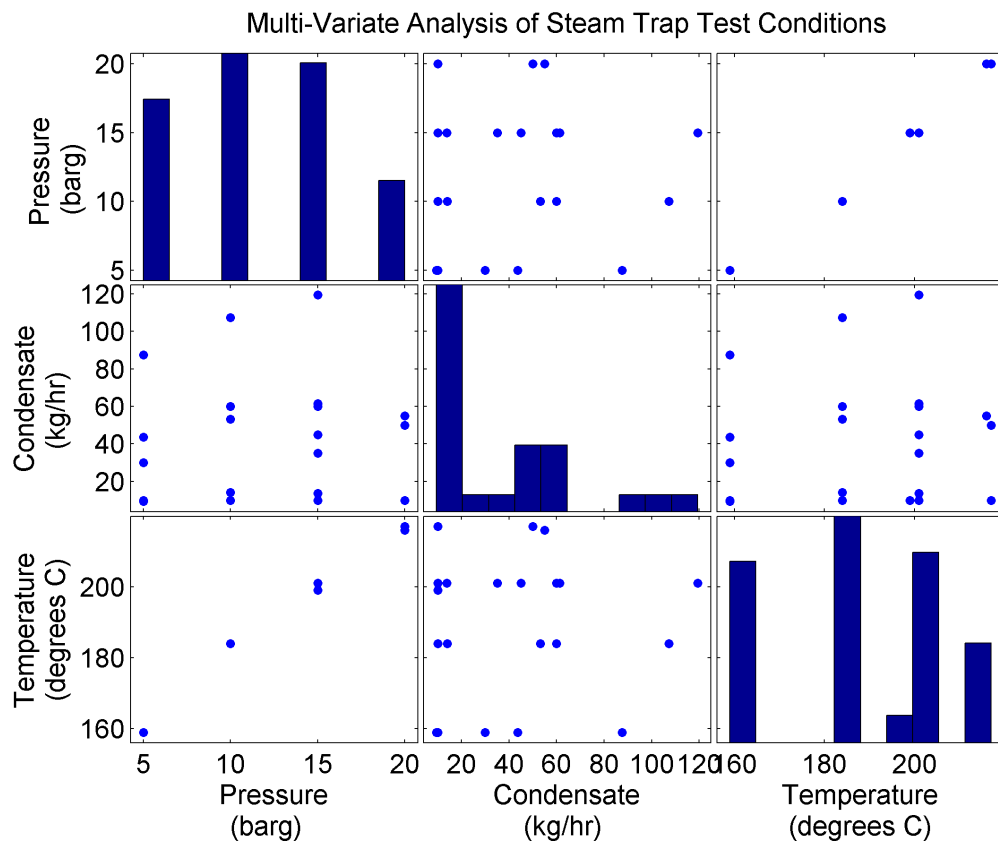


Figure 5.7: Multi-Variate Analysis of Steam Trap Test Conditions

and clearly there is no relationship. This is expected as there is no link between these two factors.

### 5.3.2 Analysis of Trap Type and Pressure / Condensate Load Relationship

The following sections review the dependence of pressure and condensate on the Steam Wastage Values for individual trap types. The RMS and Kurtosis evaluations for acoustic emission are used to investigate the relationship of pressure and condensate load. The first data set used to investigate this relationship is the Fixed Orifice Trap type, as it has no mechanisms and thus the resulting acoustic data will be free from extraneous data and the effects can be reviewed in their purest form.

As an explanation for Figures 5.9 to 5.14, the colour of the data points indicate the region of condensate load or the pressure in the pressure and condensate load graphs respectively. In other words, in an RMS and Pressure graph, the colour will denote the condensate load indications. The colours have been set with the thresholds listed in Table 5.4, additionally this is graphically shown in Figure 5.8.

Colour	Pressure (barg) (Outer Marker Colour)	Condensate (kg/hr) (Inner Marker Colour)
Red	> 12	> 80
Yellow	< 12 and > 6	< 80 and > 20
Green	< 6	< 20

Table 5.4: Operational Condition Condensate and Pressure Indicator

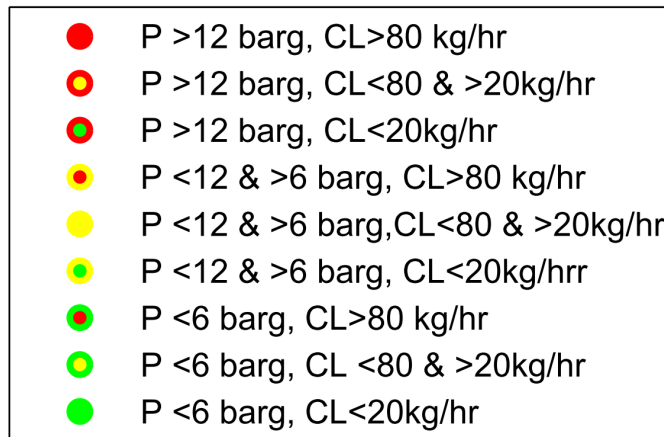


Figure 5.8: Operational Parameter Analysis Colour Legend

## Feature Extraction

### RMS

The RMS value is the square root of the arithmetic mean of the sum of the squares of the original values. The equation for the RMS value given a set of  $n$  values  $(x_1, x_2, \dots, x_n)$  is shown in Equation 5.1:

$$x_{rms} = \sqrt{\frac{x_1^2 + x_2^2 + \dots + x_n^2}{n}} \quad (5.1)$$

RMS is often used as a measure of power of a signal or apparatus and the relevance of the power.

### Kurtosis

Kurtosis is more commonly referred to as “skewness”. The Kurtosis of a normal distribution is 3 and depending on the skewness of the signal, the value of the Kurtosis changes. Matlab defines the Kurtosis by Equation 5.2,

$$Kurtosis = \frac{E(x - \mu)^4}{\sigma_{SD}^4} \quad (5.2)$$

where  $\mu$  is the mean of  $x$ ,  $\sigma_{SD}$  is the standard deviation of  $x$ , and  $E(t)$  represents the expected value of the quantity  $t$ .

### Fixed Orifice

The Fixed Orifice Trap was introduced in Chapter 2. The data considered for this analysis (in Figure 5.9) includes a number of signals at different pressure and condensate load levels. A complete list of data sets is included in Appendix D.

**Pressure Analysis** The analysis of pressure for the Fixed Orifice Trap shows that the RMS values of the recorded data can be banded into high, medium and low levels although they overlap each other.

The analysis shows that an increase in pressure results in an increase in RMS, which makes sense as with a higher pressure, more energy is contained in the flow, causing a higher acoustic emission. Another point worth noting is that the data sets (marked by similar colour indicators) are clearly clustered together for a given condition, yet still distributed. This shows that signals are related, but are not necessarily deterministically repeatable, in other words, statistics may need to be applied. Kurtosis, on the other hand, is more widely distributed, especially, at low

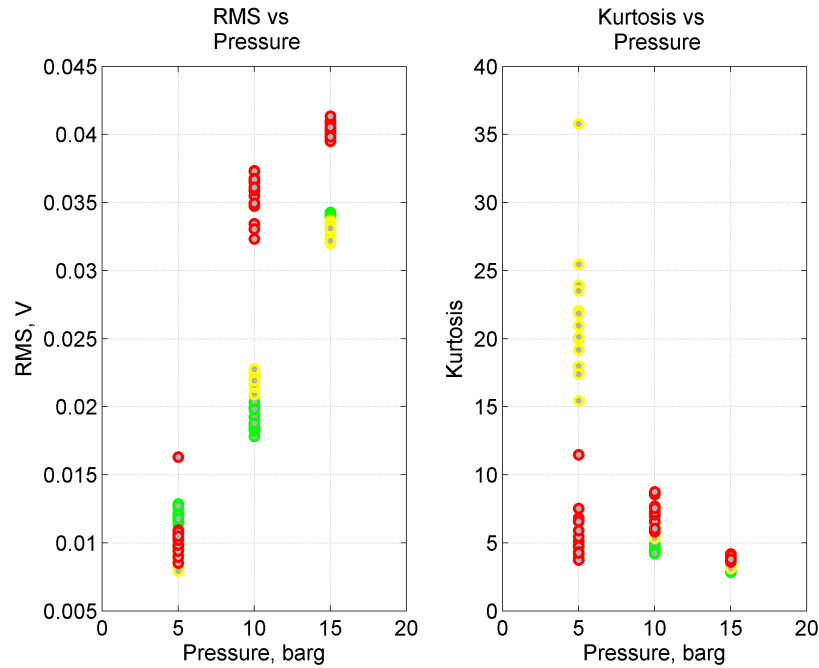


Figure 5.9: Fixed Orifice Pressure vs. RMS and Kurtosis Load Review

pressure. Kurtosis does not provide any useful features to assist in the understanding of the trap type and pressure relationship.

**Condensate Load Analysis** Reviewing the relationship between RMS and condensate load, the higher the condensate load the higher the RMS value. This makes sense as the higher the condensate the more mass is contained in the flow of the pipe and thus a higher acoustic emission is contained. Another point worth noting is that the values are all clustered together, suggesting that the experimental conditions are consistent.

Upon review there does not seem to be a relationship between Kurtosis and condensate load. Although most of the experimental values are clustered, there is no deterministic relationship between the values.

For this reason, Fixed Orifice Traps are difficult to diagnose acoustically by a survey engineer, as a key measure is the volume of the acoustic emission of the flow. As shown in Figure 5.9, both the steam and condensate load are related to an increased RMS.

### Non-Impulsive Steam Traps

As with the Fixed Orifice Trap, the data considered for this pressure and condensate load analysis includes a number of signals at different pressure levels. It is worth noting that there is no high pressure data, the reason for this is that the trap considered for the Float Trap has a maximum pressure limit of 14 barg. A complete list of data sets is included in Appendix D.



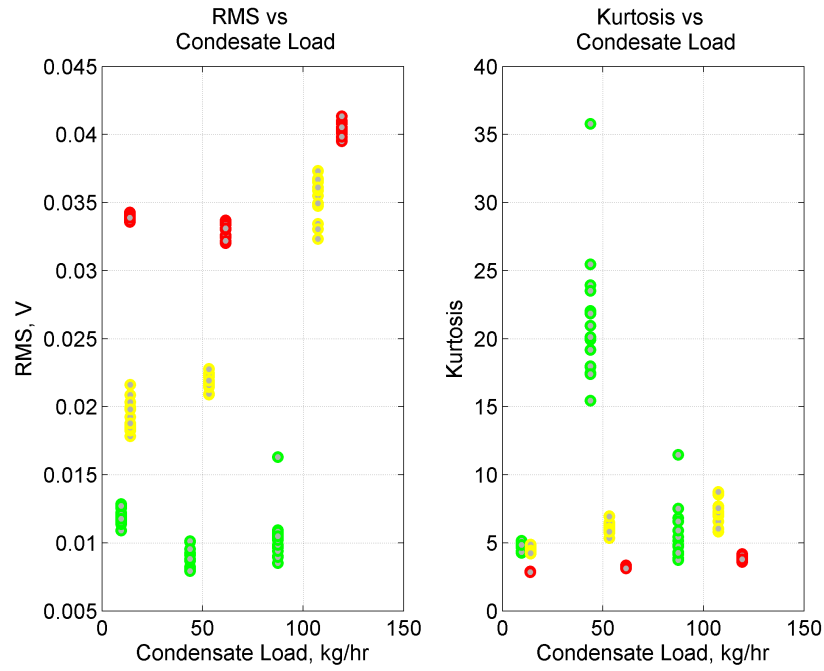


Figure 5.10: Fixed Orifice Condensate Load vs. RMS and Kurtosis Review

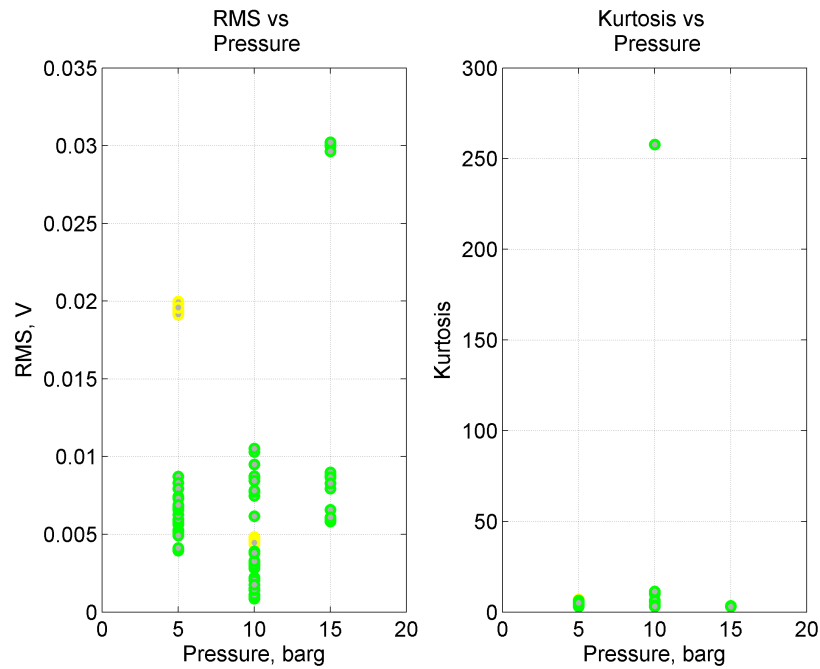


Figure 5.11: Float Trap Pressure vs. RMS and Kurtosis Review

**Pressure Analysis** The Pressure analysis for the Float Trap is shown in Figure 5.11. There does not seem to be a relationship between RMS and pressure. The RMS value does not provide any information on the relationship between these factors for the non-impulsive trap category. Likewise, Kurtosis does not provide any specific information.

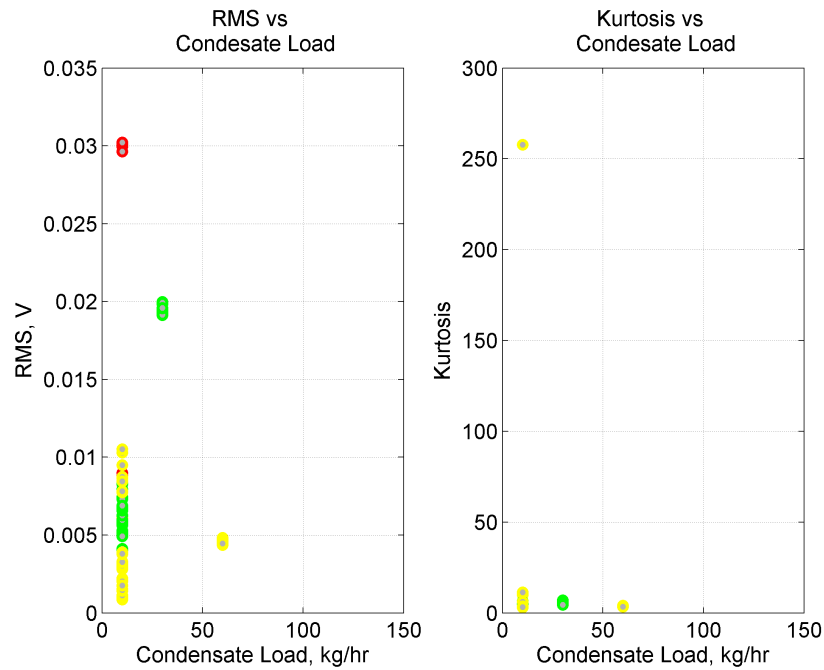


Figure 5.12: Float Trap Kurtosis Condensate Load vs. RMS and Kurtosis Review

**Condensate Load Analysis** The condensate load analysis for the Float Trap is shown in Figure 5.12. Reviewing the relationship between Kurtosis and RMS and condensate load, the higher the condensate load the higher the RMS value.

Both Kurtosis and RMS do not seem to assist in the determination of the Float Trap relationship with pressure and condensate load.

### Impulsive Steam Traps

The data considered for the pressure and condensate load analysis includes a number of signals at different pressure levels. A complete list of data sets is included in Appendix D.

**Pressure Analysis** There appears to be no relationship between RMS and pressure for this trap type. This can be explained as the trap signal is impulsive and, depending on the operation, the trap could show highly varying RMS values, with several impulses within a data recording. Equally, Kurtosis does not assist in the understanding of the relationship between pressure and RMS.

**Condensate Load Analysis** Reviewing the relationship between RMS and condensate load for Thermodynamic Traps highlights an interesting point. Essentially, the RMS is not related to the condensate load, which makes sense due to the operation of the trap. However, with regards to the condensate load, the higher the pressure, the lower the RMS value, as seen in Figure 5.14. In

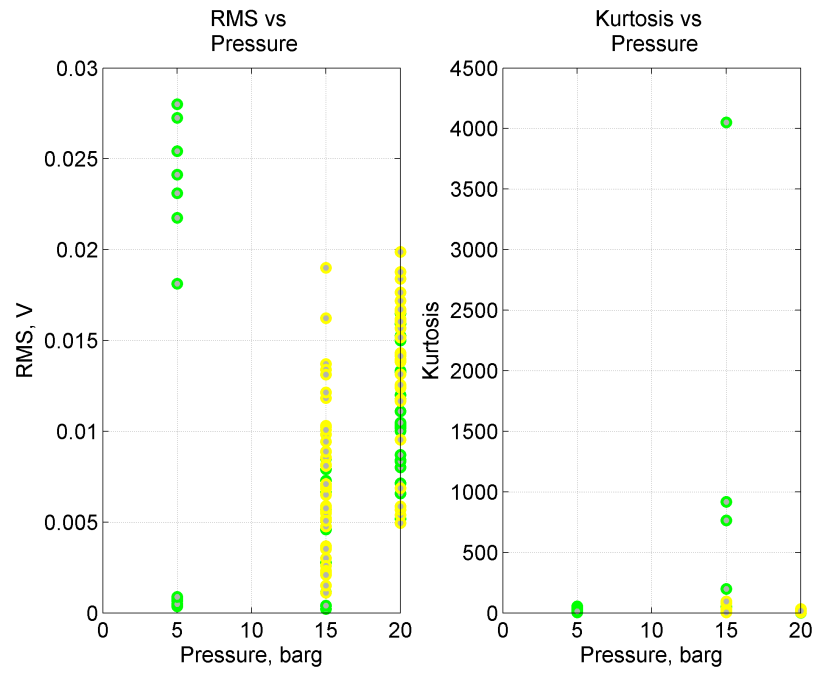


Figure 5.13: Thermodynamic Trap Pressure vs. RMS and Kurtosis Review

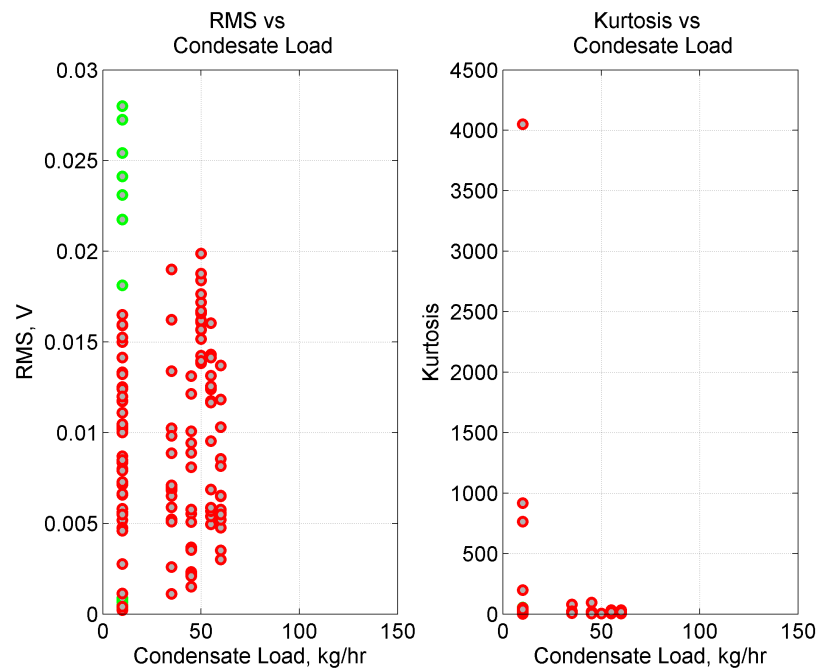


Figure 5.14: Thermodynamic Trap Condensate Load vs. RMS and Kurtosis Review

terms of the Kurtosis and condensate load in Non-Impulsive Traps, the two are not related. There are a number of outliers, all related to high pressure and a relatively low condensate load.

### **Discussion of Steam Trap Type acoustic emission in relation to Pressure and Condensate Load**

This section demonstrates that Steam Trap operations can be highly random in nature. The acoustic emission from the three characteristic Steam Traps show that the level of noise is useful in traps that have no mechanism, such as the Fixed Orifice Trap. This makes sense as the mechanism will interfere with the acoustic response of the Steam Trap.

Key Points of the preliminary analysis are:

- 1) Interface 1 - Pressure & Temperature relationship. The analysis has shown that the temperature and pressure are related, suggesting that the measurement of temperature could be used to estimate pressure.
- 2) Interface 2 - Steam Trap Type and Condensate Load relationship. The relationship of Condensate Load to the Steam Trap Type was measured with RMS and Kurtosis. Only for the Orifice Trap, using an RMS measurement, could a relationship be established. In the other traps, mechanisms interfere with this measurement.
- 3) Interface 3 - Steam Trap Type and Pressure relationship. The relationship of Steam Trap type to the pressure was measured with RMS and Kurtosis. Only for the Orifice Trap, using an RMS measurement, could a relationship be established. In the other traps, mechanisms interfere with this measurement.

## **5.4 Acoustic Analysis Techniques applied to the Steam Wastage Data**

The failure modes listed previously require the application of a number of signal processing methods to be applied to highlight characteristic features for the diagnosis. Analysis methods, which have been highlighted in the background review of Chapter 2, have shown a number of methods that have been applied to condition monitoring applications. Resulting from the background research, the following methods have been applied to the identification and feature selection in Acoustic Steam Wastage Data:

- 1) **Time Domain Averaging and Statistics** - This technique will be applied to the initial pressure and Condensate Load indication.
- 2) **Fast Fourier Transform for Steam Trap Signals** - This technique is suited to stationary signal feature extraction, as in stationary signals, the frequency content does not change with time. Frequency analysis allows the features of the signal to be highlighted. As the frequency

analysis considers the whole length of the signal, no distinction is made on when a specific frequency occurs.

- 3) **Short-Time Fourier Transform for Steam Trap Signals** - The disadvantage of the frequency is that it considers the frequency content across the whole signal. However, time-frequency analysis highlights the dynamics within the signal, providing an additional dimension over the FFT approach by dividing the signal up into discrete time units. For this reason, this approach is applied to non-stationary signals allowing frequency content in a specific section of the signal to be identified and analysed.

Although it is expected that time or time-frequency approaches will be more suited to the impulsive trap category for example, for prudence, all techniques will be applied to all trap types.

## 5.5 Summary

The following are the findings and observations that have been made:

- 1) The Steam Traps have been reviewed and categorised by response to three categories: Fixed Orifice, Non-Impulsive and Impulsive. For each category one example trap type was defined for further investigation.
- 2) A number of parameters were outlined and the scope of the investigation has been defined and limited.
- 3) The variability in the acquired data as well as the complexity of the variety of data has been shown. For this, a multivariate analysis was used to assess the relationship between operational parameters. It has been demonstrated that the data sets, as a whole, across the three different trap sets, span the conditions well.
- 4) Using basic measurements of Kurtosis and RMS for each trap type, the difficulty in consistently measuring the Steam Wastage has been made apparent. It has been discovered that RMS and Kurtosis values resulting from acoustic emission data cannot be used to conclusively determine Pressure, Condensate Load or Steam Wastage Values in Steam Traps.
- 5) The chaotic and variable nature of Steam Trap operational behaviour has been introduced.

*This chapter has reviewed the operational parameters of this research and an overview to the structure of the following three analysis chapters. The next three chapters will analyse the Steam Trap as per the three acoustic emission categories identified in this chapter. It is worth noting that Chapter 6 provides an overview of the techniques and measures that are applied to all three analysis chapters.*

## Chapter 6

# Fixed Orifice Steam Trap Analysis

*This chapter presents the analysis of Fixed Orifice Steam Trap data. The recorded data has been processed using time and frequency methods and the results are presented and interpreted.*

### 6.1 Acoustic Signals for Fixed Orifice Trap

For this research, this trap provides an idealised scenario and assists in the acoustic determination of steam and condensate leakages. The noise emission from this trap is solely due to fluid flow, phase changes and dimensional flow path changes. The signal for the long time large scale (tens of seconds) can be classed as stationary. However, on a smaller time scale (seconds) a pulsating phenomenon is observed, which is a reflection of the inherent chaotic nature of the signal. This trap can be classed as non-stationary when considered at a shorter time scale.

This investigation will review the purist scenario of high steam leakage with low condensate load and high condensate load with low Steam Wastage. These specific scenarios have been chosen to reduce the presented data size to a manageable volume. Furthermore, the Orifice Trap allows these two scenarios to be investigated in their purest form, i.e. not being affected by mechanism or other temporary processes. Additionally, an intermediate scenario of medium steam leakage and medium condensate load are presented. The following sections will present the signal processing data and investigate steam leakage at different scales.

Another point worth noting is that as there is no mechanism in the Orifice Trap, there is a constant flow rate of a mixture of steam and condensate. The flow rate is limited by the pressure and the size of the orifice of the trap, but uniquely (compared to other traps) if pressure is applied to the trap, there will always be a flow of a kind. The acoustic data for this trap type has been recorded using the Steam Wastage Monitor as well as the Steam Wastage Rigs presented in earlier chapters. The data presented covers a wide range of conditions up to 20 barg and 87.5 kg/hr

condensate load. The datasets have been divided into three pressure ranges (high, medium and low) within each the Condensate Load and Steam Wastage Value will be considered. Overall these datasets generate 153 data points which are used in the subsequent analysis to correlate the operational conditions with the acoustic emission.

The data considered for the analysis is displayed in the Table 6.1.

Filename	SWV (kg/hr)	Pressure (barg)	Condensate (kg/hr)	Temperature (°C)
UK_12_01_09_11_11_48	4.62	5	9.5	159
UK_12_01_09_11_54_59	1.65	5	43.7	159
UK_12_01_09_14_23_07	0.57	5	87.5	159
UK_12_01_09_11_11_48	7.79	10	14.1	159
UK_12_01_09_11_54_59	2.51	10	53.1	159
UK_12_01_09_14_23_07	0.27	10	107	159
UK_12_01_09_11_11_48	11.63	15	13.8	159
UK_12_01_09_11_54_59	3.6	15	61.4	159
UK_12_01_09_14_23_07	-0.26	15	87.5	159

Table 6.1: Fixed Orifice Trap Acoustic Data Summary

### 6.1.1 Characteristics of the Acoustic Signals

As an introduction to the acoustics of the Orifice Trap, three signals have been plotted in Figures 6.1, 6.3 and 6.5. These examples are all at 5 barg pressure and provide the reader an overview of the format of Fixed Orifice data at low, medium and high Steam Wastage Values. It is worth noting that the time domain representations for all nine operational condition examples will be shown as part of the frequency analysis in Section 6.2.2 of this chapter.

Additionally, as explained, the response of the signals depend on the scale at which the signal is being analysed. Over minutes, the signal will appear to be largely stationary. On a shorter time scale, the waveform can be considered. When the signal is considered on the level of one second or less, the rate of change of the signal is clearly displayed. For this reason, for each of the displayed examples, a shorter time scale plot is presented.

Figure 6.1 shows a high Condensate Load example of 87.5 kg/hr and low Steam Wastage of 0.57 kg/hr. A strong background noise level is displayed with a slight amplitude rise over the 2 minute period of the recording. Some randomly placed instantaneous spikes are also shown. A closer view of the signal is provided in Figure 6.2 where the same signal is shown on a 1 second and 0.1 second time scale. The non-stationary behaviour is clearly shown at both scales although the one second sample does include a small spike between 0.6 and 0.7 seconds.

Figure 6.3 shows a case of medium Condensate Load (43.7 kg/hr) and a medium Steam Wastage (1.85 kg/hr). The same clear background noise band is displayed as with the first example with a comparable magnitude. However, the spikes have become more frequent in number

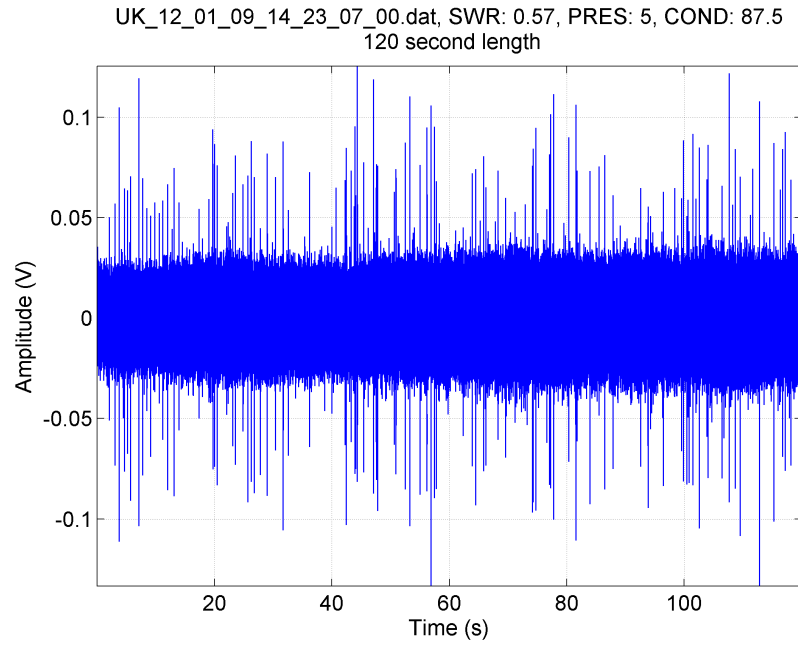


Figure 6.1: Orifice Trap 5 barg Low Steam Wastage Time Plot

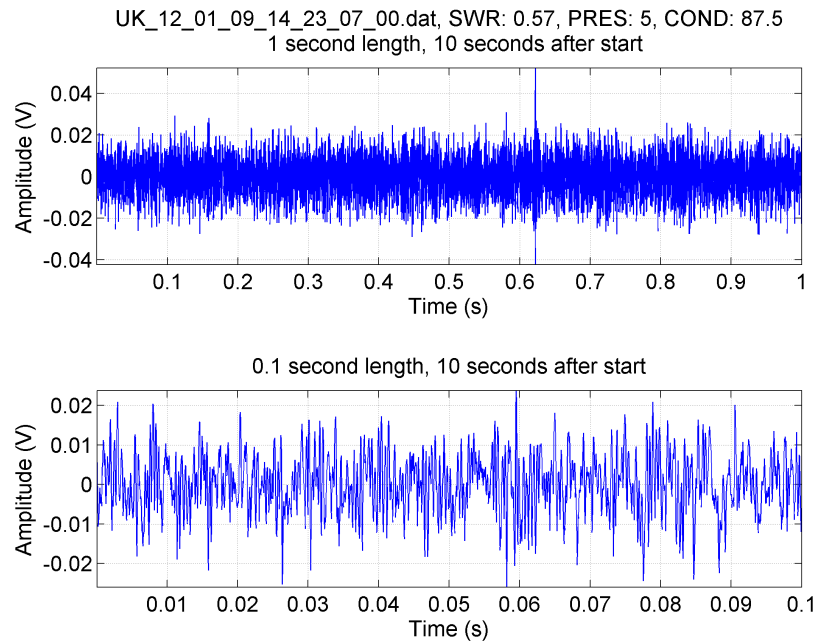


Figure 6.2: Orifice Trap 5 barg Low Steam Wastage Time Plot Zoomed

and higher in amplitude. This may be related to the increased density of the condensate load and the impact on pipe structure. Considering the shorter time scale shown in Figure 6.4, a similar response is displayed as in the previous example with lesser overall amplitudes. In the 1 second example, the amplitude is now around half of the previous example. The same is true for the 0.1 second example.



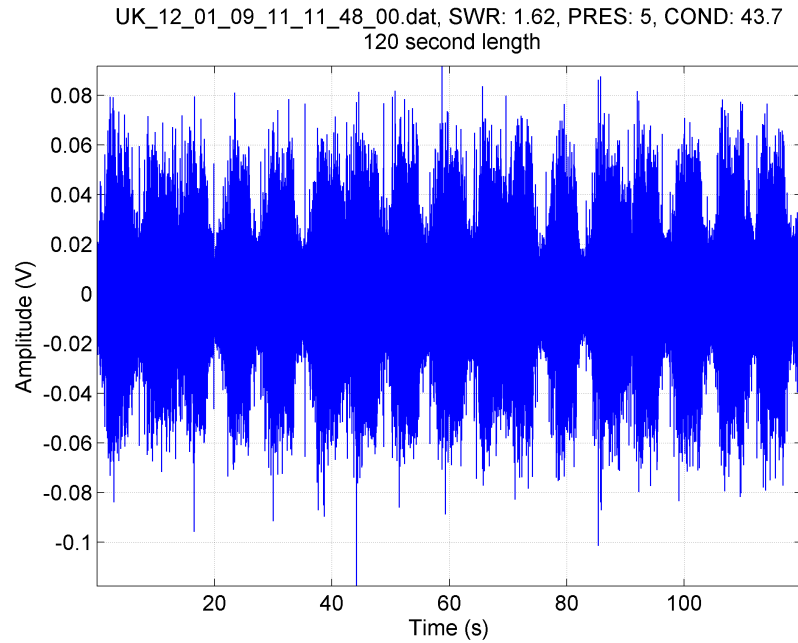


Figure 6.3: Orifice Trap 5 barg Medium Steam Wastage Time Plot

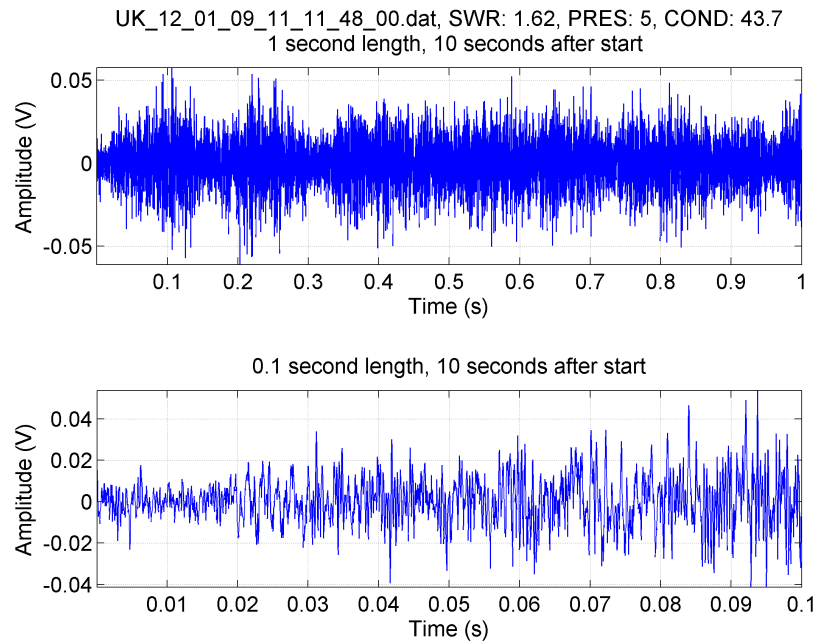


Figure 6.4: Orifice Trap 5 barg Medium Steam Wastage Time Plot Zoomed

Finally, Figure 6.5 shows a low Condensate Load (9.5 kg/hr) and high Steam Wastage (4.62 kg/hr) example. The strong background signal is now not visible as the shape of the signal is wave like. From a two-phase flow regime point of view, this behaviour is very slug-like where there are high energy and low energy regions of the recording. Considering the signal at the shorter time scales, shown in Figure 6.6, the signal is fairly stationary, although it does include

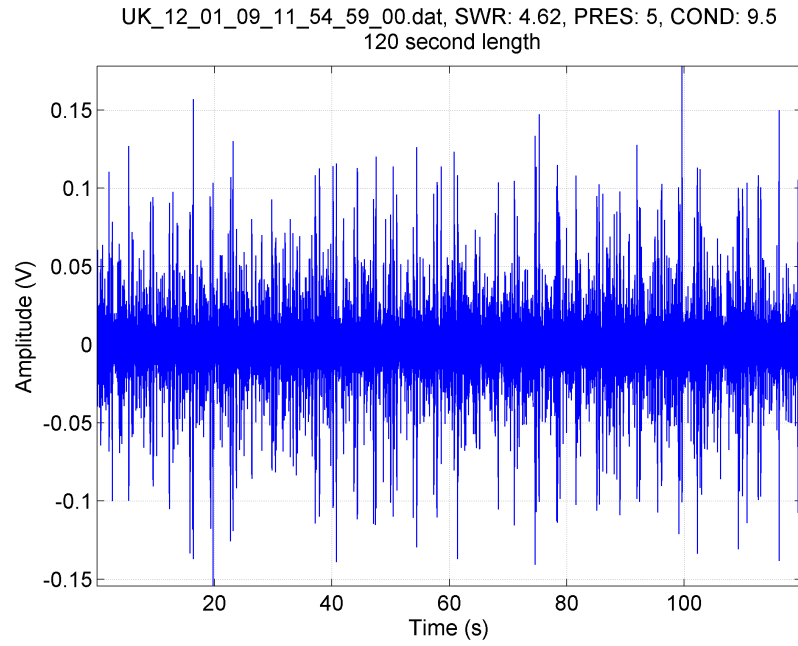


Figure 6.5: Orifice Trap 5 barg High Steam Wastage Time Plot domain

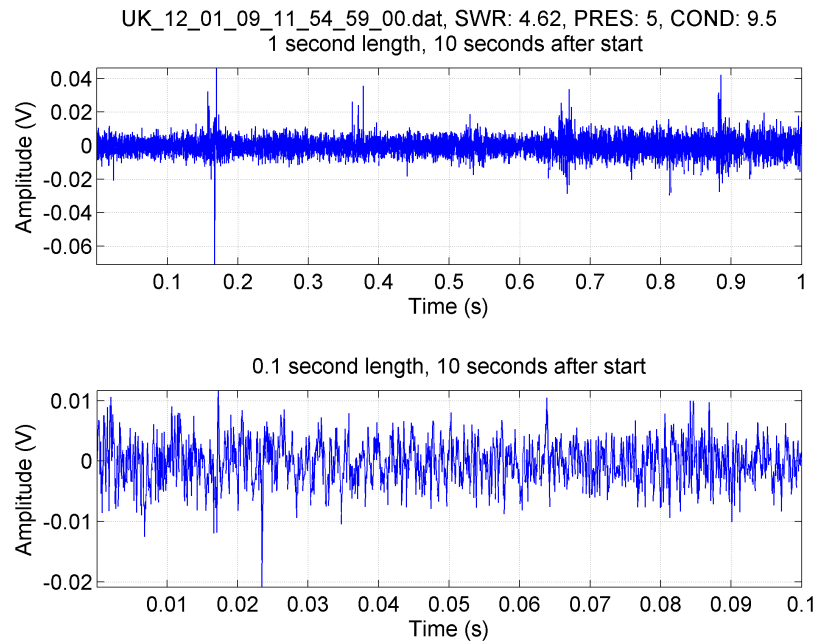


Figure 6.6: Orifice Trap 5 barg High Steam Wastage Time Plot Zoomed

some slow modulation. The time scale of 0.1 seconds also shows a trend of the signal growing in amplitude as time progresses.

**Discussion** The length of the data samples presented are 2 minutes long and the stationary nature of the signal can clearly be seen. As previously explained, the Fixed Orifice Trap is an ideal case as there is always flow present and no mechanism to interfere with the flow. The different

manifestations of modulations occurring at different mixtures between steam and condensate have been introduced.

### 6.1.2 Feature Extraction of Acoustic Trap Signals

A number of features have been calculated using the signals presented. Additional to the RMS and Kurtosis calculations presented in Chapter 5, a number of features were calculated, namely: Standard Deviation, Maximum, Variance, Mean, Sum and Median. The following section provides a short explanation of each of these features including the equation used for calculation.

#### Standard Deviation

The standard deviation ( $\sigma_{SD}$ ) is defined as the square root of the average value of  $(X - \mu)^2$ :

$$\sigma_{SD} = \sqrt{E[(X - \mu)^2]} \quad (6.1)$$

Here, the operator  $E$  denotes the average or expected value of  $X$  and  $\mu$  is the mean. The Standard Deviation allows the spread of the distribution of the signal points to be analysed. A low value indicates that the values in the data set are close to the mean, a high value indicates that the values of the data set are more widely distributed.

#### Maximum Individual Value

The Maximum Individual Value is determined by an iterative process rather than calculation.

$$x_{1,2,\dots,n} = x_n < x_{max} \quad (6.2)$$

The Maximum Individual Value determines the maximum value of any point within the data point set that make up the signal. Although this feature is not expected to provide much useful output as the maximum point does not relate to the remainder of the data points within the signal data set, it is an easy feature to measure and select.

#### Variance

The variance can be expressed as:

$$\text{Var}(X) = E[(X - \mu)^2] \quad (6.3)$$

It is clear from the equation that the variance is defined as the standard deviation squared.

The variance is a measure of how widely the values are spread apart. The calculated value of the variance can only be zero or positive as the value is squared. If the value of the variance is zero, the data set is invariant. Consequently, the closer the value of variance is to zero the smaller the difference in values within a data set.

### Mean

The arithmetic mean is essentially the average value.

$$\bar{x} = \frac{1}{n} \cdot \sum_{i=1}^n x_i \quad (6.4)$$

The mean of a data set is defined as the average of the data set. It is calculated by adding all the values within the set and dividing by the number of data points within the set.

### Sum of Total signal

The Sum of Total Signal is calculated by adding all points within the data set as shown in Equation 6.5.

$$x_{sum} = |x_1| + |x_2| + \dots + |x_n| \quad (6.5)$$

When comparing the sum parameter between different data sets, it is important to ensure that the number of points is constant so that the values can be compared.

### Median

The median is defined as the value for which half of the population of values is above and half of the values is below the median value. For a series of values placed in order of magnitude, the Median is given by

$$Median = \frac{n^{th}}{2} value \quad (6.6)$$

It should be noted that for skewed distributions, the mean and median are not the same value, as the mean will be the arithmetic average and the median will be the value of half of the population.

## 6.2 Application of Signal Processing

### 6.2.1 Time Domain Analysis

The following section reviews key features of the time domain representation for the Fixed Orifice trap, for which the time domain signal was analysed by splitting the signal into 15 second subsets. Steam Wastage has been plotted on the x-axis and the calculated feature on the y-axis. In addition, the marker contains two colours to allow Pressure and Condensate Load indications to be represented (in a similar way to that in Chapter 5). Using this approach, four parameters can be displayed in one graph which reduces the number of figures required to consider all permutations of data combinations.

The markers have been implemented by a two-dot system, in which the inner colour indicates the level of Condensate Load and the outer colour the Pressure level. The Condensate Load and Pressure have been differentiated into a range of high, medium and low, as detailed in Table 6.2. A visual representation is provided in Figure 6.7 to show an applied context.

Colour	Pressure (barg) (Outer Marker Colour)	Condensate (kg/hr) (Inner Marker Colour)
Red	> 12	> 80
Yellow	< 12 and >6	< 80 and > 20
Green	< 6	< 20

Table 6.2: Fixed Orifice Trap Condensate and Pressure Indicator

●	P >12 barg, CL>80 kg/hr
●	P >12 barg, CL<80 & >20kg/hr
●	P >12 barg, CL<20kg/hr
●	P <12 & >6 barg, CL>80 kg/hr
●	P <12 & >6 barg, CL<80 & >20kg/hr
●	P <12 & >6 barg, CL<20kg/hrr
●	P <6 barg, CL>80 kg/hr
●	P <6 barg, CL <80 & >20kg/hr
●	P <6 barg, CL<20kg/hr

Figure 6.7: Orifice Colour Legend

The results of the time domain evaluations of the features introduced in the previous sections are shown in Figures 6.8, 6.9, 6.10 and 6.11.

Figure 6.8 show the RMS and Kurtosis measurements for the Fixed Orifice Trap data set. The RMS measurement is not related to Steam Wastage, as a high RMS value can be related to either high or low Steam Wastage Values. Considering the coloured markers, RMS also does not

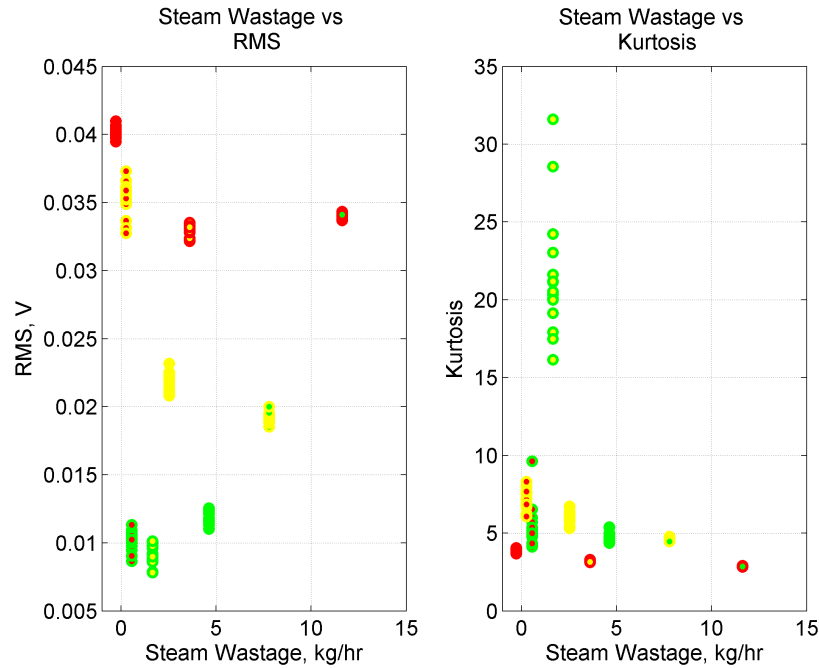


Figure 6.8: Orifice Trap Time Domain RMS and Kurtosis

seem to be related to condensate load or pressure. However, there does appear to be a linear tendency between the RMS and an increase in condensate load and pressure. Considering the high RMS values (approximately 0.035), the Condensate Load is inversely proportional to the Steam Wastage Value. This is an expected result as the Fixed Orifice has a limited pass area and no mechanism, so when the steam leakage increases, the condensate load must decrease. Furthermore, considering the pressure value, these high values are in the medium and high ranges. The results also make sense as the higher the pressure, the greater the energy contained, resulting in a higher RMS value. Equally, considering the low RMS values (below 0.015), Steam Wastage Values are inversely proportional to the condensate load indicator.

There appears to be no relationship between Kurtosis measurement and Steam Wastage Measurement in Figure 6.8. Nor does there seem to be a relationship between Kurtosis and the Condensate Load or Pressure.

Figure 6.9 shows the relationship between Standard Deviation of the Fixed Orifice Trap data set. The Standard Deviation shows the same pattern and nearly the same values as the RMS calculations. The analysis applied to the RMS will also be applied towards the Standard Deviation.

With regard to the Maximum Individual Value, such values seem to funnel towards higher Steam Wastage i.e., the values are spread wider at low Steam Wastage Values and more clustered (as a set, as well as for different conditions) towards the higher end. Low Maximum Individual Values are proportional to the Steam Wastage Values, which is explainable, even at higher pressures. The high Maximum Individual Values are related to medium Condensate Load and low

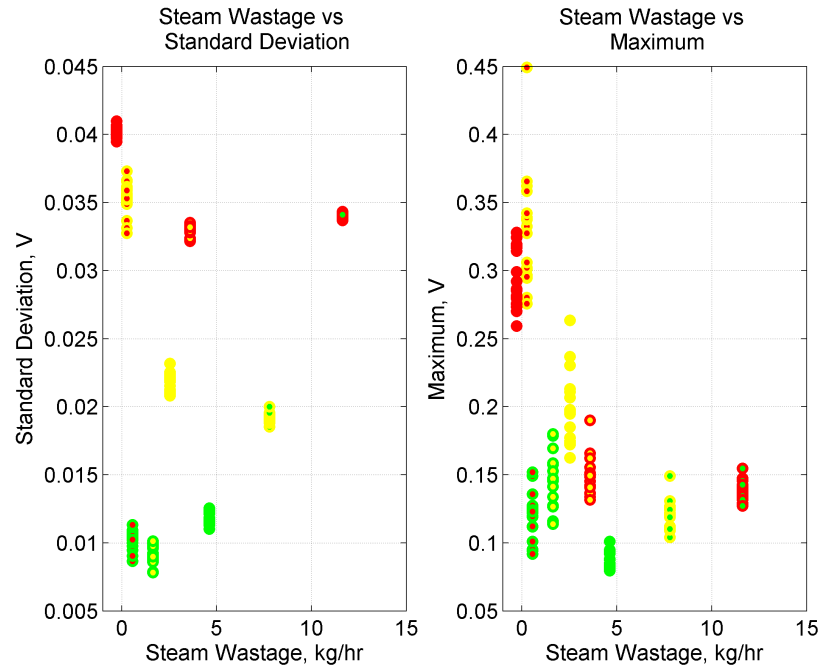


Figure 6.9: Orifice Trap Time Domain Standard Deviation and Maximum

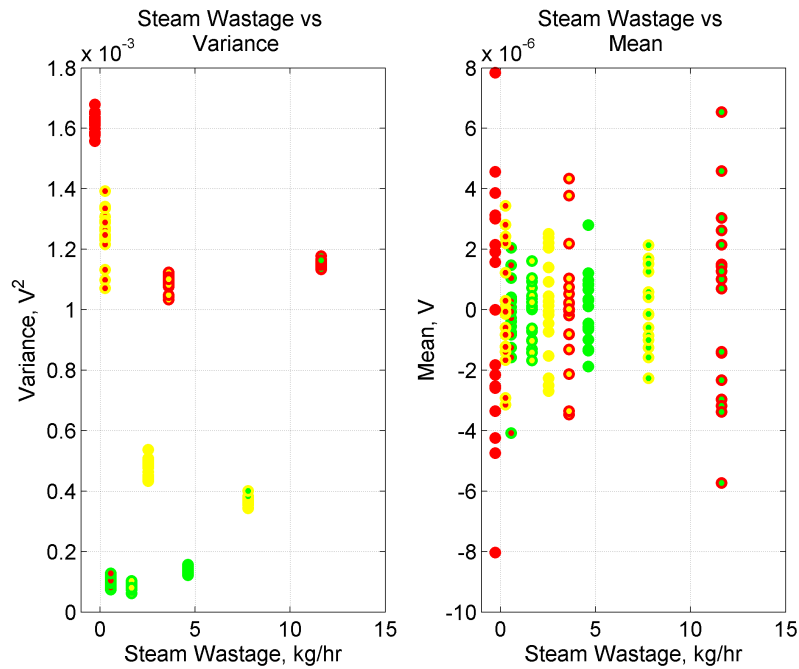


Figure 6.10: Orifice Trap Time Domain Variance and Mean

Pressure. A reason for this effect is that condensate load has a higher density and thus contains more momentum, producing higher Maximum Individual Values.

Figure 6.10 shows the relationship between Variance of the acoustic emission signal and Steam Wastage for the Fixed Orifice Trap. It can be seen that the calculation of the Variance value increases with pressure. This makes sense as the higher the pressure, the higher the energy con-

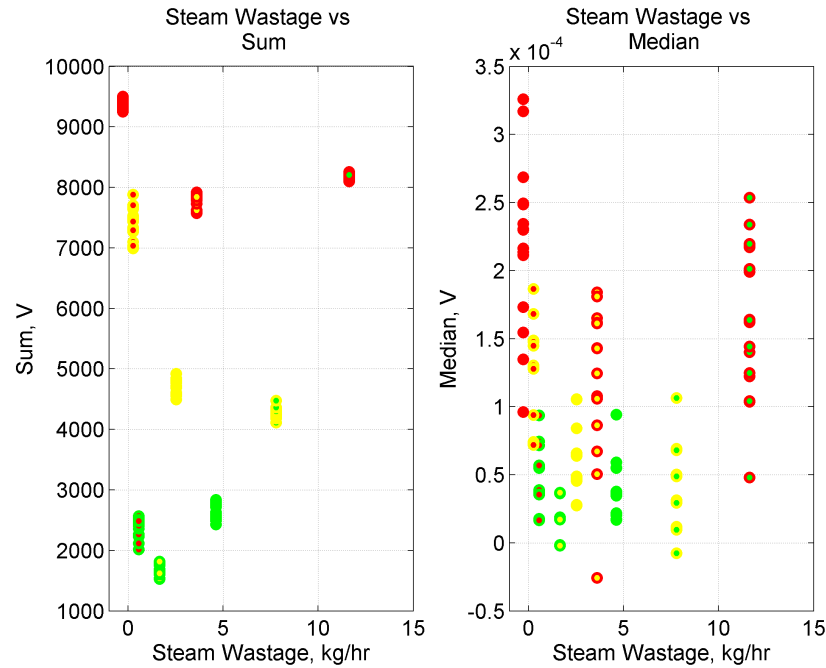


Figure 6.11: Orifice Trap Time Domain Sum and Median

tained in the pipe, thus the sum is greater. As the Variance is of the same value as the RMS value, the plot is similar to the RMS plot.

Considering the Mean values in relation to Steam Wastage, the Mean values centred around zero are more widely spread with higher Steam Wastage. Additionally, lower pressure and condensate reduce the spread of the Mean value within a data set.

Figure 6.11 shows the relationship between the sum of the total signal and the Steam Wastage value. The plot looks similar in layout to RMS and the same analysis and reasoning can be applied to this analysis.

Considering the Median, the signals are highly proportional and clustered between Steam Wastage and the Median value, although they are widely spread. Median values for low pressure conditions are more closely clustered than for higher pressure conditions. Additionally, high condensate load values produce a wider spread Median measurement, which may be caused by the two-phase slug flows.

**Discussion** It is clear from the signals that these methods can be used as an indication of condensate load or pressure, but cannot be used for Steam Wastage Measurement. For this reason, frequency and time frequency methods have been applied to the analysis.



## 6.2.2 Frequency Domain Analysis

In terms of the method in which the signal is divided into segments, the frequency analysis uses the same approach as the time domain analysis. The function to create the Fourier Transform was the standard m-file `fft.m`. The FFT was applied over 1024 points to speed up the process. Thereafter, a number of features were calculated to allow the data segments to be compared. To conclude, the energy contained within different frequency ranges of the FFT are reviewed.

Firstly a sample of the signals are presented. For the high, medium and low pressure and Condensate Load, each one example is presented to provide the reader with an overview, hence nine example plots are shown.

The Fourier Transform plots are all very comparable. For this reason, only one plot is presented in full size. The remaining eight are shown on four-to-a-page overviews.

The Fourier Transforms were calculated using a 15 second length of the sample signal. The process by which the Fourier Transforms were calculated are as follows:

- 1) A signal was divided into 15 second long data segments.
- 2) For each of the data segments, the Fourier Transform was calculated with a length of 16,384 points (equal to  $2^{14}$ ). This allows approximately 1.2 Hz per resolution bin.
- 3) A number of features (discussed earlier in Chapter 6) were calculated for comparison.
- 4) The Fourier Transform was plotted on a graph together with the time domain representation to assist in the analysis of the Fourier Spectrum in relation to the time domain signal.

In Figure 6.12, an example plot is shown. From the time domain signal, it can be clearly seen that the signal is noise-like, with a number of instantaneous speaks. Furthermore, there is a base noise band, which is steady throughout the 15 second time frame. The noise rises and falls twice within the sample length. This demonstrates typical behaviour of an Orifice Trap resulting from the two-phase flow nature of the steam and condensate mixture that presents itself at the trap. The operational conditions in this example dataset is 5 barg pressure and low condensate load (9.5 kg/hr), resulting in a high Steam Wastage of 4.62 kg/hr.

Figures 6.13 and 6.14 show other low pressure examples of the Fixed Orifice trap. It is worth noting that in both cases, the spectrum remains very peak-like although the peak frequencies shift. In the medium condensate load example, the peaks are mainly located below 1 kHz and at a low intensity level. For the high condensate load example, there are two significant intensity peaks located at 1kHz and 2kHz respectively with no features much beyond 3.5 kHz.

Considering the medium pressure examples in Figures 6.15 to 6.17, there does not seem to be any specific peaks. The noise seems to decay with frequency until about 3.5 kHz for all three

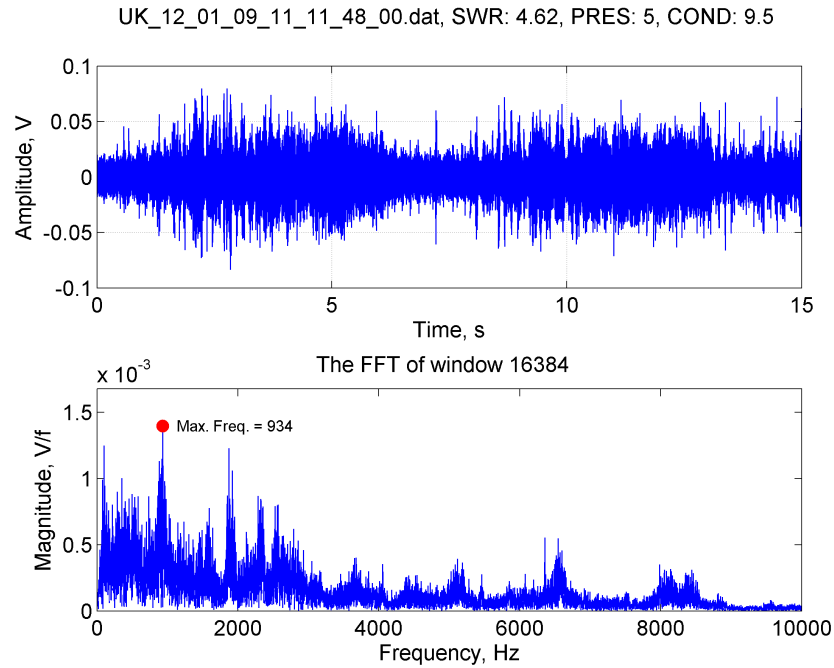


Figure 6.12: Orifice Trap FFT  
5 barg CL=9.5 kg/hr SWV=4.62 kg/hr

examples. From a time domain perspective, the signal at the high Condensate Load / low Steam Wastage is less noisy, trends are visible, but they are not abrupt in nature. Reviewing the opposite condition of low Condensate Load / high Steam Wastage, the signal in the time domain shows frequent peaks and changes, however, the baseline remains trendless. A reason for this could be that at higher condensate load, the steam leakage is interrupted by a slug of condensate, resulting in a higher rate of instantaneous events. In the high steam leakage case, the exchange between steam and condensate passing through the orifice is more rapid, resulting in trending of the baseline noise.

For the high pressure examples, Figures 6.18 to 6.20, a similar response is seen as compared with the medium pressure. There are no clear peaks and the intensity decays with the increase in frequency of the Fourier Spectrum. Comparing the three examples, a significant peak is seen at about 1 kHz that seems to shift lower in the frequency domain as the Steam Wastage level increases. From a time domain perspective, the response is largely flat across the three examples and higher in magnitude than the low or medium pressure examples previously described. The reason for the largely flat response of the time domain signal could be due to the pressure exerted on the flow. Interestingly, the high Condensate Load example (Figure 6.20) seems to indicate a low level of background instantaneous peaks which has also been observed in the other two examples of this Condensate Load condition at the other two pressures.

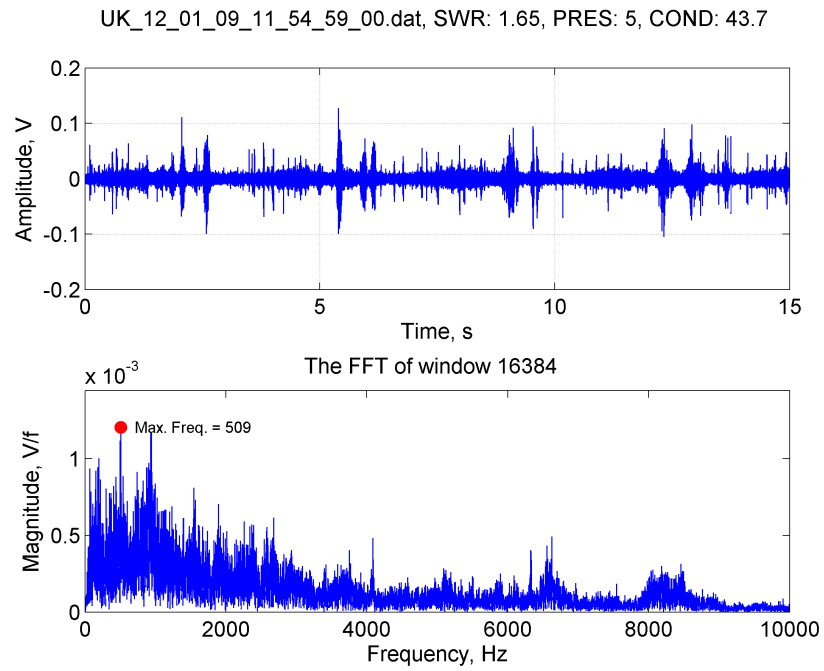


Figure 6.13: Orifice Trap FFT  
5 barg CL=43.7 kg/hr SWV=1.65 kg/hr

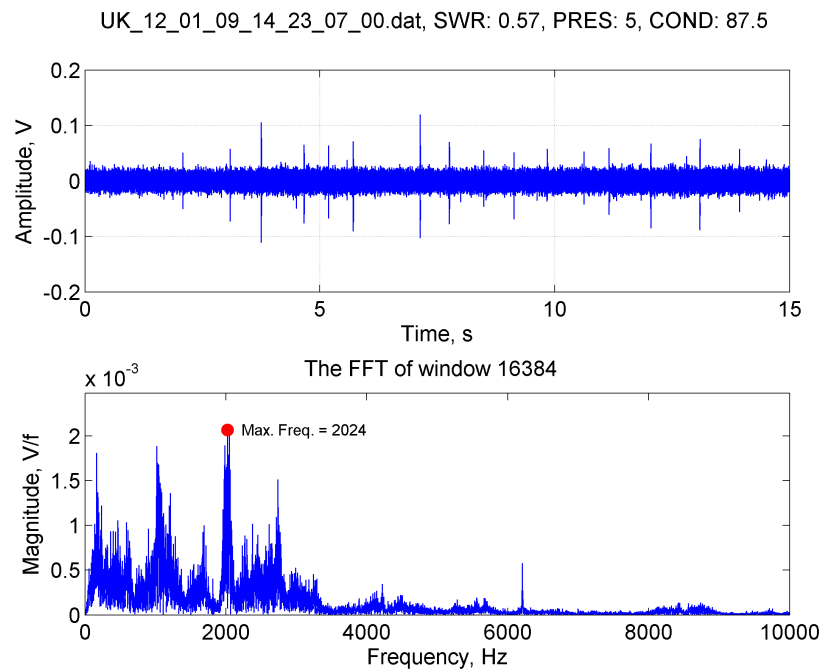


Figure 6.14: Orifice Trap FFT  
5 barg CL=87.5 kg/hr SWV=0.57 kg/hr

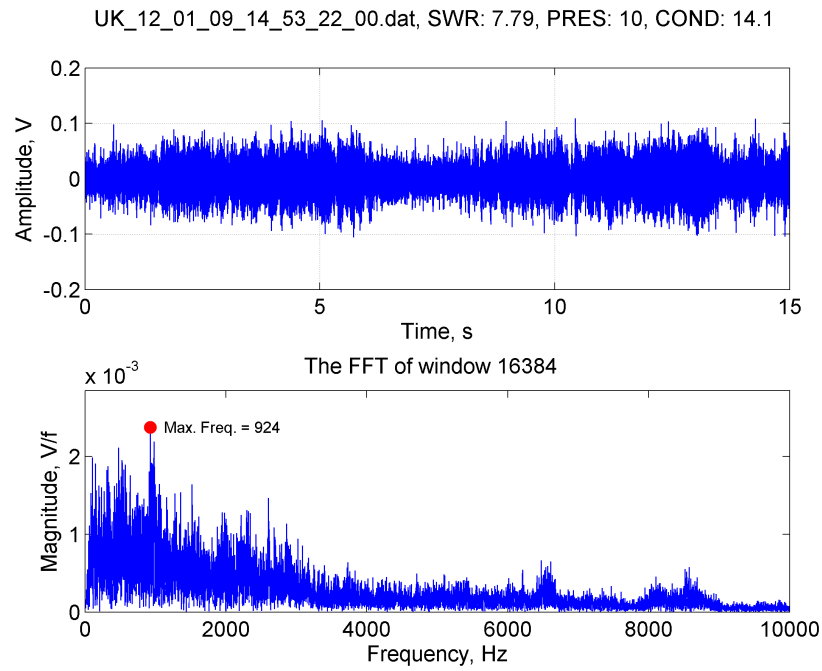


Figure 6.15: Orifice Trap FFT  
10 barg CL=14.1 kg/hr SWV=7.79 kg/hr

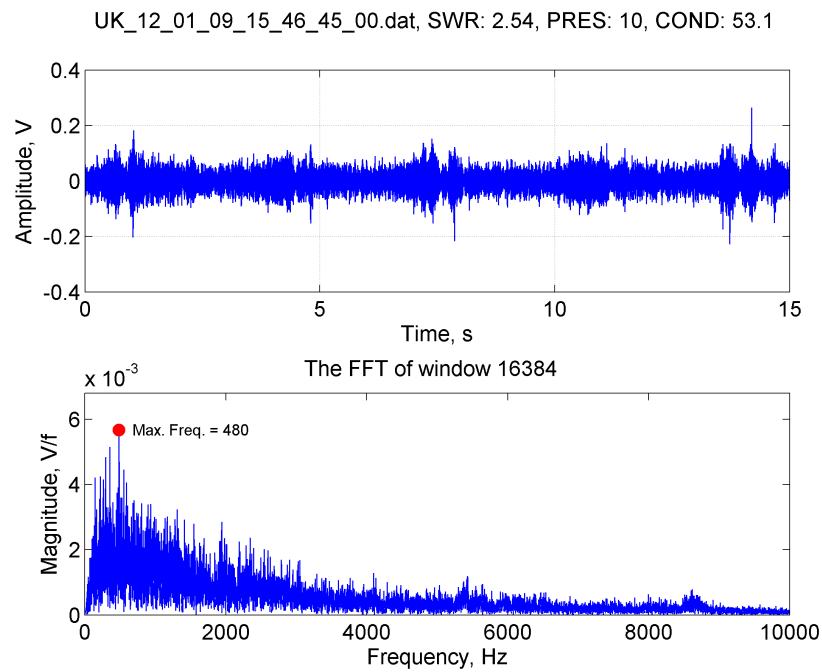


Figure 6.16: Orifice Trap FFT  
10 barg CL=53.1 kg/hr SWV=2.51 kg/hr

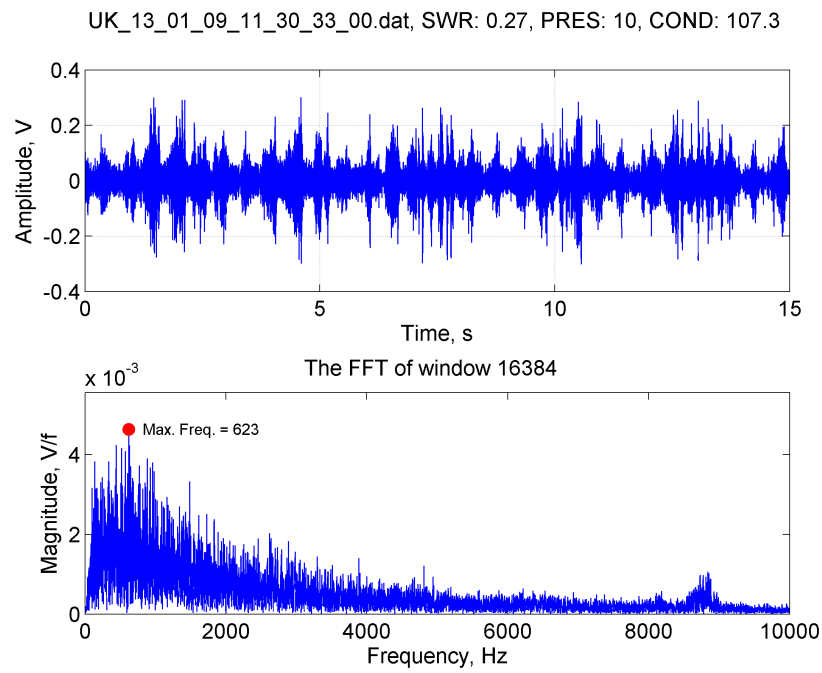


Figure 6.17: Orifice Trap FFT  
10 barg CL=107 kg/hr SWV=0.27 kg/hr

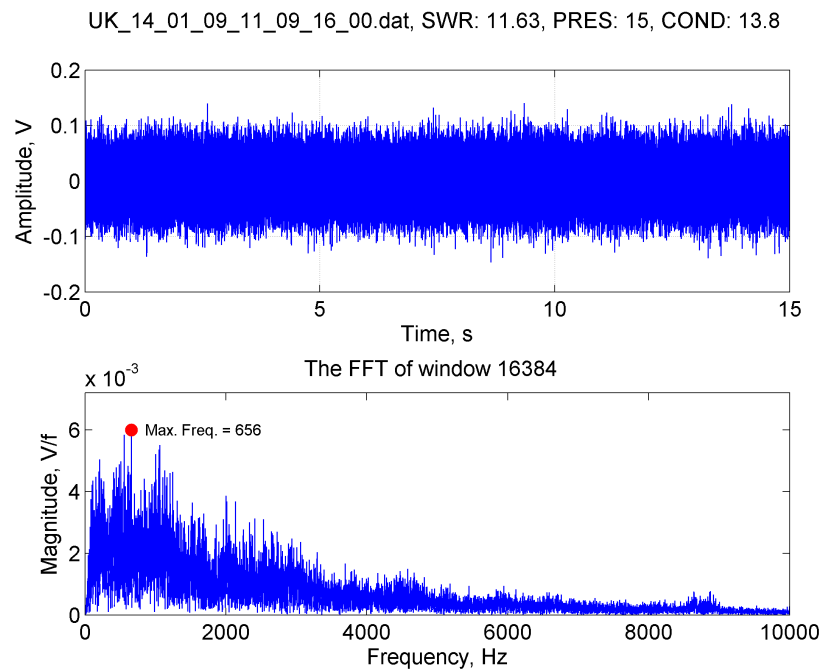


Figure 6.18: Orifice Trap FFT  
15 barg CL=13.8 kg/hr SWV=11.63 kg/hr

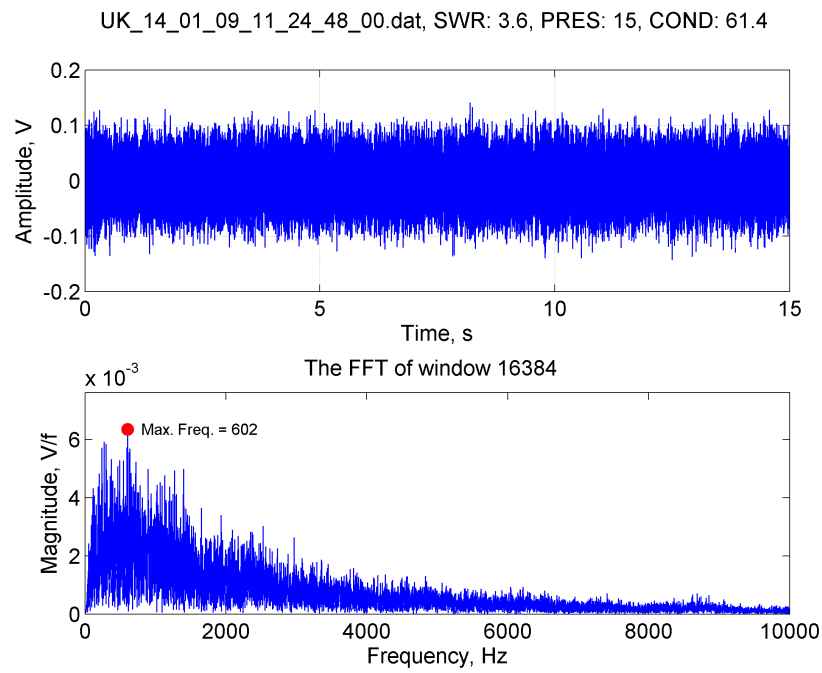


Figure 6.19: Orifice Trap FFT  
15 barg CL=61.4 kg/hr SWV=3.6 kg/hr

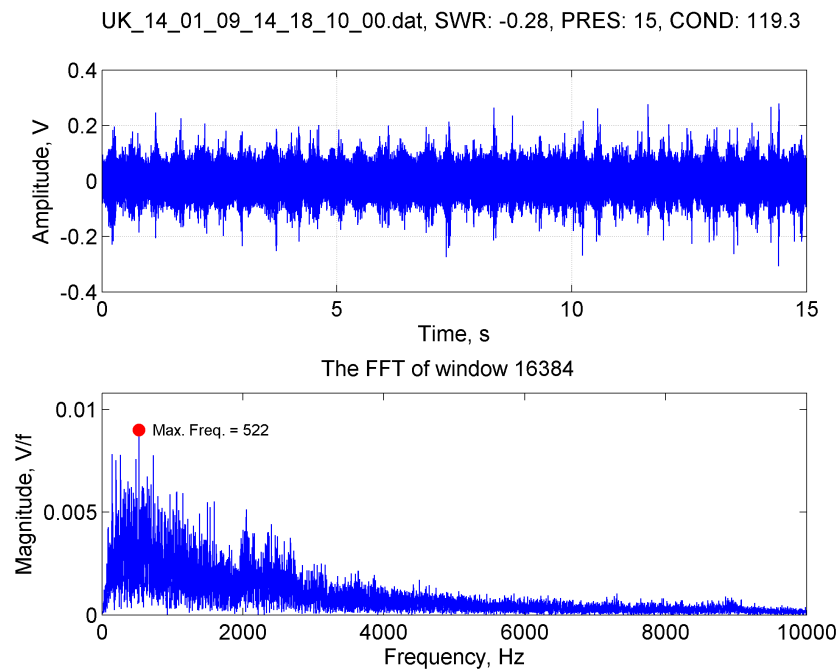


Figure 6.20: Orifice Trap FFT  
15 barg CL=87.5 kg/hr SWV=-0.26 kg/hr

The next section features summary plots previously seen for the time domain analysis. The parameters evaluated using the Fourier Transform as an input signal are RMS, Kurtosis, Standard Deviation, Maximum Individual Value, Variance, Mean, Sum of Total Signal and Median Value, introductions to which were given in Sections 5.3.2 and 6.1.2 respectively.

Figure 6.21 shows the RMS and Kurtosis evaluated and plotted against Steam Wastage. The same trend is being seen as compared to the time domain signal. The Steam Wastage is inversely proportional to the condensate load, as expected. The higher the pressure, the higher the steam RMS value. It is worth noting that the values are not closely clustered together. The RMS values could be used as an indicator of Steam Wastage, but it is certainly not conclusive, especially at low pressure conditions. If the condensate values could be determined by another method, the RMS evaluation could be used for Steam Wastage identification, which can be clearly seen through the points with a green inner circle, where the condensate load is low and the RMS measure is proportional with Steam Wastage Value (and Pressure Value).

Considering the Kurtosis evaluation in the same Figure, the values are not related and do not provide any trends. This was also found in the time domain analysis.

Figure 6.22 considers the Standard Deviation and the Maximum Individual Value. The Standard Deviation of the measurements for the Short-Time Fourier Transform signals shows the same trend as the time domain evaluations, with no conclusive trends. Likewise, the Maximum Individual Values do not yield any correlation with Steam Wastage.

Figure 6.23 considers the Variance and the Mean value of the Fourier Transform. The Variance

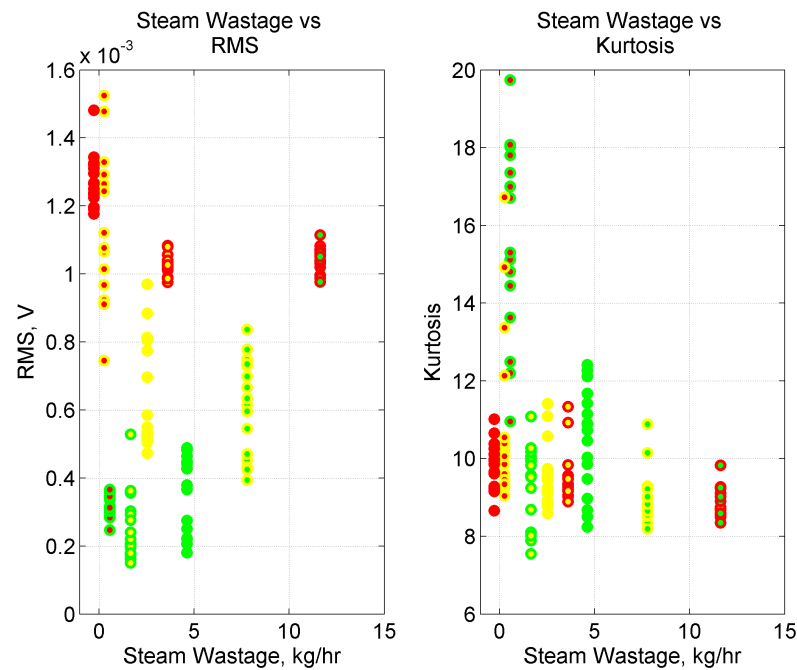


Figure 6.21: Orifice Trap Frequency Domain RMS and Kurtosis

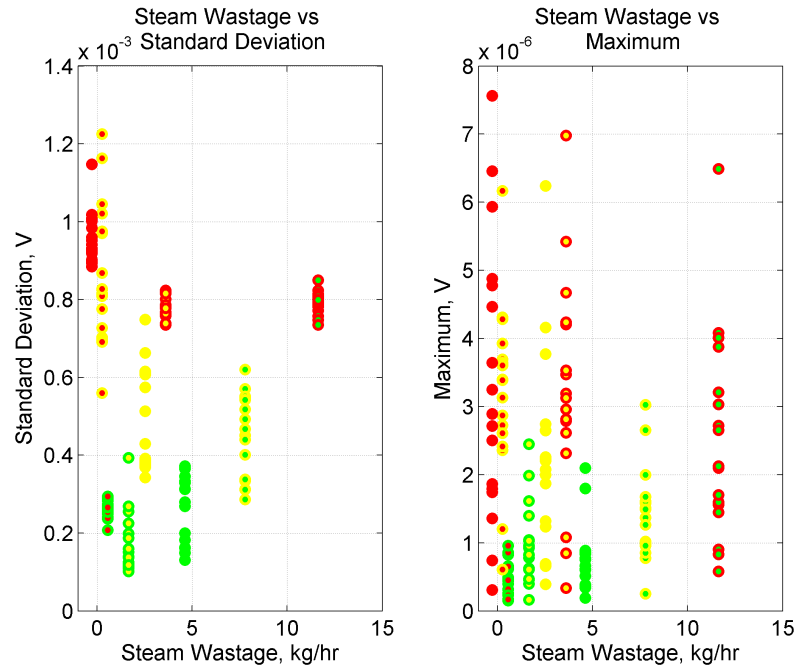


Figure 6.22: Orifice Trap Frequency Domain Standard Deviation and Maximum

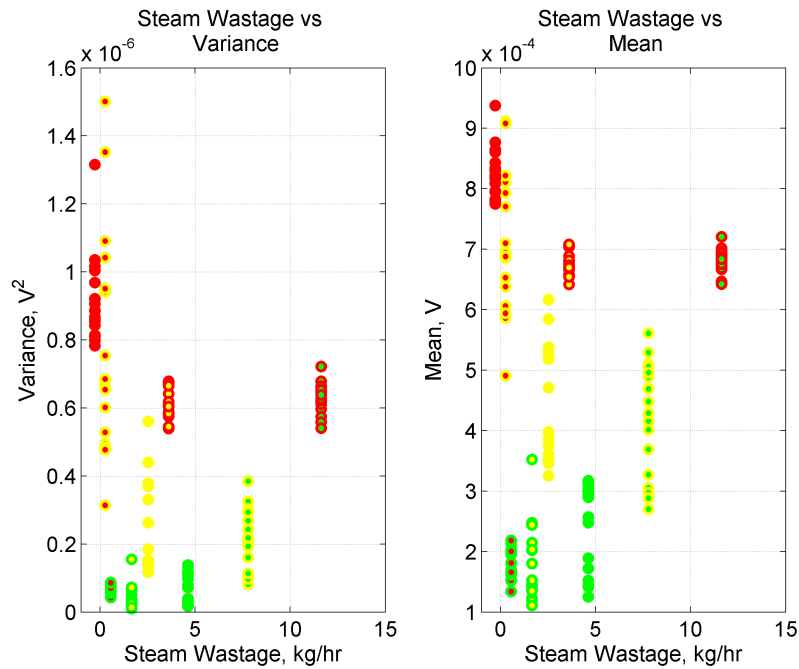


Figure 6.23: Orifice Trap Frequency Domain Variance and Mean

calculation of the Fourier Transform of the signals segments shows the same trend as the time domain calculation, providing no conclusive trends. Likewise, the Mean values do not yield any correlation with the Steam Wastage other than the one already explained as part of the RMS evaluation.

Figure 6.24 considers the sum of the Total Signal and the Median Value. No specific or useful



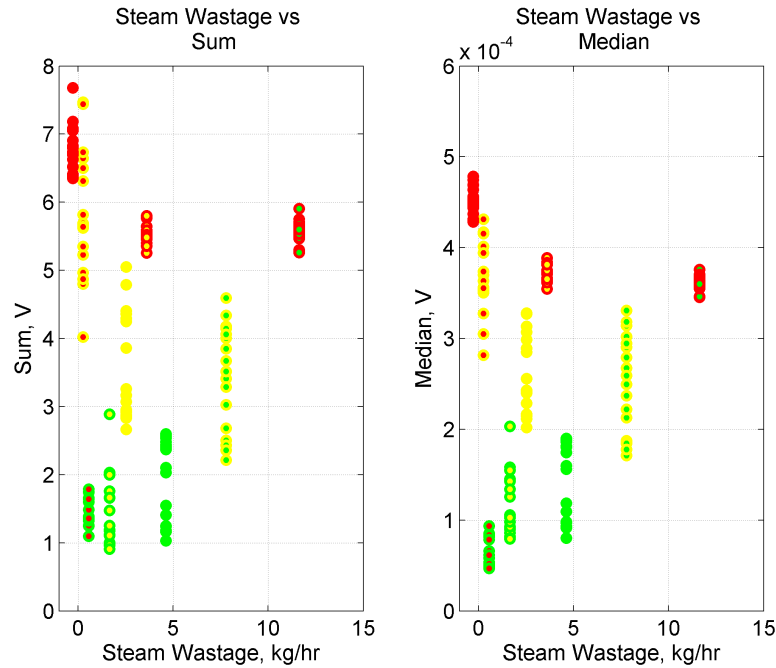


Figure 6.24: Orifice Trap Frequency Domain Sum and Median

trend has been identified. However, the two plots are nearly identical in their evaluation, which makes sense as the median is the average value. The Fourier Transform provides the locations (in terms of frequency) of the total energy as component of the individual frequency bins, thus the Median should form a similar response to the total energy of the Fourier Transform.

It is clear from these four plots of parameters calculated from the Fourier Transform, that these methods can be used as an indication of condensate load or pressure, but cannot be used for Steam Wastage Measurement.

From the review of the individual plots, a number of peaks were identified, which could not be specifically correlated to a condition. For this reason, the Crest Value has been allied to the Fourier Transform. The Crest Value has been calculated by dividing the Maximum Individual Value of a frequency range with the mean of the values within the range. Three frequency ranges were selected, namely: 1Hz to 1kHz, 1kHz to 2kHz, 2kHz to 3kHz, 3kHz to 4kHz, 4kHz to 5kHz and 5kHz to 6kHz. Figures 6.25 and 6.26 show these plotted, but there is no clear correlation between Crest Value and Steam Wastage Value. Another feature of this plot is that the Crest Value across frequency ranges as ratios remain the same, in other words, there is no relative change when comparing the Crest Value for the operational conditions in terms of the frequency range.

**Discussion** As mentioned previously, the Fourier Spectrum considers the complete 15 seconds and the representative frequencies within this signal segment. From the time domain and respective frequency analysis it can be seen that there are changes to the frequency content within the

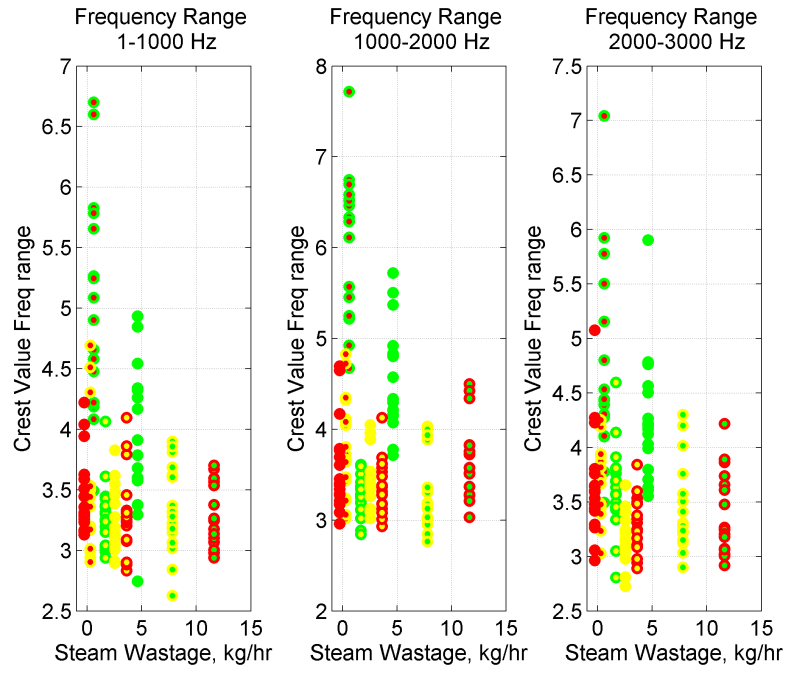


Figure 6.25: Orifice Trap Frequency Domain Frequency Bins Part 1

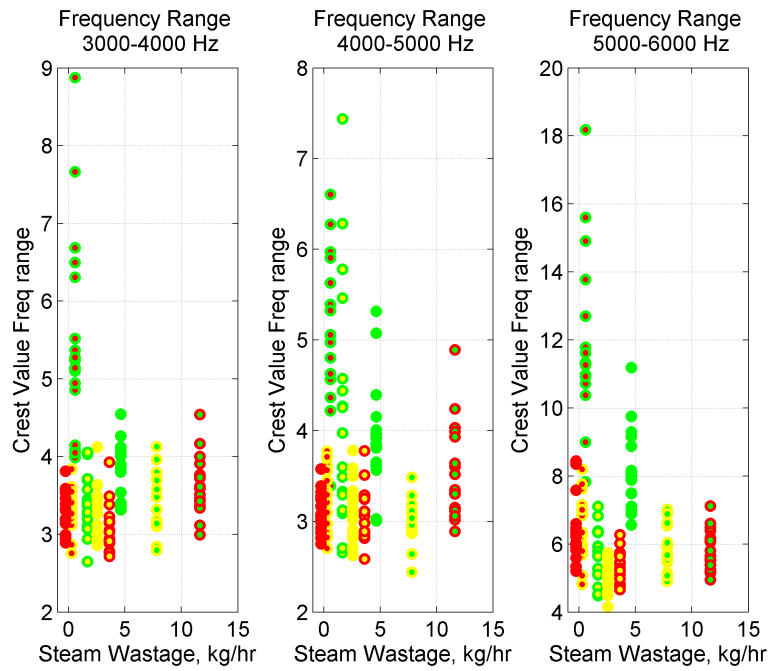


Figure 6.26: Orifice Trap Frequency Domain Frequency Bins Part 2

15 second recording. For this reason, time-frequency analysis is presented in the next section to allow the review of the contributing components to be identified.

### 6.2.3 Time-Frequency Analysis

The time-frequency analysis approach has been explained in Chapter 2. This approach allows both the frequency and time domain components to be identified. The steps used for this application are as follows:

- 1) A signal was segmented into 15 second long data segments.
- 2) For each of the data segments, the Short-Time Fourier Transform was calculated with a length of 2048 points (equal to  $2^{11}$ ) using a Hamming window. This allows for approximately 9.88 Hz per resolution bin. The reason for the decrease in frequency bin resolution (compared to the frequency analysis) is that this method is computationally more intensive. Additionally, the time and frequency resolutions are inversely proportional. In other words, if the time domain resolution is increased, the frequency resolution will be decreased. The window size chosen allows for an acceptable frequency and time resolution.
- 3) A number of features (discussed earlier in Chapter 6) were calculated for comparison.
- 4) The time-frequency domain was plotted on a graph together with the time domain representation to assist in the analysis.

In Figure 6.27 an example plot for the STFT is shown. This signal is the same example that was used for the frequency analysis representation. From the time domain signal, it can be clearly seen that the signal is noise-like, with a number of instantaneous speaks. Furthermore, there is a base noise band, which is steady throughout the 15 second period. However the noise rises and falls twice within the sample length. This demonstrates the typical behaviour of an Orifice Trap resulting from the two-phase flow nature of the steam and condensate mixture that presents itself at the trap. This dataset is specifically for a 5 barg Pressure reading and low Condensate Load (9.5 kg/hr), resulting in a high Steam Wastage of 4.62 kg/hr. Clearly, the time-frequency map in the same figure shows those time domain features as well as the corresponding frequency domain changes.

From the time-frequency map, the high intensity time domain spikes can be seen to spread across nearly the complete frequency range (vertically). The low frequency noise band can be seen up to about 3 kHz. Where the spikes and the background noise meet, the intensity is increased to an orange value. These same features were shown in Chapter 4 where low frequency signals manifested themselves as vertical, impulse like responses spread across the frequency range and high frequency noise presented itself as horizontal values.

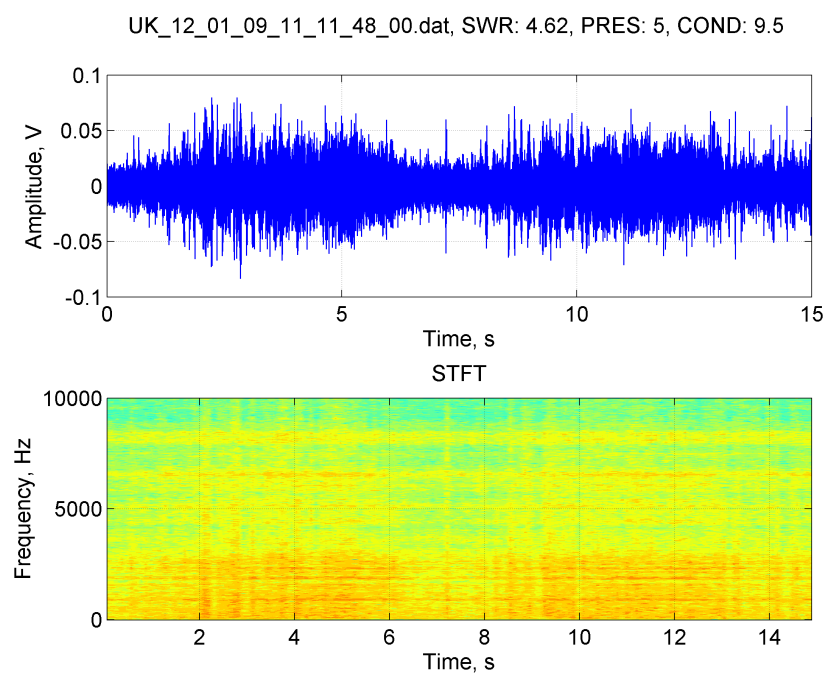


Figure 6.27: Orifice Trap STFT  
5 barg CL=9.5 kg/hr SWV=4.62 kg/hr

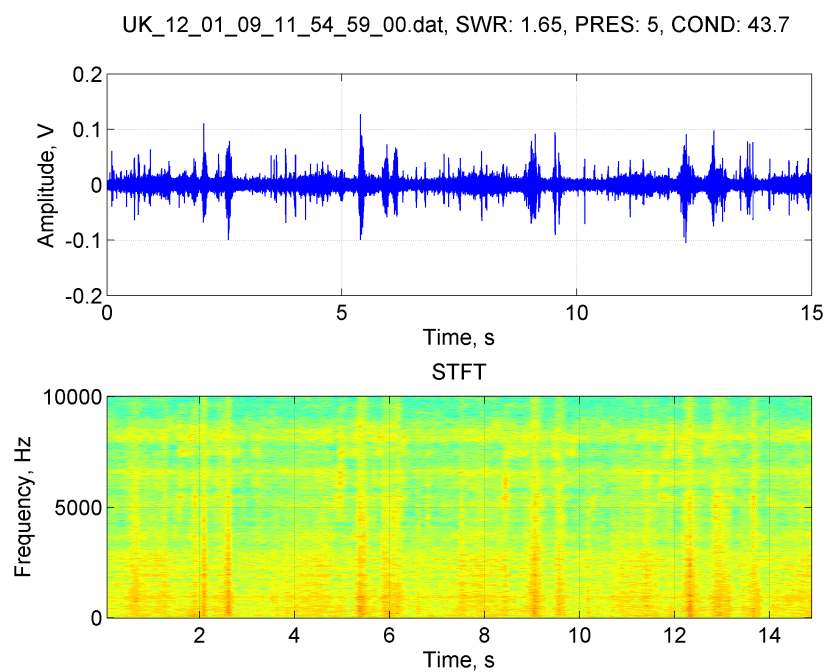


Figure 6.28: Orifice Trap STFT  
5 barg CL=43.7 kg/hr SWV=1.65 kg/hr

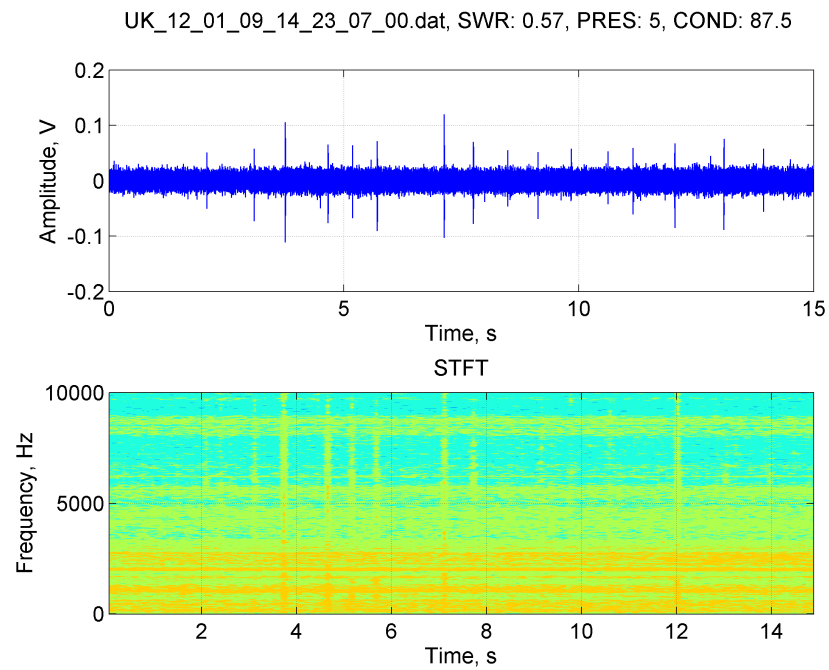


Figure 6.29: Orifice Trap STFT  
5 barg CL=87.5 kg/hr SWV=0.57 kg/hr

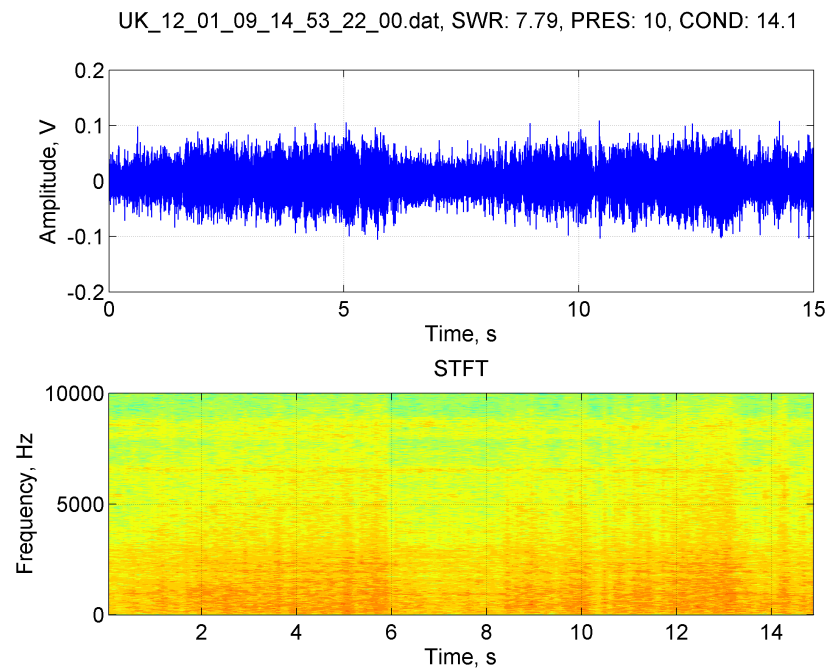


Figure 6.30: Orifice Trap STFT  
10 barg CL=14.1 kg/hr SWV=7.79 kg/hr

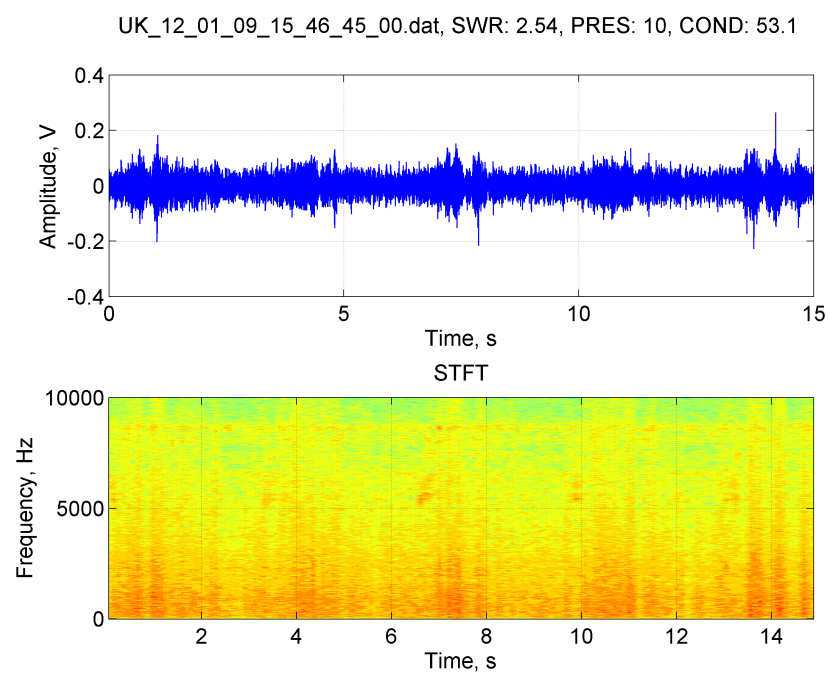


Figure 6.31: Orifice Trap STFT  
10 barg CL=53.1 kg/hr SWV=2.51 kg/hr

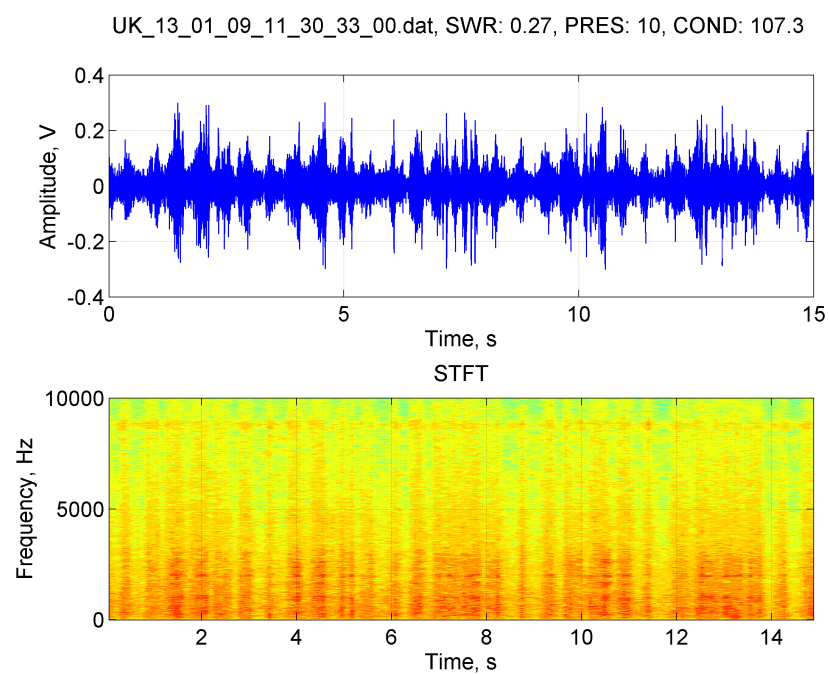


Figure 6.32: Orifice Trap STFT  
10 barg CL=107 kg/hr SWV=0.27 kg/hr

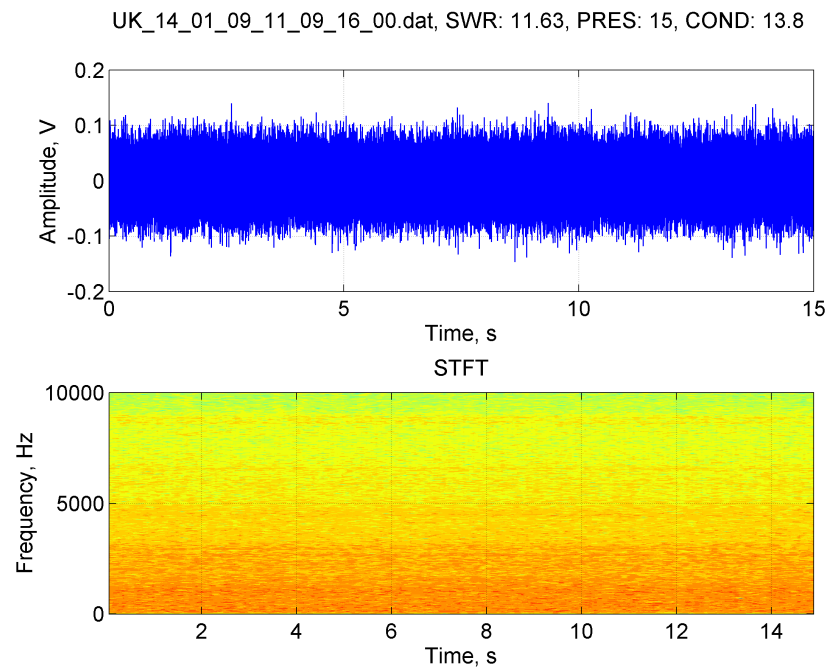


Figure 6.33: Orifice Trap STFT  
15 barg CL=13.8 kg/hr SWV=11.63 kg/hr

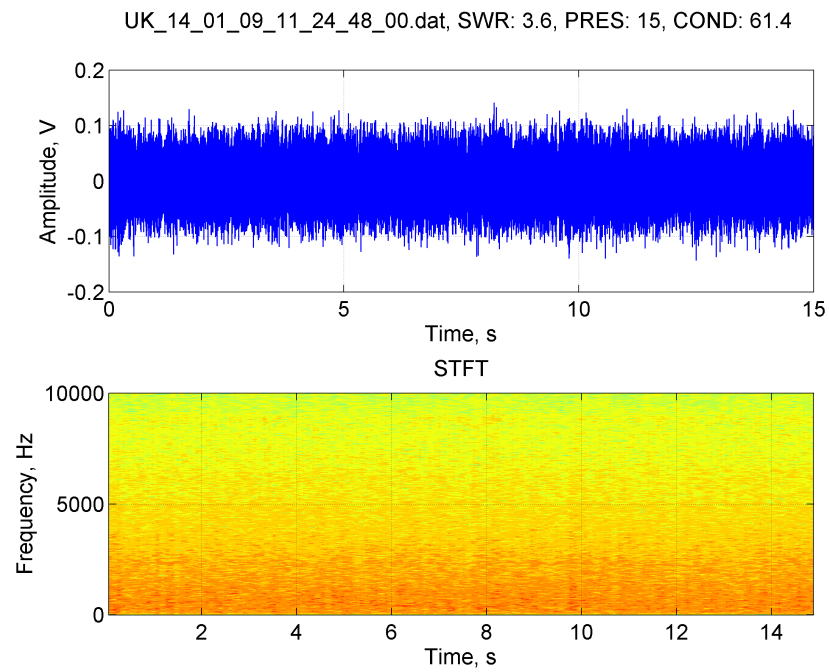


Figure 6.34: Orifice Trap STFT  
15 barg CL=61.4 kg/hr SWV=3.6 kg/hr

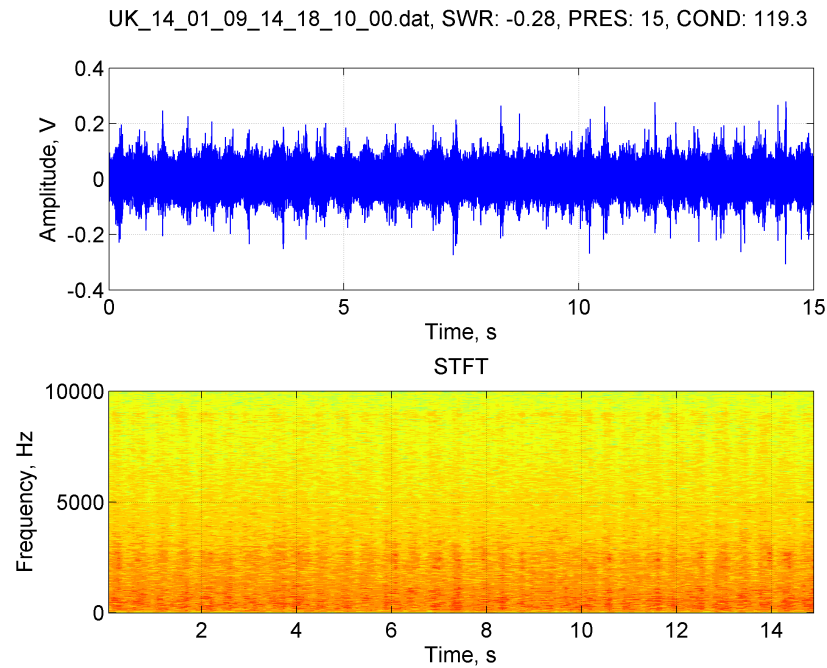


Figure 6.35: Orifice Trap STFT  
15 barg CL=87.5 kg/hr SWV=-0.26 kg/hr

Figures 6.28 and 6.29 show the other two conditions for the low pressure example. The spikes are clearly shown in the time-frequency map and the features of the Fourier spectrum are also shown.

Figures 6.30, 6.31 and 6.32 show the three medium pressure conditions. These plots show the trend of spikes building. At the low Condensate Load, there are two clear flat bursts. At the medium level, there are approximately four events and at the high Condensate Load there are over 25 events. The level of intensity is also higher than the low pressure examples.

Figures 6.33, 6.34 and 6.35 show the three high pressure conditions in terms of the STFT. These plots show compared, with the other conditions the highest intensity. The low and medium Condensate Load shows spikes, only the high Condensate Load shows many fluctuating intensity values (over 30). Due to high pressure, the lower Condensate Loads are not shown the time-frequency maps.

The next part features the summary plots previously seen for the time domain analysis. The parameters evaluated using the Fourier Transform as an input signal are RMS, Kurtosis, Standard Deviation, Maximum Individual Value, Variance, Mean, Sum of Total Signal and Median Value, introductions to which were given in Sections 5.3.2 and 6.1.2 respectively.

Figure 6.36 shows the RMS and Kurtosis evaluated and plotted against Steam Wastage. The same trend is being seen as compared to the time domain and frequency domain signal analysis.



Steam Wastage is inversely proportional to the Condensate Load, as expected. The higher the pressure, the higher the steam RMS value. It is worth noting that the values are not closely clustered together. RMS values could be used as an indicator, but certainly are not conclusive, especially at low pressure values. If the Condensate Load Values could be determined by another method, the RMS evaluation could be used for Steam Wastage identification, which can be clearly seen through the points with a green inner circle, where the Condensate Load is low and the RMS measure is proportional to Steam Wastage Value (and Pressure Value).

Considering the Kurtosis evaluation in the same Figure, the values are not related and do not provide any trends. This was also found in the time domain analysis.

Figure 6.37 considers the Standard Deviation and the Maximum Individual Value. The Standard Deviation of the measurements for the Short-Time Fourier Transform signals shows the same trend as the previous evaluations for the Fixed Orifice Trap, with no conclusive trends. Likewise, the Maximum Individual Values do not show any correlations with the Steam Wastage.

Figure 6.38 considers the Variance and the Mean of the STFT. The Variance calculation of the STFT of the signal segments show the same trend as in previous calculations, providing no conclusive outcomes. Likewise, the Mean Individual Values does not yield any correlation with the Steam Wastage other than the one already explained as part of the RMS evaluation.

Figure 6.39 considers the sum of the Total Signal and the Median Value. No specific or useful trend has been identified.

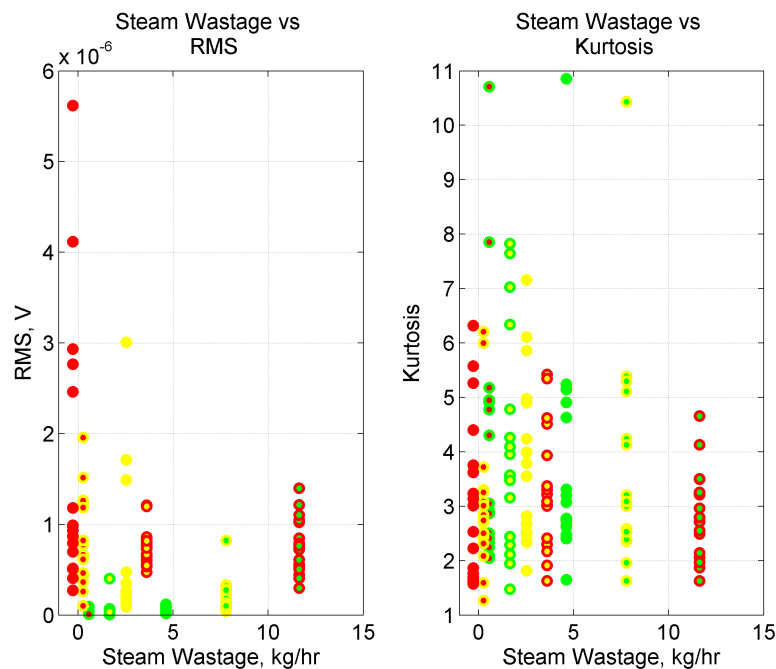


Figure 6.36: Orifice Trap STFT RMS and Kurtosis

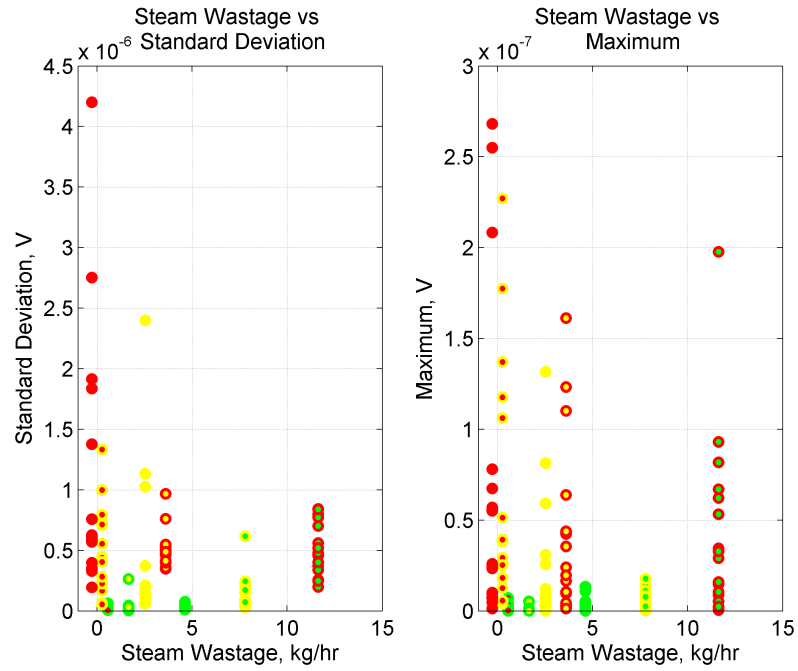


Figure 6.37: Orifice Trap STFT Standard Deviation and Maximum

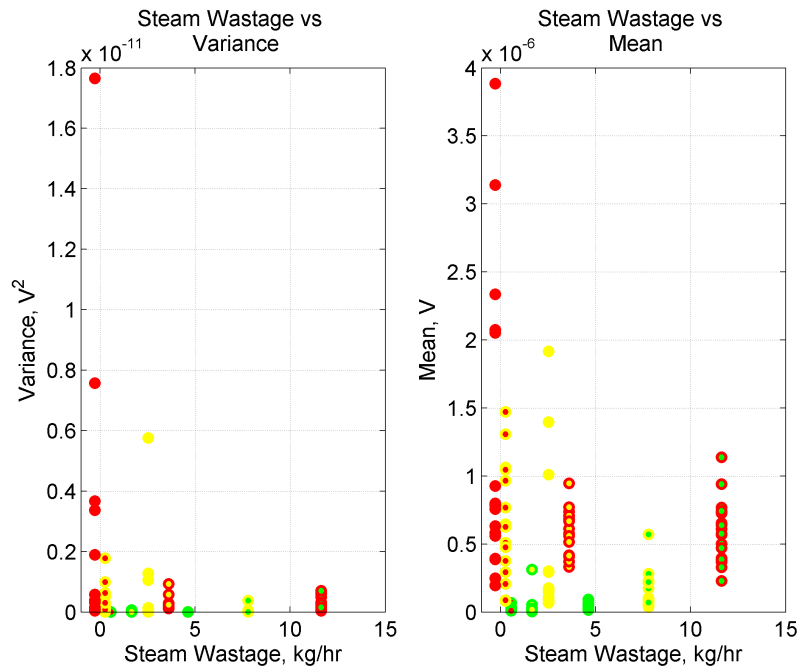


Figure 6.38: Orifice Trap STFT Variance and Mean

It is clear from these four plots of parameters calculated from the STFT that these methods can be used as an indication of condensate load or pressure, but cannot be used for Steam Wastage measurement. However, this analysis has been the best method in displaying the behaviour of the trap.

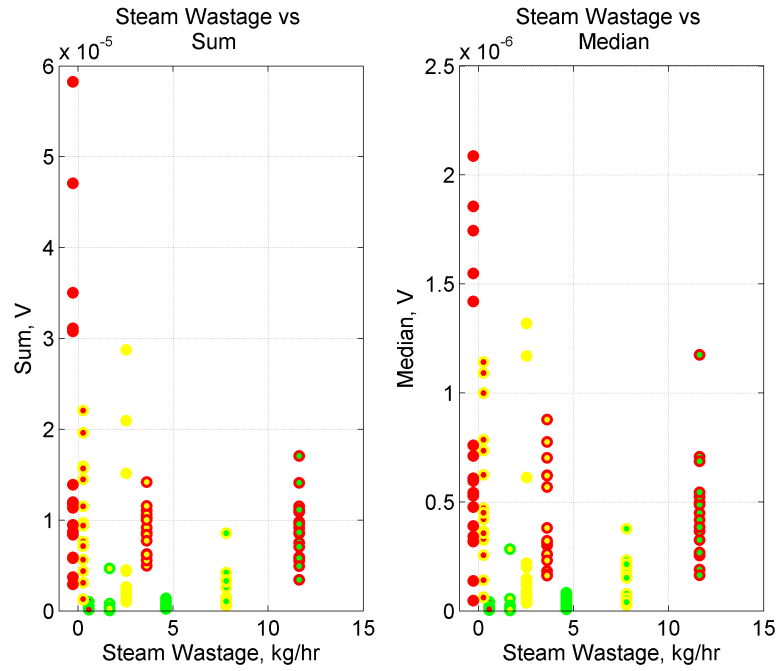


Figure 6.39: Orifice Trap STFT Sum and Median

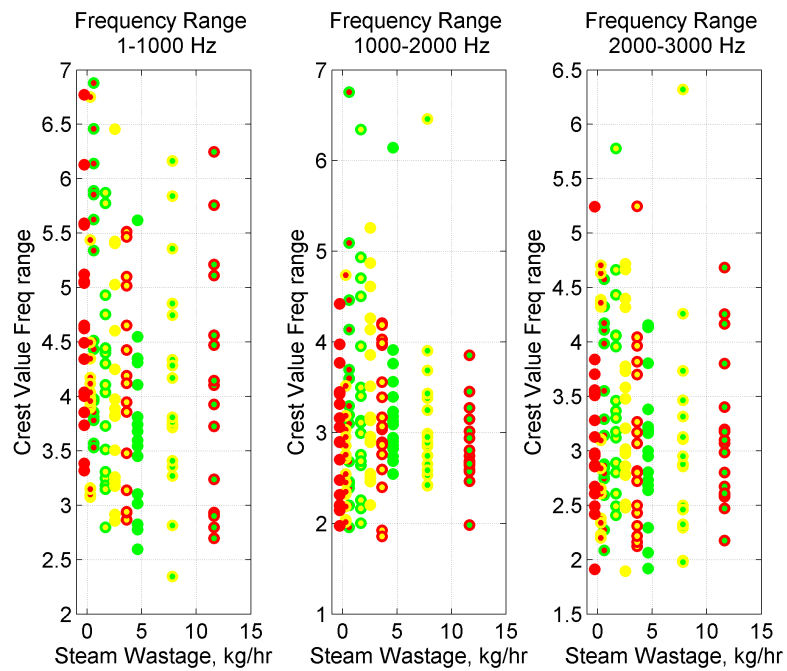


Figure 6.40: Orifice Trap STFT Frequency Bins Part 1

From the review of the individual plots, a number of peaks were identified, which could not be specifically correlated to a condition. For this reason, the Crest Value has been applied to the STFT. The Crest Value has been calculated by dividing the Maximum Instantaneous Value of a frequency range with the mean of the values within the range. Three frequency ranges were selected, namely: 1 Hz to 1 kHz, 1 kHz to 2 kHz, 2 kHz to 3 kHz, 3 kHz to 4 kHz, 4 kHz to 5 kHz

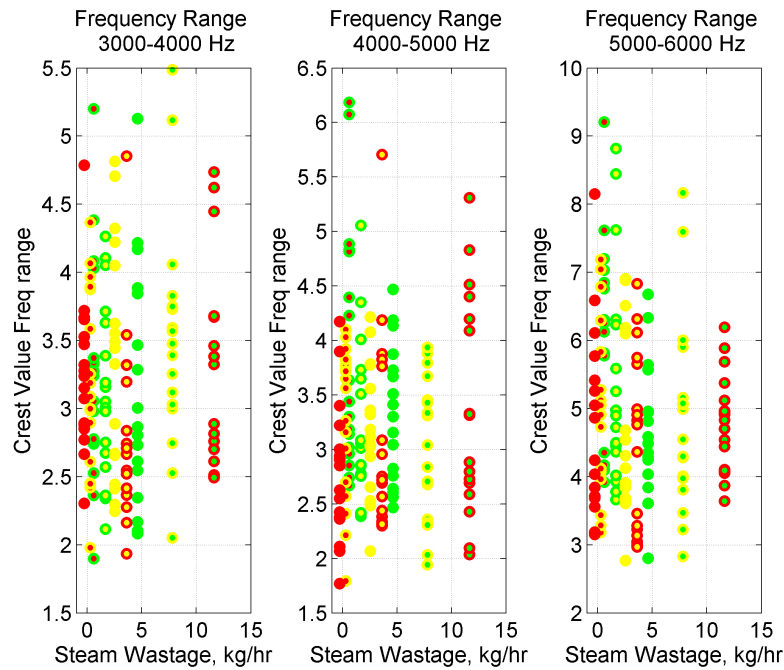


Figure 6.41: Orifice Trap STFT Frequency Bins Part 2

and 5 kHz to 6 kHz. Figures 6.40 and 6.41 show these plotted, but there is no clear correlation between Crest Value and Steam Wastage Value. Another feature of this plot is that the Crest Value across frequency ranges as ratios remain the same, in other words, there is no relative change when comparing the Crest Value for the operational conditions in terms of the frequency range.

**Discussion** As mentioned previously, the STFT considers the complete 15 seconds and the representative frequencies within this signal segment. From the time domain and respective STFT analysis, it can be seen that changes to the time domain are reflected in the STFT content within the 15 second recording. It has been shown that the time-frequency analysis is the best method to capture both behaviours highlighting the contributing components.

### 6.3 Summary

The following are the findings and observations that have been made:

- The time domain acoustic emission of the Fixed Orifice Trap has been presented and the stationary nature of signal demonstrated. Periods where the signal is non-stationary have also been shown.
- Time domain processing has not been very successful, as the signal observes little modulation and is largely stationary. Using basic statistic measurements the complicated nature and difficulty in consistently relating Steam Wastage to the acoustic emission has been shown.

- Frequency domain processing has been equally inconclusive. The example data sets presented show a high variability in resonant peaks. Due to the stationary nature of the signal, it was expected that the frequency domain analysis would be best suited. However, the variability and the chaotic nature of Fixed Orifice Trap has resulted in an inconclusive estimation of Steam Wastage from the acoustic emission.
- The time-frequency method has been shown to be the most suitable approach, as this highlights the operational nature of the trap by simultaneously evaluating the time and frequency domain.
- This chapter has reviewed the “ideal” scenario of the Orifice Trap (i.e. no mechanism that interferes with the flow). From Chapter 5, generally Pressure and Condensate Load increase the intensity of the signal. However, no specific inherent noise characteristic related to Steam Wastage has been discovered. Overall, it has been discovered that RMS and Kurtosis values resulting from the acoustic emission data cannot conclusively be used to determine Pressure, Condensate Load or Steam Wastage Values in Steam Traps.
- Finally, although this trap represents an “ideal” case, it has not been possible to link the trap with the two phase flow behaviour. The reason for this is that measurements are not taken at the same scale. Signal processing features over and above the measurement of RMS and Kurtosis have been introduced, such as the Standard Deviation and Variance, but these also have not been successful in determining a trend.

*This chapter applied digital signal processing techniques to orifice type traps. The next chapter will cover non-impulsive traps, which includes a mechanism and can observe both a modulating and stationary behaviours.*

## Chapter 7

# Non-Impulsive Steam Trap Analysis

*This chapter presents the analysis of Non-Impulsive Steam Trap data. The data has been recorded and processed using time and frequency methods. An explanation of the acoustic data and an overview of digital signal processing is presented.*

### 7.1 Acoustic Signals for Non-Impulsive Trap

For this research, this trap provides an idealised scenario for Non-Impulsive Traps. Non-Impulsive Traps are defined as traps that have slowly modulating response. The traps in this category are Float, Bi-metal and Thermostatic. The mechanisms in these traps manifest themselves by a slow opening and closing sequence, which also does not display any distinct or repeatable markers in the acoustical response. Additionally, these traps can observe a modulating cycle (where they open and close repeatedly), which is not always clearly distinguishable in the acoustic signal. For this reason, these traps are very difficult to diagnose and differentiation between condensate flow and steam leakage is not easily determined.

The signal for the long time large scale (tens of seconds) can sometimes be classed as stationary due to flat response of the signal. However, on a shorter time scale (seconds) a pulsating phenomenon is observed, which is a reflection of the inherent chaotic nature of the signal as well as the mechanism. Overall, this trap can be classed as mainly non-stationary when considered across the operational ranges.

Although there are a number of traps within this category of acoustic response, the Steam Trap chosen for analysis in this category is the Float Trap, as it provides a representative signal for this acoustic category and allows a manageable size of data to be presented.

The acoustic signal for this trap type has been recorded using the Steam Wastage Rigs, which were introduced in Chapter 3. The signals presented cover a wide range of conditions up to 14

barg (as this is the operational limit of the Float Trap design chosen for this investigation) and 60 kg/hr condensate load. Overall these datasets generate 221 data points which are used in the subsequent analysis to correlate the operational conditions with the acoustic emission.

The data sets used in the analysis are displayed in Table 7.1. The data sets are not as uniformly distributed as they were for the Orifice Trap. The reason for this is that the modulating mechanism influences the flow through the trap and through that the operational conditions that can be attained. Operational conditions and Steam Wastage Values are shown in the table below.

Filename	SWV (kg/hr)	Pressure (barg)	Condensate (kg/hr)	Temperature (°C)
UK_21_05_07_13_32_02	1.88	5	10	159
UK_14_05_07_13_40_04	2.71	5	10	159
UK_16_07_07_10_21_02	4.08	5	30	159
UK_21_05_07_15_29_31	0.68	10	10	184
UK_08_05_07_10_23_31	1.68	10	10	184
UK_03_05_07_10_34_32	4.1	10	10	184
UK_30_04_07_11_33_33	7.48	10	10	184
UK_08_05_07_14_59_58	-0.39	10	60	159
UK_01_05_07_11_29_04	9.29	15	10	199

Table 7.1: Float Trap Acoustic Data Summary

### 7.1.1 Characteristics of the Acoustic Signals

As an introduction to the acoustics of the Non-Impulsive Trap category, three signals have been plotted in Figures 7.1, 7.3 and 7.5. These figures show examples at 5 barg pressure and provide the reader with an overview of the format of Non-Impulsive trap data at low and medium Steam Wastage Values. A high Steam Wastage Value was not achieved by this trap at the low pressure condition.

Additionally, a magnified representation of each of the three examples is provided to show the changes to the time domain signal at different time scale levels. It is worth noting at this point that time domain representations for all nine example conditions will be shown as part of the Frequency analysis in Section 7.2.2 of this chapter.

Figure 7.1 shows a low Condensate Load example of 10 kg/hr and low Steam Wastage of 1.88 kg/hr. A strong background noise level is displayed with a slight amplitude rise over the 2 minute period of the recording. Some randomly occurring instantaneous spikes are also shown. A closer view of the signal is provided in Figure 7.2 where the same signal is shown on a 1 second and 0.1 second time scale. The noisy nature of the flow through the Steam Trap is clearly shown at both scales although the one second sample does include a small spike at around 0.3 seconds.

Figure 7.3 shows another case of low Condensate Load (10 kg/hr) and medium Steam Wastage (2.71 kg/hr). The same clear background noise band is displayed as with the first example with a

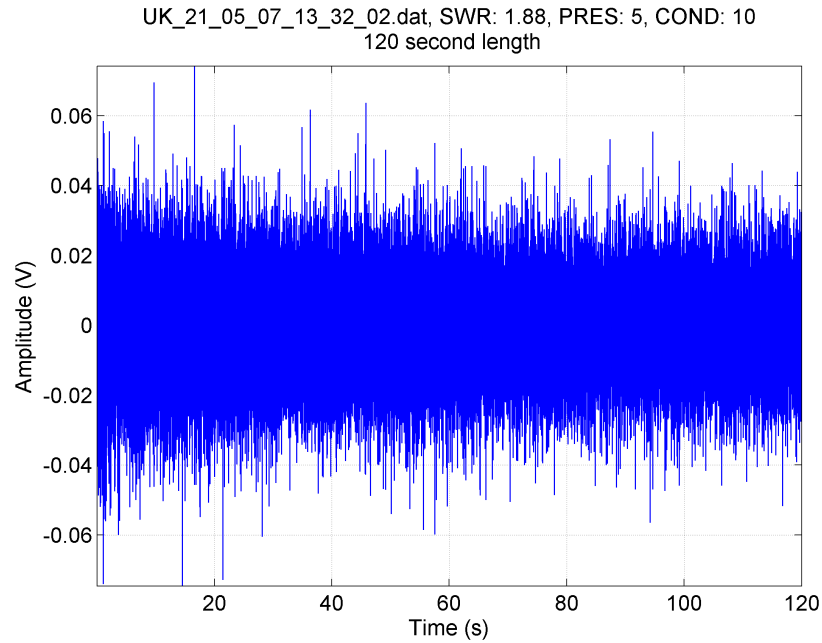


Figure 7.1: Float Trap 5 barg Low Steam Wastage Time Plot

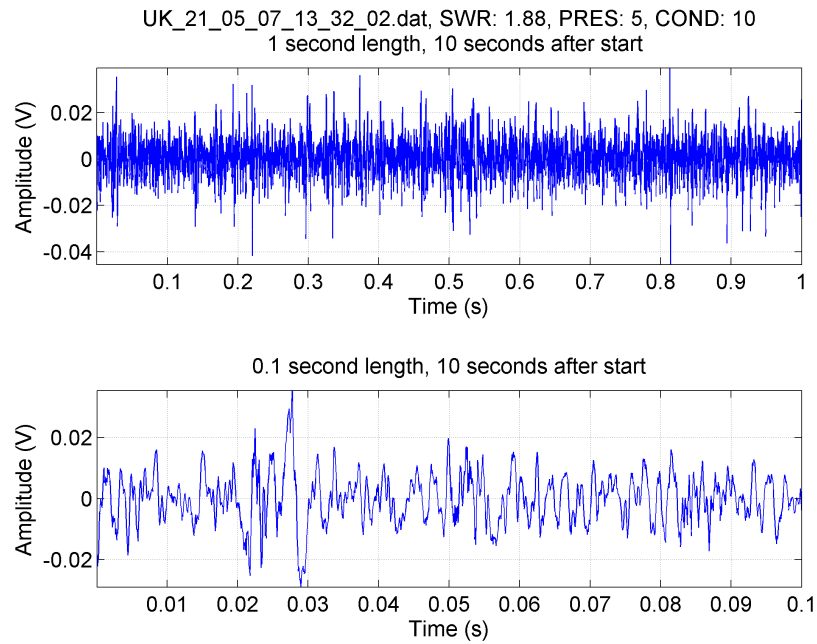


Figure 7.2: Float Trap 5 barg Low Steam Wastage Time Plot Zoomed

comparable magnitude. However, the spikes have become less pronounced and lower in amplitude. Considering the shorter time scale shown in Figure 7.4, a similar response is displayed as in the previous example with more overall spikes. In the 1 second example, the amplitude is now around half of the previous example and the same is true for the 0.1 second example.

Finally, Figure 7.5 shows high Steam Wastage (4.08 kg/hr) and low Condensate Load (30



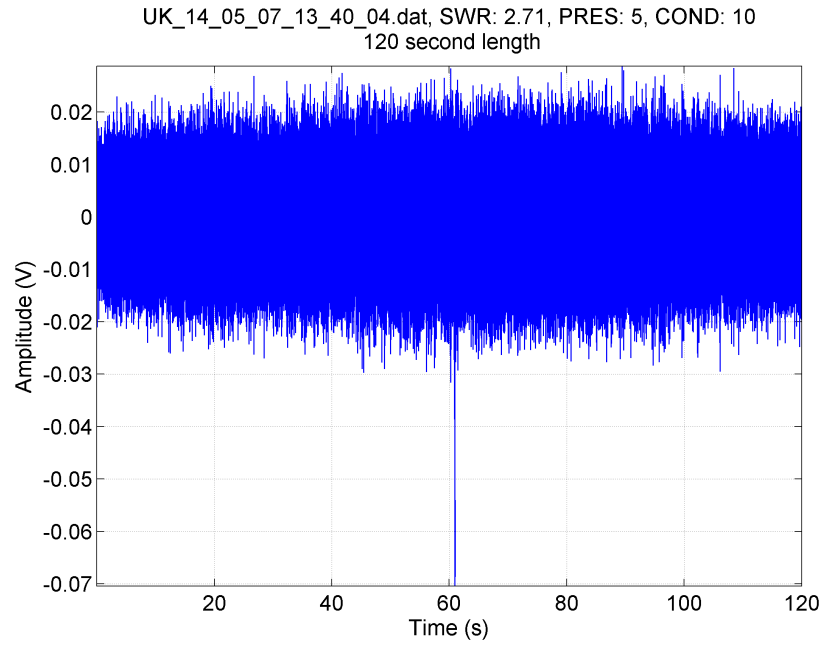


Figure 7.3: Float Trap 5 barg Medium Steam Wastage Time Plot

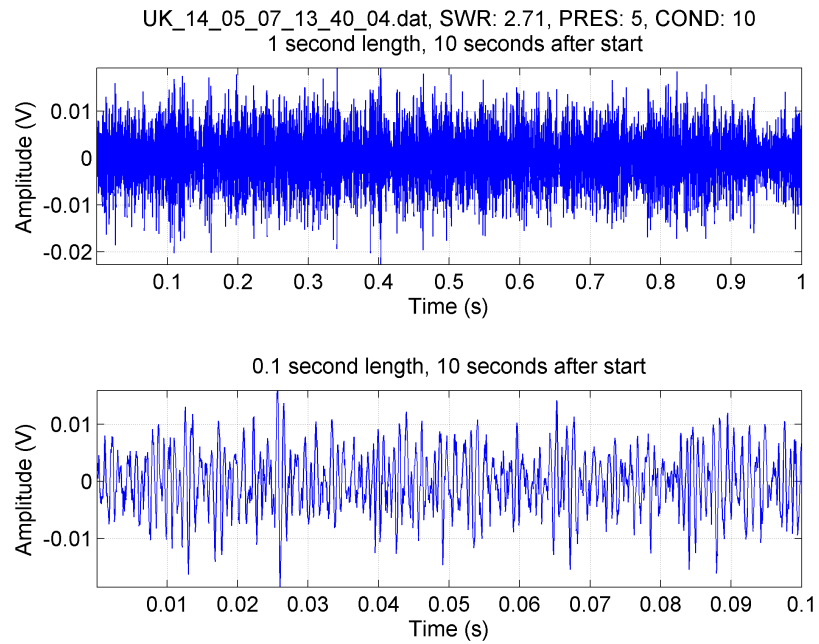


Figure 7.4: Float Trap 10 barg Low Steam Wastage Time Plot Zoomed

kg/hr). The strong background signal is now reduced, but the spikes are more pronounced. Considering the signal at the smaller time scales, as shown in Figure 7.6, the signal is fairly stationary, although clear spikes are observed. The time scale of 0.1 seconds shows also a trend of the signal growing in amplitude as the time progresses.

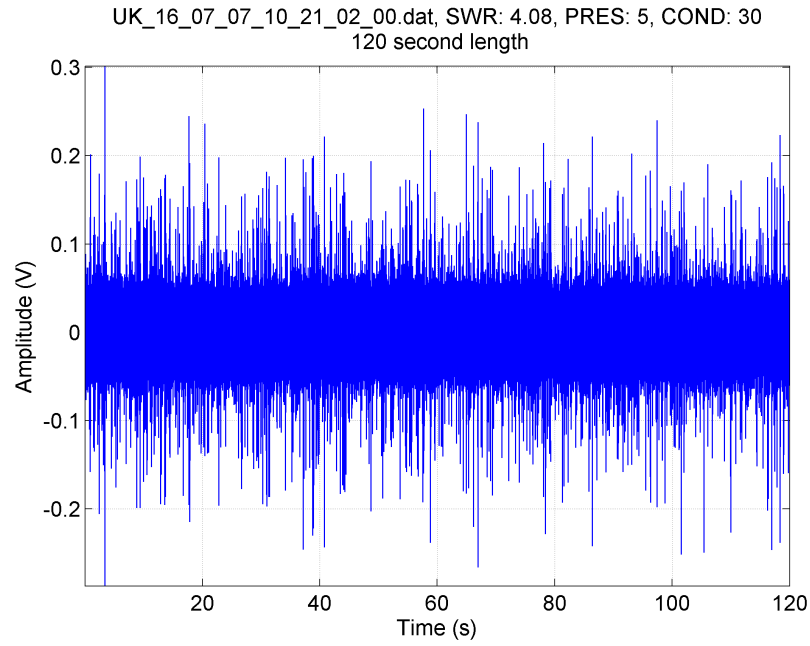


Figure 7.5: Float Trap 5 barg High Steam Wastage Time Plot

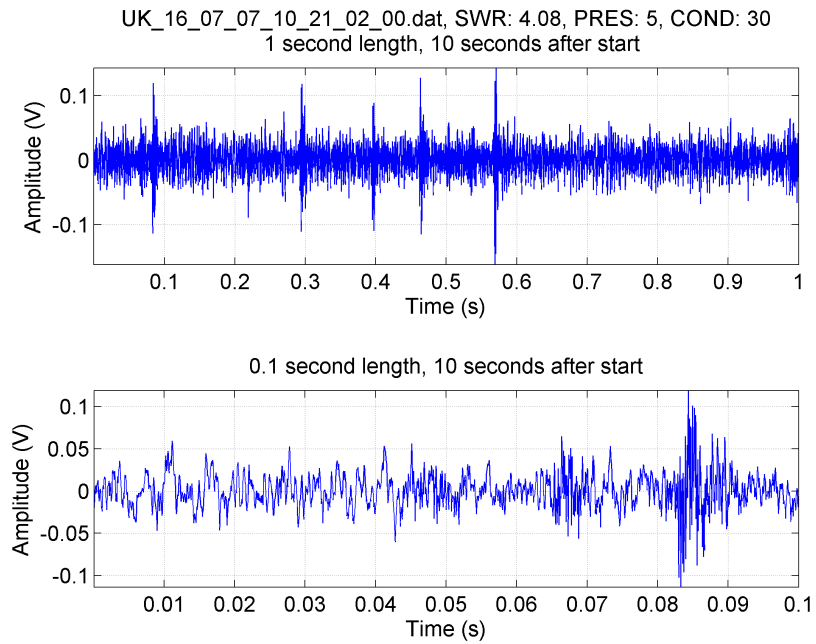


Figure 7.6: Float Trap 5 barg High Steam Wastage Time Plot Zoomed

**Discussion** The length of the data samples presented are 2 minutes long. The different manifestations of modulations occurring at different mixtures between steam and condensate have been introduced. The Float Trap contains a float that rises and falls with the condensate load. As the data recordings presented are from a wearing trap, there are no periods where the signal diminished. Furthermore, the Float Trap is also known as a continuous discharge trap as its mechanism

is usually in a dynamic state of openness.

## 7.2 Application of Signal Processing

### 7.2.1 Time Domain Analysis

The following section reviews key features of the time domain representation for the Float Trap, for which the time domain signal was analysed by splitting the signal into 15 second sub-sets. Steam Wastage has been plotted on the x-axis and the calculated feature on the y-axis. In addition, the marker contains two colours to allow Pressure and Condensate Load indications to be represented (in a similar way as it was presented in Chapter 5). Using this approach, four parameters can be displayed in one graph which reduces the number of figures required to consider all permutations of data combinations.

The markers have been implemented by a two-dot system, in which the inner colour indicates the level of Condensate Load and the outer colour the Pressure level. The Condensate Load and Pressure have been differentiated into a range of high, medium and low, as detailed in Table 7.2. A visual representation is provided in Figure 7.7 to provide an applied context of the application.

Colour	Pressure (barg) (Outer Marker Colour)	Condensate (kg/hr) (Inner Marker Colour)
Red	> 12	> 80
Yellow	< 12 and >6	< 80 and > 20
Green	< 6	< 20

Table 7.2: Float Trap Condensate and Pressure Indicator

Features used in the analysis have been introduced in Sections 5.3.2 and 6.1.2 and include: RMS, Kurtosis, Standard Deviation, Maximum, Variance, Mean, Sum and Median. The results










	P >12 barg, CL>80 kg/hr
	P >12 barg, CL<80 & >20kg/hr
	P >12 barg, CL<20kg/hr
	P <12 & >6 barg, CL>80 kg/hr
	P <12 & >6 barg, CL<80 & >20kg/hr
	P <12 & >6 barg, CL<20kg/hrr
	P <6 barg, CL>80 kg/hr
	P <6 barg, CL <80 & >20kg/hr
	P <6 barg, CL<20kg/hr

Figure 7.7: Float Trap Colour Legend

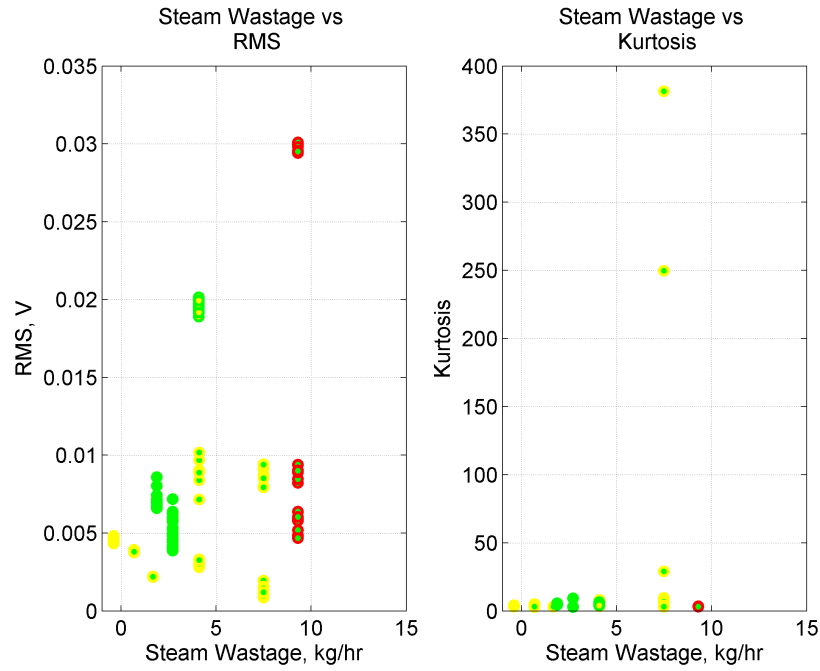


Figure 7.8: Float Trap Time Domain RMS and Kurtosis

of the time domain evaluations of the features introduced in the previous sections are shown in Figures 7.8, 7.10, 7.11 and 7.12.

Figure 7.8 shows the RMS and Kurtosis measurements for the Float Trap data set. The RMS measurement is not related to Steam Wastage. Considering the coloured markers in the signal sets presented a high RMS value which is related to a higher condensate load (above 0.011 V). For the low Condensate Load examples shown, the higher the Pressure, the higher the Steam Wastage Value. This makes sense as the pressure loading on the orifice is greater and will lead to a higher steam flow. The low pressure and condensate load examples seem to be clustered close together, however the medium pressure is further spread apart. In comparison to the Fixed Orifice trap, the Float Trap, due to its mechanism, has lower RMS values at lower Pressure and Condensate Load. This could be due to the mechanism causing a dampening effect on the flow. Referring to Figure 5.5 of the key parameters Venn Diagram, the multi-dimensionality of this investigation becomes clear.

Considering the Kurtosis measurement in relationship with the Steam Wastage measurement in Figure 7.8, two clear outlier data points can be seen. For this reason, the Kurtosis data has been plotted separately in Figure 7.9. This shows that there is no relationship between Kurtosis and Steam Wastage. In addition, there does not seem to be a relationship between Kurtosis and Condensate Load or Pressure.

Figure 7.10 shows the relationship between Standard Deviation of the Float Trap data set. The Standard Deviation shows the same pattern and nearly the same values as the RMS calculations.

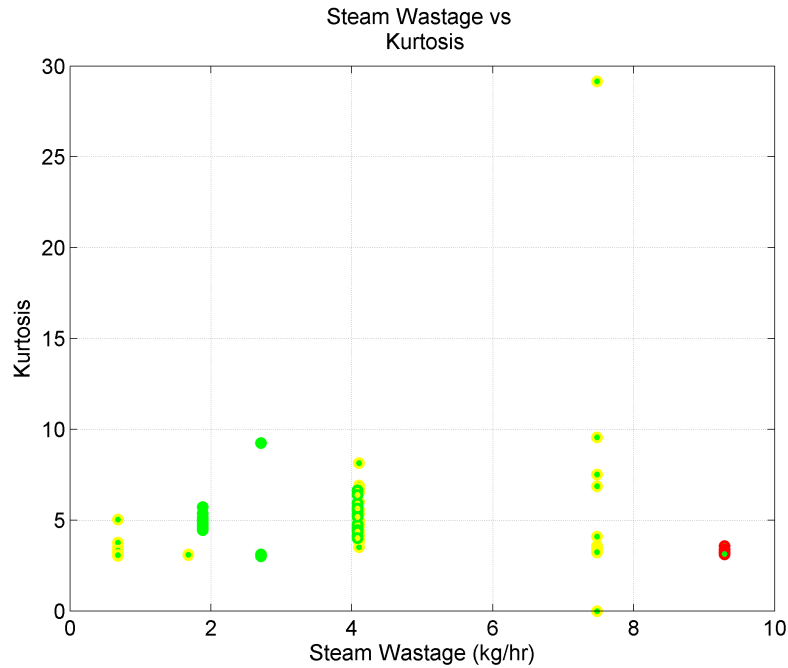


Figure 7.9: Float Trap Time Domain Kurtosis Only

The analysis applied to the RMS will also be applied to Standard Deviation.

Considering the Maximum Individual Value, the values seem to funnel towards low Steam Wastage, i.e. the values are spread wider at low Steam Wastage Values and less clustered towards the higher end. However, the higher condensate load is the exception, which is significantly higher, even compared to the higher pressure. This could be caused by the higher density of the condensate load, resulting in a higher peak value. It is also worth noting that at the higher condensate load, the calculated maximum values are further spread apart compared with the other conditions.

Figure 7.11 shows the relationship between Variance of the acoustic emission signal and Steam Wastage for the Float Trap. It can be seen that the calculation of the Variance value increases with pressure. This makes sense as the higher the pressure, the higher the energy contained in the pipe and thus the sum is greater. As the Variance is of the same value as the RMS value, the plot is similar to the RMS plot. The high pressure / high Steam Wastage data set also has a wide Variance between the data sets, although individual runs within sets are closely clustered.

Considering the Mean values in relation to Steam Wastage, the Mean values centred around zero are more widely spread with higher Steam Wastage. Additionally, lower pressure and condensate reduce the spread of the mean value within a data set. Interestingly the medium condensate load example is very clustered at around zero, suggesting that the values are very stable and comparable. The higher condensate load also showed the highest individual value, suggesting that the condensate load stabilises the traps operations. This has been found in operational cases.

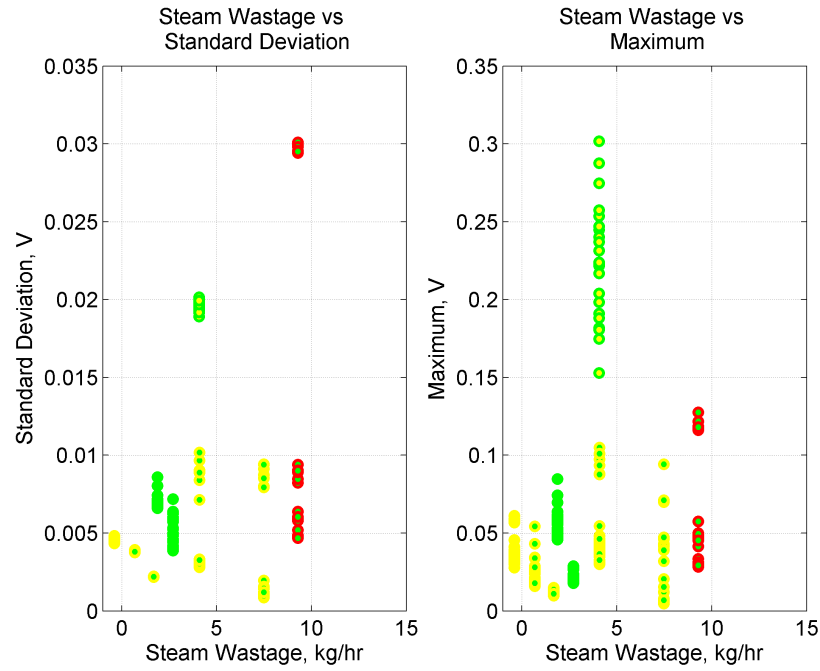


Figure 7.10: Float Trap Time Domain Standard Deviation and Maximum

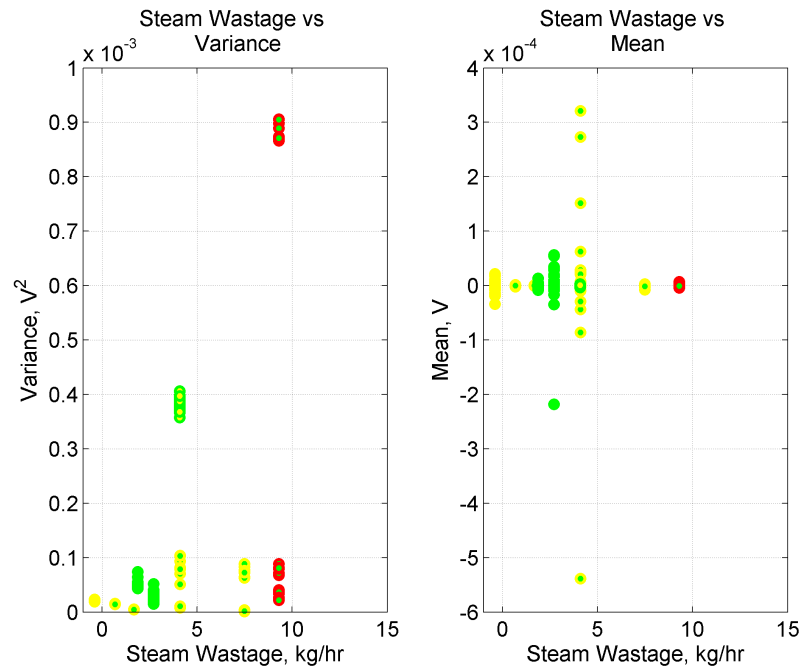


Figure 7.11: Float Trap Time Domain Variance and Mean

On the other hand, the medium pressure medium Steam Wastage example is widely spread. As a complete dataset, the high pressure example is also very clustered around zero.

Considering the mean values in relation to Steam Wastage, the Mean values centred around zero are more widely spread with higher Steam Wastage. Additionally, lower pressure and condensate reduce the spread of the mean value within a data set.

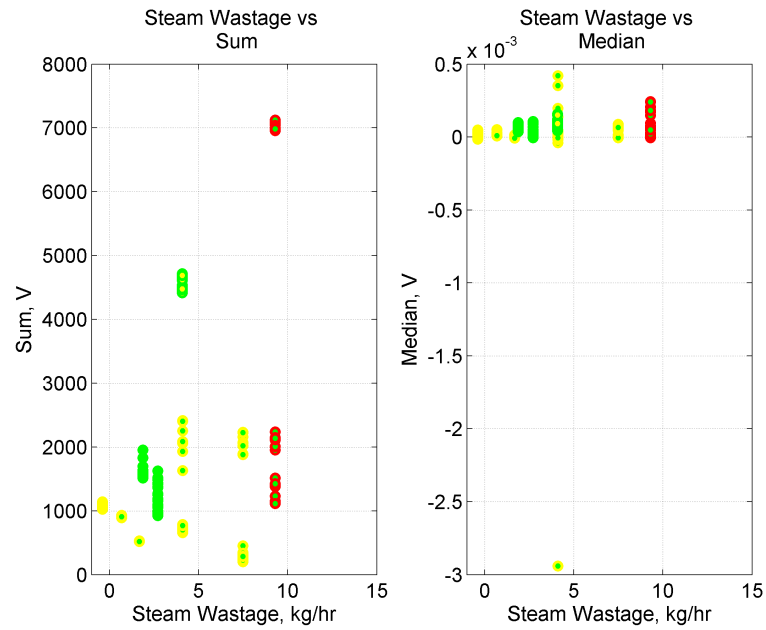


Figure 7.12: Float Trap Time Domain Sum and Median

Figure 7.12 shows the relationship between the Sum of the total signal and the Steam Wastage value. The plot looks similar in layout to RMS and the same analysis and reasoning can be applied to this analysis.

Considering the median, the signals are not proportional as cluster. There is a outlier at -2.9 which has been removed so that the data cluster can be analysed. This has been plotted in Figure 7.13.

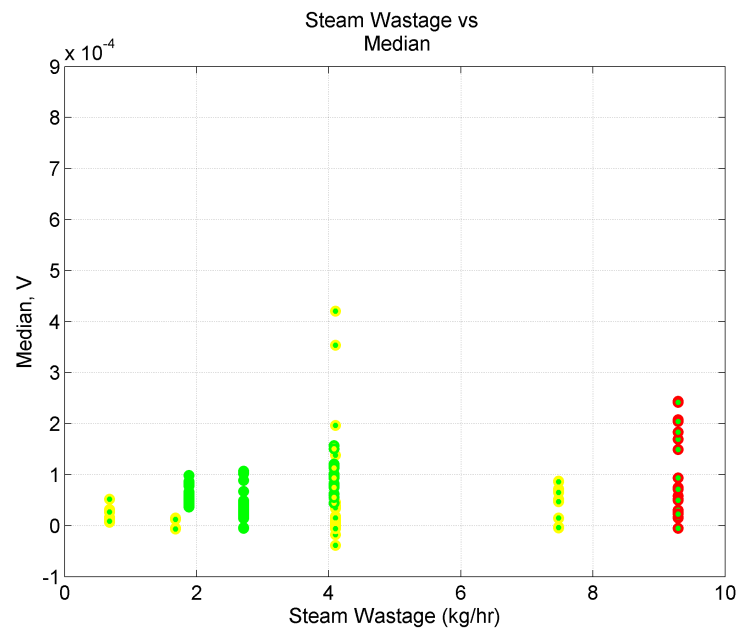


Figure 7.13: Float Trap Time Domain Median Only

**Discussion** It is clear from the signals that these methods can be used, but no coherent assessment can be made of the Steam Wastage Value. For this reason, frequency and time-frequency methods have been applied to the analysis, which will be shown in the subsequent sections.



## 7.2.2 Frequency Domain Analysis

In terms of the method in which the signal is divided into segments, the frequency analysis uses the same approach as the time domain analysis. The function to create the Fourier Transform was the standard m-file `fft.m`. The FFT was applied over 1024 points to speed up the process. Thereafter, a number of features were calculated to allow the data segments to be compared. To conclude, the energy contained within different frequency ranges of the FFT are reviewed.

Firstly, a sample of the time domain representation of the dataset is presented. Nine representative Pressure and Condensate Load examples is presented to provide the reader with an overview of the trap performance.

The Fourier Transform plots are all very comparable. For this reason, only one plot is presented in full size. The remaining eight are shown on four-to-a-page overviews.

The Fourier Transforms were calculated using a 15 second length of the sample signal. The process by which the Fourier Transforms were calculated are as follows:

- 1) A signal was divided into 15 second long data segments.
- 2) For each of the data segments, the Fourier Transform was calculated with a length of 16,384 points (equal to  $2^{14}$ ). This allows approximately 1.2 Hz per resolution bin.
- 3) A number of features (discussed earlier in Chapter 6) were calculated for comparison.
- 4) The Fourier Transform was plotted on a graph together with the time domain representation to assist in the analysis of the Fourier Spectrum in relation to the time domain signal.

In Figure 7.14, an example plot is shown. From the time domain signal, it can be clearly seen that the signal is noise-like, with a number of instantaneous speaks. The signal appears to be stationary with a base noise band, which is steady throughout the 15 second time frame. This response is quite typical for a Float Trap that is on a constant load, passing some flow. The continuous discharge nature of the trap is shown, as there are no distinct features of modulation recognised. The operational conditions in this example dataset is 5 barg pressure and low Condensate Load (10 kg/hr), resulting in a high Steam Wastage of 1.88 kg/hr.

Figures 7.15 and 7.16 show other low pressure examples of the Float Trap. It is worth noting that in both cases, the spectrum remains very peak-like, although the peak frequencies shift as shown in the FFT plots. In the low Condensate Load example, the two main peaks are located between 1 kHz and 1.5 kHz. For the medium Condensate Load example, a new lower peak is identified at around 300 Hz. The other main peak is located at around 1.2 kHz. Another lower peak is also seen at about 3 kHz.

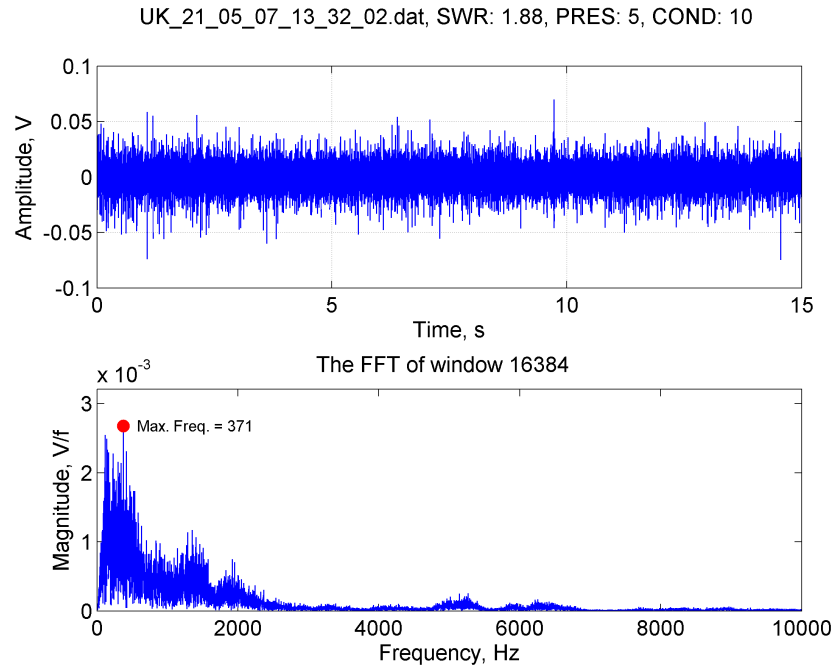


Figure 7.14: Float Trap FFT  
5 barg CL=10 kg/hr SWV=1.88 kg/hr

Considering the medium pressure examples in Figures 7.17 to 7.21, there does not seem to be any specific peaks. However, some points are worth noting. The noise spectrum has no distinct features, but all the peak values are located below 2 kHz and are flat in response. The medium Steam Wastage Value in Figure 7.19 displays a flat time domain response although high instantaneous events are also registered. The maximum frequency is 49 Hz, which is very much lower than the maximum peak values for this range of pressure to the other examples shown.

The high pressure example shown in Figure 7.22 the time domain signal response is noise like, as in the previous examples. The FFT shows two peaks at around 1 kHz and around 3 kHz.

The next section features summary plots previously seen for the time domain analysis. The parameters evaluated using the Fourier Transform as an input signal are RMS, Kurtosis, Standard Deviation, Maximum Individual Value, Variance, Mean, Sum of Total Signal and Median value, introductions to which were given in Sections 5.3.2 and 6.1.2 respectively.

Figure 7.23 shows the RMS and Kurtosis evaluated and plotted against Steam Wastage. The same trends that have been observed in the time domain analysis are being observed for the frequency analysis. Steam Wastage is inversely proportional to Condensate Load, as expected. The higher the Pressure and Steam Wastage Value, the higher the RMS value. The RMS values are closely clustered together for the respective condition pairs with no outliers. This has resulted from the FFT, as it averages the energy across the signal, hence any outliers are averaged out unless they are very high in magnitude. The RMS values could be used as an indicator of Steam Wastage, but it is certainly not conclusive, especially at low pressure conditions. If the condensate

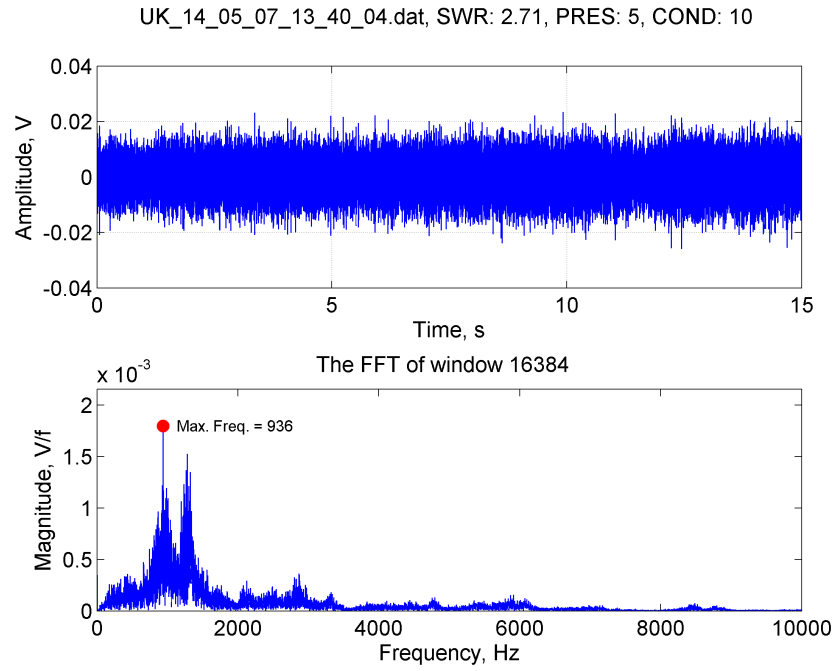


Figure 7.15: Float Trap FFT  
5 barg CL=10 kg/hr SWV=2.71 kg/hr

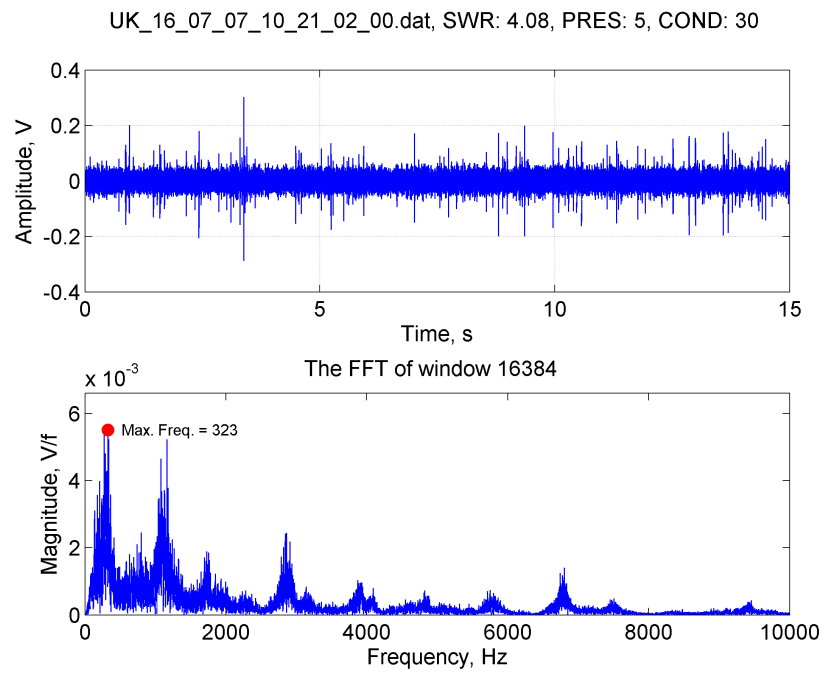


Figure 7.16: Float Trap FFT  
5 barg CL=30 kg/hr SWV=4.08 kg/hr

values could be determined by another method, the RMS evaluation could be used for steam leakage identification, which can clearly be seen through the points with a green inner circle, where the Condensate Load is low and the RMS measure is proportional with the Steam Wastage Value (and Pressure).

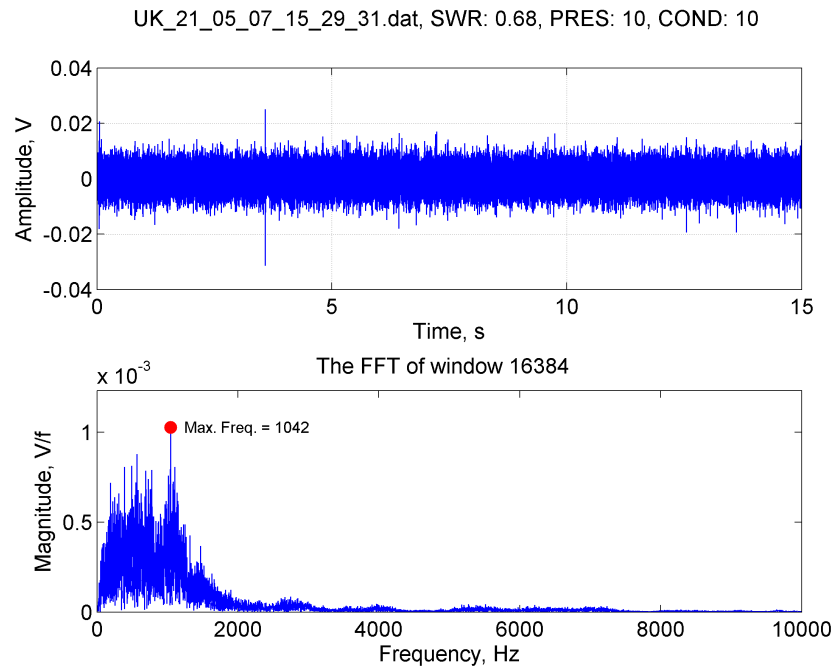


Figure 7.17: Float Trap FFT  
10 barg CL=10 kg/hr SWV=0.68 kg/hr

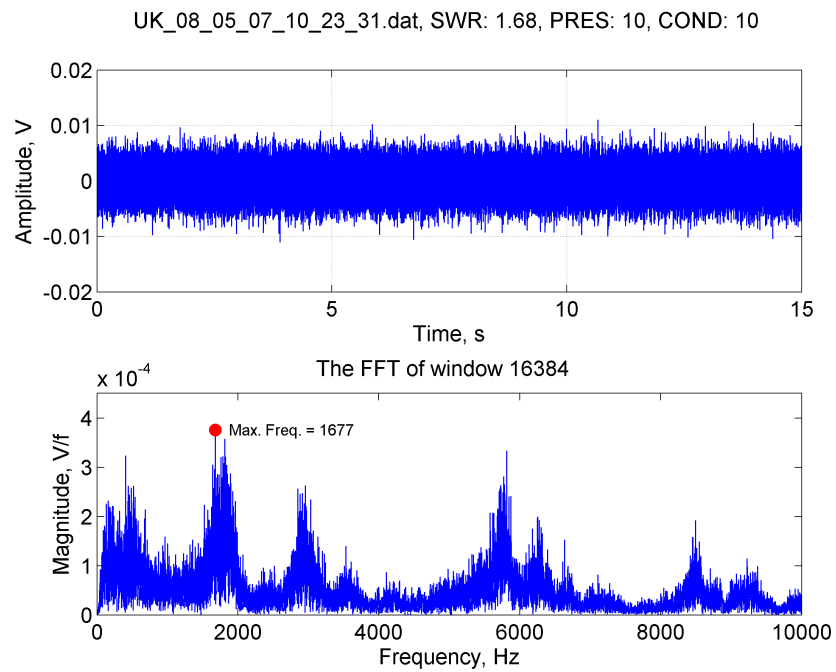


Figure 7.18: Float Trap FFT  
10 barg CL=10 kg/hr SWV=1.68 kg/hr

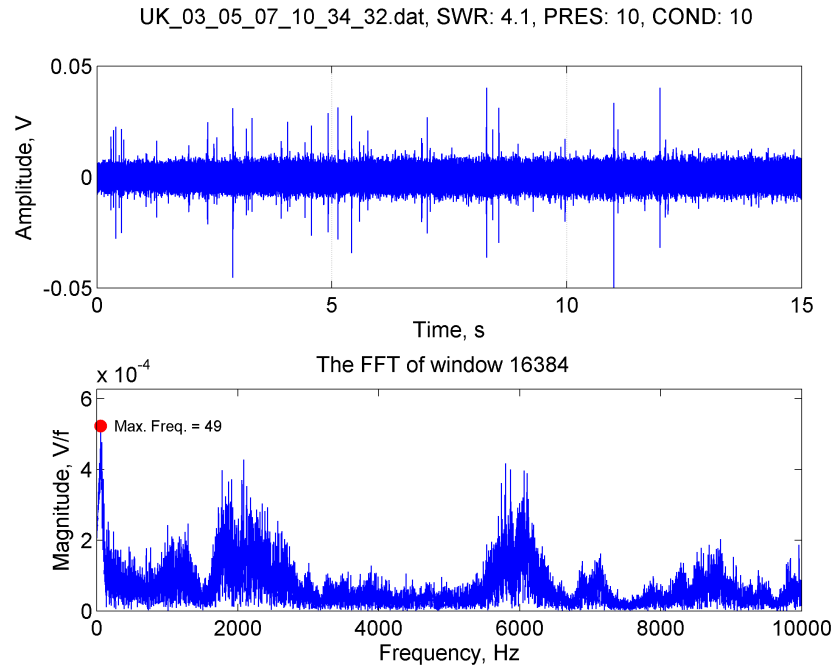


Figure 7.19: Float Trap FFT  
10 barg CL=10 kg/hr SWV=4.1 kg/hr

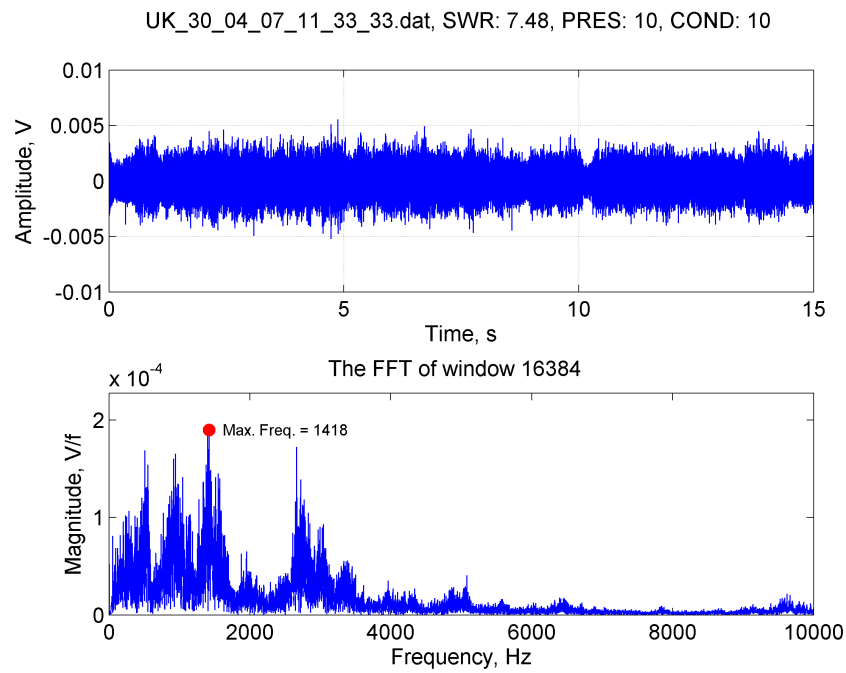


Figure 7.20: Float Trap FFT  
10 barg CL=10 kg/hr SWV=7.48 kg/hr

Interestingly, the Kurtosis evaluation in the same Figure, is fairly well clustered and a “region based” algorithm may be applied to classify the conditions.

Figure 7.24 considers the Standard Deviation and the Maximum Individual Value. The Standard Deviation of the measurements for the Fourier Transform signals show some trend similar

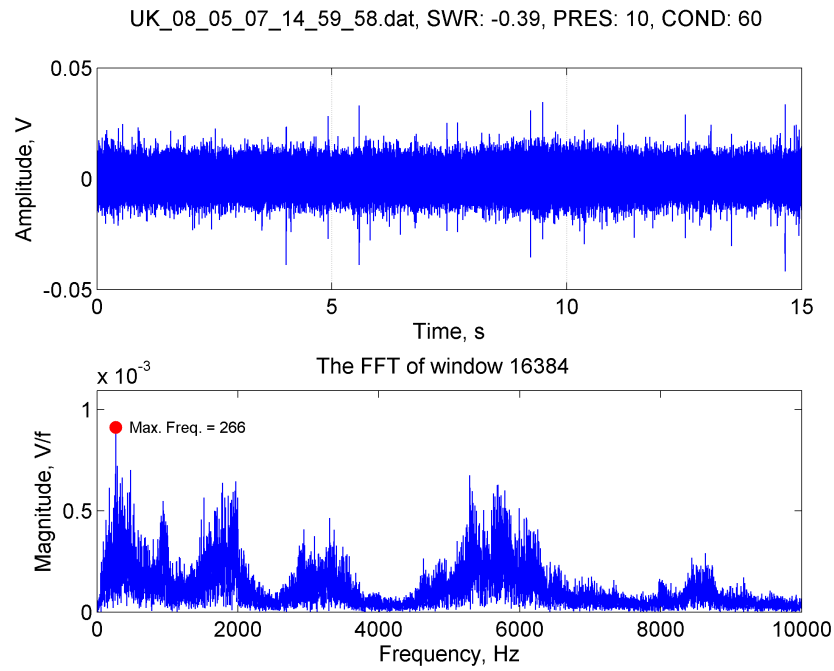


Figure 7.21: Float Trap FFT  
10 barg CL=60 kg/hr SWV=-0.39 kg/hr

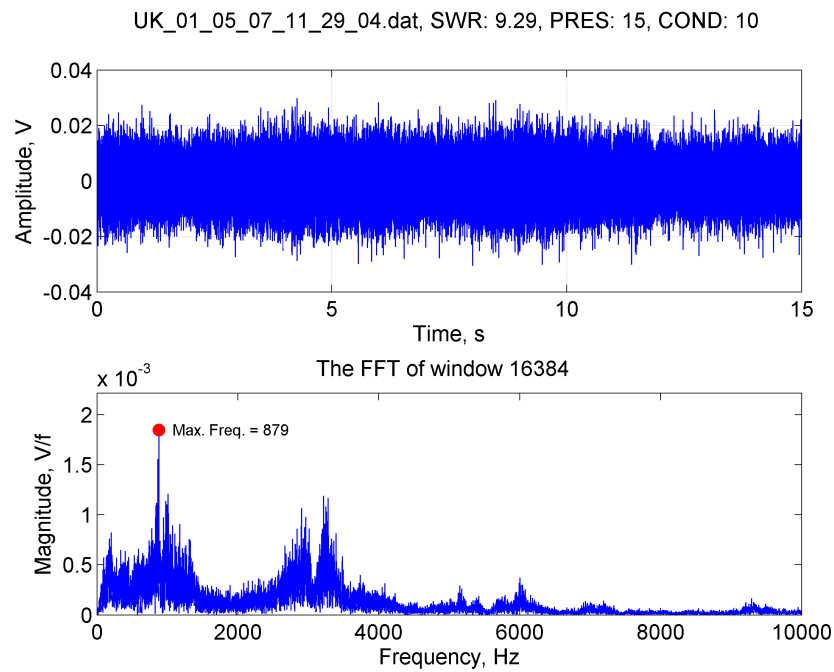


Figure 7.22: Float Trap FFT  
15 barg CL=10 kg/hr SWV=9.29 kg/hr

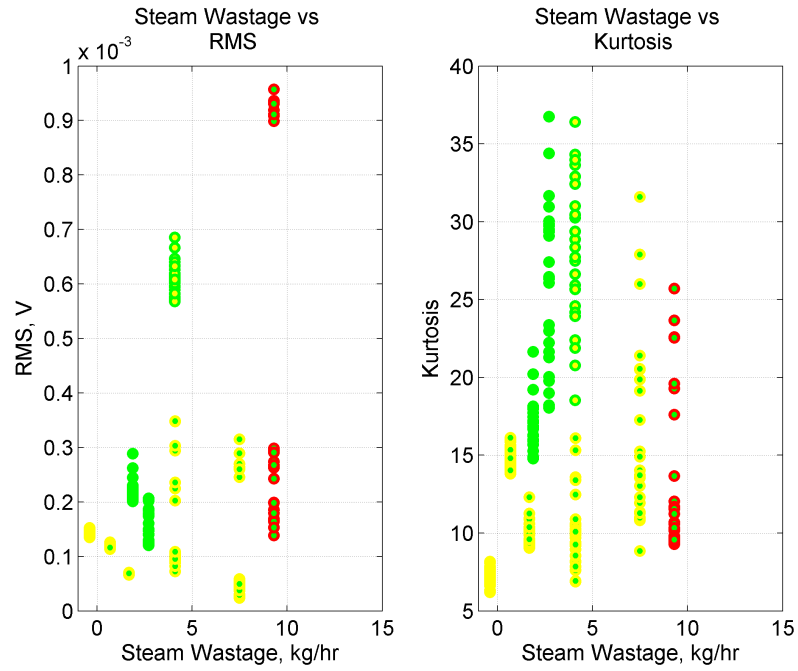


Figure 7.23: Float Trap Frequency Domain RMS and Kurtosis

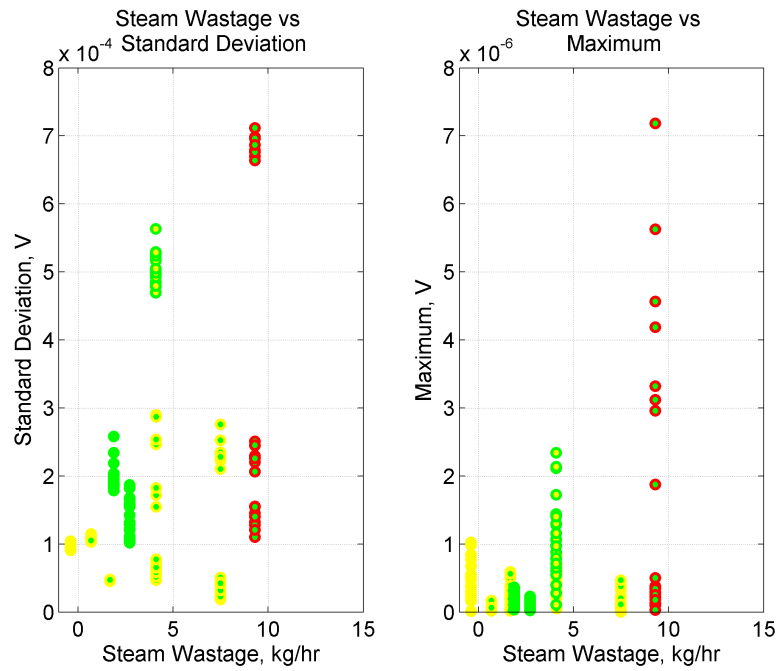


Figure 7.24: Float Trap Frequency Domain Standard Deviation and Maximum

to the RMS measurement, which could be clustered by average value and used as an indicator of Steam Wastage. However, the Maximum Individual Values do not show any correlation with Steam Wastage.

Figure 7.25 considers the Variance and the Mean value of the Fourier Transform. The Variance calculation of the Fourier Transform of the signal segments shows the same trend as it did in the

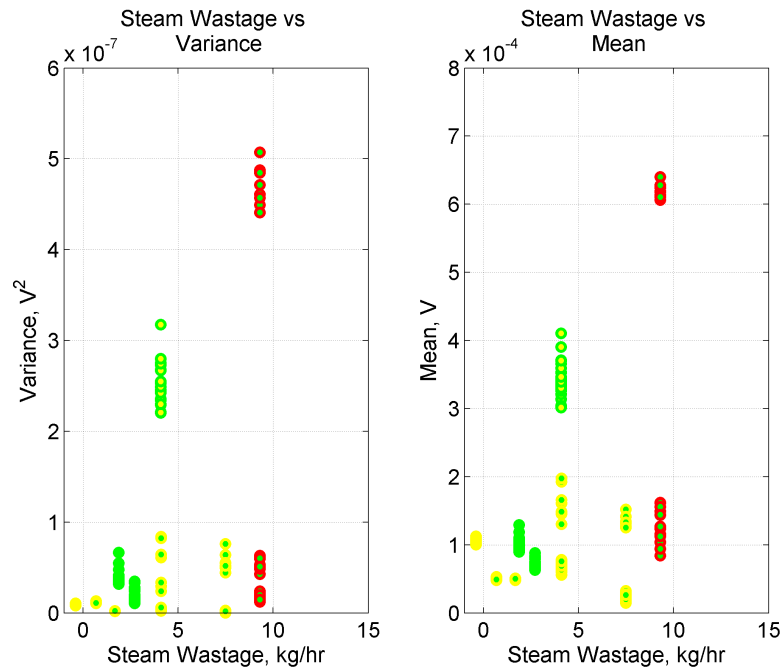


Figure 7.25: Float Trap Frequency Domain Variance and Mean

time domain calculation, providing no conclusive trends. Likewise, the Mean Values do not yield any correlation with the Steam Wastage other than the one already explained as part of the RMS evaluation.

Figure 7.26 considers the sum of the Total Signal and the Median Value. No specific or useful trend has been identified. However, the two plots are nearly identical in their evaluation, which makes sense as the Median is the average value. The Fourier Transform provides the locations (in terms of frequency) of the total energy as component of the individual frequency bins. The Median should form a similar response to the total energy of the Fourier Transform.

It is clear from these four plots of parameters calculated from the Fourier Transform, that these methods can be used as an indication of condensate load or pressure, but cannot be used for Steam Wastage measurement.

From the review of the individual plots, a number of peaks were identified, which could not be specifically correlated to a condition. For this reason, the Crest Value has been allied to the Fourier Transform. The Crest Value has been calculated by dividing the Maximum Individual Value of a Frequency Range with the mean of the values within the Range. Three frequency ranges were selected, namely: 1 Hz to 1 kHz, 1 kHz to 2 kHz, 2 kHz to 3 kHz, 3 kHz to 4 kHz, 4 kHz to 5 kHz and 5 kHz to 6 kHz. Figures 7.27 and 7.28 show these plotted, but there is no clear correlation between Crest Value and Steam Wastage Value. Another feature of this plot is that as ratios remain the same, the Crest Value across frequency ranges remain the same. In other words, there is no relative change when comparing the Crest Value for the operational conditions



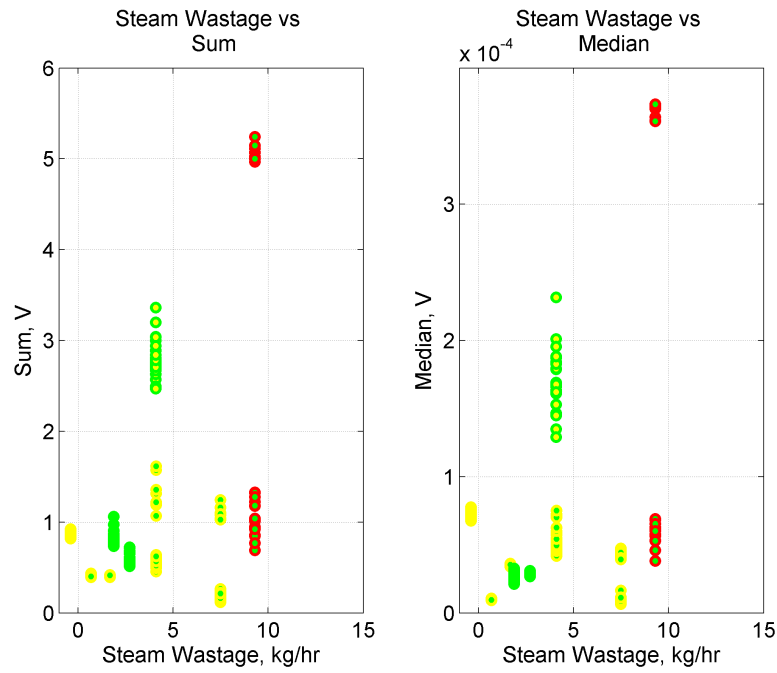


Figure 7.26: Float Trap Frequency Domain Sum and Median

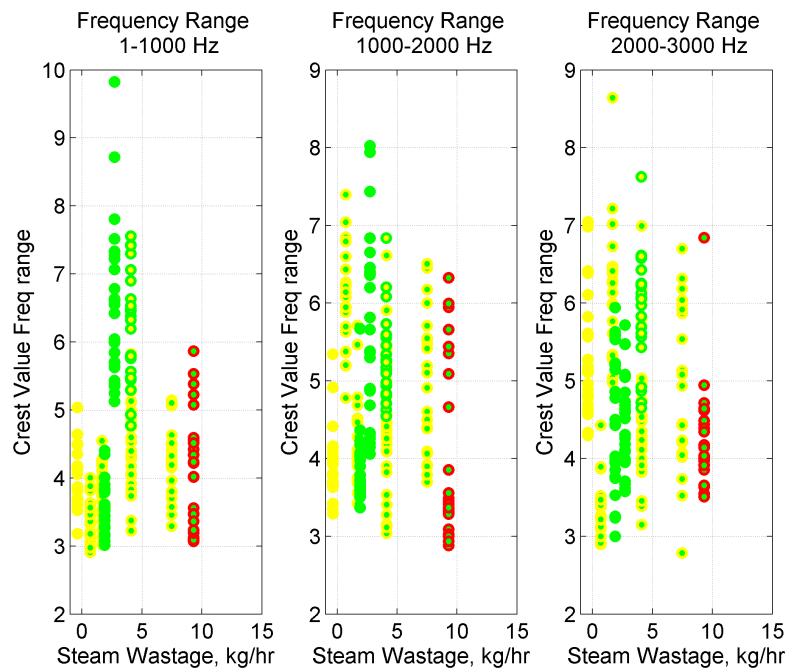


Figure 7.27: Float Trap Frequency Domain Frequency Bins Part 1

in terms of the frequency range.

**Discussion** As mentioned previously, the Fourier Spectrum considers the complete 15 seconds and the representative frequencies within this signal segment. From the time domain and respective frequency analysis, it can be seen that there are changes to the frequency content within the 15 second recording. For this reason, the time-frequency analysis is presented in the next section

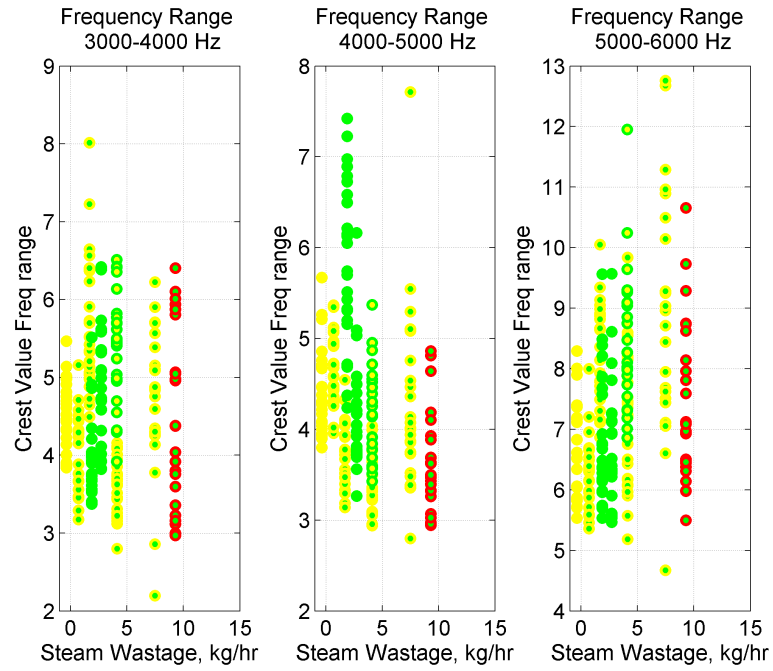


Figure 7.28: Float Trap Frequency Domain Frequency Bins Part 2

to allow the review of the contributing components to be identified.

As the FFT is an average representation of the frequency content across the data sample, it is highly affected by any dynamic or transient content. When the signal is stationary in nature, the FFT will be comparable and consistent. As the mechanism of the Float Trap introduces transient events, the FFT will not show these unless they are regular and consistent. Furthermore, the two-phase flow introduces transient effects as the flow regime changes dynamically. For this reason, it is advantageous to combine both temporal and transient analysis, which is shown in the next section through the application of the Short-Time Fourier Transform.

### 7.2.3 Time-Frequency Analysis

The time-frequency analysis approach has been explained in Chapter 2. This approach allows both the frequency and time domain components to be identified. The steps used for this application are as follows:

- 1) A signal was segmented into 15 second long data segments.
- 2) For each of the data segments, the short-Time Fourier Transform was calculated with a length of 2048 points (equal to  $2^{11}$ ) using a Hamming window. This allows for approximately 9.88 Hz per resolution bin. The reason for the decrease in frequency bin resolution (compared to the frequency analysis) is that this method is computationally more intensive. Additionally, the time and frequency resolutions are inversely proportional. In other words, if the time domain resolution is increased, the frequency resolution will be decreased. The window size chosen allows for an acceptable frequency and time resolution.
- 3) A number of features (discussed earlier in Chapter 6) were calculated.
- 4) The time-frequency map and time domain plotted on a graph for detailed analysis.

In Figure 7.29 an example plot for the STFT is shown. This signal is the same example that was used for the frequency analysis representation. From the time domain signal, it can be clearly seen that the signal is noise-like, with a number of low level instantaneous peaks. Furthermore, there is a base noise band, which is steady throughout the 15 second period. Comparing the time frequency representation with the FFT (see Figure 7.29), it is clear that there is not much change to the spectrum over the 15 second interval. In this case, the FFT could be used as a representation for the signal. The Time-Frequency map in the same figure reflects the stationary nature of the frequency content for the signal time scale of 15 seconds. From the time-frequency map, some higher intensity areas can be identified, however the bulk of the signal content is contained below 2.2 kHz. The operational conditions in this example dataset is 5 barg pressure and low Condensate Load (10 kg/hr), resulting in a high Steam Wastage of 1.88 kg/hr.

Figures 7.30 and 7.31 show the other two conditions for the low pressure example. For Figure 7.30, a similar time domain noise pattern is presented and compared to the previous example. However, in the frequency domain, a high peak at around 1 kHz which stretches the length of the shown signal. This high energy signature is reflected in the Fourier Transform as a clear peak. In Figure 7.31, a number of spikes can be seen and their high intensity impact is clearly visible in the time-frequency map across the complete frequency range (vertically). The low frequency noise band can be seen up to about 2 kHz and then another thinner horizontal band at 3 kHz. Where the spikes and the background noise meet, the intensity is increased to an increased value

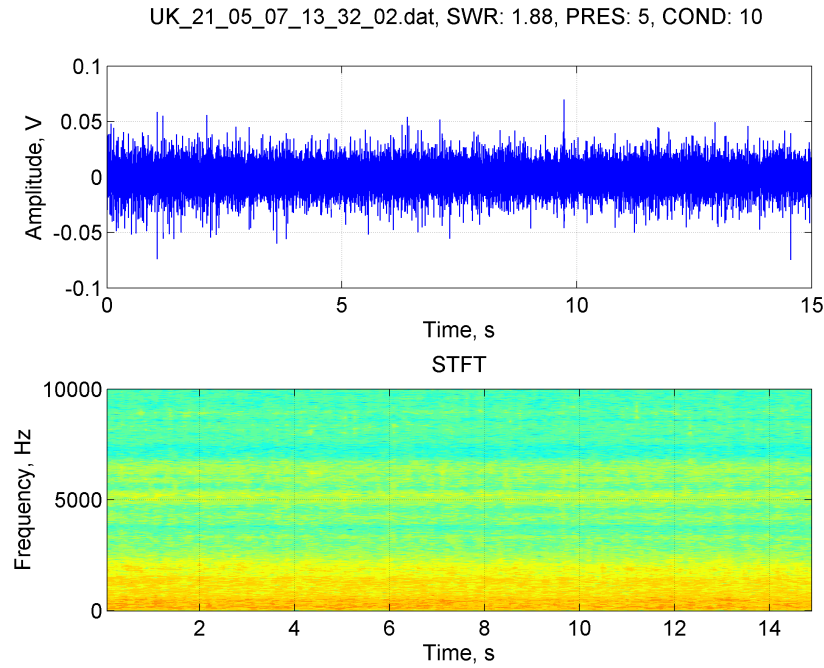


Figure 7.29: Float Trap STFT  
5 barg CL=10 kg/hr SWV=0.65 kg/hr

(orange). This effect is clearly shown above 4 kHz. These same features were shown in Chapter 4 where low frequency signals manifested themselves as vertical, impulse like responses spread across the frequency range and high frequency noise presented itself as horizontal values.

Figures 7.32 to 7.36 show the medium pressure examples. Figure 7.32 shows a strong intensity response in a band up to about 2 kHz in the frequency range. The low intensity observed in the Fourier Transforms is reflected in the time-frequency maps in Figures 7.33 to 7.35 where a low intensity frequency response is observed in the ranges of about 1 kHz and 3 kHz. Another point worth noting is that Figure 7.34 shows an instantaneous peak at 11 seconds and about 500 Hz, which can be clearly be related to the instantaneous peak in the time domain.

The high pressure example shown in Figure 7.37 shows two high intensity bands at around 1 kHz and 3 kHz, similar to the lower intensity bands seen in Figure 7.35. Both of these cases are related to a higher Steam Wastage Value of 9.29 kg/hr and 7.48 kg/hr respectively.

The next part features the summary plots previously seen for the time domain analysis. The parameters evaluated using the Fourier Transform as an input signal are RMS, Kurtosis, Standard Deviation, Maximum Individual Value, Variance, Mean, Sum of Total Signal and Median value, introductions to which were given in Sections 5.3.2 and 6.1.2 respectively.

Figure 7.38 shows the RMS and Kurtosis evaluated and plotted against Steam Wastage. The same trend is being seen as compared to the time domain and frequency domain signal analysis. Steam Wastage is inversely proportional to Condensate Load, as expected. If the condensate values could be determined by another method, the RMS evaluation could not be used for steam

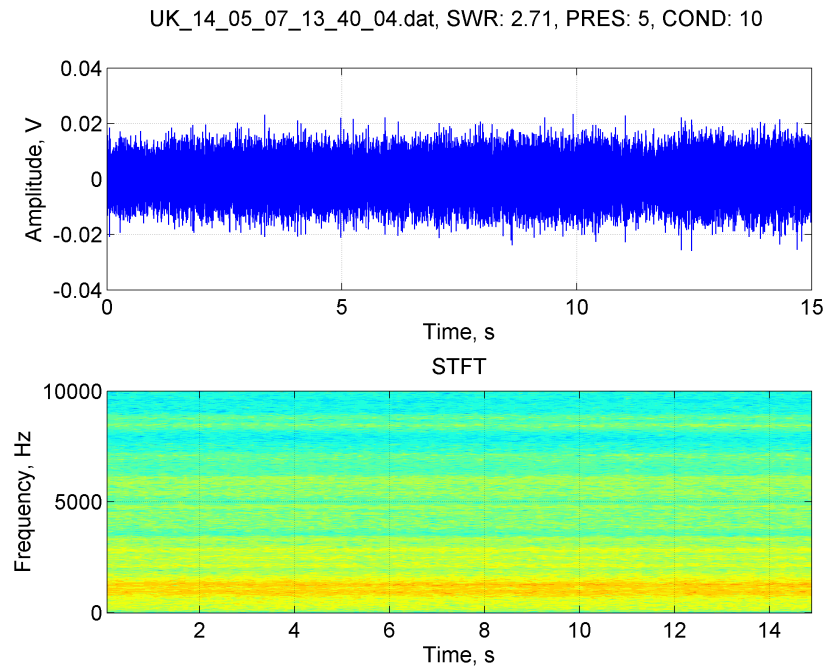


Figure 7.30: Float Trap STFT  
5 barg CL=10 kg/hr SWV=2.71 kg/hr

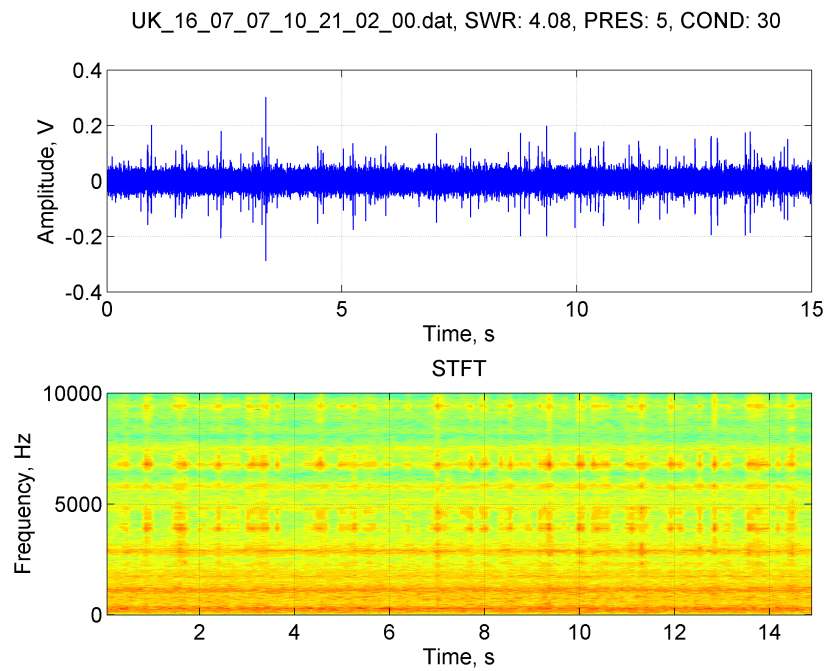


Figure 7.31: Float Trap STFT  
5 barg CL=30 kg/hr SWV=4.08 kg/hr

leakage identification. The reason for this is that the mechanism affects the response of the trap. Considering the Kurtosis evaluation in the same figure, the values are not related and do not provide any trends. This was also found in the time domain analysis.

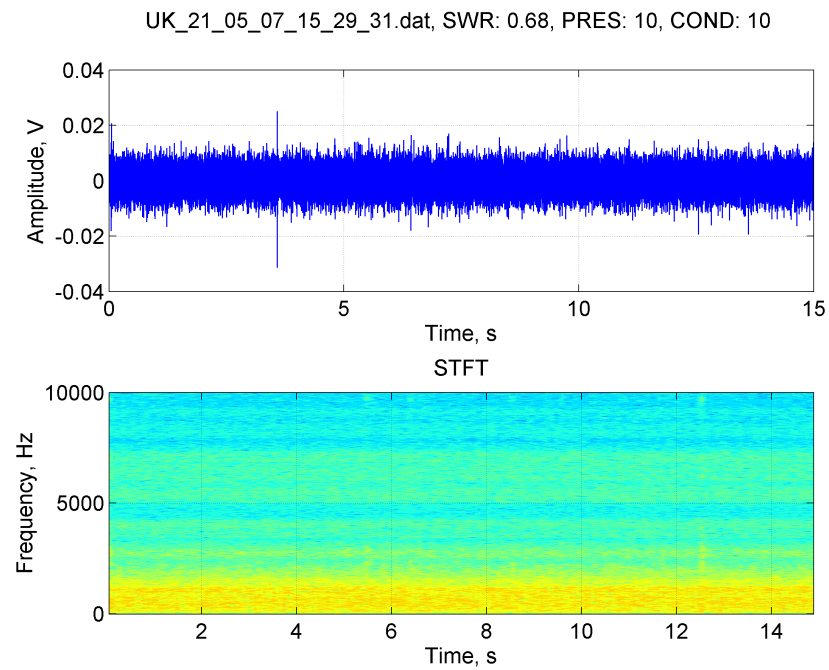


Figure 7.32: Float Trap STFT  
10 barg CL=10 kg/hr SWV=0.68 kg/hr

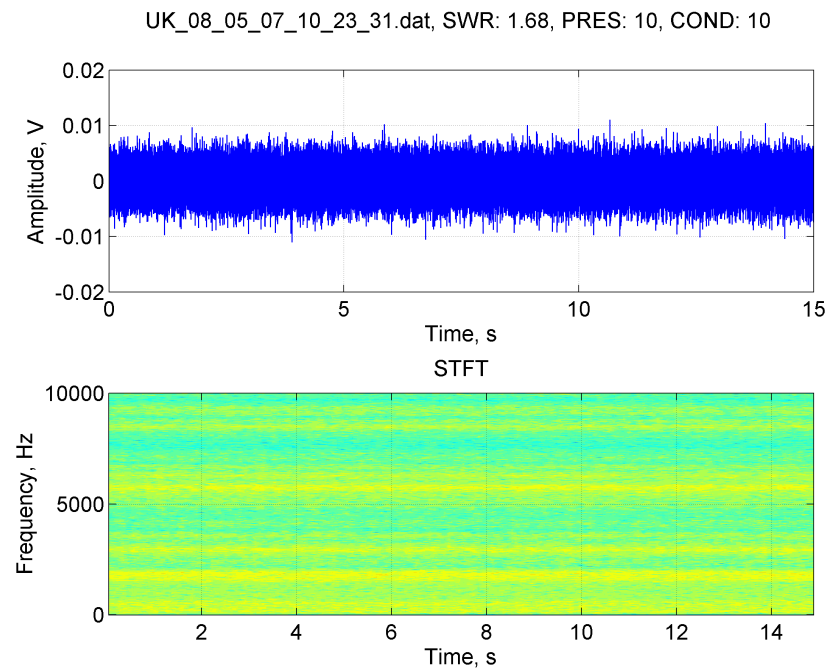


Figure 7.33: Float Trap STFT  
10 barg CL=10 kg/hr SWV=1.68 kg/hr

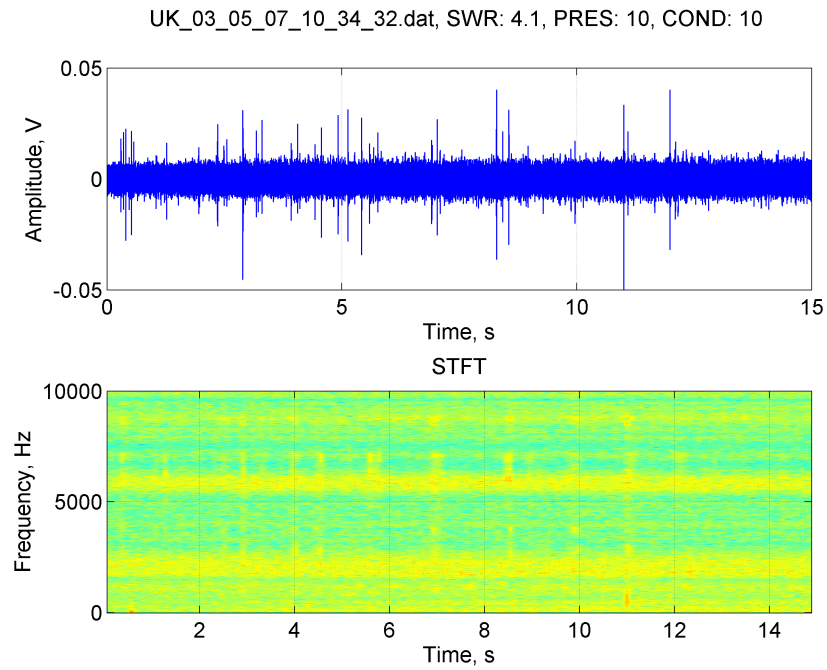


Figure 7.34: Float Trap STFT  
10 barg CL=10 kg/hr SWV=4.1 kg/hr

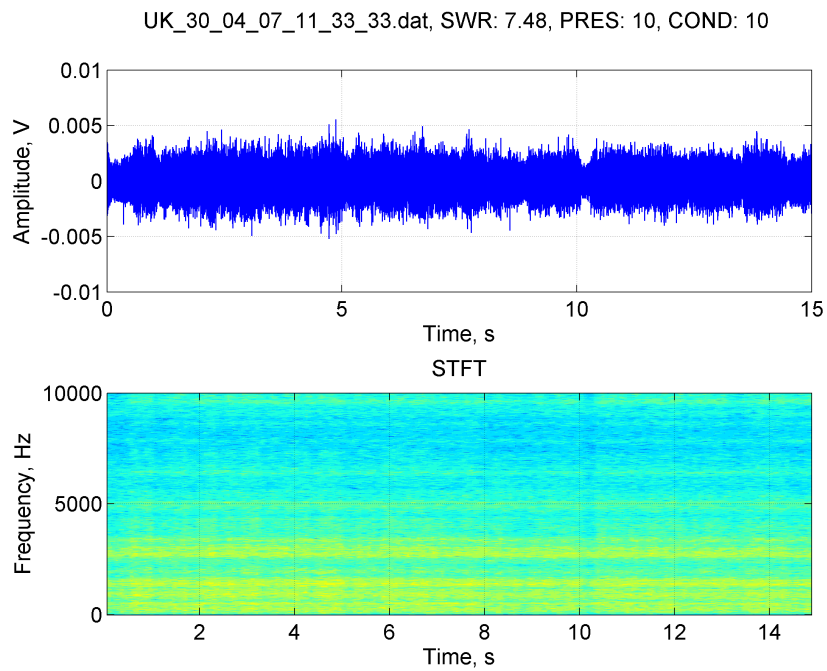


Figure 7.35: Float Trap STFT  
10 barg CL=10 kg/hr SWV=7.48 kg/hr

Figure 7.39 considers the Standard Deviation and the Maximum Individual Value. The Standard Deviation of the measurements for the Short-Time Fourier Transform signals shows the same trend as the previous evaluations for the Fixed Orifice Trap, with no conclusive trends. Likewise, the Maximum Individual Values do not show any correlation with the Steam Wastage.

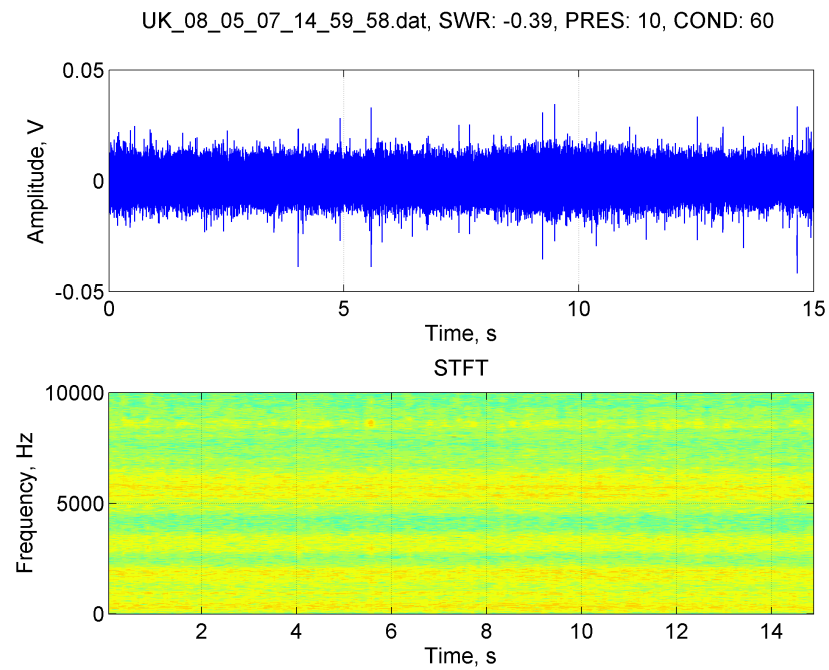


Figure 7.36: Float Trap STFT  
10 barg CL=60 kg/hr SWV=-0.39 kg/hr

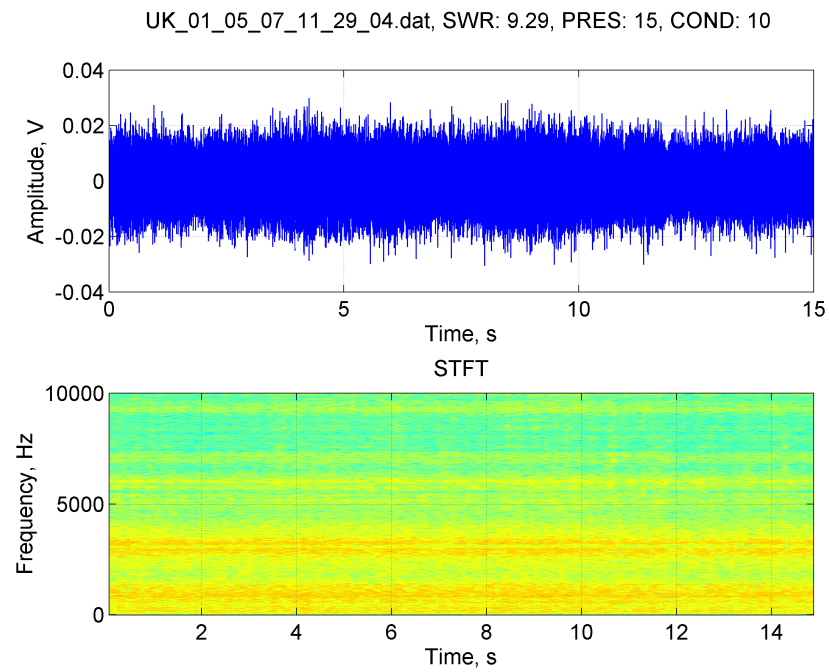


Figure 7.37: Float Trap STFT  
15 barg CL=10 kg/hr SWV=9.29 kg/hr



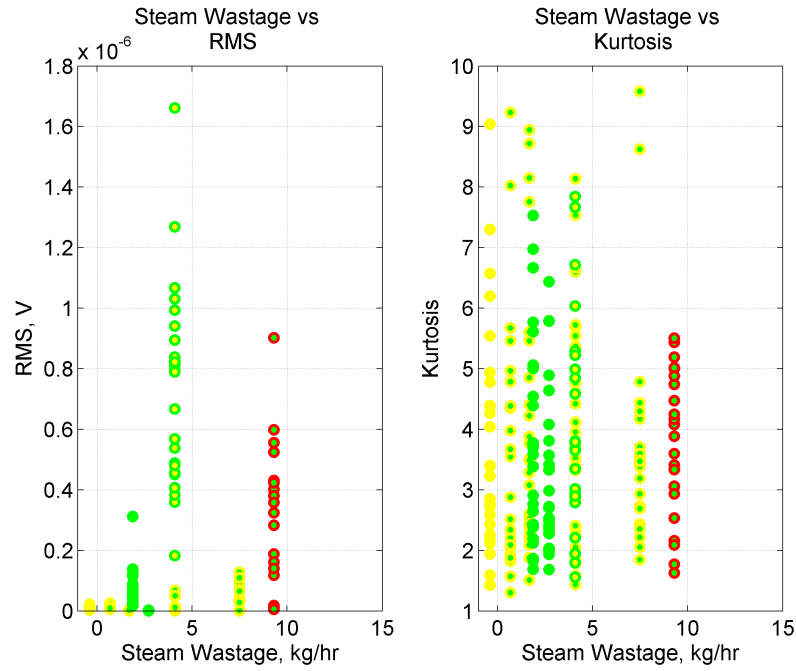


Figure 7.38: Float Trap STFT RMS and Kurtosis

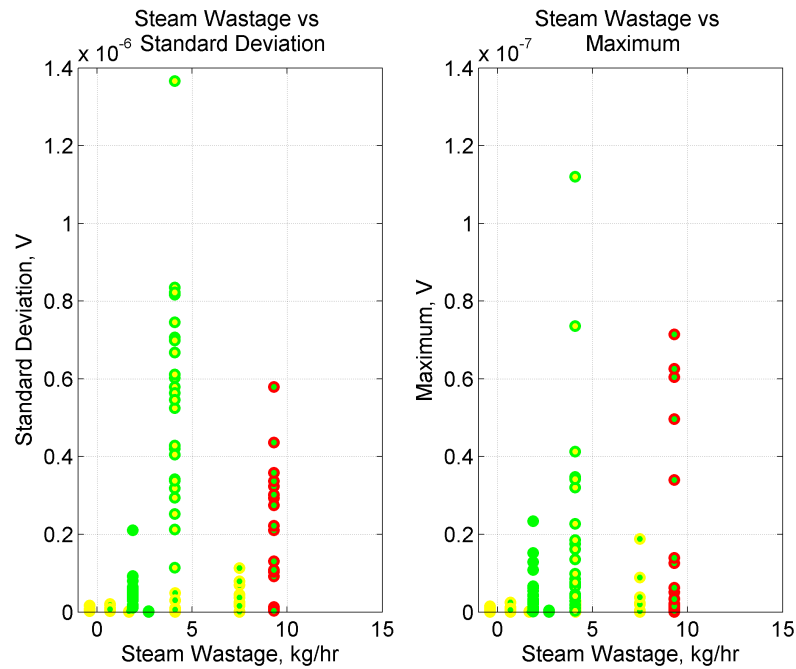


Figure 7.39: Float Trap STFT Standard Deviation and Maximum

Figure 7.40 considers the Variance and the Mean value of the STFT. The Variance calculation of the STFT of the signal segments shows an outlier. This can be related to the instantaneous spike that has already been highlighted in the previous section. The same trend as discovered in the the previous calculations is observed for the time-frequency evaluation, and thus no conclusive outcomes have been found. Likewise, the Mean Individual Values does not yield any correlation

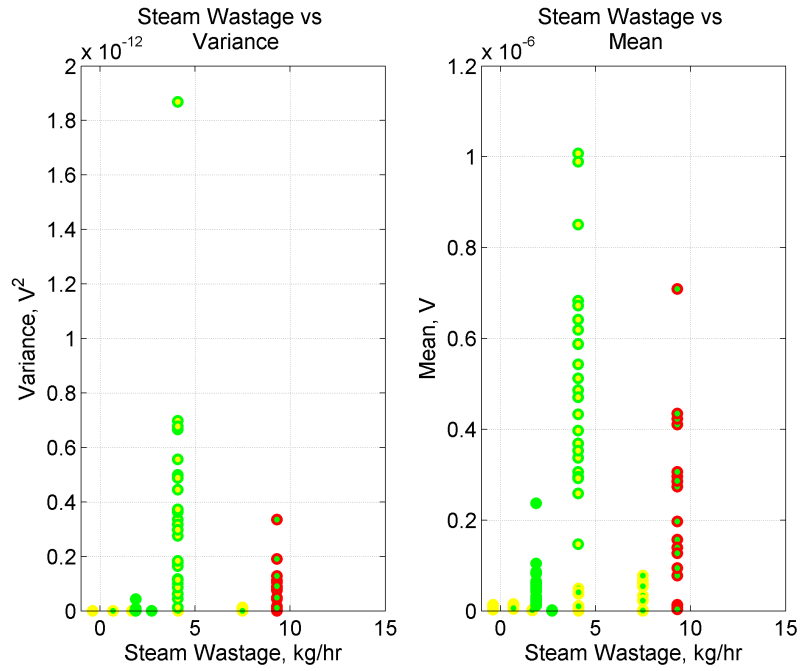


Figure 7.40: Float Trap STFT Variance and Mean

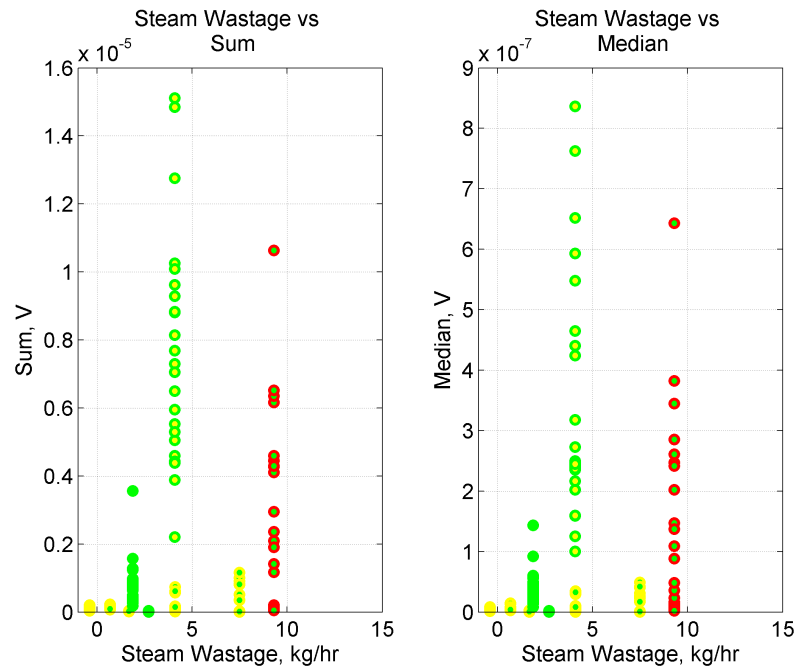


Figure 7.41: Float Trap STFT Sum and Median

with the Steam Wastage other than the one already explained as part of the RMS evaluation.

Figure 7.41 considers the sum of the Total Signal and the Median Value. No specific or useful trend has been identified.

It is clear from these four plots of parameters calculated from the STFT that these methods can be used, but only when the data is piece-wise evaluated rather than averaged, as shown in the

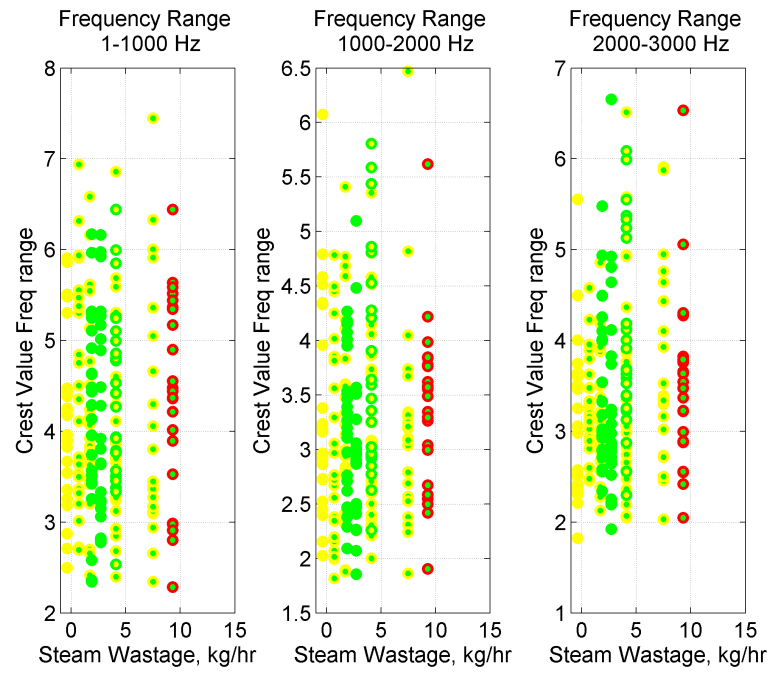


Figure 7.42: Float Trap STFT Frequency Bins Part 1

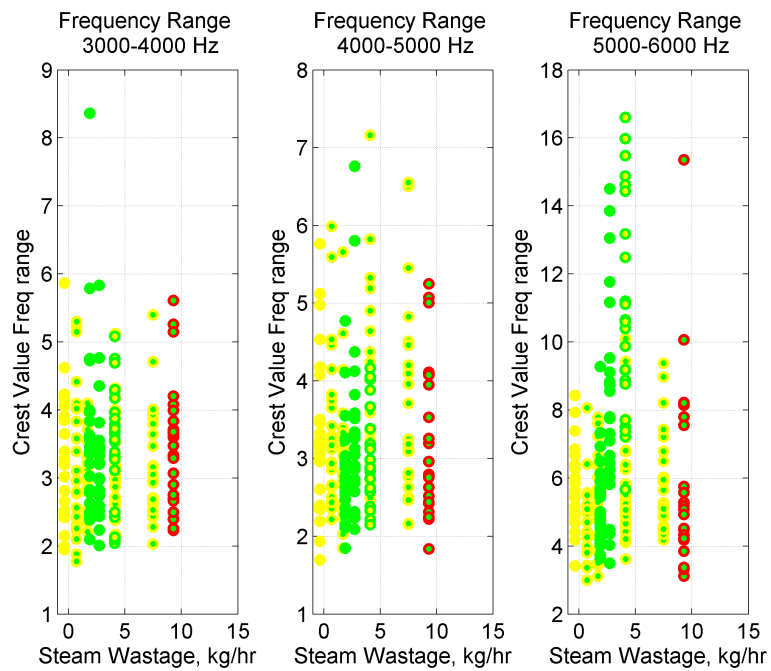


Figure 7.43: Float Trap STFT Frequency Bins Part 2

previous section. For this reason, this approach cannot be used for Steam Wastage measurement. However, when some good repeatable dynamic features exist, this analysis has been the best method for displaying the behaviour of the trap.

From the review of the individual plots, a number of peaks were identified, which could not be specifically correlated to a condition. For this reason, the Crest Value has been applied to the

STFT. The Crest Value has been calculated by dividing the Maximum Instantaneous value of a Frequency Range with the mean of the values within the Range. Three frequency ranges were selected, namely: 1 Hz to 1 kHz, 1 kHz to 2 kHz, 2 kHz to 3 kHz, 3 kHz to 4 kHz, 4 kHz to 5 kHz and 5 kHz to 6 kHz. Figures 7.42 and 7.43 show these plotted, but there is no clear correlation between Crest Value and Steam Wastage Value. Another feature of this plot is that as ratios remain the same, the Crest Value across frequency ranges remain the same. In other words, there is no relative change when comparing the Crest Value for the operational conditions in terms of the frequency range.

**Discussion** As mentioned previously, the STFT considers the complete 15 seconds and the representative frequencies within this signal segment. From the time domain and respective STFT analysis, it can be seen that changes to the time domain are reflected in the STFT content within the 15 second recording. It has been shown that the time-frequency analysis is the best method to capture both behaviours highlighting the contributing components.

### 7.3 Summary

This chapter has investigated the Float Trap. The following are the findings and observations that have been made:

- The time domain acoustic emission of the Float Trap has been presented and the modulating nature of the trap is more clearly visible than in the Orifice Trap. Periods in which the signal is largely stationary have also been shown.
- Time domain processing has not been successful, even though the signal observes some modulation. Using basic statistic measurements the complicated nature and difficulty in consistently relating the Steam Wastage to the acoustic emission has been demonstrated.
- Frequency domain processing has been equally inconclusive. However, compared with the Fixed Orifice Trap, the response shows (in some cases) some clear peaks, but the example data sets presented also show a high variability in resonant peaks. The variability and the chaotic nature of Float Trap has resulted in an inconclusive estimation of Steam Wastage from acoustic emission.
- Similar to the Orifice Trap, the time-frequency method has been shown to be the most suitable approach, as this highlights the operational nature of the trap by simultaneously evaluating the time and frequency domain. It must be noted that this is the most computationally intensive signal processing method being considered.

- No specific inherent noise characteristic related to Steam Wastage has been discovered. Overall, it has been discovered that RMS and Kurtosis values resulting from acoustic emission data cannot conclusively be used to determine Pressure, Condensate Load or Steam Wastage Values in Steam Traps. Other statistical methods, such as Standard Deviation and Variance, also have been unsuccessful in determining a trend or estimating Steam Wastage.
- It has not been possible to link the trap behaviour with the two-phase flow regimes.
- In this case, a statistical approach based on frequency or time-frequency evaluations would be best suited.

*This chapter applied digital signal processing techniques to the Float Trap. The next chapter will cover Impulsive Traps, which have a strong modulating behaviour.*

## Chapter 8

# Impulsive Steam Trap Analysis

*This chapter presents the analysis of Impulsive Steam Trap data. The data has been recorded and processed using time and frequency methods and their results are presented with an explanation of the acoustic data and an overview of digital signal processing.*

### 8.1 Acoustic Signals for Impulsive Trap

The Impulsive Trap category includes the Thermodynamic and Inverted Bucket Traps. These traps have a clear impulse response within their acoustic response. This impulse type response provides a clearer signature compared to the other two trap categories. These impulses can be used for timing and cycle counting, as the impulses signify the times when the trap mechanism is open. Conversely, the impulses can provide a measure of the seal of the trap mechanism, as between impulses at a low load, the trap should be silent as it is closed and there is no flow. Thus the impulse can be used as a good measure of leakage. These traps are the easiest to diagnose by an engineer as the impulse provides a good marker for the position within the cycle. Furthermore, the impulse can be heard without the use of sophisticated tools as the acoustic response is detectable at low kHz and is, thus, within the range of human hearing.

Although there are a number of traps within this category of acoustic response, the Steam Trap chosen for analysis of this category is the Thermodynamic Trap, as it provides a representative signal for this acoustic category and allows a manageable size of data to be presented. Overall these datasets generate 200 data points which are used in the subsequent analysis to correlate the operational conditions with the acoustic emission.

The acoustic data for this trap type has been recorded using the Steam Wastage Monitor as well as the Steam Wastage Rigs. The data sets used in the analysis are displayed in Table 7.1 and cover a range of operating conditions up to 20 barg and 60 kg/hr Condensate Load. As previously

seen, the datasets have been divided into three pressure ranges (high, medium and low), within each the Condensate Load and Steam Wastage Value will be considered. The Condensate Load and Steam Wastage Values are also shown in the table.

Filename	SWV (kg/hr)	Pressure (barg)	Condensate (kg/hr)	Temperature (°C)
UK_08_08_07_11_07_24	0.19	5	10	159
UK_18_04_07_14_51_34	1.62	15	10	201
UK_19_04_07_15_29_59	1.12	15	35	201
UK_20_04_07_14_58_26	0.38	15	45	201
UK_19_04_07_14_00_46	-0.37	15	60	201
UK_16_04_07_14_31_44	10.96	20	10	217
UK_16_04_07_15_10_49	9.65	20	10	217
UK_16_04_07_15_41_03	7.28	20	50	217
UK_17_04_07_10_18_16	1.39	20	55	216

Table 8.1: Thermodynamic Trap Acoustic Data Summary

## 8.2 Application of Signal Processing

In terms of signal processing, three methods will be described (time domain, frequency domain and time-frequency).

### 8.2.1 Characteristics of the Acoustic Signals

As an introduction to the acoustics of the Non-Impulsive Trap category, three signals have been plotted in Figures 8.1, 8.3 and 8.5. These figures show examples at 15 barg pressure and provide the reader an overview of the format of Impulsive Trap data at low and medium Steam Wastage Values. High Steam Wastage Values were not achieved by this trap at this pressure condition. Additionally, a magnified representation of each of the three examples is provided to show the changes to the time domain signal at different time scale levels. It is worth noting at this point that time domain representations for all nine example conditions will be shown as part of the Frequency analysis in Section 8.2.3 of this chapter.

Figure 8.1 shows a low condensate example of 10 kg/hr and low Steam Wastage of 1.62 kg/hr. The background noise level is significantly lower compared to the previous two trap types. Furthermore, the sharp impulses are clearly visible. Eight impulses can be seen in the total length display. It is worth noting the lower level noise just before and after the impulse. This can be caused by condensate and is akin with the noise seen in the previous two traps. A more detailed view of the signal is provided in Figure 8.2 in which the same signal is shown on a 1 second and 0.1 second time scale. The noisy nature of the flow through the Steam Trap is clearly shown at the 1 second scale. Additionally, a number of small “blips” can be seen between 0.4 and 0.8 second

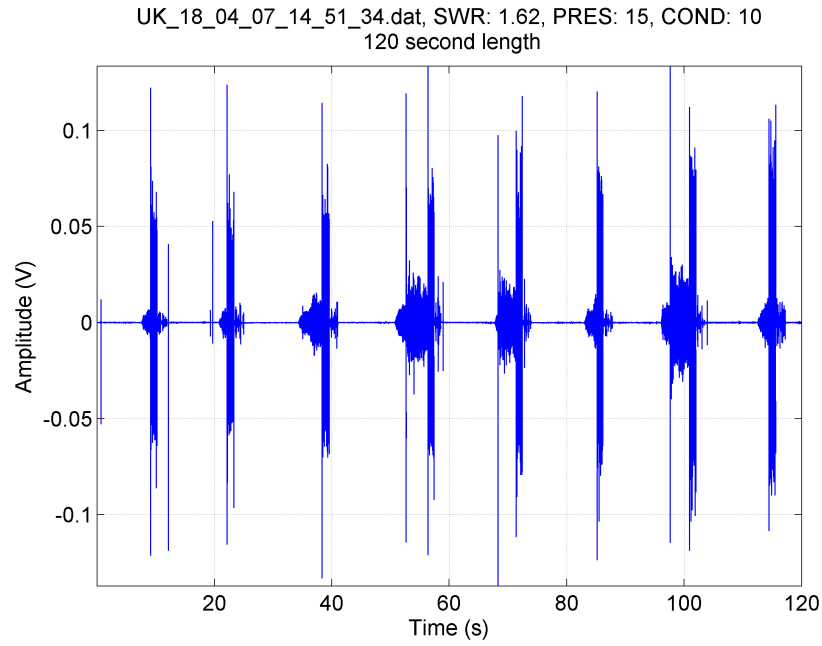


Figure 8.1: Thermodynamic Trap 15 barg High Steam Wastage Time Plot

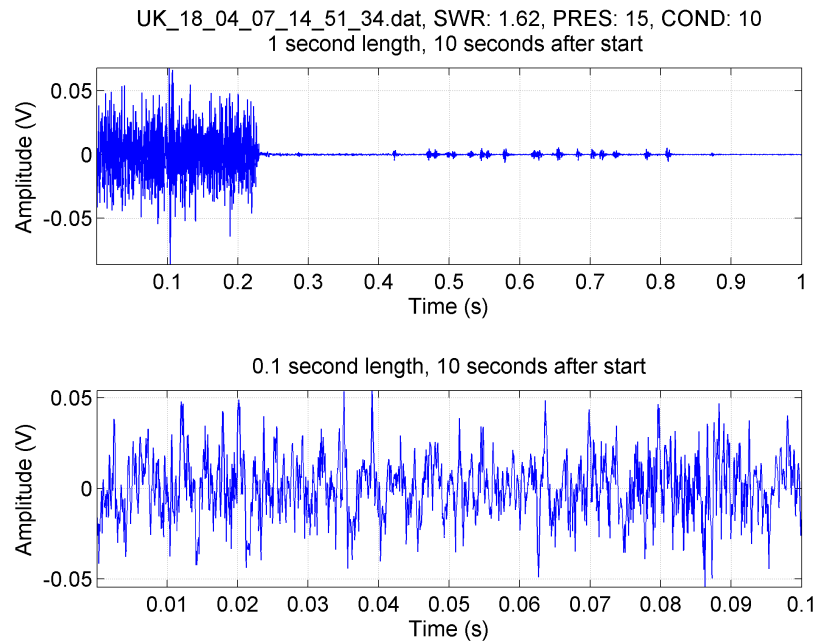


Figure 8.2: Thermodynamic Trap 15 barg High Steam Wastage Time Plot Zoomed

markers in this graph. The rapid reduction of the signal to a very low level is clearly shown. At the 0.1 second scale (the lower graph), the signal looks similar to the one observed for previous Steam Trap types, although the scale is significantly higher.

Figure 8.3 shows another case of medium Condensate Load (35 kg/hr) and a medium Steam Wastage (1.12 kg/hr). The similar response is shown compared to the previous signal, both in



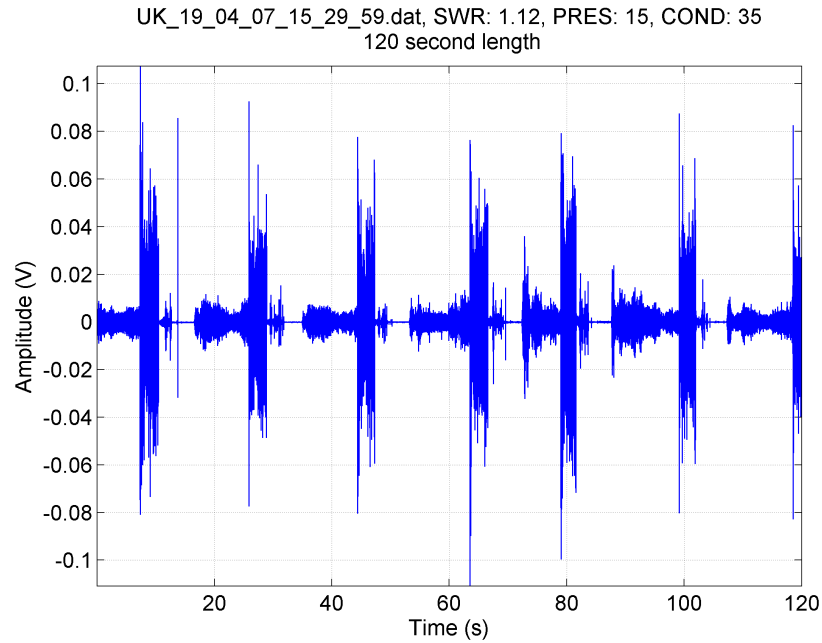


Figure 8.3: Thermodynamic Trap 15bar Medium Steam Wastage Time Plot

magnitude of the spikes and the shape. However, only six and a half impulses are observed. The impulses are wider and opening/closing sequences are bigger. A reason for this could be the increase in the condensate load. At the shorter time scale of 0.1 seconds (Figure 8.4), the same pattern is repeated as was observed in the previous example. At the end of the opening sequence, the noise drops to a very low level. The amplitude of the respective higher and lower level are also comparable. At the scale of 0.1 seconds, a similar signal response is observed as in the previous example.

Finally, Figure 8.5 shows a low Steam Wastage (-0.37 kg/hr) and higher Condensate Load (60 kg/hr). The signal observed is similar to the previous two examples. However, as the condensate load is high, there is almost no shut off visible. The amplitude has remained the same. Equally, at the lower scale of -0.37 kg/hr Steam Wastage Value, there appears to be little movement. Considering the signal at the shorter time scales, shown in Figure 8.6, the signal is comparable.

**Discussion** The length of the data samples presented are 2 minutes long. The different manifestations of modulations occurring at different mixtures between steam and condensate have been covered. The Thermodynamic Trap contains a disc that lifts off the seat to open and falls back onto the seat to close. With the condensate load, the number of opening/closing sequences increases. Either side of the opening, there are additional features which provide further information on the operational conditions. As the data recordings presented are from an operational trap, there are no periods where the signal is silent.

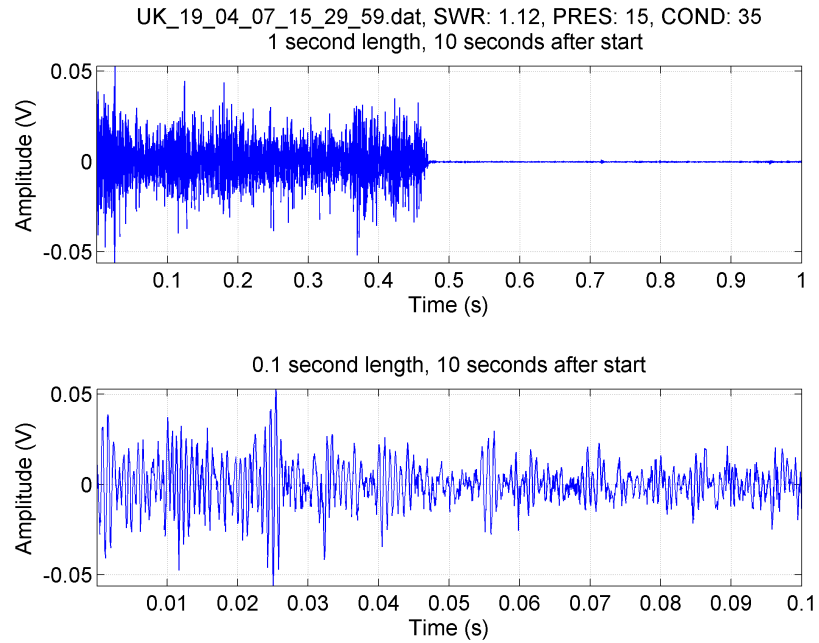


Figure 8.4: Thermodynamic Trap 15bar Medium Steam Wastage Time Plot Zoomed

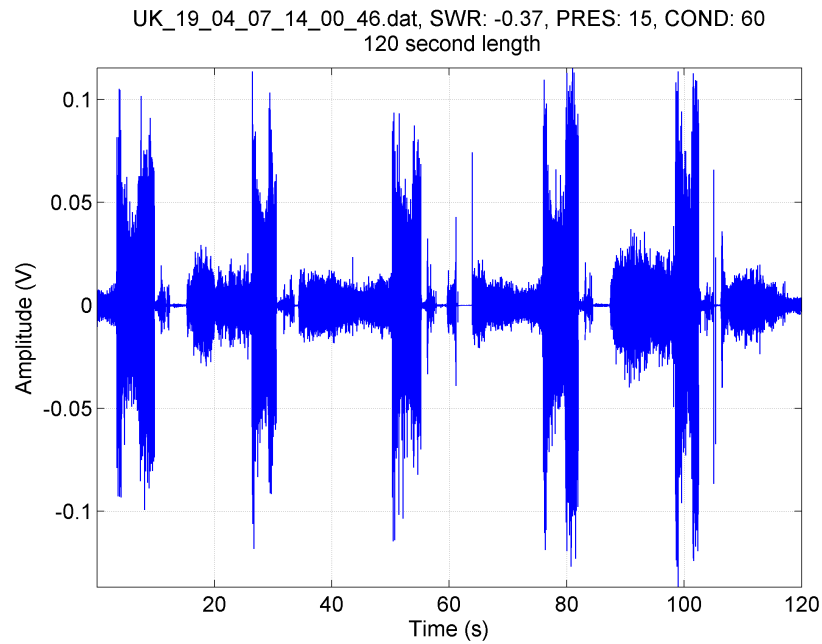


Figure 8.5: Thermodynamic Trap 15 barg Low Steam Wastage Time Plot

### 8.2.2 Time Domain Analysis

The following section reviews key features of the time domain representation for the Thermodynamic Trap, for which the time domain signal was analysed by splitting the signal into 15 second sub-sets. Steam Wastage has been plotted on the x-axis and the calculated feature on the y-axis. In addition, the marker contains two colours to allow Pressure and Condensate Load indications

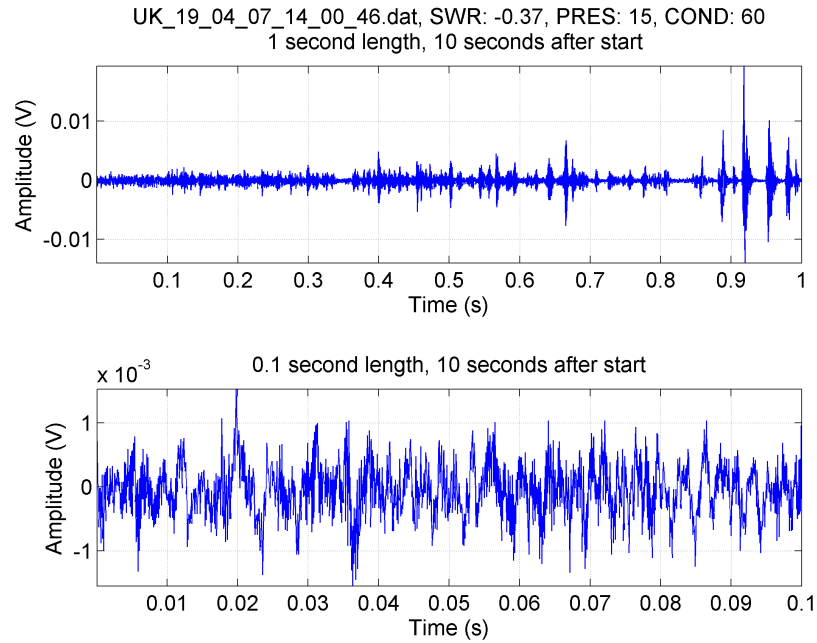


Figure 8.6: Thermodynamic Trap 15 barg Low Steam Wastage Time Plot Zoomed

to be represented (in a similar way as in Chapter 5). Using this approach, four parameters can be displayed in one graph which reduces the number of figures required to consider all permutations of data combinations.

The markers have been implemented by a two-dot system, in which the inner colour indicates the level of Condensate Load and the outer colour the Pressure level. The Condensate Load and Pressure have been differentiated into a range of high, medium and low, as detailed in Table 8.2. A visual representation is provided in Figure 8.7 to provide an applied context of the application.

Colour	Pressure (barg) (Outer Marker Colour)	Condensate (kg/hr) (Inner Marker Colour)
Red	> 12	> 80
Yellow	< 12 and > 6	< 80 and > 20
Green	< 6	< 20

Table 8.2: Thermodynamic Trap Condensate and Pressure Indicator

Features used in the analysis have been introduced in Sections 5.3.2 and 6.1.2 and include: RMS, Kurtosis, Standard Deviation, Maximum, Variance, Mean, Sum and Median. The results of the time domain evaluations of the features introduced in the previous sections are shown in Figures 8.8, 8.9, 8.10 and 8.11.

Figure 8.8 show the RMS and Kurtosis measurements for the Thermodynamic data set. The RMS measurement is not related to the Steam Wastage or Condensate Load. No clear trends are observed between the different signals and the operational conditions. This is further support for the complex multi-dimensionality of this investigation, referred to in Figure 5.5 of the Venn



Figure 8.7: Thermodynamic Trap Colour Legend

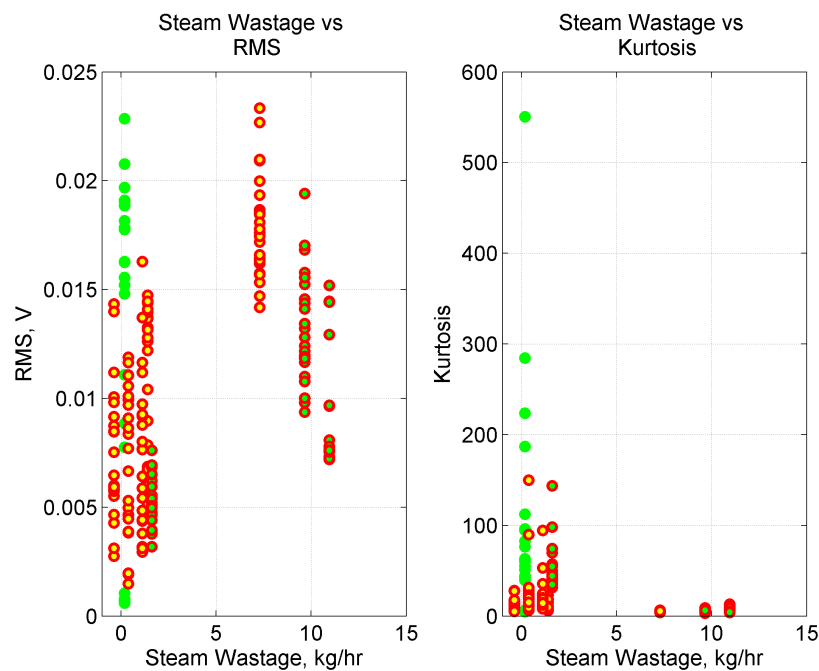


Figure 8.8: Thermodynamic Trap Time Domain RMS and Kurtosis

Diagram of the key parameters. In Figure 8.8, there is no relationship between Kurtosis and Steam Wastage. One point worth noting is that the Kurtosis of the low Steam Wastage, low pressure and low condensate load examples (green dots) is very widely spread. In addition, there does not seem to be a relationship between the Kurtosis with the Condensate Load or Pressure. This observation is supported, as the signal is non-stationary in nature and the periodicity and scales of the impulses are not consistent.

Figure 8.9 shows the relationship between Standard Deviation of the Thermodynamic Trap data set. The Standard Deviation shows the same pattern and nearly the same values as the RMS calculations. The observations from the RMS will also apply to the evaluation of the Standard Deviation. Considering the Maximum Individual Value, the values seem to be very much over-

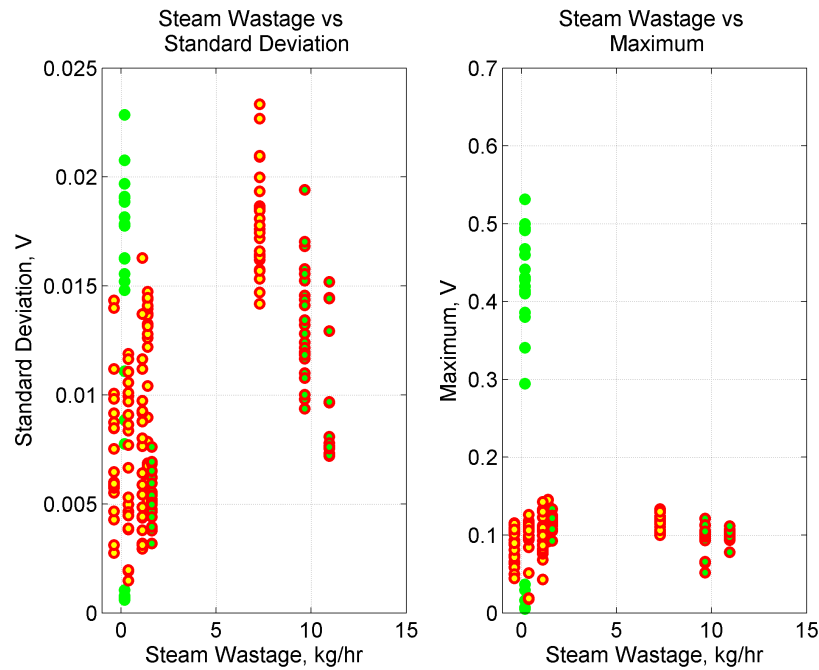


Figure 8.9: Thermodynamic Trap Time Domain Standard Deviation and Maximum

lapped and no trends are visible with regard to Steam Wastage and Condensate Load. However, the higher pressure examples seem a lot more consistent and centre around 0.1 V. Only the green dots (low Pressure, Condensate Load and Steam Wastage) seem to be very widely spread and show a high Maximum Individual Value.

Figure 8.10 shows the relationship between Variance of the acoustic emission signal and Steam Wastage for the Thermodynamic Trap. The Variance shows a similar trend to the RMS although the higher values are more widely spread. Other than the low pressure example, the Variance could be used in the examples shown to evaluate Steam Wastage at a basic level. Clearly, the process is very chaotic and due to the high separation between individual data sets, statistical methods would have to be employed to achieve a good correlation. Considering the Mean values in relation to Steam Wastage, the Mean values centred around zero are more widely spread with higher Steam Wastage. Again, this could be used as a comparative method, i.e. if the variance from the Mean is large, for an individual set of data, it is likely that the Steam Wastage is low. This makes sense as the impact of the impulses will affect the Mean value and be more dominant in the lower Steam Wastage case than the higher Steam Wastage cases.

Figure 8.11 shows the relationship between the Sum of Total Signal and the Steam Wastage Value. The plot looks similar in layout to RMS, however, there seems to be a clearer differentiation between the higher Steam Wastage and lower Steam Wastage examples. For example, a simple threshold algorithm might be applied to the sum measurement, set at about 2000. Should a centre of gravity approach be chosen, the signal could be separated into two consistent parts. Consid-

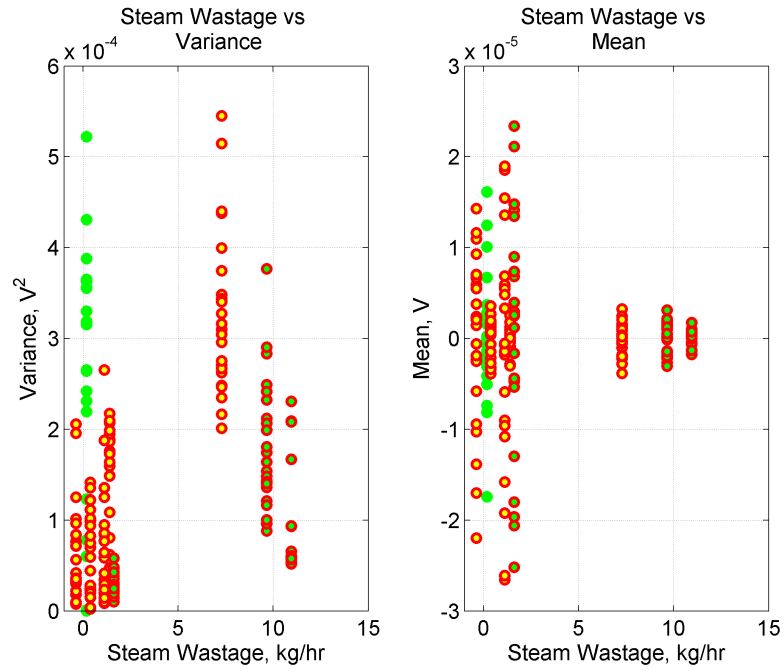


Figure 8.10: Thermodynamic Trap Time Domain Variance and Mean

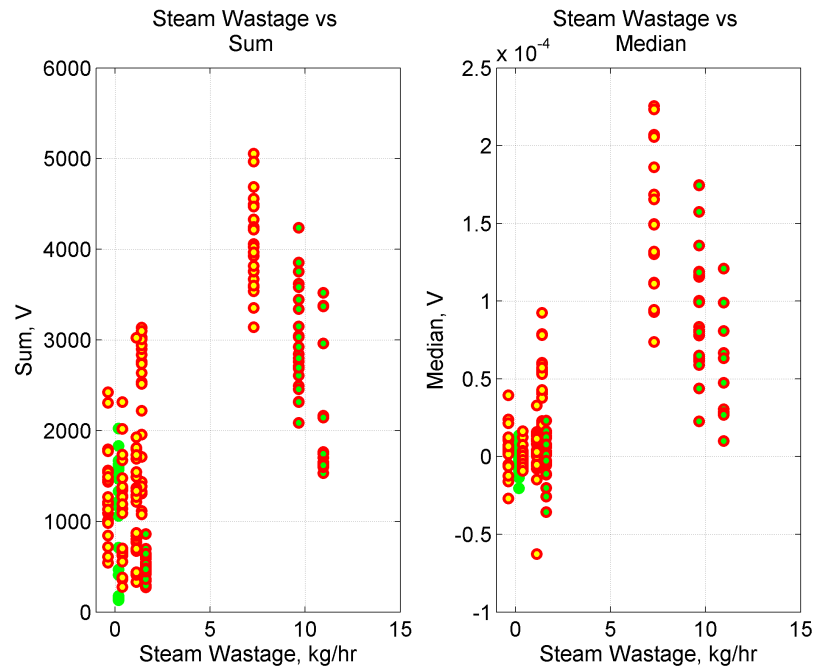


Figure 8.11: Thermodynamic Trap Time Domain Sum and Median

ering the Median, the signals are proportional (as a cluster set) with Steam Wastage. Should a centre of gravity approach be employed, and the centre of gravity of a set tends to zero, then the likelihood is high that Steam Wastage is low. Likewise, should the centre of gravity have a value of above 0.5, then Steam Wastage could be deemed significant.

**Discussion** It is clear from the signals that these methods can be used, and that the Maximum Individual Value, Sum of Total Signal and Median could be used together with simple thresholding techniques to highlight low and high Steam Wastage Values. These methods would be relatively simple to apply from computational point of view although they would additionally require statistical approaches, as an individual value would not provide a coherent assessment of the Steam Wastage Value. In the next section, frequency and time-frequency methods have been applied to the signals and the results presented.

### 8.2.3 Frequency Domain Analysis

In terms of the method in which the signal is divided into segments, the frequency analysis uses the same approach as the time domain analysis. The function to create the Fourier Transform was the standard m-file `fft.m`. The FFT was applied over 1024 points to speed up the process. Thereafter, a number of features were calculated to allow the data segments to be compared. To conclude, the energy contained within different frequency ranges of the FFT are reviewed.

Firstly, a sample of the signals are presented. As the Fourier Transform plots are all very comparable, only one plot is presented in full size and the remaining eight are shown on two four plots to a page overviews.

The Fourier Transforms were calculated using a 15 second length of the sample signal. The process by which the Fourier Transforms were calculated are as follows:

- 1) A signal was divided into 15 second long data segments.
- 2) For each of the data segments, the Fourier Transform was calculated with a length of 16,384 points (equal to  $2^{14}$ ). This allows approximately 1.2 Hz per resolution bin.
- 3) A number of features (discussed earlier in Chapter 6) were calculated for comparison.
- 4) The Fourier Transform was plotted on a graph together with the time domain representation to assist in the analysis of the Fourier Spectrum in relation to the time domain signal.

Figure 8.12 shows an example of a time domain representation of 15 seconds together with the FFT. The operational conditions for this trap are Steam Wastage of 0.19 kg/hr, Pressure of 5 barg and Condensate Load of 10 kg/hr. The time domain shows a quiet section for approximately 13.5 seconds of the signal (with one spike at about 12 seconds). The last approximate 1.5 seconds contain an opening sequence. Reviewing the FFT in the plot below in the same figure, the low energy of the FFT is clear.

Figures 8.13 to 8.16 show example plots for the 15 bar condition, covering a number of Condensate Loads and Steam Wastage Values for the Thermodynamic Trap. Figure 8.13 shows a clean signal with a very low base signal. The operational conditions of 10 kg/hr of Condensate Load and Steam Wastage Value of 1.62 kg/hr make sense. The signal is clean and very low, except for when the trap opens. When it opens, the initial spike is the opening, the prolonged noise after the opening is the steam leakage, as the noise has little modulation, i.e. the response is consistent in amplitude until it rapidly falls off, when the trap shuts. For this reason, the Fourier Transform is very low in energy and shows no distinct peaks.

Figure 8.14 shows a stronger base signal as well as a clear opening sequence, as in the previous example. The operational conditions are Condensate Load of 35 kg/hr and an associated Steam



Wastage of 1.12 kg/hr. The opening spike is less pronounced and the following noise contains more variance in amplitude, this is the Condensate Load and Steam Wastage interaction. The FFT contains more energy and shows a peak at 1.5 kHz.

Figure 8.15 shows another example, containing a lot of energy. The operational conditions are a Condensate Load of 45 kg/hr, providing a steam leakage of 0.38 kg/hr. The time domain representation for this example has no clear start. There seems to be an opening/closing event at about 8 seconds, but this is difficult to determine as the signal is very noisy. The FFT shows a low peak at 580Hz and energy well distributed throughout the Frequency Domain, which makes sense considering the time domain representation above.

Lastly, for this pressure range, Figure 8.16 shows a Condensate Load of 60 kg/hr and a Steam Wastage of -0.37 kg/hr, which can be regarded as zero steam loss. The time domain shows an opening sequence which is sharp and immediate; the flow period (from approximately 7 to 9.5 seconds) has a variable amplitude and a sharp shut-off with a very low level of signal response thereafter. The FFT reflects this, as there is a sharp response at 382 Hz and the remaining energy is distributed at a low level across the spectrum.

Figures 8.17 to 8.20 show the example data set for 20 barg with a number of Steam Wastage and Condensate Loads.

Figure 8.17 provides an example of low Condensate Load of 10 kg/hr and a high Steam Wastage of 10.96 kg/hr. Comparing the time domain response with the low pressure example, the increase in the base line is clearly visible, i.e. the trap does not seem to be closing properly. The opening and closing event is shorter and more symmetrical; the baseline seems to be modulating slightly (but not much), which could be related to high Pressure together with low Condensate Load. The FFT contains a lot of energy, especially up to 1.5 kHz. There is another peak visible at around 3 kHz, which seems to be a periodically occurring frequency when high Steam Wastage occurs, but is not consistent within all examples of high Steam Wastage.

In Figure 8.18 a slightly lower Steam Wastage (9.65 kg/hr) is presented for the same Condensate Load of 10 kg/hr. The time domain provides a similar response to the previous example as does the frequency response. However, in the FFT, the peak at around 3 kHz is slightly lower than in the previous example.

Figure 8.19 shows an example of a higher Condensate Load of 50 kg/hr and a slightly lower Steam Wastage of 7.28 kg/hr. The time domain representation is more variable and there are short periods of closing of the mechanism visible at approximately 6, 7.5 and 14 seconds. The FFT at the lower frequencies is more pronounced and rolls off at about 2.5 kHz to a low level. There is no peak at 3kHz visible although the Steam Wastage is still significant. Interestingly, the two peaks at about 500 Hz and 1.5 kHz are still visible and have nearly doubled in magnitude.

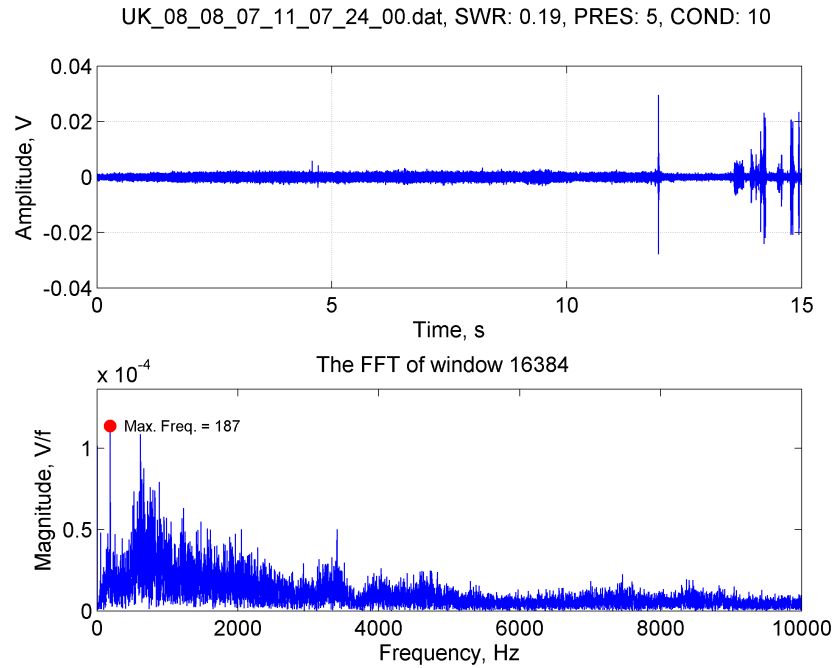


Figure 8.12: Thermodynamic Trap FFT  
5 barg CL=10 kg/hr SWV=0.19 kg/hr

Figure 8.20 shows an example of fairly low Steam Wastage of 1.39 kg/hr together with a Condensate Load of 55 kg/hr. Two opening sequences appear to have occurred within this section of the signal. Again, there seem to be short periods where the mechanism seems to close, which are located at approximately 2.5, 4, 8, 10 and 13 seconds. In this example, the FFT has one peak running up to about 800 Hz and rolls off at about 3.5 kHz. The two peaks observed in the three previous examples are no longer clearly visible.

The next section features summary plots previously seen for the time domain analysis. The parameters evaluated using the Fourier Transform as an input signal are RMS, Kurtosis, Standard Deviation, Maximum Individual Value, Variance, Mean, Sum of Total Signal and Median value, introductions to which were given in Sections 5.3.2 and 6.1.2 respectively.

Figure 8.21 shows the RMS and Kurtosis evaluated and plotted against Steam Wastage. A similar trend observed in the time domain analysis is being observed for the frequency analysis. However, in this trend, the values are so closely related that no distinction can be made for Steam Wastage based on the RMS value. As expected, Steam Wastage is inversely proportional to the Condensate Load. Interestingly, the higher RMS value is being observed by the lower pressure example. This could be caused by the high signal strength impulses and clear opening and closing sequences, which emit a lot of energy. As the FFT is also an averaging process and the impulse nature of the Thermodynamic Trap is very much transient, the impulse outliers in the time domain signal are averaged out unless they are very high in magnitude. Kurtosis evaluation in the same figure is clustered at a low level and this measurement does not provide any meaningful

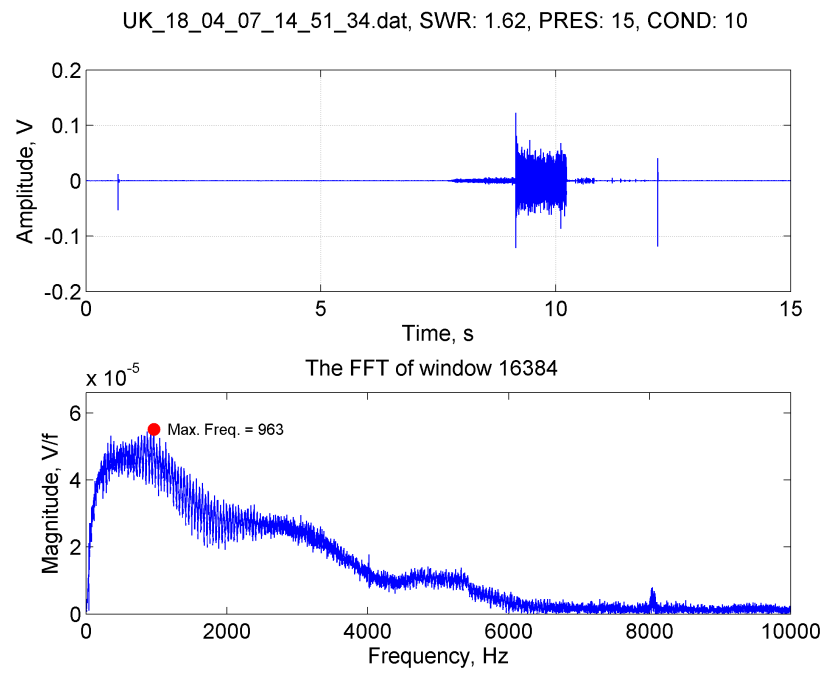


Figure 8.13: Thermodynamic Trap FFT  
15 barg CL=10 kg/hr SWV=1.62 kg/hr

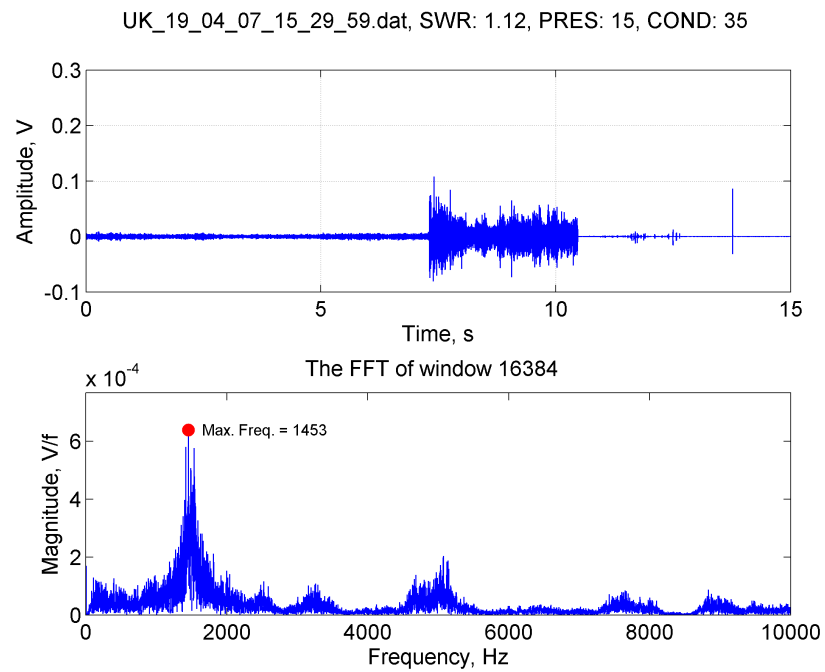


Figure 8.14: Thermodynamic Trap FFT  
15 barg CL=35 kg/hr SWV=1.12 kg/hr

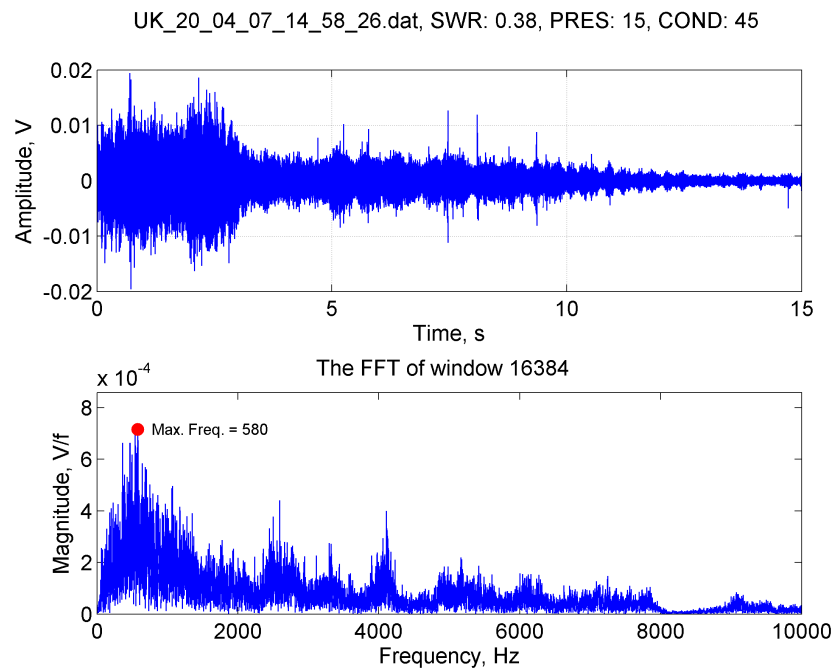


Figure 8.15: Thermodynamic Trap FFT  
15 barg CL=45 kg/hr SWV=0.38 kg/hr

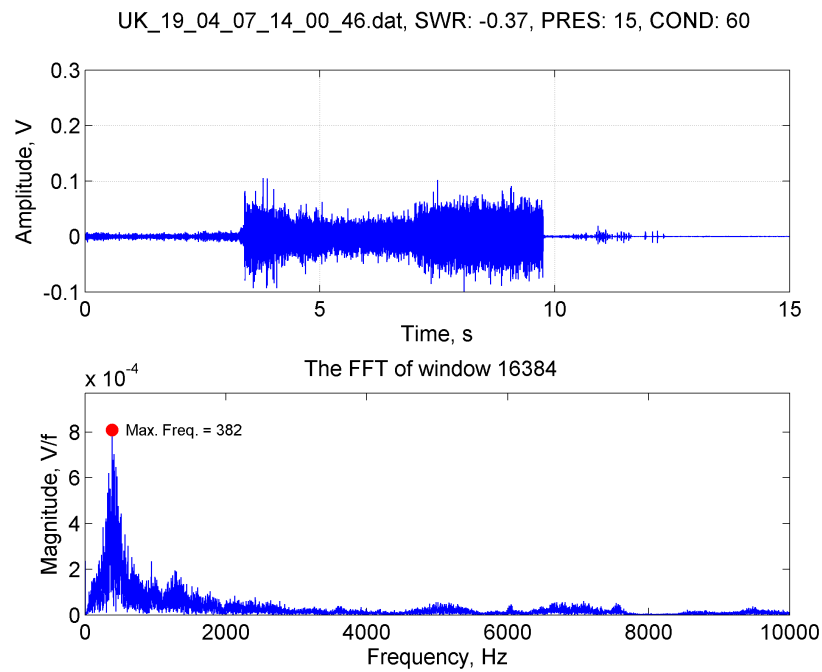


Figure 8.16: Thermodynamic Trap FFT  
15 barg CL=60 kg/hr SWV=-0.37 kg/hr

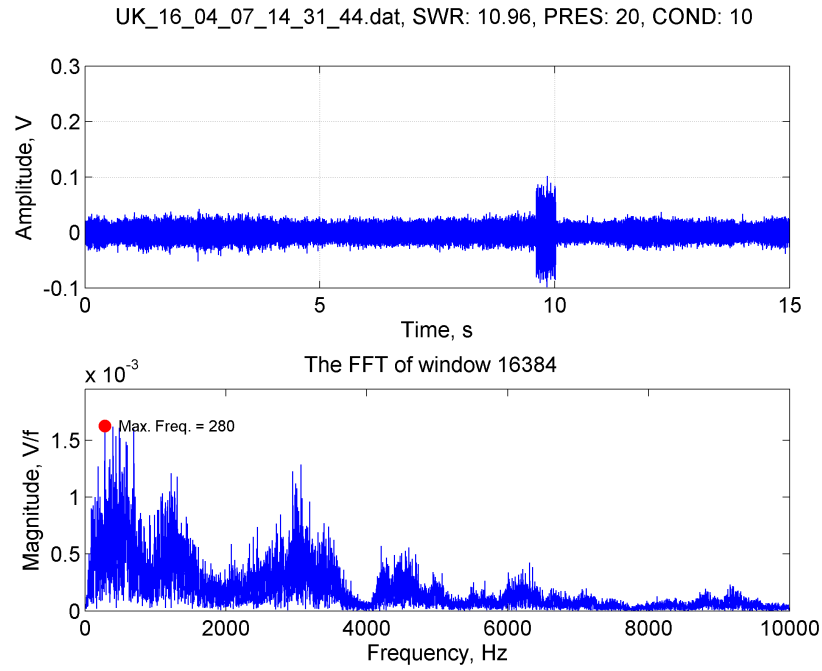


Figure 8.17: Thermodynamic Trap FFT  
20 barg CL=10 kg/hr SWV=10.96 kg/hr

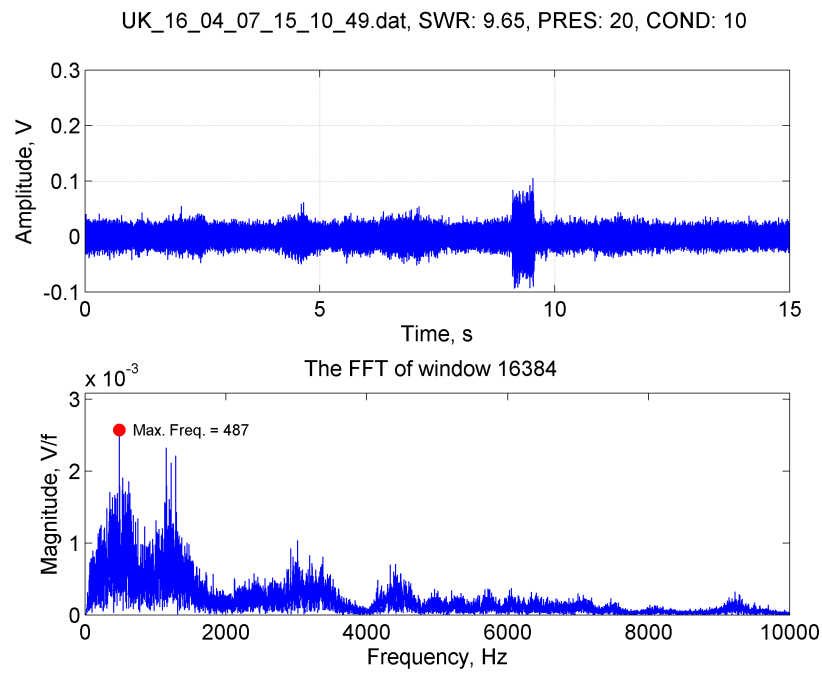


Figure 8.18: Thermodynamic Trap FFT  
20 barg CL=10 kg/hr SWV=9.65 kg/hr

information.

Figure 8.22 considers the Standard Deviation and the Maximum Individual Value. The calculations of Standard Deviation of the Fourier Transform signals show some trends similar to the RMS measurement. The Maximum Individual Values do not show any correlation with Steam

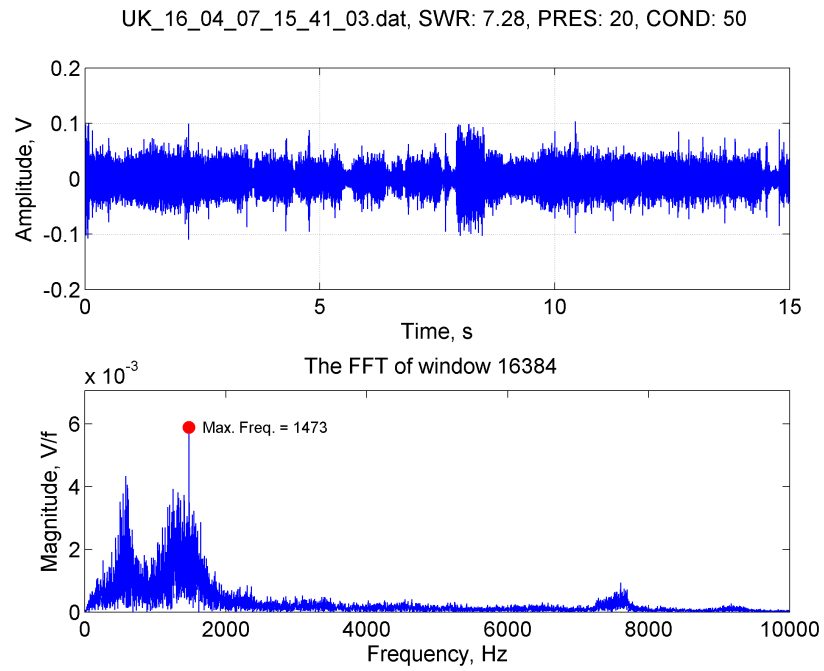


Figure 8.19: Thermodynamic Trap FFT  
20 barg CL=50 kg/hr SWV=7.38 kg/hr

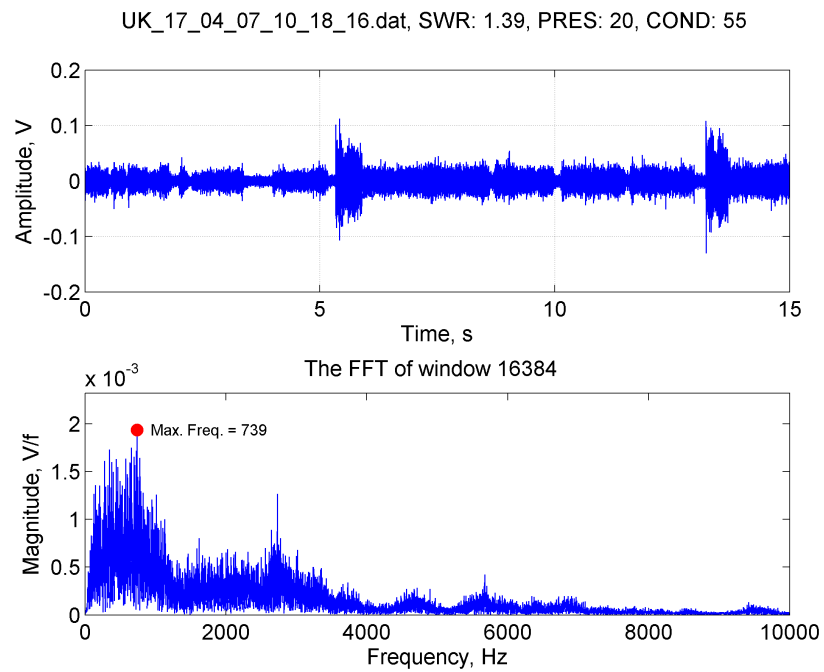


Figure 8.20: Thermodynamic Trap FFT  
20 barg CL=55 kg/hr SWV=1.39 kg/hr

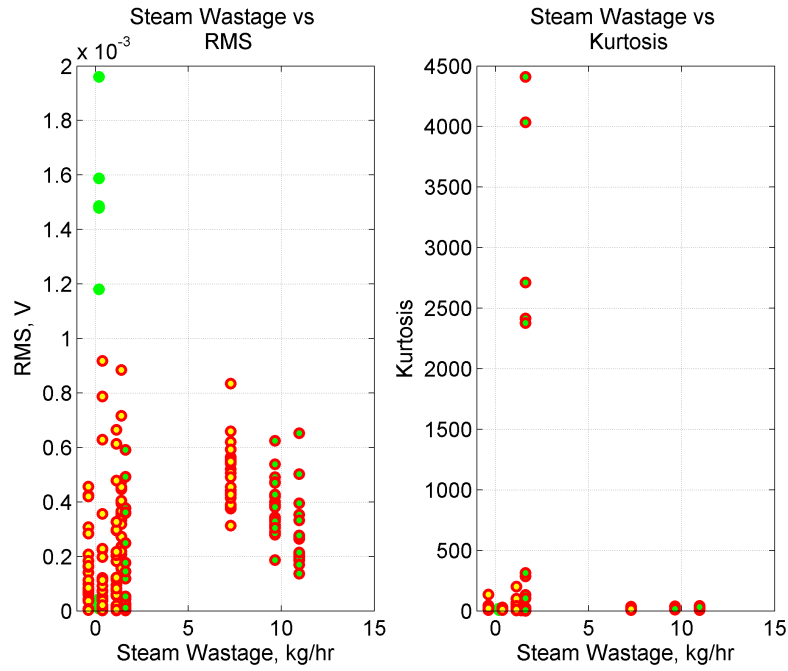


Figure 8.21: Thermodynamic Trap Frequency Domain RMS and Kurtosis

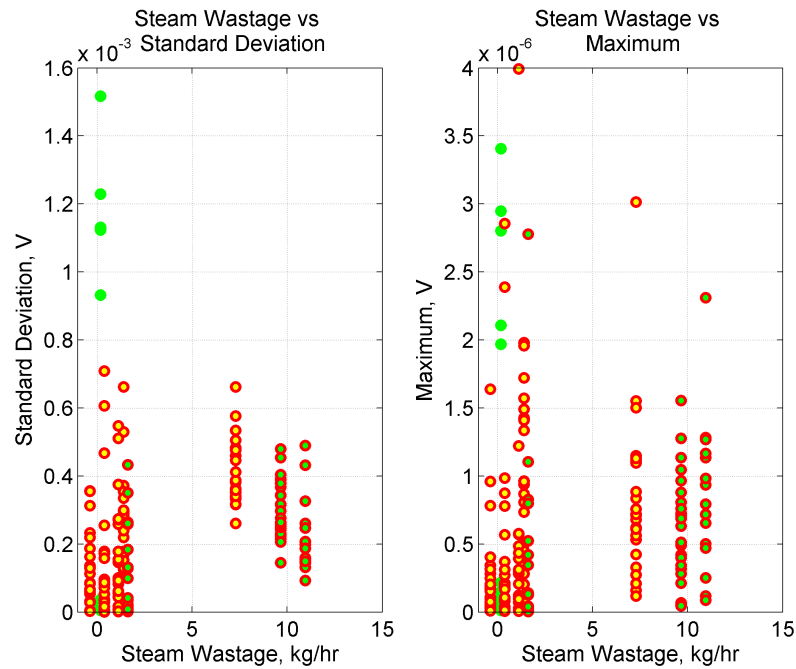


Figure 8.22: Thermodynamic Trap Frequency Domain Standard Deviation and Maximum

Wastage. Neither is useful for Steam Wastage measurement for Thermodynamic Traps.

Figure 8.23 considers the Variance and the Mean value of the Fourier Transform. The Variance calculation of the Fourier Transform of the signals segments shows the same trend as in the time domain calculation, providing no conclusive trends. Likewise, the Mean Individual Values do not show any correlation with Steam Wastage other than the one already explained as part of the

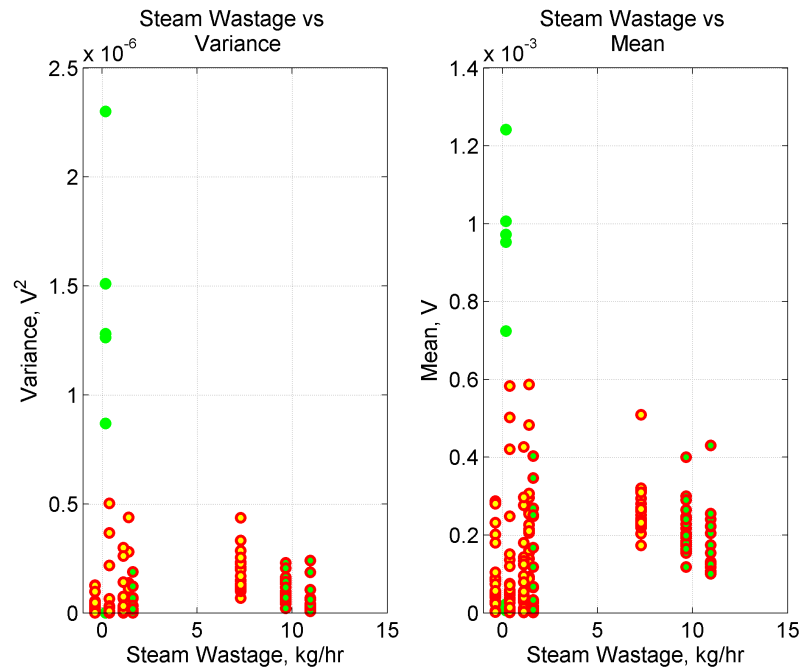


Figure 8.23: Thermodynamic Trap Frequency Domain Variance and Mean

RMS evaluation.

Likewise, Figure 8.24 considers the Sum of Total Signal and the Median Value. No specific or useful trend has been identified. However, the two plots are nearly identical in their evaluation, which makes sense as the median is the average value. The Fourier Transform provides the locations (in terms of frequency) of the total energy as component of the individual frequency bins, thus the calculation of the Median should form a similar distribution of values compared with the distribution of the total energy of the Fourier Transform.

It is clear from these four plots of parameters calculated from the Fourier Transform, that these methods cannot be used for Steam Wastage measurement. This is expected as the Thermodynamic Trap has a transient response which varies depending on the conditions presented.

The Crest Value has been applied to the Fourier Transforms resulting from the signals. The Crest Value has been calculated by dividing the Maximum Instantaneous Value of a frequency range with the mean of the values within the range. Three frequency ranges were selected, namely: 1 Hz to 1 kHz, 1kHz to 2 kHz, 2 kHz to 3 kHz, 3 kHz to 4 kHz, 4 kHz to 5 kHz and 5 kHz to 6 kHz. Figures 8.25 and 8.26 show these plotted. There is no clear correlation between Crest Value and Steam Wastage Value. Another feature of this plot is that the Crest Value across frequency ranges as ratios remain the same. In other words, there is no relative change when comparing the Crest Value for operational conditions in terms of the frequency range. However, the overall values seem to rise slightly in the second two bins compared with the first. In any case, this does not provide any advantages in determining Steam Wastage.



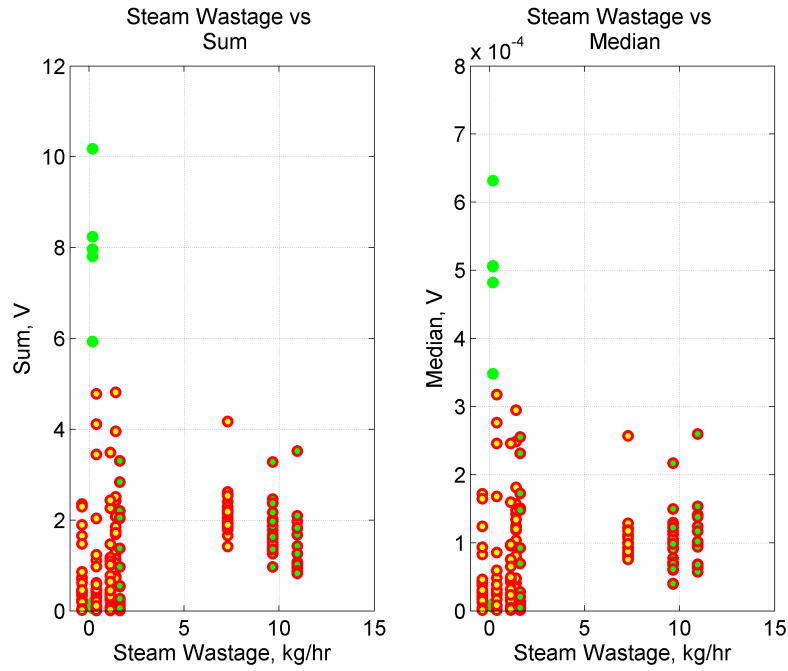


Figure 8.24: Thermodynamic Trap Frequency Domain Sum and Median

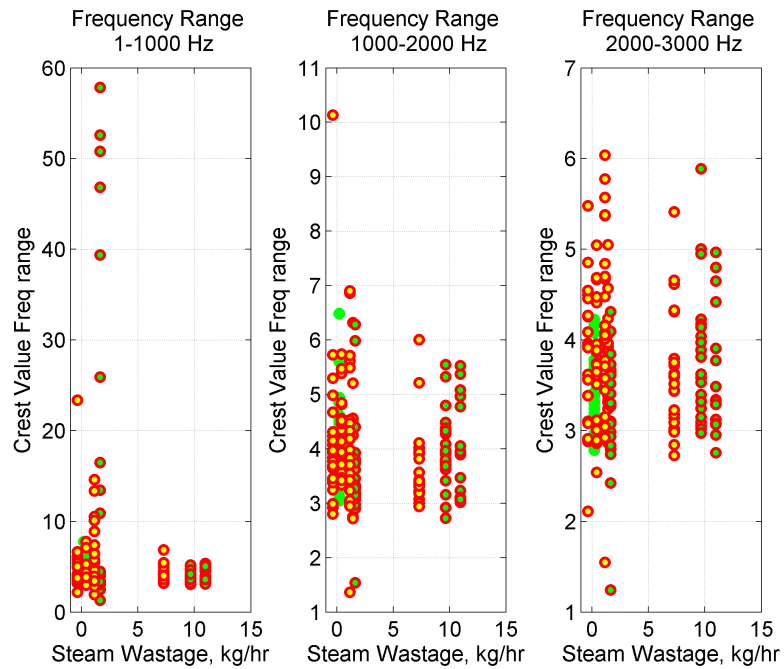


Figure 8.25: Thermodynamic Trap Frequency Domain Frequency Bins Part 1

**Discussion** As mentioned previously, the Fourier Spectrum considers the complete 15 seconds and the representative frequencies within this signal segment. From the time domain and respective frequency analysis, it can be seen that there are changes to the frequency content within the 15 second recording. For this reason, time-frequency analysis is presented in the next section to allow the review of the contributing components to be identified.

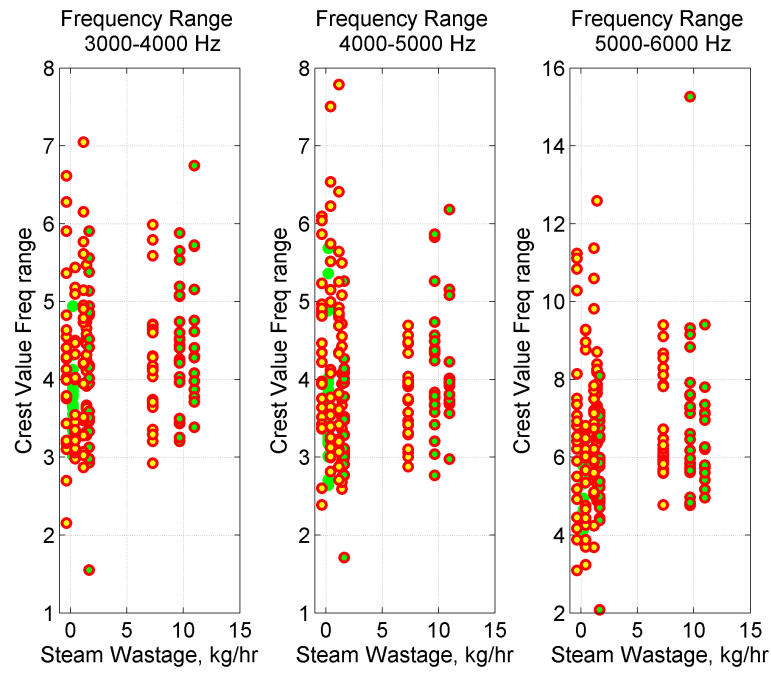


Figure 8.26: Thermodynamic Trap Frequency Domain Frequency Bins Part 2

As the FFT is an average representation of the frequency content across the data sample, it is highly affected by any dynamic or transient content. When the signal is stationary, the FFT will be comparable and consistent. As the mechanism of the Thermodynamic Trap introduces transient events, the FFT will not show these unless they are regular and consistent. Furthermore, the two-phase flow introduces transient effects as the flow regime changes dynamically. For this reason, it is advantageous to combine both temporal and transient analysis, which is shown in the next section through the application of the Short-Time Fourier Transform.

### 8.2.4 Time-Frequency Analysis

The time-frequency analysis approach has been explained in Chapter 2. This approach allows both the frequency and time domain components to be identified. The steps used for this application are as follows:

- 1) A signal was segmented into 15 second long data segments.
- 2) For each of the data segments, the Short-Time Fourier Transform was calculated with a length of 2048 points (equal to  $2^{11}$ ) using a Hamming window. This allows for approximately 9.88 Hz per resolution bin. The reason for the decrease in frequency bin resolution (compared to the frequency analysis) is that this method is computationally more intensive. Additionally, the time and frequency resolutions are inversely proportional. In other words, if the time domain resolution is increased, the frequency resolution will be decreased. The window size chosen allows for an acceptable frequency and time resolution.
- 3) A number of features (discussed earlier in Chapter 6) were calculated.
- 4) The time-frequency map and time domain plotted on a graph for detailed analysis.

Figure 8.27 shows an example of a time domain representation of 15 seconds together with the STFT. The operational conditions for this trap are Steam Wastage of 0.19 kg/hr, Pressure of 5 barg and Condensate Load of 10 kg/hr. The time domain shows a quiet section for approximately 13.5 seconds of the signal (with one spike at about 12 seconds). The last approximate 1.5 seconds contain an opening sequence. Reviewing the STFT in the plot below in the same figure, the low energy of the signal is clearly shown. The higher energy at the end of the time domain signal is also shown, with high intensity points running from the low kHz up to about 3.5 kHz. The STFT clearly shows the transient dynamic of the signal.

Figures 8.28 to 8.31 show example plots for the 15 barg condition, covering a number of Condensate Loads and Steam Wastage Values for the Thermodynamic Trap. Figure 8.28 shows a very clean signal with a very low base signal. The operational conditions of 10 kg/hr of Condensate Load and Steam Wastage Value of 1.62 kg/hr make sense. The signal is clean and very low, except for when the trap opens. When it opens the initial spike is the opening, the prolonged noise after the opening is the steam leakage, as the noise has little modulation, i.e. the response is consistent in amplitude until it rapidly falls off, when the trap shuts. The STFT shows clearly when the mechanism opens as the energy clearly increases from a deep low blue to a turquoise green level. Thereafter, the opening is clearly shown by a vertical region, shown by a high orange level from low frequency up to just below 4 kHz and above that a green level up to 10 kHz. After the opening, the smaller blips show between 10 seconds to about 11 seconds, which looks similar to

the opening sequence. However, the closing sequence has less of a consistent frequency content shown by a speckled frequency map. After the closing sequence the signal returns to a blue low level intensity.

Figure 8.29 shows a stronger base signal as well as a clear opening sequence, much as the previous example. The operational conditions are a Condensate Load of 35 kg/hr and an associated Steam Wastage of 1.12 kg/hr. The opening spike is less pronounced and the following noise contains more variance in amplitude, this is the Condensate Load and Steam Wastage interaction. The STFT maps the frequency domain exactly. In comparison to the previous example, the baseline is slightly higher in amplitude, which is reflected in the green and turquoise map up to about 7.5 seconds. The opening sequence can clearly be identified by the orange and green vertical block. Additionally, the slight decrease in amplitude is also visualised by the reduced orange section as the time progresses. When the trap closes, the amplitude is less than it was at the beginning of the signal, which is shown by the deep blue and turquoise frequency map. Even the instantaneous peak at about 14 seconds is registered in the frequency map by the vertical bar.

Figure 8.30 shows another example, containing a lot of energy. The operational conditions are a Condensate Load of 45 kg/hr, providing a Steam Wastage of 0.38 kg/hr. The time domain representation for this example has no clear start. There seems to be an opening /closing event at about 8 seconds, but this is difficult to determine as the signal is very noisy. The STFT shows clearly that there is an opening just after 8 seconds, as the clear vertical energy region is seen, which has been observed in the previous examples. The baseline is significantly greater in amplitude, which is reflected in the orange map of the STFT, which covers up to about 2 kHz. The low peak of 580 Hz seen in the FFT is not visible in this mapping although the dynamics and transient changes are clearly displayed.

Lastly, for this pressure range, Figure 8.31 shows a Condensate Load of 60 kg/hr and a Steam Wastage of -0.37 kg/hr, which can be regarded as zero steam loss. The time domain shows an opening sequence which is sharp and immediate, the flow period (from approximately 7 to 9.5 seconds) has a variable amplitude and a sharp shut-off, with a very low level signal response thereafter. This frequency map shows the clear opening sequence as well as the slight reduction in the middle of the opening sequence, which is reflected by the reduction in the orange content of the frequency map between four and seven seconds. The lower baseline after the opening is also shown by a deeper blue frequency map, as well as the residual acoustic emission in turquoise between 10 to 12 seconds.

Figures 8.32 to 8.35 show example data sets for 20barg with a number of Steam Wastage and Condensate Loads.

Figure 8.32 provides an example of a low Condensate Load of 10kg/hr and a high Steam Wastage of 10.96 kg/hr. Comparing the time domain response with the low pressure example, the increase in the baseline is clearly visible, i.e. the trap does not seem to be closing properly. The opening and closing event is shorter and more symmetrical. The baseline seems to be modulating slightly (but not much) which could be related to high Pressure together with low Condensate Load.

The STFT contains a lot more energy than the previous examples at lower pressure. The orange section has now increased in frequency to about 5kHz. The opening is clearly distinguished at just before 10 seconds. The baseline remains high, which makes sense as Steam Wastage is high as well. The slightly modulating nature of the baseband is reflected in the time-frequency map by speckled changes in the orange green band in the frequency map.

In Figure 8.33, slightly lower Steam Wastage (9.65 kg/hr) is presented for the same Condensate Load of 10 kg/hr. The time domain provides a similar response to the previous example as does the frequency response. The STFT is similar to the first example at this pressure. Although there are some differences. The time domain changes at just after 2 and 4 seconds. Additionally, there is higher intensity signal content between 4 to 6 kHz. Additionally, the opening/closing and the baseband are clearly visible in the same way as in the previous example.

Figure 8.34 shows an example of a higher Condensate Load of 50 kg/hr and a slightly lower Steam Wastage of 7.28 kg/hr. The time domain representation is more variable and there are short periods of closing of the mechanism visible at approximately 6, 7.5 and 14 seconds. The STFT shows a very high intensity below 2kHz as well as a clear opening and closing sequence. Above 2 kHz, the signal is fairly flat. There is a horizontal band at between 7.5 kHz to 8 kHz. The low level signal seen at approximately 2.5, 4, 8, 10 and 13 seconds are also reflected in the orange band below 2kHz within the frequency map.

Figure 8.35 shows an example of fairly low Steam Wastage at about 1.39 kg/hr together with a Condensate Load of 55 kg/hr. Two opening sequences appear to have occurred within this section of the signal. The STFT shows two clear opening and closing events at just before 6 seconds and 14 seconds. The short periods observed in the time domain where the mechanism seems to close, are located at approximately 2.5, 4, 8, 10 and 13 seconds and are also clearly visible in the frequency map. This signal seems to have the lowest energy in the baseband, which makes sense as this has the lowest Steam Wastage Value of the four signals reviewed.

The next section features summary plots previously seen for the time domain analysis. The parameters evaluated using the Fourier Transform as an input signal are RMS, Kurtosis, Standard Deviation, Maximum Individual Value, Variance, Mean, Sum of Total Signal and Median value, introductions to which were given in Sections 5.3.2 and 6.1.2 respectively.

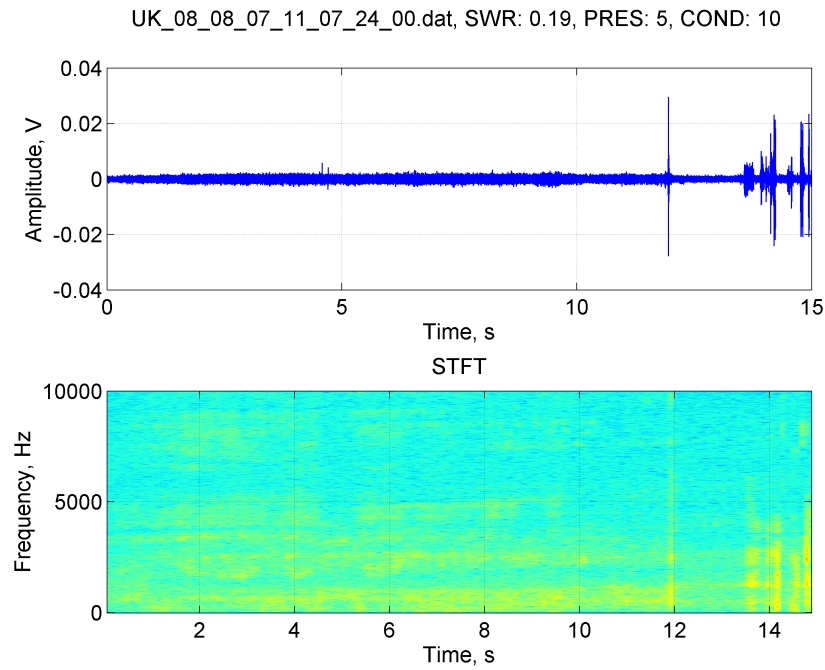


Figure 8.27: Thermodynamic Trap STFT 5 barg CL=10 kg/hr SWV=0.19 kg/hr

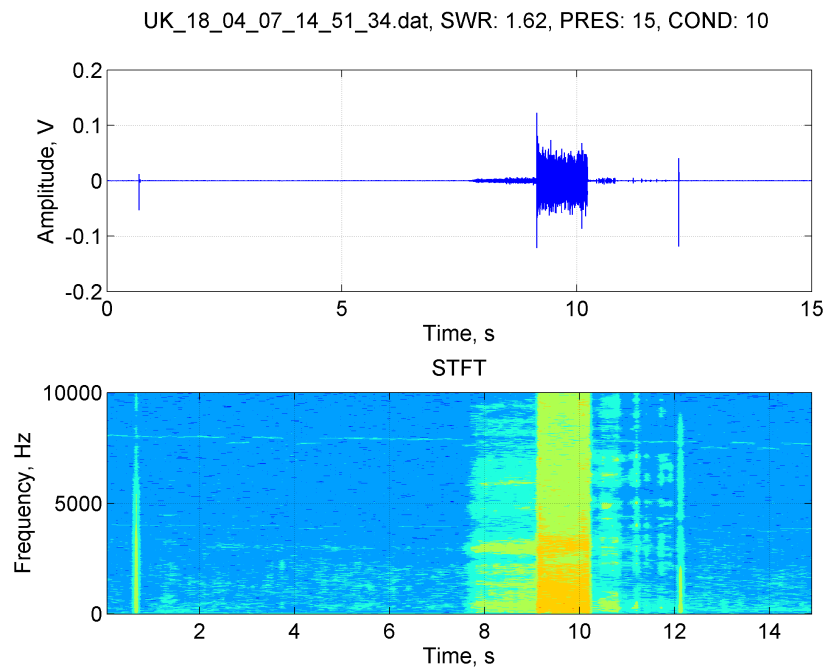


Figure 8.28: Thermodynamic Trap STFT  
15 barg CL=10 kg/hr SWV=1.62 kg/hr

Figure 8.36 shows the RMS and Kurtosis evaluated and plotted against Steam Wastage. Steam Wastage is inversely proportional to Condensate Load, as expected. The same trend is being seen as compared to the frequency domain signal analysis. Considering the Kurtosis evaluation in the same figure, the values are not related and do not provide any trends, which was also found by the time domain analysis. The reason why no trend trend can be identified within these plots

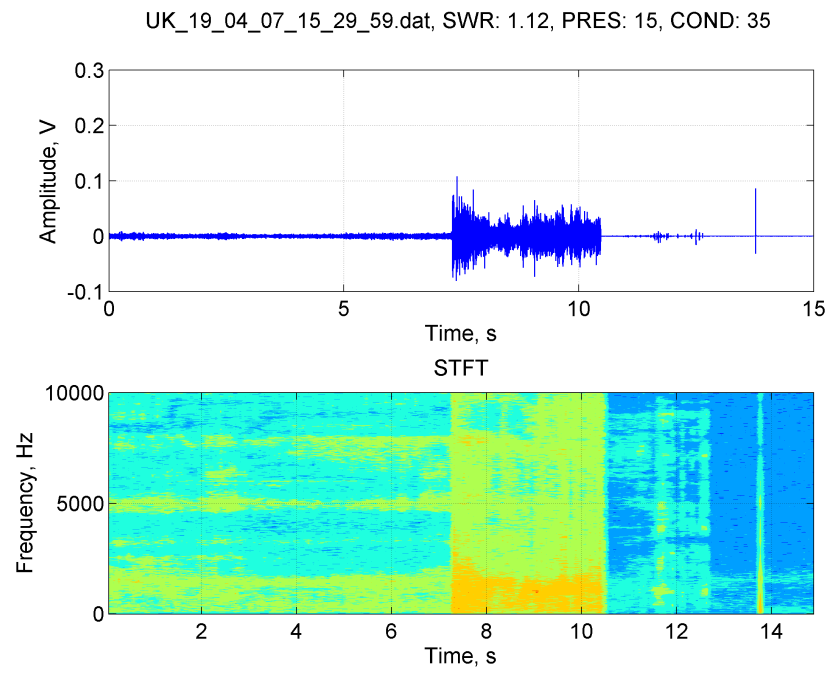


Figure 8.29: Thermodynamic Trap STFT  
15 barg CL=35 kg/hr SWV=1.12 kg/hr

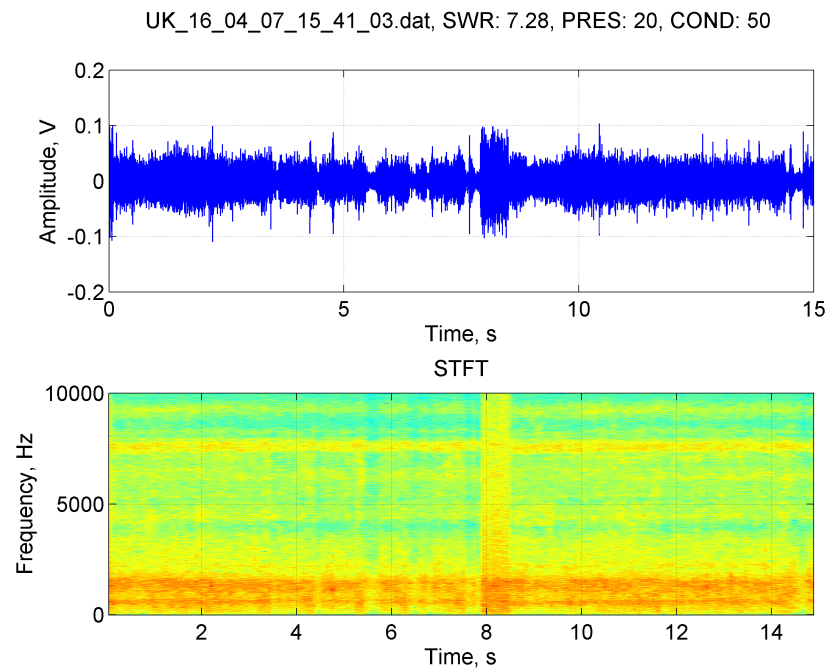


Figure 8.30: Thermodynamic Trap STFT  
15 barg CL=45 kg/hr SWV=7.38 kg/hr

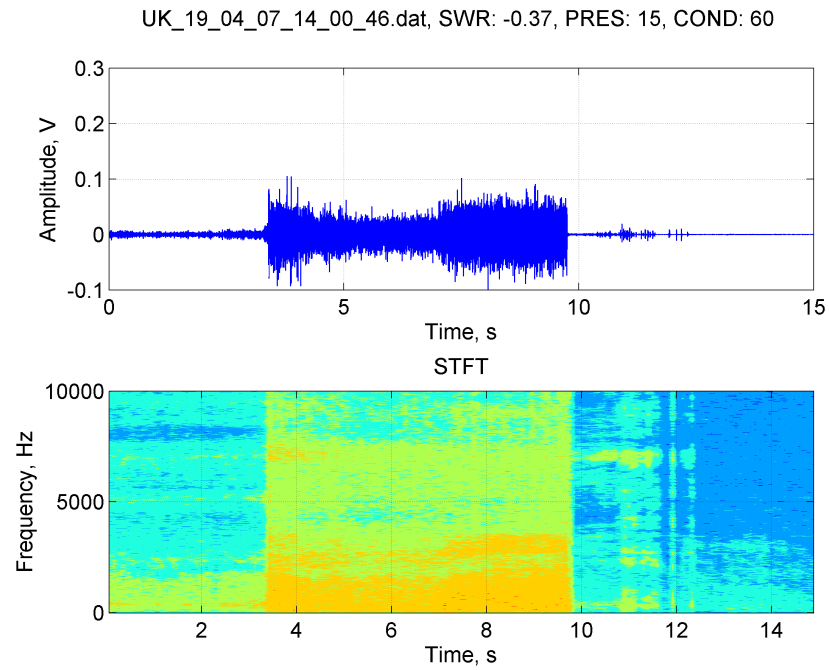


Figure 8.31: Thermodynamic Trap STFT  
15 barg CL=60 kg/hr SWV=-0.37 kg/hr

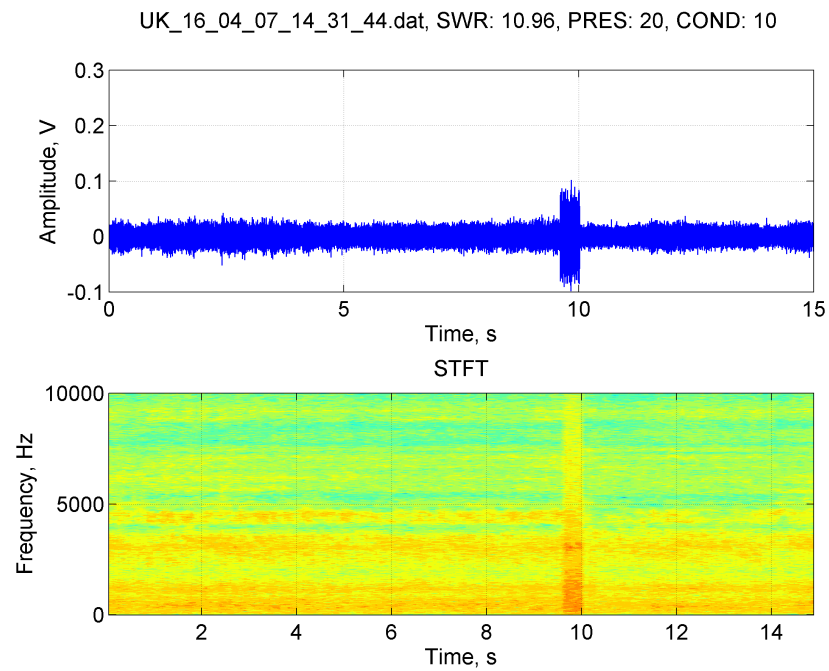


Figure 8.32: Thermodynamic Trap STFT  
20 barg CL=10 kg/hr SWV=10.96 kg/hr

is that the mechanism affects the response of the trap and the transient effects are not captured through this method, but averaged out and thus no trend is visible.

Similarly, Figure 8.37 considers the Standard Deviation and the Maximum Individual Value. The Standard Deviation of the measurements for the STFT of the signals shows the same trend



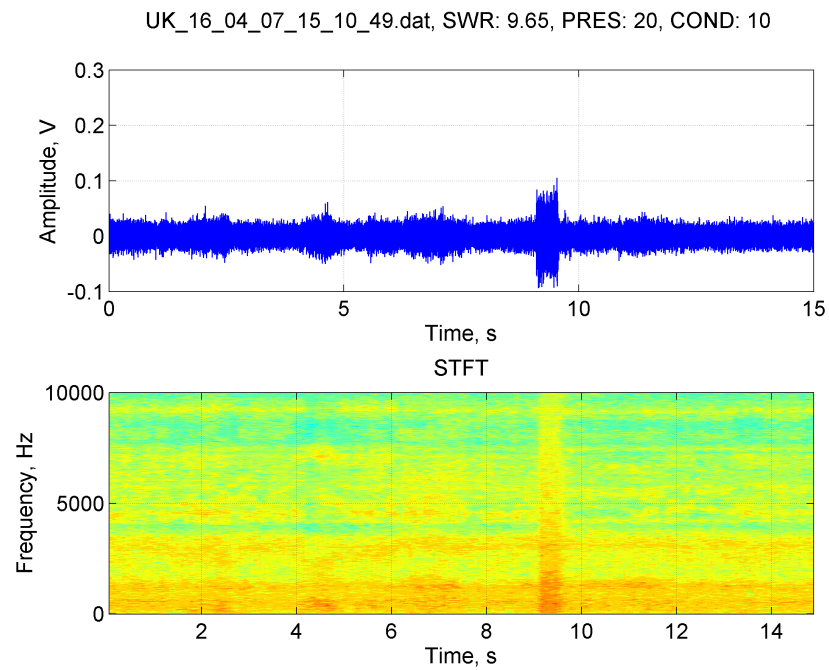


Figure 8.33: Thermodynamic Trap STFT  
20 barg CL=10 kg/hr SWV=9.65 kg/hr

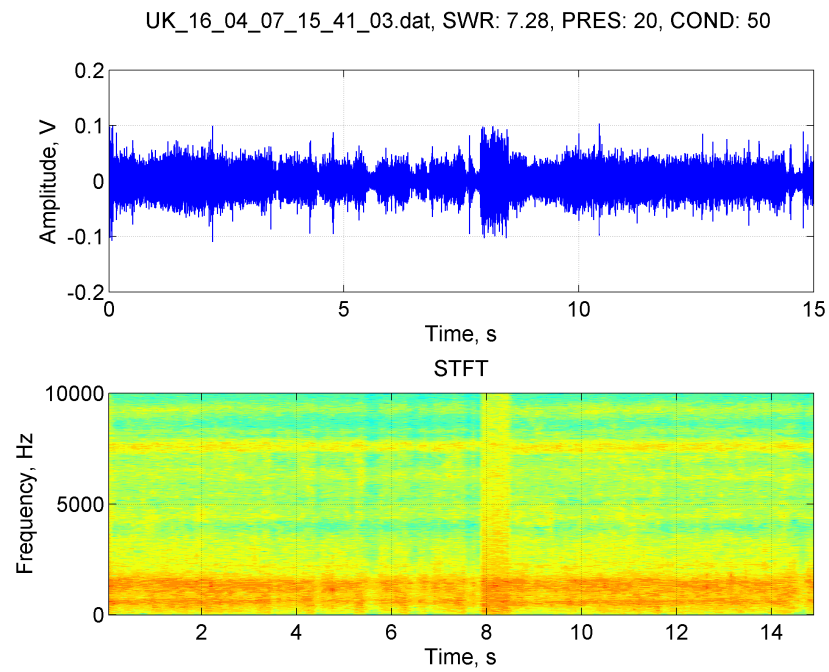


Figure 8.34: Thermodynamic Trap STFT  
20 barg CL=50 kg/hr SWV=7.28 kg/hr

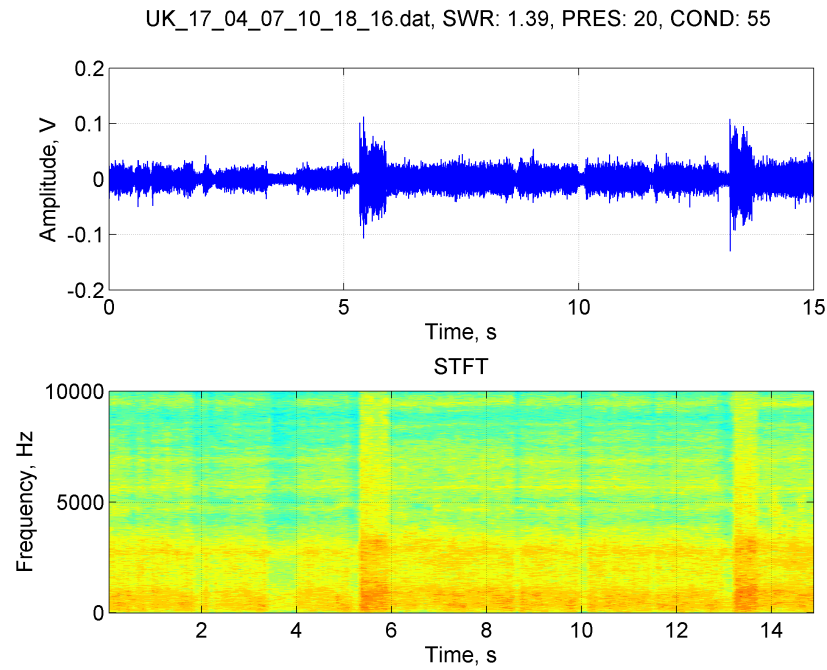


Figure 8.35: Thermodynamic Trap STFT  
20 barg CL=55 kg/hr SWV=1.39 kg/hr

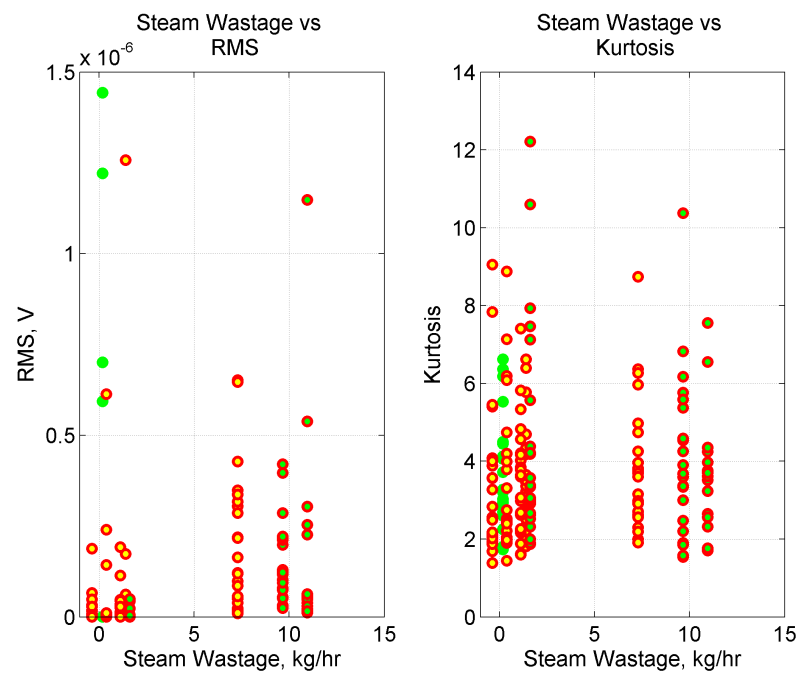


Figure 8.36: Thermodynamic Trap STFT RMS and Kurtosis

as the previous evaluations for the frequency domain, with no conclusive trends. Likewise, the Maximum Individual Values does not show any correlation with Steam Wastage.

Figure 8.38 considers the Variance and the Mean value of the STFT. The Variance calculation of the STFT of the signal segments show a number of outliers. However, these do not affect the overall trend, which has been discovered in the the previous frequency evaluation, and thus

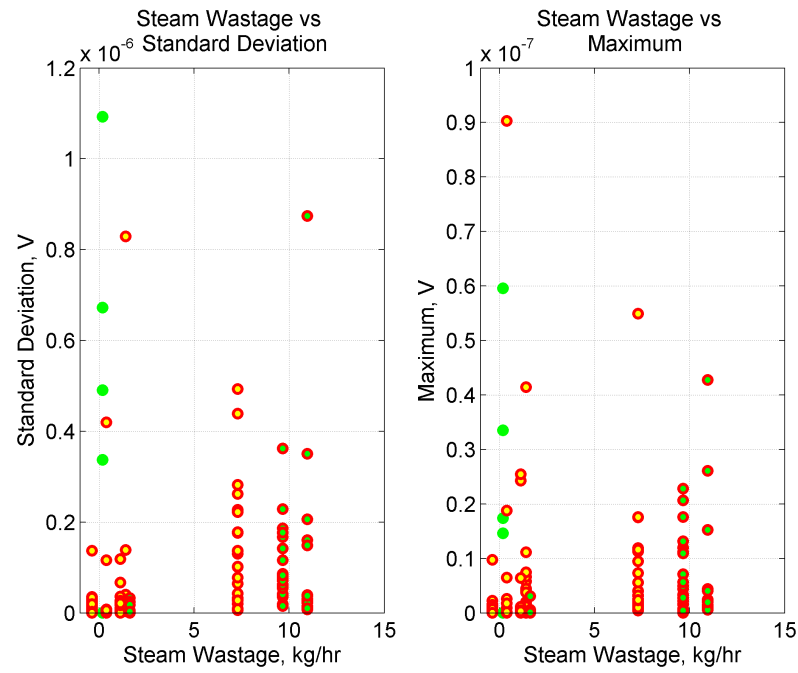


Figure 8.37: Thermodynamic Trap STFT Standard Deviation and Maximum

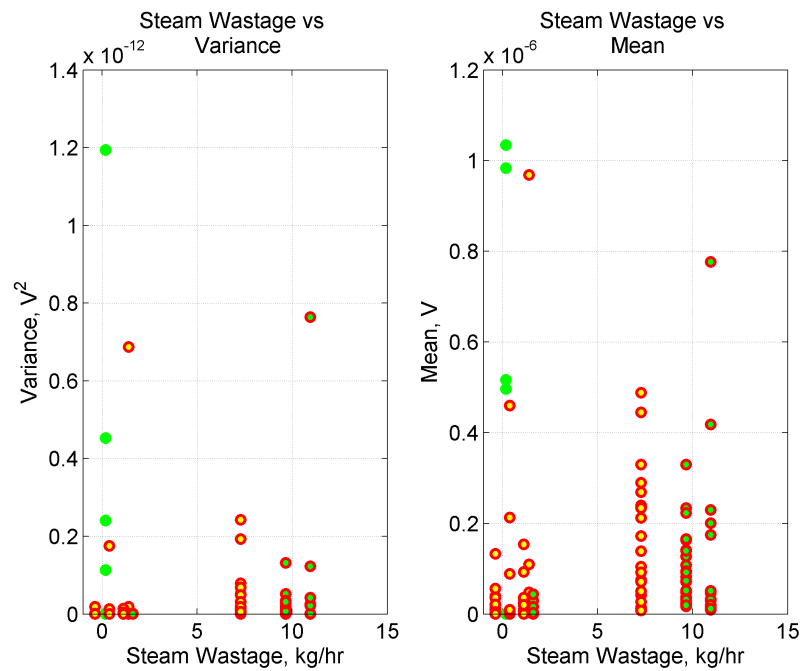


Figure 8.38: Thermodynamic Trap STFT Variance and Mean

no conclusive outcomes have been found. Likewise, the Mean Individual Values do not yield any correlation with the Steam Wastage other than the one already explained as part of the RMS evaluation.

Figure 8.39 considers the sum of the Total Signal and the Median Value. No specific or useful trend has been identified.

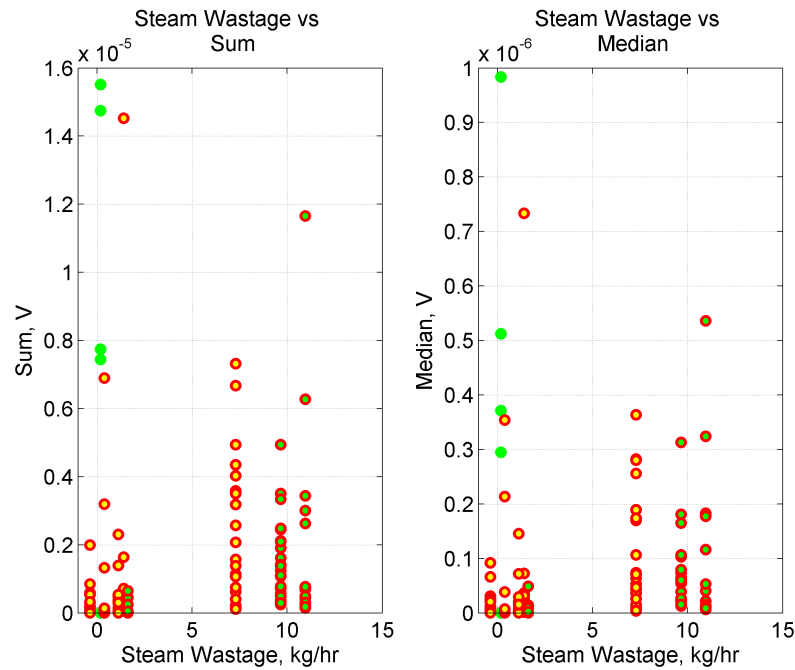


Figure 8.39: Thermodynamic Trap STFT Sum and Median

It is clear from these four plots of parameters calculated from the STFT that these methods cannot be used, as the features are averaged and thus reduces the advantages of having both the time and frequency content. For this reason, this approach cannot be used for Steam Wastage measurement.

The Crest Value has been applied to the STFT in Figures 8.40 and 8.41. The Crest Value has been calculated by dividing the Maximum Individual Value of a frequency range with the mean of the values within the range. Three frequency ranges were selected, namely: 1 Hz to 1 kHz, 1 kHz to 2 kHz, 2 kHz to 3 kHz, 3 kHz to 4 kHz, 4 kHz to 5 kHz and 5 kHz to 6 kHz. Figures 8.40 and 8.41 show these, but there is no clear correlation between Crest Value and Steam Wastage Value. Another feature of this plot is that the Crest Value across frequency ranges as ratios remain the same. In other words, there is no relative change when comparing the Crest Value for the operational conditions in terms of the frequency range. This feature is averaged and thus the transient features are not clearly highlighted.

**Discussion** As mentioned previously, the STFT considers the complete 15 second sample and the representative frequencies within this signal segment. From the time domain and respective STFT analysis, it can be seen that changes to the time domain are reflected in the STFT content within the 15 second recording. It has been shown that the time-frequency analysis is the best method to capture both behaviours highlighting the contributing components. However, extracting averaged features from the STFT does not take advantage of the additional dimensionality of

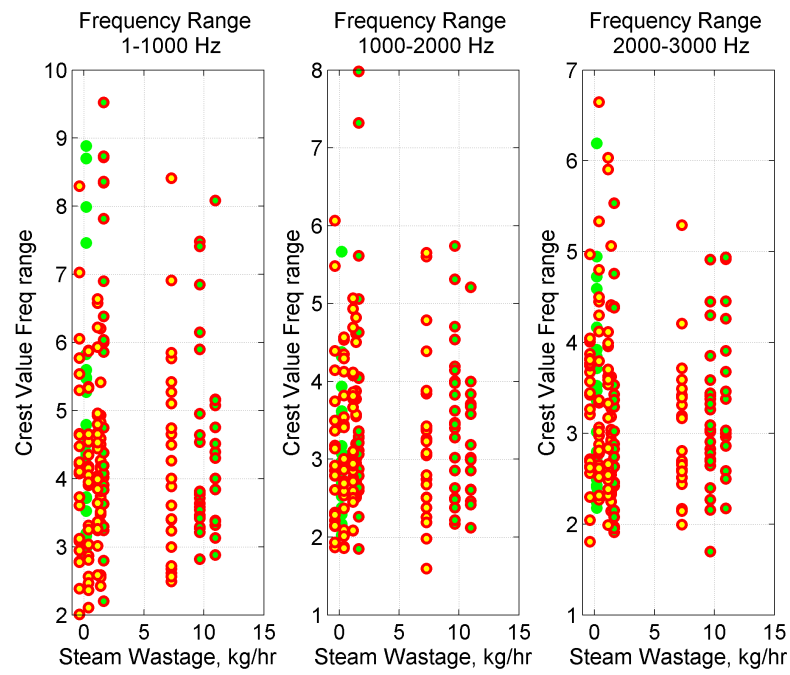


Figure 8.40: Thermodynamic Trap STFT Frequency Bins Part1

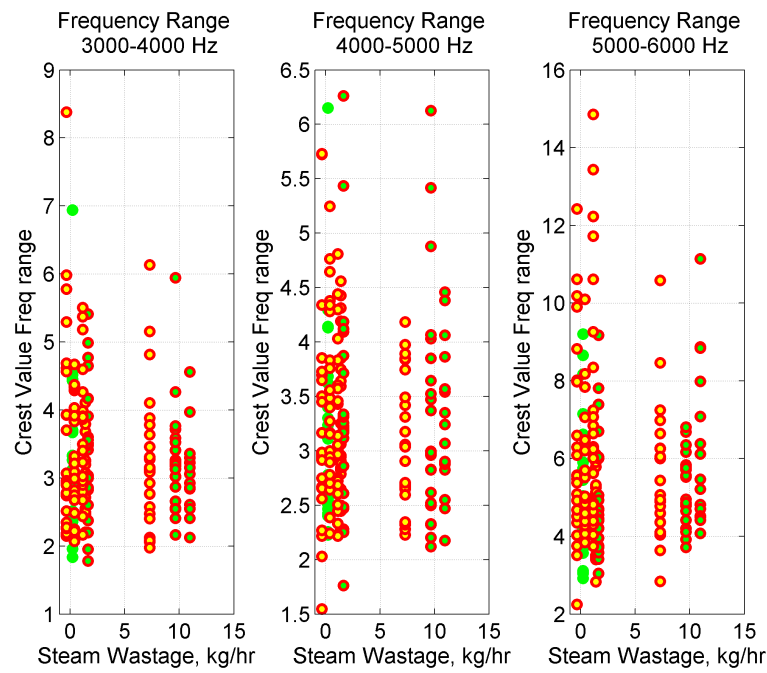


Figure 8.41: Thermodynamic Trap STFT Frequency Bins Part 2

the STFT.

### 8.3 Summary

This chapter has investigated the Thermodynamic Trap. The following are the findings and observations that have been made:

- Time-domain acoustic emission of the Thermodynamic Trap has been presented and the clear modulating nature of the trap shown.
- Time-domain processing has been successful, as the signal observed clear modulation by the trap operation (opening / closing sequence).
- Frequency-domain processing has been highly inconclusive, largely due to the mechanism. The example data sets still show a high degree of variability.
- Much like the time-domain processing, the time-frequency method has been shown to be a suitable approach, as this highlights the operational nature of the trap by simultaneously evaluating the time and frequency domain. It must be noted that this is the most computationally intensive signal processing method being considered.
- No specific inherent noise characteristic related to Steam Wastage has been discovered. Overall, it has been discovered that RMS and Kurtosis values resulting from acoustic emission data cannot conclusively be used to determine Pressure, Condensate Load or Steam Wastage Values in Steam Traps. Other statistical methods, such as the Standard Deviation and Variance, also have been unsuccessful in determining a trend or estimating Steam Wastage.
- It has not been possible to link the trap behaviour with two-phase flow regimes.
- The Impulse Steam Trap type can be classified using time domain features to detect the overall cycling rate, as there is a clear marker of the opening / closing sequence. For this, a simple algorithm counting the number of open sequences can be designed. It is clear that shortening the analysis time frame, i.e. 15 seconds and below will result in increased uncertainty. Steam Traps such as the Thermodynamic Steam Trap cycle is typically less than 10 times per minute, which is an average of 2.5 times in 10 seconds. Any shorter time period will result in an inaccurate prediction of premature failure. In this case, a statistical time domain approach based would be best suited. A time-frequency approach may also be advantageous. However, it is computationally significantly more expensive.

*This chapter applied digital signal processing techniques to Thermodynamic Traps. The next chapter provides a summary of key results for this investigation.*

## Chapter 9

# Key Results Summary

*This penultimate chapter summarises the key findings and discusses potential sources of error.*

### 9.1 Steam Trap Test Rig

- 1) A test rig was successfully built to establish Steam Wastage of operational traps.
- 2) Overall, the Steam Wastage Rig has performed well, but the repeatability of Steam Wastage measurement of Steam Traps has been difficult to undertake. It has become apparent that there is an issue with time scale. The Steam Trap and flow dynamics change every few seconds. Steam Wastage is only evaluated over the complete test run. The result of which is an acoustic trace which changes rapidly, especially if a trap being tested includes a mechanism.
- 3) The importance of maintaining constant conditions throughout the experiment is of high importance, but is difficult to achieve with a complex responding feedback process, as is the case in Steam Traps, especially those with a mechanism.

### 9.2 Heterodyne Circuit

- 1) The signal resulting from the heterodyne is not narrowband but a representation of the broadband response, with a bias to the higher frequencies around 40kHz.
- 2) The heterodyne circuit does frequency shifting of the higher frequencies to the low kHz bandwidth.
- 3) The time-frequency analysis of the input frequency sweep response has shown a complex frequency shifting pattern.

## 9.3 Common Features in the Signal Analysis

It has been shown that each of the three trap categories have different responses. These can be highlighted using time, frequency and time-frequency approaches. For each of the trap categories the following summarises common features.

### 9.3.1 Orifice Traps Common Features

- 1) Signified by a signal which is largely stationary with little or no modulation.
- 2) Frequency or time-frequency signal analysis is the best approach.
- 3) No specific algorithm has been identified.

### 9.3.2 Non-Impulsive Traps Common Features

- 1) Signified by largely stationary signal with some modulation.
- 2) Frequency or time-frequency signal analysis is the best approach.
- 3) No specific algorithm has been identified.

### 9.3.3 Impulsive Traps Common Features

- 1) Signified by a highly modulated signal.
- 2) The time domain is the best approach for processing, as it has low overhead and provides sufficient data.
- 3) No specific algorithm has been identified.

## 9.4 Sources of Error

It has been shown that the determination of Steam Wastage from a Steam Trap through the analysis of the acoustic emission is difficult. The potential sources of error are highlighted in the list below:

- Steam Wastage Measurement - The measurement of Steam Wastage according to the standards is a time average result, but the two-phase flow, especially when a trap mechanism interferes is a dynamic problem. The result of which is that Steam Wastage cannot be correlated in real terms at the same rate that Steam Wastage is determined. Steam Wastage is time averaged, whereas acoustic emission is measured instantaneously.



- Multiple Parameters - As has been shown in Chapter 5, there are a number of parameters that affect Steam Wastage, including Temperature, Pressure, Condensate Load and Steam Trap type. These parameters can be measured, but some can only be loosely defined. The two-phase nature of the flow dynamics makes controlling some of the key variables such as Condensate Load and Pressure difficult, all of which affect the Steam Wastage observed.
- Heterodyne Circuit - Chapter 4 investigated the heterodyne circuit and showed how data is transferred from broadband to a narrowband low frequency output. The time-frequency analysis of the input signal sweep showed that although low and high frequency data is passed through the circuit, its origins cannot be conclusively reconstructed. This explains the lack of clear frequency translation and the difficulty in the signal analysis.
- Scales of Magnitudes - Experiments were carried out to relate acoustic emission signatures to operational conditions. The time scales at which these (acoustic emission and operational conditions) are measured differ. For that reason, there is a discrepancy between the different parameters. This cannot easily be adjusted, as some parameters, such as Steam Wastage need to be measured over a longer period to provide sufficient accuracy, whereas acoustic emission is measured over a far shorter period. This makes it difficult to relate a specific operational condition or Steam Wastage Value to an acoustic emission profile. This is a similar matter to the Multiple Variable Error, but this is time-based rather than parameter-based.

*This chapter complete the analysis work. The next and final chapter covers the contribution to knowledge, recommendations and suggests further work.*

## Chapter 10

# Conclusions and Recommendations

*This is the final chapter to discuss and evaluate the approaches investigated in this thesis. Further work will also be discussed.*

### 10.1 Contribution to Knowledge

**1) The acoustic emission properties of Steam Traps have been systematically evaluated.**

Three major trap types have been analysed. Analysis of Steam Traps including opening and closing patterns has been performed. Acoustic emission characteristics of major Steam Traps have been established.

**2) Characteristics of heterodyne signal have been analysed.**

The frequency folding characteristics of the heterodyne circuit have been investigated and understood.

**3) The relationship between the acoustic emission and Steam Wastage, Pressure and Condensate Load have been assessed for a number of conditions.**

Overall, it has become clear that the Orifice Trap is better for the setting of operational conditions due to its stationary response. This is because the Orifice Trap has no modulating mechanism. However, it has also been shown that as the response for the Orifice Trap is stationary, there are no specific features that can be used to establish an instantaneous leak. On the other hand, the Thermodynamic Trap, having a clear opening and closing sequence, can be readily used to analyse its operational condition, as there are artefacts within the signal to allow the operation to be understood. However, it has also been shown that the setting of op-

erational scenarios is significantly more difficult compared to a Orifice Trap, as demonstrated in Chapter 5.

**4) Inherent random operational behaviour has been discovered for three types of Steam Trap.**

The random nature of Steam Traps has been discussed. Statistical quantities are introduced in the condition assessment to take into account of the variability of the data and an averaging approach must be taken.

**5) The complexity of multiple parameter analysis in relation to operational traps has been discussed.**

The operation of Steam Traps is affected by a number of parameters, some of which are listed in Table 5.3. In an effort to make the investigation more manageable, these parameters were limited. Additionally, the major interaction interfaces of key parameters were defined. The analysis work has shown that when considering a relationship between only two parameters in isolation to the other parameters, an analysis can be undertaken. However, to understand the relationship of acoustic emission to Steam Wastage, relationships of all contributing parameters must be taken into account to allow a correlation between Steam Wastage and acoustic emission. Additionally, the operation of Steam Traps introduces an instability to the steam and condensate loop which results in a complex dynamic feedback process further complicating the ability to understand the relationship between acoustic emission and Steam Wastage.

## 10.2 Recommendations and Further Work

There are a number of areas where further work could be conducted, both from an academic and application point of view, as listed below:

- 1) The environmental process conditions for which the traps have been tested could be extended. For this work, only traps of 1/2" diameter have been used. The process conditions have been limited to 15 barg and up to 200 kg/hr of condensate load. It would be advantageous to extend the investigation to larger sized traps as well as higher pressures and condensate loads. Furthermore, the very low pressure applications would be of interest, as many district heating systems use low pressure (1-2 barg) steam. Although these lower pressures result in smaller leakage rates, the opportunity for application is still large as these Steam Traps are usually very inaccessible.
- 2) The sensor probe used could be further investigated and/or a specific probe built with known characteristic responses. The low bandwidth output signal from the heterodyne is useful, as it reduces the computational effort in the analysis. Heterodyne circuits can be made in hardware, as well as software. It may be advantageous, especially given the improvements in speed and ability of microchips, that the signal be sampled at full length and then heterodyned in software. This approach may also reduce some of the observed uncertainty of measurement, especially related to the "frequency folding" feature of the heterodyne circuit, which is discussed in Chapter 4.
- 3) The application of Wavelets and other DSP techniques may enhance the feature recognition for trap diagnosis. This may especially apply to the the filtering abilities of the wavelet function. No specific work has been carried out using wavelets and care will have to be taken that the correct "Mother-wavelet" is chosen for the signal analysis.
- 4) The application of automatic pattern recognition would be another suitable area for further work. These automatic pattern recognition techniques would include Fuzzy Logic and Neural Network approaches. The neural network may be especially of further interest as it is analogous to the survey engineer's approach for diagnosing traps.

## 10.3 Final Summary Overview

In summary, the following table highlights the past, the present and the potential future direction of the knowledge development in this field of study. As previously indicated no published condition monitoring literature has been found specifically related to Steam Traps.

Period	Knowledge
<hr/>	
<b>Before</b>	<ol style="list-style-type: none"> <li>1) No specific study of Steam Wastage levels for Steam Traps existed.</li> <li>2) No specific knowledge of Steam Trap acoustic emission responses existed.</li> <li>3) No specific knowledge existed regarding the chaotic nature of Steam Traps and their interaction with two-phase flow and the corresponding steam leakage.</li> </ol>
<hr/>	
<b>During</b>	<ol style="list-style-type: none"> <li>1) Steam Wastage levels for Steam Traps have been established.</li> <li>2) Specific knowledge of Steam Trap acoustic emission responses has been established and signal processing approach recommendations have been made.</li> <li>3) Specific knowledge on the chaotic feedback nature of Steam Traps and their interaction with two-phase flow and the corresponding steam leakage has been established.</li> </ol>
<hr/>	
<b>Future</b>	<ol style="list-style-type: none"> <li>1) Extension of the experimental scope.</li> <li>2) Further detailed investigation into the heterodyne process, considering a software approach.</li> <li>3) Application of additional DSP techniques.</li> <li>4) Application of higher level pattern recognition.</li> </ol>
<hr/>	

## References

- [1] A. Addali, A. Al-lababidi, H. Yeung, D. Mba, and F Khan. Acoustic emission and gas-phase measurement in two-phase flow. *Proceedings of the Institution of Mechanical Engineers Part E: Journal of Process Mechanical Engineering*, 224, pp 281–290, 2010. Cited on page 30
- [2] Glenn Allgood. Steam trap condition monitoring - Confidential. Technical report, Spirax Sarco Inc., 2007. Cited on page 32
- [3] Xiaolei Shirley Ao, Jed Matson, Peter Kucmas, Oleg Khrakovsky, and Xuesong Scott Li. Ultrasonic clamp-on flow measurement of natural gas, steam and compressed air. Technical report, Panametrics, Waltham, MA, 2009. Cited on page 29
- [4] Armstong. The sound steam traps make. Audio Tape, 1980. Cited on page 17, 93
- [5] ASME. PTC 39-2005 - Performance Test Codes - Steam Traps. Technical report, Performance Test Codes, 1989. Cited on page 6
- [6] Neil Barton. A review of steam flowmetering technology. Technical report, NEL Laboratories, 2004. Cited on page 33
- [7] V. Blazquez. Is ultrasound leak detection reliable for steam traps? *Hydrocarbon Processing*, Vol. 80, No: 2, pp 99–100, 2001. Cited on page 29
- [8] Heinz Bloch. Consider an advanced method of steam trap condition monitoring. *Hydrocarbon Processing*, Vol. 84, p 9, 2005. Cited on page 19
- [9] Jonathan Boyd and Julie Varley. Measurement of gas hold-up in bubble columns from low frequency acoustic emissions. *Chemical Engineering Journal*, Vol. 88, pp 111–118, 2002. Cited on page 38
- [10] Simon Braun. *Mechanical Signature Analysis: Theory and Applications*. Academic Press, 1986. Cited on page 41, 43
- [11] Christopher E. Brennen. *Cavitation and Bubble Dynamics (Oxford Engineering Science Series)*. Oxford University Press, USA, 1995. Cited on page xi, 38, 39, 40

- [12] Christopher E. Brennen. *Fundamentals of Multiphase Flows*. Cambridge University Press, 2005. Cited on page 33
- [13] P. Bruck, G. Zysk, and T. Esselman. Steam incident investigation at east 41st street and lexington avenue new york. Technical report, ABS Consulting, 18th July 2007. Cited on page 14
- [14] Carbon Trust. Energy and cost savings from steam trap replacement. Technical report, Carbon Trust, 2004. Cited on page 26
- [15] Carbon Trust. Energy efficient operation of heat distribution systems. Technical report, Carbon Trust, 2005. Cited on page 16
- [16] Carbon Trust. Steam boiler equipment. Technical report, Carbon Trust, 2008. Cited on page 52
- [17] Richard Carmichael. Condensate Trap, GB 2397032. Patent, 2006. Spirax Sarco. Cited on page 5
- [18] Richard Carmichael. Condensate Trap, GB 2440548. Patent, 2008. Spirax Sarco. Cited on page 5
- [19] Richard Carmichael, Poczka Christopher, and Ramadas Nishal. Steam Trap Monitoring, GB 2457924. Patent, 2009. Spirax Sarco. Cited on page 5
- [20] Richard Carmichael and Christopher Poczka. Carbon Trust Grant Application: STAPS - Steam Trap Acoustic Performance Sensor. Technical report, Spirax Sarco, Carbon Trust, 2006. Cited on page 53
- [21] Richard Carmichael and Christopher Poczka. Condensate Trap, GB 2429936. Patent, 2007. Spirax Sarco. Cited on page 5
- [22] Richard Carmichael, Christopher Poczka, and Nishal Ramadas. Developments in or relating to a Condensate Recovery System, GB 2457923. Patent, 2010. Spirax Sarco. Cited on page 5
- [23] Stephen Chapman. *Matlab Programming for Engineers*. Cengage Learning, 2007. Cited on page 4, 95
- [24] P. Chen, P. Chua, and G. Lim. A study of hydraulic seal integrity. *Mechanical Systems and Signal Processing*, Vol. 21, pp 1115–1126, 2007. Cited on page 49

- [25] Sze-Foo Chien. Predicting wet-steam flow regime in horizontal pipes. In *Meeting on Petroleum Engineering*, Tianjin, November 1988. Society of Petroleum Engineers. Cited on page xi, 34
- [26] ConEddison. Steam use efficiency and demand reduction. Technical report, ConEddison, December 2007. Cited on page 16
- [27] James W. Cooley and John W. Tukey. An algorithm for the machine calculation of complex fourier transform series. *The American Mathematical Society - Mathematics of Computation*, Vol. 19, Iss. 90, No. 30, pp 297–301, 1965. Cited on page 44
- [28] Cypress Envirosystem. *Wireless Steam Trap Monitor (WSTM-100)*, 2008. Cited on page 18
- [29] DECC. Climate Change Act 2008. Technical report, Department of Energy and Climate Change, November 2010. Cited on page 53
- [30] Robert Evans, Jonathan Blotter, and Alan Stephens. Flow rate measurments unsinf flow-induced pipe vibration. *Journal of Fluids Engineering, Transactions of the AMSE*, Vol. 126, pp 280–284, 2004. Cited on page 49
- [31] Federal Energy Management Program. Steam trap performance assessment. Technical report, Department of Energy, 2006. Cited on page 14, 26, 52
- [32] William File. *Cost Effective Maintenance: Design and Implementation*. Butterworth-Heinemann, 1991. Cited on page 16
- [33] Jacob Fraden. *Handbook of Modern Sensors: Physics, Designs, and Applications*. Springer, 2003. Cited on page 63
- [34] Stephen Frank. Selecting the right steam trap. *Hydrocarbon Processing*, Vol. 85, p 79, July 2006. Cited on page 19
- [35] Michael Fuchs. Kondensatableiter, EP 1630470a1. Patent, 2004. ARI-Armaturen. Cited on page 18, 20
- [36] L. J. Giacoletto. *Electronics Designer's Handbook*. McGraw-Hill, 2nd edition, 1977. Cited on page 71
- [37] Andrew Gillespie. *Foundations of Economics*. OUP Oxford, 29 Mar 2007. Cited on page 19, 51
- [38] Mark A. Goodmann. How ultrasound and infrared work together. *Proceedings Thermosense XII*, Vol. 4020, pp 94–98, 2000. Cited on page 19, 25



- [39] John Grimond. For want of a drink (Interview with John Grimond). *The Economist*, May 20th, Special Report, 2010. Cited on page 54
- [40] Thomas Hahn, Thomas Berger, and Michael Buckingham. Acoustic resonances in the bubble plume formed by a plunging water jet. *Proceedings of the Royal Society A*, Vol. 459, pp 1751–1782, 2003. Cited on page 38
- [41] Peter Hauptmann, Niels Hoppe, and Alf Püttmer. Application of ultrasonic sensors in the process industry. *Institute of Physics Publishing - Measurement Science and Technology*, Vol. 13, pp 73–83, 2002. Cited on page 50
- [42] G. F. Hewitt. Thermopedia. Technical report, Department of Chemical Engineering and Chemical Technology, Imperial College, 2009. Cited on page 33
- [43] Chenquan Hua, W. Changming Wang, Yanfeng Geng, and Tianming Shi. Noninvasive flow regime identification for wet gas flow based on flow-induced vibration. *Chinese Journal of Chemical Engineering*, Vol. 18, Iss. 5, pp 795–803, 2010. Cited on page 37
- [44] Emmanuel C. Ifeachor and Barrie W. Jervis. *Digital Signal Processing: A Practical Approach (Electronic Systems Engineering)*. Addison-Wesley, 1993. Cited on page 4
- [45] Vinay Ingle and John Proakis. *Digital Signal Processing Using MATLAB (ISE)*. Nelson Engineering, 2006. Cited on page 4
- [46] Alan Isaacs, editor. *A Dictionary of Physics (Oxford Paperback Reference)*. Oxford University Press, USA, 2000. Cited on page 26, 62
- [47] Andrew Jardine, Daming Lin, and Dragan Banjevic. A review on machinery diagnostics and prognostics implementing condition-based maintenance. *Mechanical Systems and Signal Processing*, Vol. 20, pp 1483–1510, 2006. Cited on page 50
- [48] Brian Johnson. Special feature: Steam today and steam tomorrow. *Valve User*, Iss. 11, 12 and 13, Special Report, 2009. Cited on page 2
- [49] W. Kaewwaewnoi, A. Prateepasen, and P. Kaewtrakulpong. Investigation of the relationship between internal fluid leakage through a valve and the acoustic emission generated from the leakage. *Measurement*, Vol. 43, pp 274–282, 2010. Cited on page 49
- [50] Jae Chan Kim. *Investigation of flow signals for condition monitoring using time-frequency analysis and wavelet transforms*. PhD thesis, University of Sussex, 2004. Cited on page 49
- [51] Stefan Kocis and Zdenko Figura. *Ultrasonic Measurements and Technologies (Sensor Physics and Techniques Series)*. Springer, 1996. Cited on page 28

- [52] Aim Lay-Ekuakille, Giuseppe Vendramin, Amerigo Trotta, and Philippe Vanderbemden. Stft-based spectral analysis of urban waterworks leakage detection. In *XIX IMEKO World Congress - Fundamental and Applied Metrology*, 2009. Cited on page 50
- [53] Oliver Lyle. *The Efficient Use of Steam*. Her Majesty's Stationery Office, 1967. Cited on page 2, 7, 13
- [54] I. Macleod, R. Rowley, M. Beesley, and P. Olleya. Acoustic monitoring techniques for structural integrity. *Nuclear Engineering and Design*, Vol. 129, Iss. 2, pp 191–200, 1991. Cited on page xi, 31
- [55] Mathworks. *Matlab Getting Started Guide*. Mathworks, 2008. Cited on page 4
- [56] Mathworks. *Signal Processing Toolbox User's Guide*. Mathworks, 2008. Cited on page 4
- [57] Mathworks. *Statistical Toolbox User Guide*. Mathworks, 2008. Cited on page 4
- [58] Frank Mittelbach, Michel Goossens, Johannes Braams, David Carlisle, and Chris Rowley. *The LaTeX Companion (Tools and Techniques for Computer Typesetting)*. Addison-Wesley Professional, 2004. Cited on page 5
- [59] S. Morozov. Development of an acoustic leak monitoring system. *Atomic Energy*, Vol. 103, Iss. 6, pp 925–931, 2007. Cited on page 51
- [60] Tomomichi Nakamura and Shigehiko Kaneko, editors. *Flow Induced Vibrations: Classifications and Lessons from Practical Experiences*. Elsevier Science, 2008. Cited on page 28, 33, 41
- [61] National Instruments. *LabView Basics I Introduction Course Manual*. National Instruments Corporation, 2006. Cited on page 4
- [62] National Instruments. *LabView Basics II Introduction Course Manual*. National Instruments Corporation, 2006. Cited on page 4
- [63] NEL Laboratories. Steam wastage of traps. Technical report, National Engineering Laboratories (NEL), 1987. Cited on page 60
- [64] M. Norton and D. Karczub. *Fundamentals of Noise and Vibration Analysis for Engineers*. Cambridge University Press, 2003. Cited on page 26, 41, 46
- [65] Gary Orlove. Non-destructive evaluation of steam trap. *Proceedings Thermosense XXI*, Vol. 3700, pp 283–288, 1999. Cited on page 19

- [66] I. Owen. The propulsion of an isolated slug through a pipe and the forces produced as it impacts upon an orifice plate. *International Journal of Multiphase Flow*, Vol:20, Iss:3, pp 659–666, 1994. Cited on page 41
- [67] I. Owen, I. Hussein, and A. Amini. The impact of water slugs on wet steam flowmeters. *Flow Measurement Instrumentation*, Vol. 2, pp 98–104, 1991. Cited on page 41
- [68] Process Engineering. Market still chequered, but robust. *Plant Technology Condition Monitoring*, July / August, p 31, 2009. Cited on page 53
- [69] PSE/007 Committee. Classification of Automatic Steam Traps - BS EN 26704:1991. Technical report, PSE/007 Industrial Valve, 1991. Cited on page 4, 7
- [70] PSE/007 Committee. Methods for Determination of Discharge Capacity of Automatic Steam Traps - BS EN 27842:1991. Technical report, PSE/007 Industrial Valve, 1991. Cited on page 4
- [71] PSE/007 Committee. Methods for Determination of Steam Loss of Automatic Steam Traps - BS EN 27841:1991. Technical report, PSE/007 Industrial Valve, 1991. Cited on page xi, 4, 22, 23, 24, 102
- [72] Mongkol Pusayatanont and Peter J. Unsworth. Effect of second phase on single phase flow meters in steam quality measurement. *The International Journal of Multiphysics*, Vol. 3, Iss. 1, pp 73–79, January 2009. Cited on page 49
- [73] Mongkul Pusayatanont. *Multiphase flow measurement based on conventional flowmeters using signal analysis*. PhD thesis, University of Sussex, 2002. Cited on page 46
- [74] A. Püttmer. New applications for ultrasonic sensors in process industries. *Ultrasonics*, 44, pp 1379–1383, 2006. Cited on page 50
- [75] A. Püttmer and V. Rajaraman. Acoustic emission based online valve leak detection and testing. In *Ultrasonics Symposium, 2007. IEEE*, pp 1854–1857. Siemens AG, 2007. Cited on page 49
- [76] Nishal Ramadas. Acoustic emission techniques applied to steam wastage estimation and fault detection in an industrial process. In *CM 2008 and MFPT 2008*, 2008. Cited on page 25, 31, 82, 95
- [77] David Ratcliffe. Steam trap performance and process plant efficiency. *Energy Management News*, Vol.10, Iss. 1, pp 1–5, 2004. Cited on page 26

- [78] Thomas Rockwell. Steam trap testing yields energy savings. Technical report, Chemical Processing, January 1995. Cited on page 19
- [79] Andres E. Rozlosnik. Infrared thermography and ultrasound both test analyzing valves. In *Thermosense - Conference No. 20, Orlando FL*, volume 3361, pp 137–153, 1998. Cited on page 18, 19, 25, 30
- [80] Michael Ryan. Steam Trap Monitor, US 4764024. Patent, 1988. Cited on page 18
- [81] M. Sharif and R. Grosvenor. Process plant monitoring and fault diagnosis. *Proceedings of the Institution of Mechanical Engineers Part E*, Vol. 212, pp 13–30, 1998. Cited on page 45
- [82] Mohamed Sharif and Roger Grosvenor. Internal valve leakage detection using an acoustic emission measurement system. *Transactions of the Institute of Measurement and Control*, Vol. 20(5), pp 233–242, 1998. Cited on page 48
- [83] Steven Smith. *Digital Signal Processing: A Practical Guide for Engineers and Scientists*. Newnes, 2002. Cited on page 4, 95
- [84] Lyubka Spasova. STAPS Reports - Confidential. Technical report, Spirax Sarco Limited, 2009. Cited on page xi, 32, 34, 35
- [85] Spirax Sarco. *Steam Utilisation Course*. Spirax Sarco Limited, 1988. Cited on page 7
- [86] Spirax Sarco. *Spiratec ST14, ST16 and ST17 Sensor Chambers and Sensors - Installation and Maintenance Sheet*, 1990. Cited on page 18
- [87] Spirax Sarco. *UP100 Ultrasonic Trap Tester - Installation and Maintenance Sheet*, 1998. Cited on page 65, 73
- [88] Spirax Sarco. *UP100 Ultrasonic Trap Tester - Technical Information Sheet*, 1998. Cited on page 17, 65, 73
- [89] Spirax Sarco. *Product Overview*. Spirax Sarco Limited, 2005. Cited on page xi, 6, 8
- [90] Spirax Sarco. *Spiratec ST14, ST16 and ST17 Sensor Chambers and Sensors - Technical Information Sheet*, 2005. Cited on page 18, 60
- [91] Spirax Sarco. *The Steam and Condensate Loop Book*. Spirax Sarco Limited, 2007. Cited on page xi, 2, 7, 9, 11, 12, 13, 15, 16, 100
- [92] G.S. Srinivasan, O. P. Singh, and R. Prabhakar. Leak noise detection and characterisation using statistical features. *Annals of Nuclear Energy*, Vol. 27, pp 329–343, 2000. Cited on page 48

- [93] James Street and M. Rasin Tek. Unsteady state gas-liquid slug flow through vertical pipe. *American Institute of Chemical Engineers Journal*, Vol. 11, Iss. 4, pp 601–607, July 1965. Cited on page 33, 34
- [94] Bin Sun, Hongjian Hang, Lu Cheng, and Yuxiao Zhao. Flow regime identification of gas-liquid two-phase flow based on hht. *Chinese Journal of Chemical Engineering*, Vol. 14, Iss. 1, pp 24–30, 2006. Cited on page 37
- [95] M. Taghvaei, S. Beck, and W. Staszewski. Leak detection in pipelines using cepstrum analysis. *Measurement Science and Technology*, Vol. 17, pp 367–372, 2006. Cited on page 47
- [96] Y. Taitel and A.E. Dukler. A model for predicting flow regime transitions in horizontal and near horizontal gas-liquid flow. *American Institute of Chemical Engineers Journal*, Vol. 22, pp 47–55, 1976. Cited on page xi, 33, 36
- [97] T. Tambouratzis and I. Pzsit. Non-invasive on-line two-phase flow regime identification employing artificial neural networks. *Annals of Nuclear Energy*, Vol. 36, pp 464–469, 2009. Cited on page 37
- [98] Chao Tan, Feng Dong, and Mengmeng Wu. Identification of gas/liquid two-phase flow regime through ert-based measurement and feature extraction. *Flow Measurement and Instrumentation*, Vol. 18, pp 255–261, 2007. Cited on page 37
- [99] John Thome. *Engineering Data Book III*. Thome, 2007. Cited on page 34
- [100] G. Thompson and G. Zolkiewski. An experiemntal investigation into the detection of internal leakage of gases through valves by vibration analysis. *Proceedings of the Institution of Mechanical Engineers Part E*, Vol. 211, pp 195–207, 1997. Cited on page 48
- [101] TLV. *Audiphone AP1*, July 1998. Cited on page 17
- [102] UE Systems. Steam trap inspection methods and steam cost analysis. Technical report, UE Systems, 2004. Cited on page 31
- [103] UE Systems. Air survey. In *Webinar*, 2009. Cited on page 17, 28, 31, 93
- [104] UE Systems. Testing steam traps - webinar. In *Web Cast*, October 2009. Cited on page 17, 93
- [105] Wenran Wang and Yunxian Tong. A new method of two-phase flow measurement by orifice plate differential pressure noise. *Flow Measurement and Instrumentation*, Vol. 6, Iss. 4, pp 265–270, October 1995. Cited on page 29, 30, 51
- [106] R. Williams. *Acoustic Emission*. Institute of Physics Publishing, 1980. Cited on page 27

- [107] Bo-Suk Yang, Won-Woo Hwang, Myung-Han Ko, and Soo-Jong Lee. Cavitation detection of butterfly valve using support vector machines. *Journal of Sound and Vibration*, Vol. 287, pp 25–43, 2005. Cited on page 50
- [108] Siril Yella, Gupta Naren, and Mark Do. Condition monitoring using pattern recognition techniques on data from acoustic emission. In *Proceedings of the 5th International Conference on Machine Learning and Applications*, 2006. Cited on page 50, 95
- [109] Yunlong Zhou, Fei Chen, and Bin Sun. Identification method of gas-liquid two-phase flow regime based on image multi-feature fusion and support vector machine. *Chinese Journal of Chemistry Engineering*, Vol. 16, No. 6, pp 832–840, December 2008. Cited on page 37

## Appendix A

# Additional Steam Trap Information

### A.1 List of Steam Trap Manufacturers

- Douglas - [www.douglas-italia.com](http://www.douglas-italia.com) or [www.douglas-ktc.com](http://www.douglas-ktc.com)
- Miyawaki - [www.miyawaki.net](http://www.miyawaki.net)
- Ayvaz - [www.ayvaz.com](http://www.ayvaz.com)
- Armstrong - [www.armstronginternational.com](http://www.armstronginternational.com)
- Hora - [www.hora.de](http://www.hora.de)
- Watson McDaniel - [www.watsonmcdaniel.com](http://www.watsonmcdaniel.com)
- Ari - [www.ari-armaturen.de](http://www.ari-armaturen.de)
- Gestra - [www.gestra.com](http://www.gestra.com)
- Nicholson - [www.nicholsonsteamtrap.com](http://www.nicholsonsteamtrap.com)
- TLV - [www.tlv.com](http://www.tlv.com)
- ADCA - [www.valsteam.com](http://www.valsteam.com)
- Yarway - [www.yarway.com](http://www.yarway.com)
- Hoffman - [www.hoffmanspecialty.com](http://www.hoffmanspecialty.com)
- Rifox - [www.rifox.de](http://www.rifox.de)
- Spirax Sarco - [www.spiraxsarco.com](http://www.spiraxsarco.com)
- GEM - [www.gemtrap.com](http://www.gemtrap.com)
- Bestobell - [www.bestobellsteamtraps.com](http://www.bestobellsteamtraps.com)

## A.2 Carbon Trust Calculation

The following calculation has been taken from the Carbon Trust application form. The UK Steam Trap population is estimated at 5 million traps of which approximately 5% are being manually serviced.

**EXAMPLE:** A trap of DN 15 size with a pressure drop across the Steam Trap of 7 barg and operating 24 hours a day and 365 years a day will operate roughly 8400 hours/pa.

If the that trap leaks 10.8 kg/hr steam this equates to approximately 90.8 tonnes pa..

The resulting CO<sub>2</sub> emissions will equate to 13.97 tonnes per annum, which equals approximately £2268 in terms of lost steam per annum.

There is a clear need for improved Steam Trap diagnostics.



## **Appendix B**

# **Heterodyne Circuit Information**

## SPECIFICATIONS

<b>Construction:</b>	Hand held ABS pistol type ultrasonic processor stainless steel sensor enclosures
<b>Circuitry:</b>	SMD/Solid State hybrid heterodyne receiver
<b>Frequency Range:</b>	35-45 kHz
<b>Indicator:</b>	10 segment LED bargraph (red)
<b>Sensitivity Selection:</b>	8 position precision attenuation
<b>Power:</b>	9 volt alkaline battery
<b>Low Battery Voltage Indicator:</b>	LED
<b>Headset:</b>	Noise isolating type: double headset wired monophonic Impedance: 16 ohms. Over 23 dB noise attenuation. Meets or exceeds ANSI specifications and OSHA standards.
<b>Transmitter:</b>	Patented warble tone transmission.
<b>Response time:</b>	300m. sec.
<b>Ambient Operating Temperature Range:</b>	32° - 120° F (0° - 50° C)
<b>Relative Humidity:</b>	10 - 95% noncondensing at up to 86°F (30°C)
<b>Storage Temperature:</b>	0° - 130°F
<b>Dimensions:</b>	5.5"x 1"x 7.9"
<b>Weight:</b>	10 oz.
<b>Probes:</b>	
<b>Scanning Module (SCM-1):</b>	Stainless Steel unisonic (single transducer) piezo electric crystal type
<b>Stethoscope (contact) Module:</b>	Stainless Steel plug-in type with 4.5" Stainless Steel wave guide
<b>Rubber Focusing Probe:</b>	Circular shaped, shields stray ultrasound signals, focuses detected signals
<b>Carrying Case:</b>	ABS plastic with die cut foam
<b>Warranty:</b>	one year, parts/labor, excluding abuse (details available on request).

Figure B.1: UP100 Heterodyne Probe Specification

## Appendix C

# Steam Wastage Rig

### C.1 Pictures Steam Wastage Rig

#### C.1.1 St Georges Road Test Shop

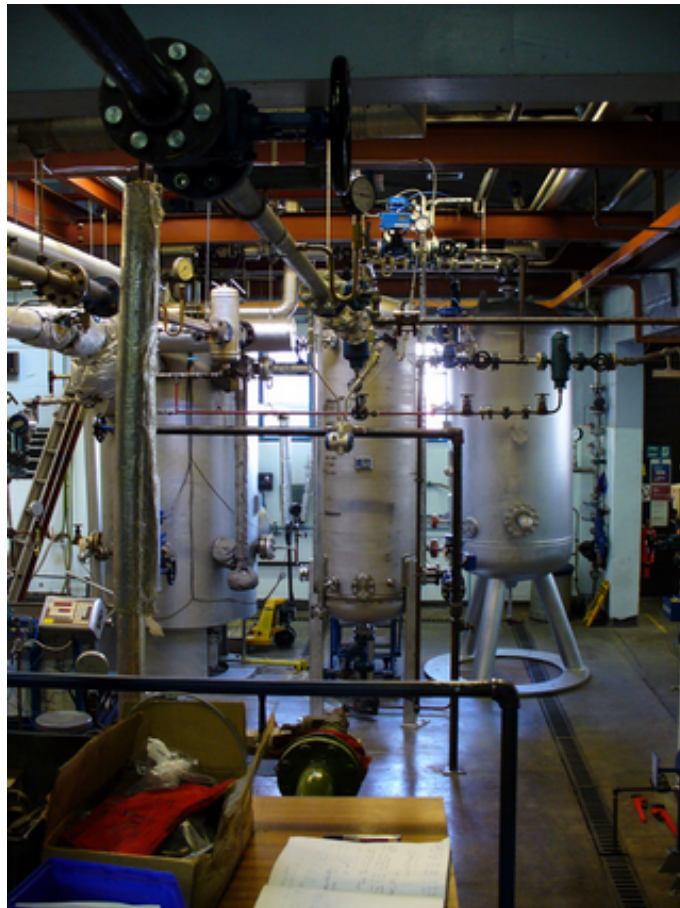


Figure C.1: SGR Rig Vessel and Flow Line



Figure C.2: SGR Rig Test Area Setup



Figure C.3: SGR Rig Condensate Heat Exchanger and Injection Setup



Figure C.4: SGR Rig Vessel Control Panel



Figure C.5: SGR Rig National Instruments Hardware





Figure C.6: SGR Rig National Instruments Hardware

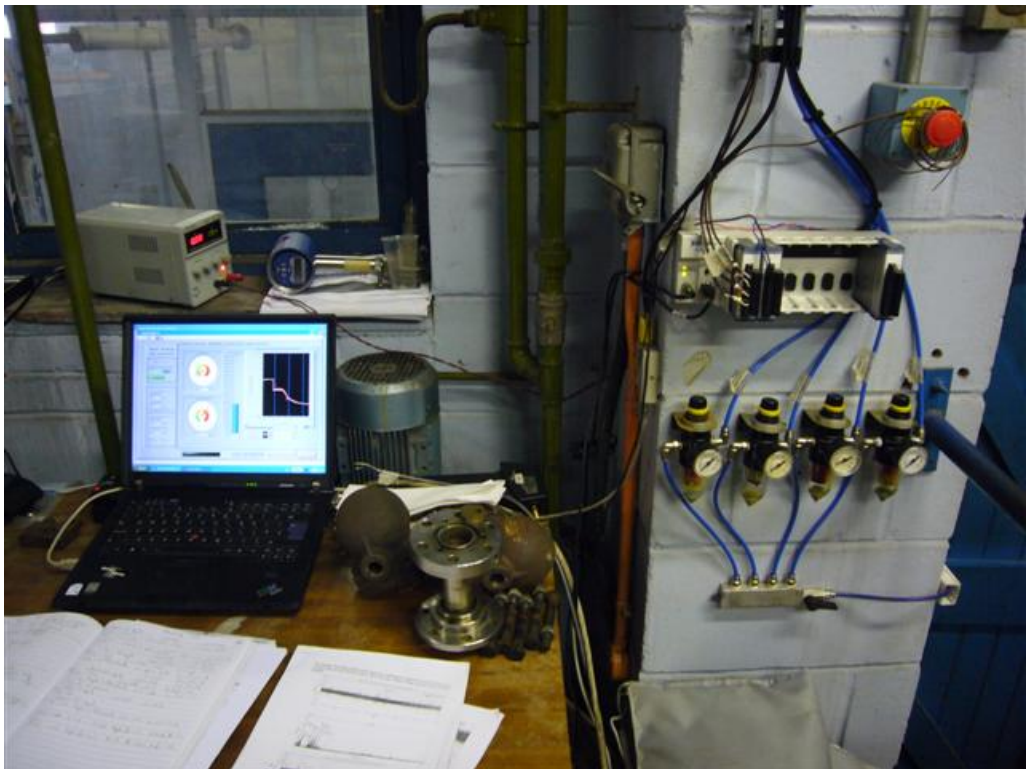


Figure C.7: SGR Rig Data Acquisition

### C.1.2 Runnings Road Test Shop



Figure C.8: Runnings Road Steam Trap Rig

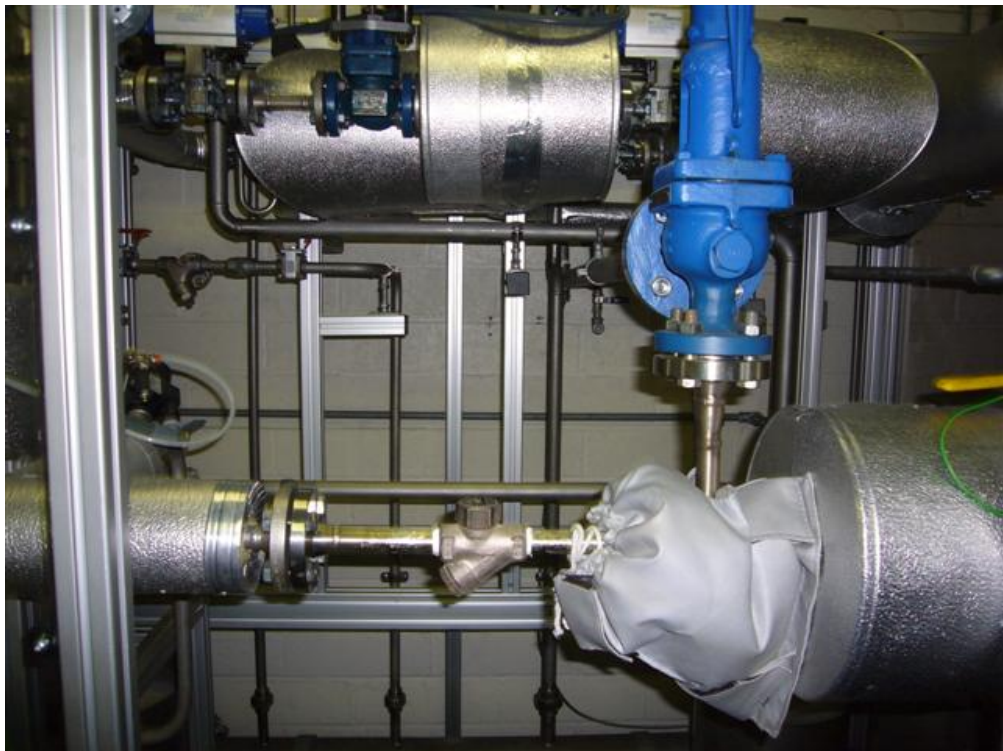


Figure C.9: Runnings Road Rig Steam Trap Test Station



Figure C.10: Runnings Road Rig Panel

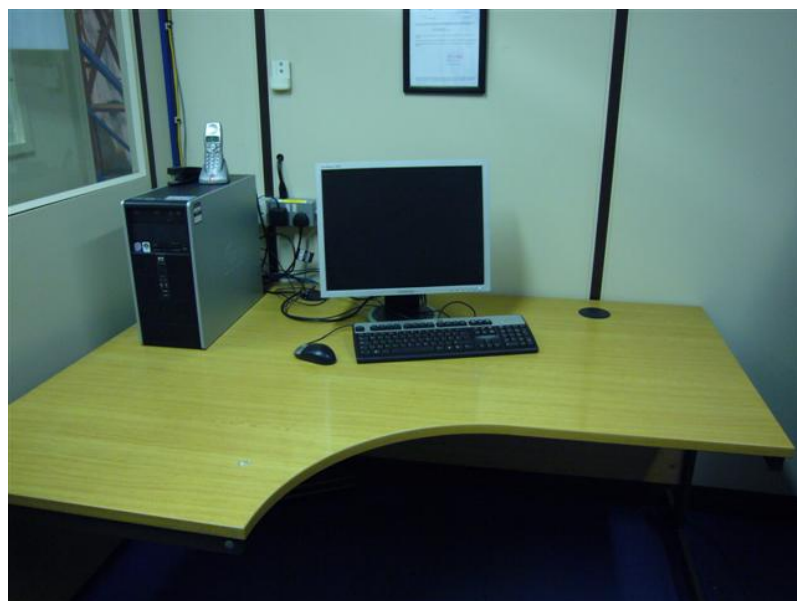


Figure C.11: Runnings Road Rig Data Acquisition



C.2 Steam Wastage Rig Schematics

C.2.1 St Georges Road Test Shop

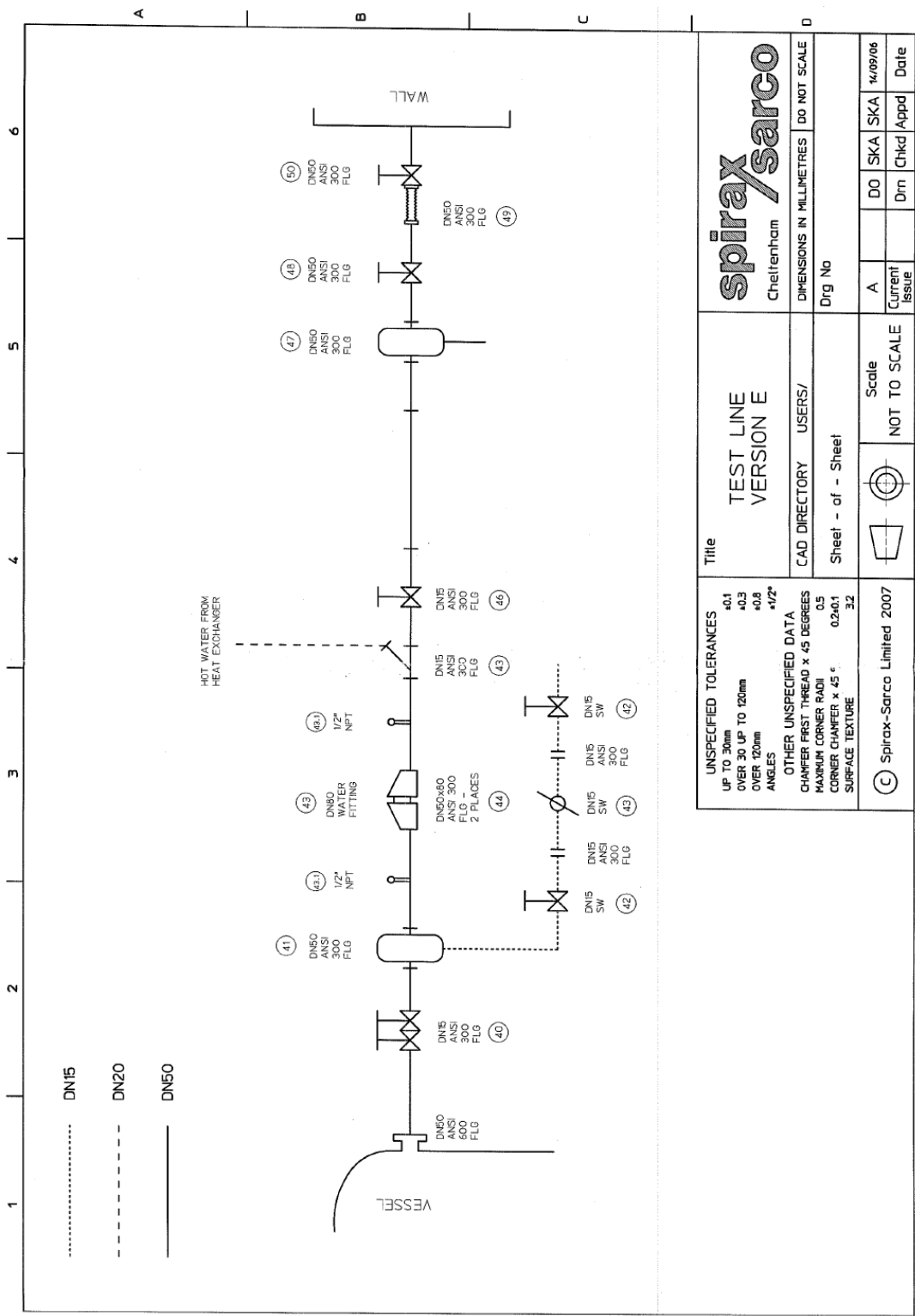


Figure C.12: SGR Rig Schematic 1 - Steam Inlet to Vessel

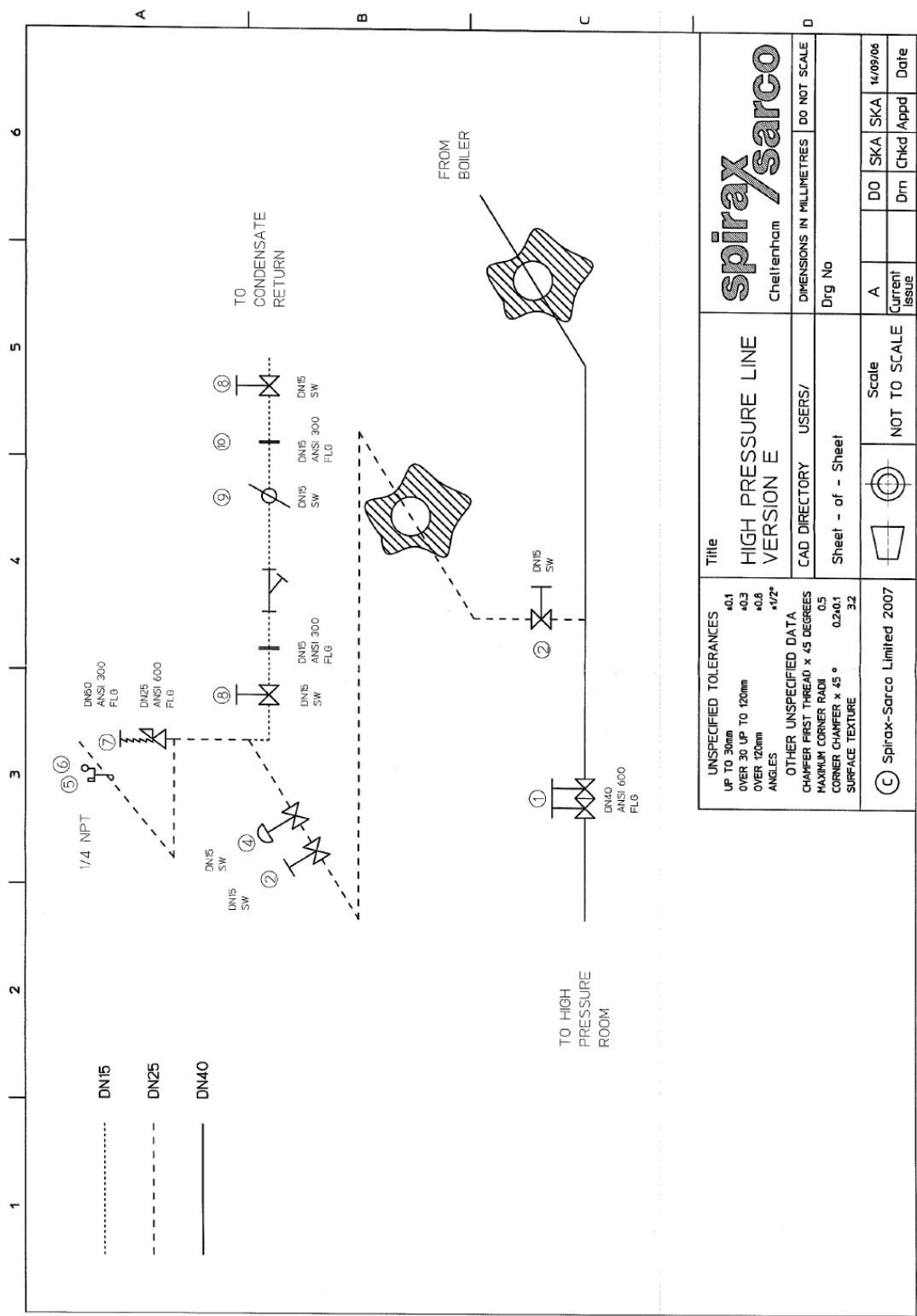


Figure C.13: SGR Rig Schematic 2 - Steam Inlet to Vessel

### C.2.2 Runnings Road Test Shop

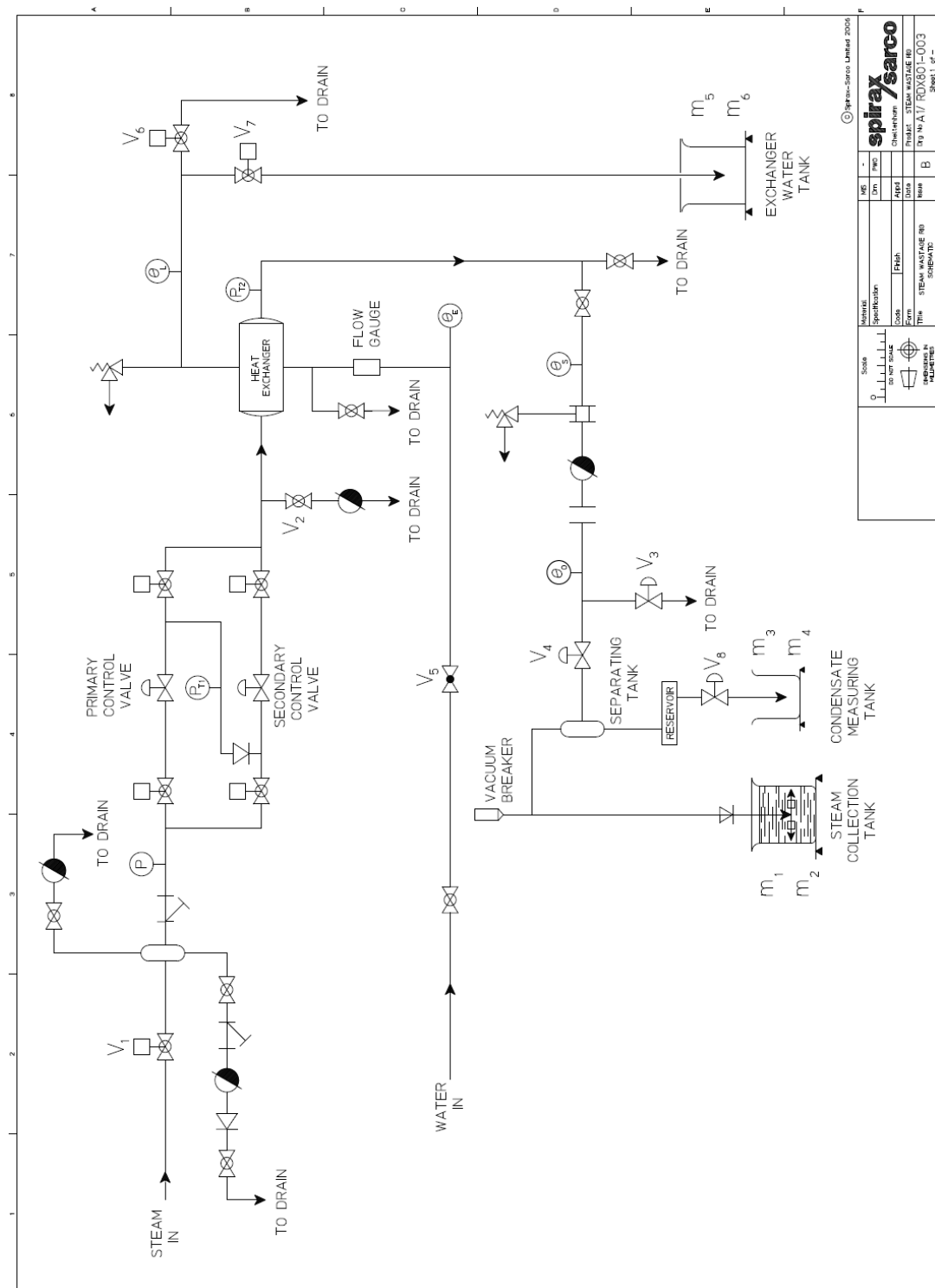


Figure C.14: RR Rig Schematic

## C.3 LabView Data Acquisition Software

### C.3.1 Software Overview Diagram

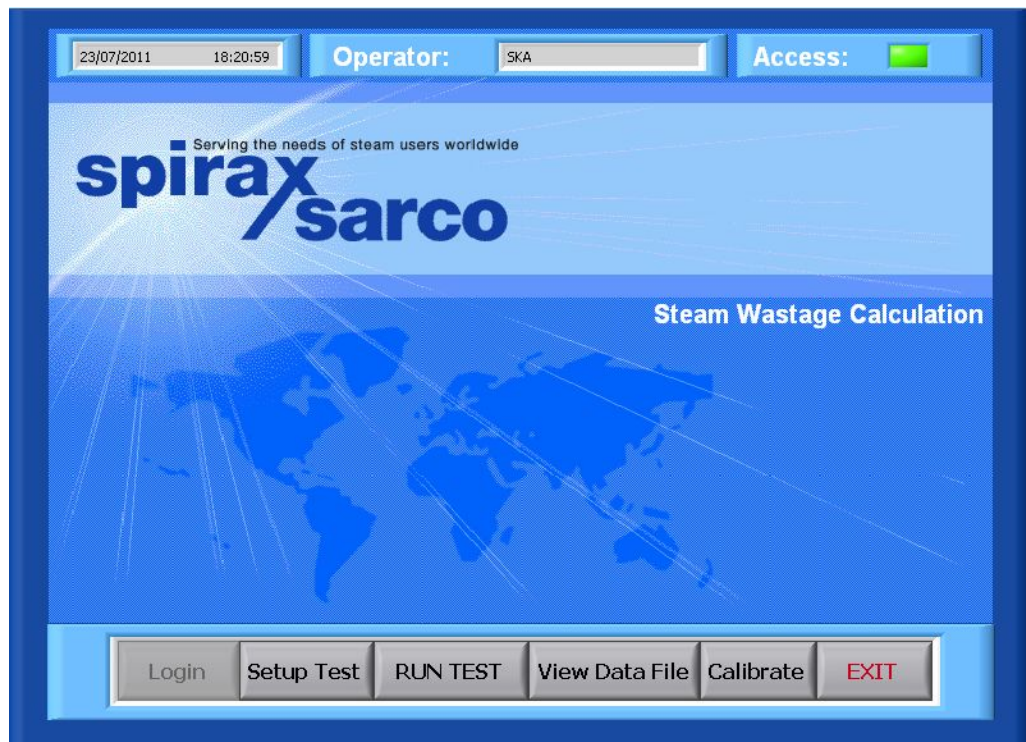


Figure C.15: LabView Start-up User Interface

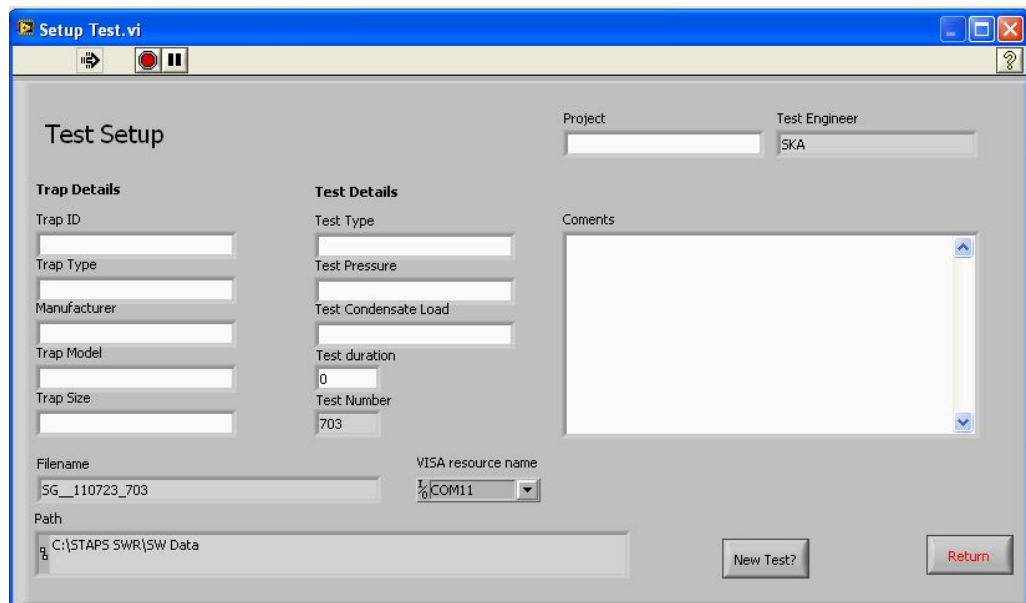


Figure C.16: LabView Data Test Setup User Interface

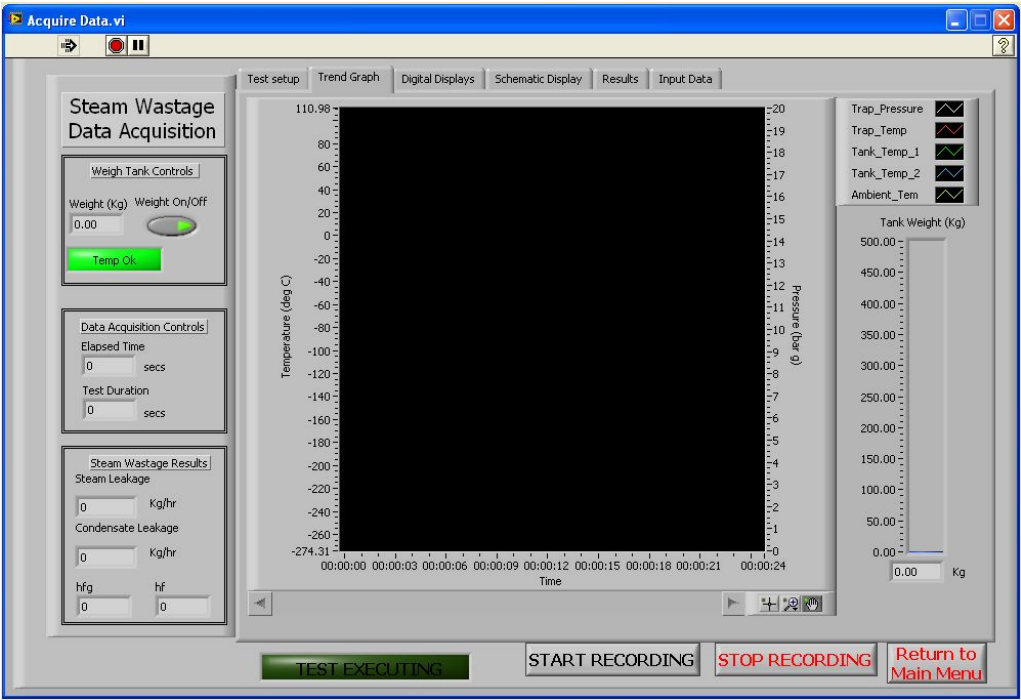


Figure C.17: LabView Data Acquisition User Interface

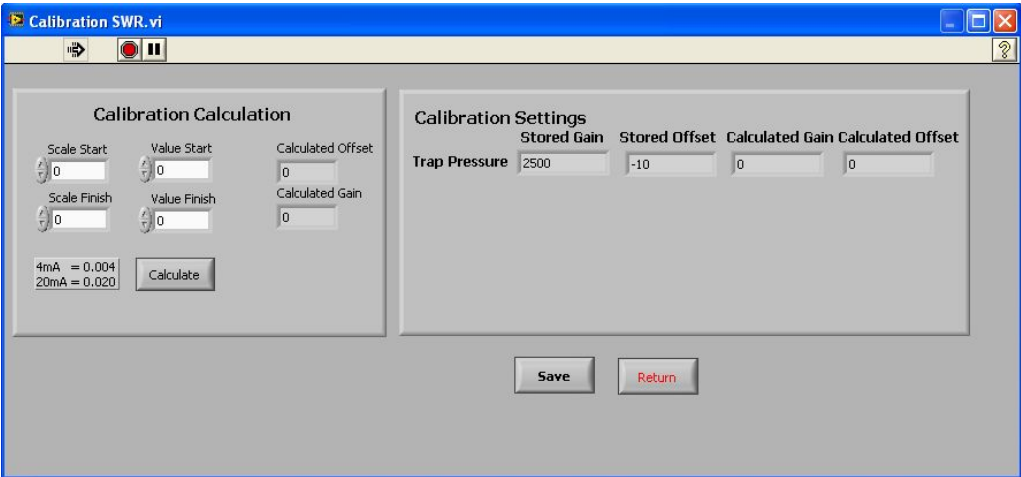
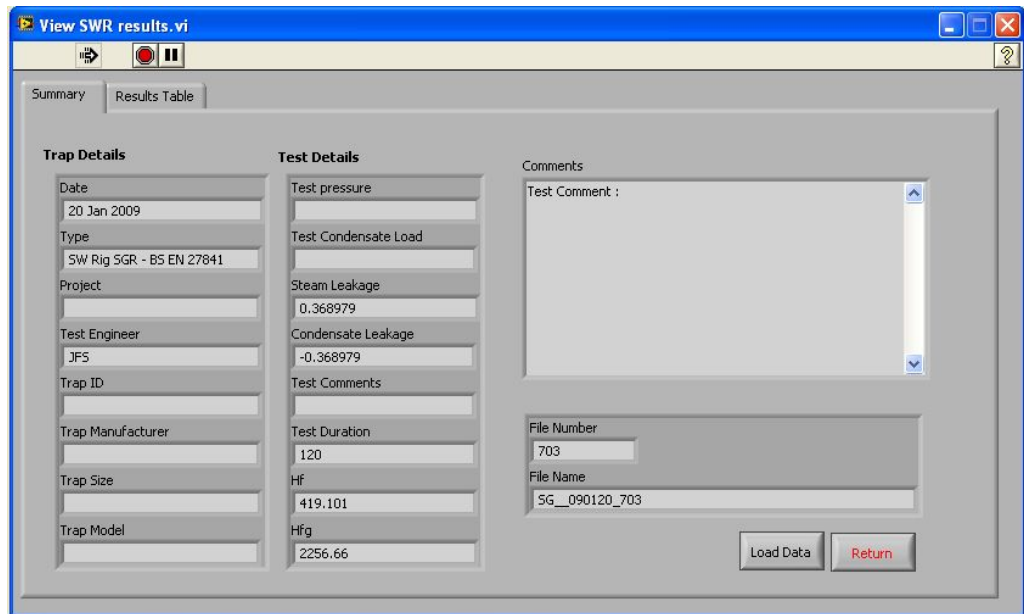


Figure C.18: LabView Sensor Calibration Coefficient User Interface



View SWR results.vi

Summary Results Table

**Trap Details**

Date: 20 Jan 2009

Type: SW Rig SGR - BS EN 27841

Project:

Test Engineer: JFS

Trap ID:

Trap Manufacturer:

Trap Size:

Trap Model:

**Test Details**

Test pressure:

Test Condensate Load:

Steam Leakage: 0.368979

Condensate Leakage: -0.368979

Test Comments:

Test Duration: 120

Hf: 419.101

Hfg: 2256.66

Comments:

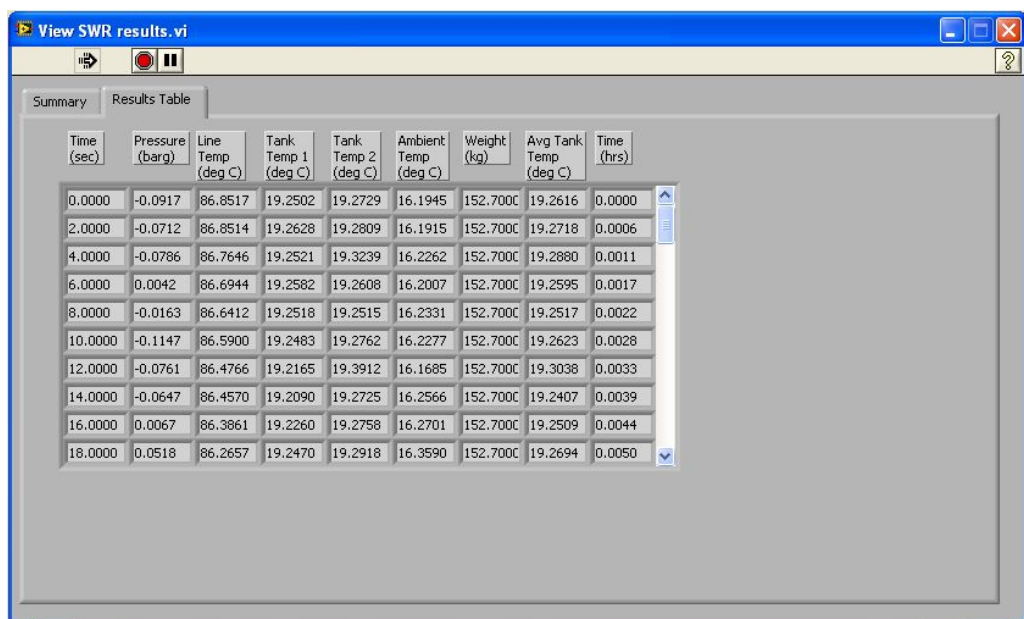
Test Comment :

File Number: 703

File Name: SG\_090120\_703

Load Data Return

Figure C.19: LabView Data Presentation User Interface Screen 1



View SWR results.vi

Summary Results Table

Time (sec)	Pressure (barg)	Line Temp (deg C)	Tank Temp 1 (deg C)	Tank Temp 2 (deg C)	Ambient Temp (deg C)	Weight (kg)	Avg Tank Temp (deg C)	Time (hrs)
0.0000	-0.0917	86.8517	19.2502	19.2729	16.1945	152.7000	19.2616	0.0000
2.0000	-0.0712	86.8514	19.2628	19.2809	16.1915	152.7000	19.2718	0.0006
4.0000	-0.0786	86.7646	19.2521	19.3239	16.2262	152.7000	19.2880	0.0011
6.0000	0.0042	86.6944	19.2582	19.2608	16.2007	152.7000	19.2595	0.0017
8.0000	-0.0163	86.6412	19.2518	19.2515	16.2331	152.7000	19.2517	0.0022
10.0000	-0.1147	86.5900	19.2483	19.2762	16.2277	152.7000	19.2623	0.0028
12.0000	-0.0761	86.4766	19.2165	19.3912	16.1685	152.7000	19.3038	0.0033
14.0000	-0.0647	86.4570	19.2090	19.2725	16.2566	152.7000	19.2407	0.0039
16.0000	0.0067	86.3861	19.2260	19.2758	16.2701	152.7000	19.2509	0.0044
18.0000	0.0518	86.2657	19.2470	19.2918	16.3590	152.7000	19.2694	0.0050

Figure C.20: LabView Data Presentation User Interface Screen 2

### C.3.2 LabView Flow Diagrams

The first example flow chart is of the central console which allows the different operations to be undertaken. On the next page the data acquisition flowchart is presented.

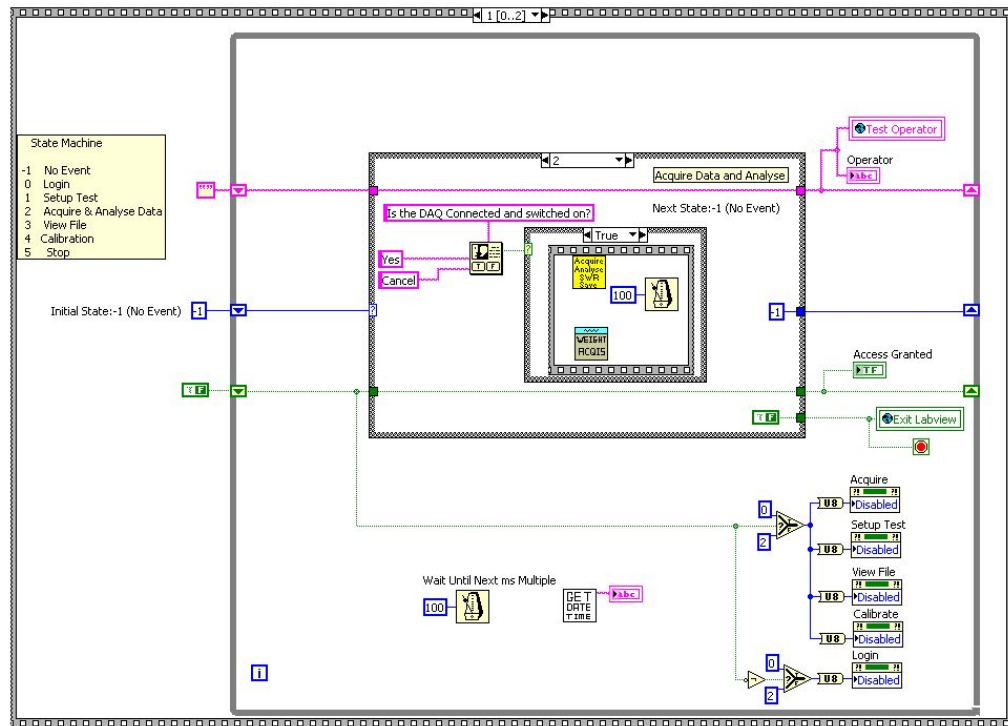


Figure C.21: LabView Front GUI Flow Chart

The flow chart for the Acquisition VI is very large and complicated. The reason for the complicated nature is that this VI was required to continuously provide up-to-date measurement values and then simultaneously record the values for a fixed period, the start of the recording determined by the operator once the conditions had sufficiently stabilised. For this reason, a queue approach was taken, allowing data to be available for recording as well as for display on the GUI, making the VI large. For this reason, the flow chart is displayed over three pages in three parts.

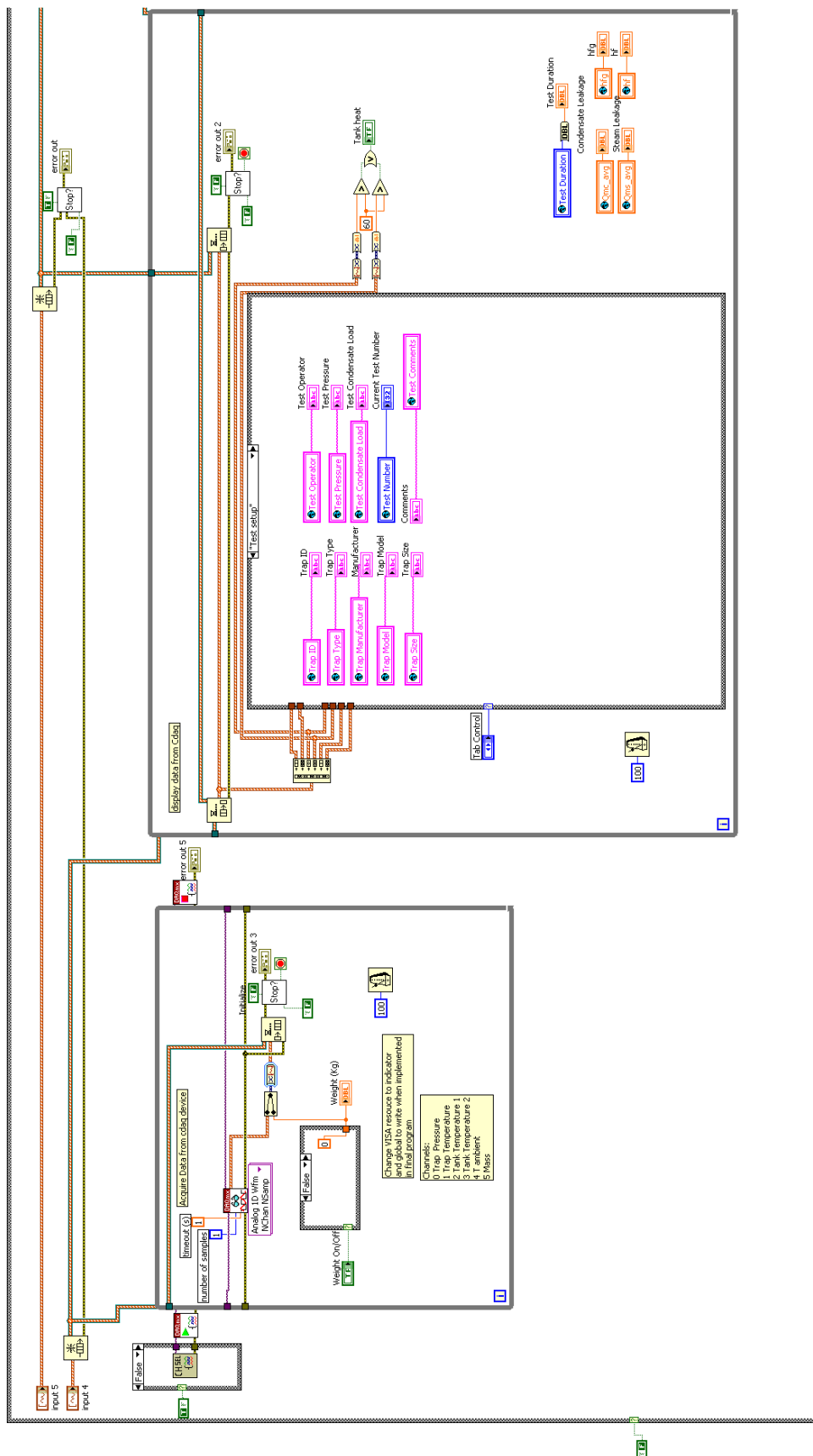


Figure C.22: LabView Data Acquisition Flow Chart Part 1



Figure C.23: LabView Data Acquisition Flow Chart Part 2

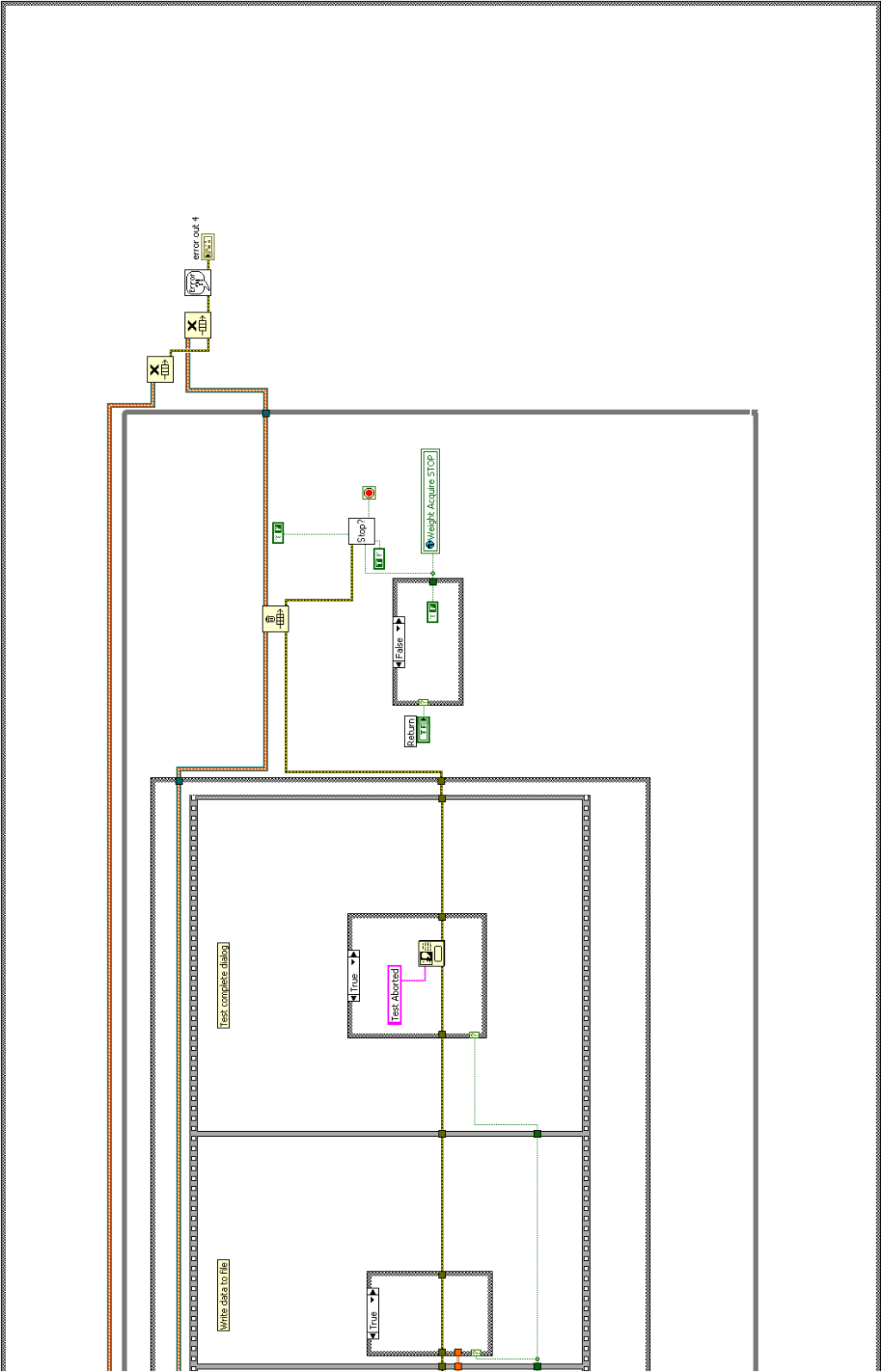


Figure C.24: LabView Data Acquisition Flow Chart Part 3

### C.3.3 List of SubVIs in Program

- 1) Acquire weight.vi - Data acquisition of weight data using RS232 protocol.
- 2) Authenticate User.vi - Authenticates and allows system access only for registered users.
- 3) Channel config virtual.vi - VI used for testing of the software by use of a simulated input signal.
- 4) Channel Config.vi - Channel setup and initialisation for data acquisition from sensors.
- 5) Convert from dynamic.vi - Converts the data type from dynamic to double data type.
- 6) Convert to dynamic.vi - Converts from Array of wave forms to dynamic data type.
- 7) Get Date Time.vi - Obtains the date and time for the indexing and saving of results file and index file.
- 8) Read cal ini SWR.vi - Reads the calibration data every time the software is started.
- 9) Read data file SWR - Reads previously recorded test data and displays it in a VI.
- 10) Read steam tables dlm.vi - Reads the steam tables stored in Steamtables.dlm to a variable.
- 11) Recall setup ini SWR.vi - Reads the settings from the `SWR_config.inifile`.
- 12) Save Setup ini SWR.vi - Save the settings to the `SWR_config.inifile`.
- 13) Should STOP swr.vi - Checks the state of the STOP flags when the program should be stopped.
- 14) SWR Calc.vi - Steam wastage calculation using Matlab with M-file calculation embedded.
- 15) Total Test Log.vi - Saves key data to an overall index file index of all tests conducted.
- 16) Write cal ini SWR.vi - Writes the calibration data to the calibration.ini file.
- 17) Write data to file SWR.vi - Writes the SWR data to the file.

### C.3.4 List of Associated INI and DLM Files

The following three files are essential for the working of the LabView program. These are a configuration file, calibration file and steam table file (for calculation of the Steam Wastage Value). The contents of the individual files is listed below.

- 1) SWR configuration exchange file - `swr_config.ini`. The following list the contents of the configuration file used in the LabView program. The purpose of this file is to transfer data from one instance of use to the other. This file is read at the start of the running of the program

and written at the end of the program when it closes. Through this method, the last usage and the test number can be incremented from one day to another without the same operator having to be present. This also ensures that no data is overwritten and that data is kept in logical chronological order.

```
[Set-up Parameters]
Demo Mode?=TRUE
Exit LabVIEW?=TRUE
Title=nnnnn
Version info=12345
Key=asdfgh
Filename=SG__090120_703
Project=""
Date=090120
Test Operator=JFS
Test Number=703
Software Path=/C/STAPS SWR
File Path=/C/STAPS SWR/SW Data
```

- 2) Calibration data exchange file - calibration.ini. These are the calibration figures for the pressure transducer.

```
[Trap Pressure]
Offset=-10.000000
Gain=2500.000000
```

## 3) Steam data tables in delimited format - steam.dlm

Pressure	Temp.	hf	hg
0.000000	100.001	419101	2.25666E06
0.100000	102.660	430327	2.24962E06
0.200000	105.128	440758	2.24305E06
0.300000	107.434	450510	2.23686E06
0.400000	109.600	459676	2.23102E06
0.500000	111.642	468331	2.22547E06
0.600000	113.577	476534	2.22019E06
0.700000	115.416	484336	2.21513E06
0.800000	117.169	491779	2.21029E06
0.900000	118.844	498898	2.20564E06
1.00000	120.449	505725	2.20116E06
1.10000	121.991	512284	2.19683E06
1.20000	123.474	518599	2.19265E06
1.30000	124.903	524690	2.18860E06
1.40000	126.283	530574	2.18467E06
1.50000	127.617	536266	2.18086E06
1.60000	128.909	541781	2.17715E06
1.70000	130.161	547130	2.17354E06
1.80000	131.376	552324	2.17002E06
1.90000	132.557	557374	2.16658E06
2.00000	133.705	562289	2.16323E06
...	...	...	...
39.0000	250.411	1.08735E06	1.71329E06
39.1000	250.559	1.08807E06	1.71252E06
39.2000	250.707	1.08879E06	1.71175E06
39.3000	250.855	1.08951E06	1.71098E06
39.4000	251.002	1.09022E06	1.71022E06
39.5000	251.149	1.09094E06	1.70945E06
39.6000	251.296	1.09165E06	1.70868E06
39.7000	251.442	1.09236E06	1.70792E06
39.8000	251.588	1.09308E06	1.70715E06
39.9000	251.734	1.09379E06	1.70639E06
40.0000	251.879	1.09450E06	1.70562E06

### C.3.5 Matlab Steam Wastage Calculation for LabView

To facilitate the calculation of the Steam Wastage in accordance with the formula from the BSEN standard for the evaluation of Steam Traps, a MatLab module inside LabView was used. This Module allowed MatLab code to be executed within a LabView VI. The code is enclosed below, but essentially it works as follows:

- 1) Reads the measured values from the experiment from a measurement variable.
- 2) Averages the Temperature Readings from the Tank,
- 3) Looks up the corresponding enthalpy values
- 4) Calculates the Steam Wastage Value and Condensate Load.

```

1 %function result = sw_estimate(exp_data)
2 %*****
3 %   Program: sw_estimation(exp_data)
4 %   Author: Christopher Poczka
5 %   Date: 19 December, 2007
6 %   Version: 2.1
7 %   Description: This script is written to be used within the NI LabVIEW
8 %   data acquisition program to calculate the steam wastage from the
9 %   experimental data. The original script was written together
10 %   with Nishal Ramadas.
11 %
12 %   Input(s): exp_data is column matrix
13 %   (Time|TrapP|TrapT|TankT1|TankT2|T Ambient|TankMass)
14 %   consisting of the data captured using the NI compact DAQ hardware
15 %*****
16
17 result=0;
18 [m,n] = size(exp_data);
19
20 % Channel Number/ exp_data file structure:
21 % 1   X   2       X   3           X 4 X 5 X   6           X   7       X
22 %TIME X PRESSURE X TRAP TEMP X T1 X T2 X T Ambient X WEIGHT X
23
24 % scripts adds avg_trap to structure (column 8)
25 exp_data = [exp_data mean(exp_data(:,4:5)')'];
26 %script adds time in hrs to structure column 9)
27 exp_data = [exp_data (exp_data(:,1)/3600)]
28 avg_trap_temp = mean(exp_data(:,3));

```

```

29
30 % constants used in the program
31 WCp = 4.19;
32 TCp = 0.05;
33
34
35 %for the latent heat content calculation use first weight-> exp_data (1,7)
36 TankMass = exp_data (1,7);
37 %HARDCODED TEST FOR WEIGHT TEST
38 %TankMass = 30;
39
40 %%DATA STRUCTURE FOR STEAM TABLE: P|T|hf|hfg
41 %sxs_steam_table =dlmread ('steam' ,'\t') ;
42
43 sxs_steam_table=steamtable;
44
45 %FIND ENTHALPHY VALUES FOR FIND ENTHALPHY VALUES FOR SW CALC
46 temp_var = abs(sxs_steam_table(:,2)-avg_trap_temp);
47 pos=find(temp_var==min(temp_var));
48 pres = sxs_steam_table(pos,1);
49 temp = sxs_steam_table(pos,2);
50 hf = sxs_steam_table(pos,3);
51 hfg = sxs_steam_table(pos,4);
52
53 % HARD CODE TEST hf + hfg values
54 % hf = 585.1;
55 % hfg = 2147.5;
56 % hf = 732.6;
57 % hfg = 2038.8;
58
59
60 % CALCULATE SW (equations taken from patrick lawler's excel sheets)
61
62 % Avg Tank Temp 1 -> exp_data(1,n+1)
63 % Avg Tank Temp 2 -> exp_data(end,n+1)
64 % Tank Mass 1 -> exp_data(1,7)
65 % Tank Mass 2 -> exp_data(end,7)
66 Qms_avg = ((exp_data(end,7)*WCp*exp_data(end,8))-(exp_data(1,7)*WCp*...
67 exp_data(1,8))-(hf*(exp_data(end,7)-exp_data(1,7)))+(TCp*TankMass*...
68 (exp_data(end,8)-exp_data(1,8))))/(hfg*exp_data(end,9));
69 Qmc_avg = exp_data(end,7) - Qms_avg;
70
71 exp_data_out=exp_data;

```

## Appendix D

### List of Data Files

The following three tables list the full number of data sets used in this document. Each entry line is an acoustic recording of 1 or 2 minutes length. Associated conditions are also listed in the tables.

#### D.1 Fixed Orifice

Filename	Condensate (kg/hr)	Pressure (barg)	SWV (kg/hr)	Temperature (°C)
UK_12_01_09_11_11_48_00.dat	9.5	5	4.62	159
UK_12_01_09_11_11_48_01.dat	9.5	5	4.62	159
UK_12_01_09_11_11_48_02.dat	9.5	5	4.62	159
UK_12_01_09_11_54_59_00.dat	43.7	5	1.65	159
UK_12_01_09_11_54_59_01.dat	43.7	5	1.65	159
UK_12_01_09_11_54_59_02.dat	43.7	5	1.65	159
UK_12_01_09_14_23_07_00.dat	87.5	5	0.57	159
UK_12_01_09_14_23_07_01.dat	87.5	5	0.57	159
UK_12_01_09_14_23_07_02.dat	87.5	5	0.57	159
UK_12_01_09_14_53_22_00.dat	14.1	10	7.79	184
UK_12_01_09_14_53_22_01.dat	14.1	10	7.79	184
UK_12_01_09_14_53_22_02.dat	14.1	10	7.79	184
UK_12_01_09_15_46_45_00.dat	53.1	10	2.54	184
UK_12_01_09_15_46_45_01.dat	53.1	10	2.54	184
UK_12_01_09_15_46_45_02.dat	53.1	10	2.54	184
UK_13_01_09_11_30_33_00.dat	107.3	10	0.27	184
UK_13_01_09_11_30_33_01.dat	107.3	10	0.27	184
UK_13_01_09_11_30_33_02.dat	107.3	10	0.27	184
UK_14_01_09_11_09_16_00.dat	13.8	15	11.63	201
UK_14_01_09_11_09_16_01.dat	13.8	15	11.63	201
UK_14_01_09_11_09_16_02.dat	13.8	15	11.63	201
UK_14_01_09_11_24_48_00.dat	61.4	15	3.6	201
UK_14_01_09_11_24_48_01.dat	61.4	15	3.6	201
UK_14_01_09_11_24_48_02.dat	61.4	15	3.6	201
UK_14_01_09_14_18_10_00.dat	119.3	15	-0.28	201
UK_14_01_09_14_18_10_01.dat	119.3	15	-0.28	201
UK_14_01_09_14_18_10_02.dat	119.3	15	-0.28	201

Table D.1: Fixed Orifice Trap Acoustic Complete Data List



## D.2 Non-Impulsive

Filename	Condensate (kg/hr)	Pressure (barg)	SWV (kg/hr)	Temperature (°C)
UK_01_05_07_11_29_04.dat	10	15	9.29	199
UK_01_05_07_11_31_15.dat	10	15	9.29	199
UK_01_05_07_11_33_25.dat	10	15	9.29	199
UK_03_05_07_10_34_32.dat	10	10	4.1	184
UK_03_05_07_10_36_41.dat	10	10	4.1	184
UK_03_05_07_10_38_47.dat	10	10	4.1	184
UK_03_05_07_10_41_19.dat	10	10	4.1	184
UK_08_05_07_10_23_31.dat	10	10	1.68	184
UK_08_05_07_10_25_38.dat	10	10	1.68	184
UK_08_05_07_10_27_43.dat	10	10	1.68	184
UK_08_05_07_14_59_58.dat	60	10	-0.39	184
UK_08_05_07_15_02_04.dat	60	10	-0.39	184
UK_08_05_07_15_04_09.dat	60	10	-0.39	184
UK_14_05_07_13_40_04.dat	10	5	2.71	159
UK_14_05_07_13_42_12.dat	10	5	2.71	159
UK_14_05_07_13_44_17.dat	10	5	2.71	159
UK_16_07_07_10_21_02.dat	30	5	4.08	159
UK_16_07_07_10_21_02.dat	30	5	4.08	159
UK_16_07_07_10_21_02.dad	30	5	4.08	159
UK_21_05_07_13_32_02.dat	10	5	1.88	159
UK_21_05_07_13_34_08.dat	10	5	1.88	159
UK_21_05_07_13_36_14.dat	10	5	1.88	159
UK_21_05_07_15_29_31.dat	10	10	0.68	184
UK_21_05_07_15_31_36.dat	10	10	0.68	184
UK_21_05_07_15_33_47.dat	10	10	0.68	184
UK_30_04_07_11_33_33.dat	10	10	7.48	184
UK_30_04_07_11_35_41.dat	10	10	7.48	184
UK_30_04_07_11_37_49.dat	10	10	7.48	184

Table D.2: Float Trap Acoustic Complete Data List

### D.3 Impulsive

Filename	Condensate (kg/hr)	Pressure (barg)	SWV (kg/hr)	Temperature ( °C)
UK_08_08_07_11_07_24_00.dat	10	5	0.19	159
UK_08_08_07_11_07_24_01.dat	10	5	0.19	159
UK_08_08_07_11_07_24_02.dat	10	5	0.19	159
UK_16_04_07_14_31_44.dat	10	20	10.96	217
UK_16_04_07_14_33_54.dat	10	20	10.96	217
UK_16_04_07_15_10_49.dat	10	20	9.65	217
UK_16_04_07_15_13_01.dat	10	20	9.65	217
UK_16_04_07_15_15_09.dat	10	20	9.65	217
UK_16_04_07_15_41_03.dat	50	20	7.28	217
UK_16_04_07_15_43_16.dat	50	20	7.28	217
UK_16_04_07_15_45_31.dat	50	20	7.28	217
UK_17_04_07_10_18_16.dat	55	20	1.39	216
UK_17_04_07_10_20_58.dat	55	20	1.39	216
UK_17_04_07_10_23_08.dat	55	20	1.39	216
UK_18_04_07_14_51_34.dat	10	15	1.62	201
UK_18_04_07_14_53_46.dat	10	15	1.62	201
UK_18_04_07_14_55_55.dat	10	15	1.62	201
UK_19_04_07_14_00_46.dat	60	15	-0.37	201
UK_19_04_07_14_02_56.dat	60	15	-0.37	201
UK_19_04_07_14_05_04.dat	60	15	-0.37	201
UK_19_04_07_15_29_59.dat	35	15	1.12	201
UK_19_04_07_15_33_12.dat	35	15	1.12	201
UK_19_04_07_15_35_23.dat	35	15	1.12	201
UK_20_04_07_14_58_26.dat	45	15	0.38	201
UK_20_04_07_15_00_37.dat	45	15	0.38	201
UK_20_04_07_15_02_45.dat	45	15	0.38	201

Table D.3: Thermodynamic Trap Acoustic Complete Data List